Electronic Supplementary Material (ESI) for Organic & Biomolecular Chemistry.

Supporting Information

Hancockiamides: Phenylpropanoid Piperazines from *Aspergillus hancockii* are Biosynthesised by a Versatile Dual Single-module NRPS Pathway

Hang Li, [†a] Alastair E. Lacey,[†b] Si Shu,[a] John A. Kalaitzis,[c] Daniel Vuong,[b] Andrew Crombie,[b] Jinyu Hu,[a] Cameron L. M. Gilchrist,[a] Ernest Lacey,[b,c] Andrew M. Piggott,[*c] Yit-Heng Chooi[*a]

[a] School of Molecular Sciences, The University of Western Australia, Perth, WA 6009, Australia

[b] Microbial Screening Technologies Pty. Ltd., Smithfield, NSW 2164, Australia

[c] Department of Molecular Sciences, Macquarie University, Sydney, NSW 2109, Australia

Table of Contents

Supplementary Experimental Procedures

1. Strains and culture conditions

The wild-type *A. hancockii* was maintained in PDA (potato dextrose agar) at 24°C. High molecular weight genomic DNA of *A. hancockii* was prepared according to the protocol described previously.[1] *Saccharomyces cerevisiae* BJ5464-NpgA (*MATα ura3-52 his3-Δ200 leu2-Δ1trp1 pep4::HIS3 prb1 Δ1.6R can1 GAL*) was used for plasmid construction and protein expression. *Aspergillus nidulans* LO7890[2] (a gift from Prof. Berl Oakley, University of Kansas) was used for heterologous expression of *hkm* genes. *Escherichia coli* 5α and 10β were used for standard DNA manipulation.

2. Cultivation and Compounds isolation

The fungus (*A. hancockii* MST FP2241) was inoculated onto jasmine rice (sterilized at 120 °C for 40 min) in 60 × 250 mL Erlenmeyer flasks, each containing 50 g of rice, and the flasks were incubated at 24 °C for 14 days. The grains were pooled and extracted with acetone (2 × 4.5 L), and the combined extract was concentrated under reduced pressure to give a crude extract (57 g in 1250 mL). The slurry was partitioned against AcOEt (2 × 2 L) and organic layer was reduced *in vacuo* forming an oily residue (15.3 g). The residue was dissolved in MeOH (900 mL), defatted with hexane (2 × 1 L) and evaporated *in vacuo* to give an enriched methanolic extract (7 g).

The methanolic extract was dissolved in $CHCl_3$ (300 mL) and absorbed onto silica gel (30 g) then dried *in vacuo* and loaded onto a silica gel column (100 g, 5 × 30 cm). The column was eluted with hexane, then 50% hexane/$CHCl_3$ and $CHCl_3$, followed by incremental steps of 1, 2, 4, 8, 16, 32, 64 and 100% MeOH/$CHCl_3$ (500 mL each fraction), to yield 11 fractions (Fr A1 to A11).

Fraction A4 (1.5 g) was purified by preparative HPLC (Hypersil C_{18}, incremental steps 58-75-100% MeCN/H_2O containing 0.01% TFA, 60 mL min^{-1}) for 16.5, 14 and 10 min, respectively, to yield hancockiamide B (**2**; t_R 14.20 min; 28.3 mg), hancockiamide C (**3**; t_R 22.00 min; 160 mg) and an enriched fraction (Fr D7/8; 110 mg). Fr D7/8 was further purified by preparative HPLC (Alltima C_{18}, isocratic 35% MeCN/H_2O, 20 mL min^{-1}) to yield hancockiamide F (**6**; t_R 25.10 min; 1.7 mg).

Fraction A6 (700 mg) was enriched by preparative HPLC (Hypersil C_{18}, incremental steps 40-60-80-100% MeCN/H_2O containing 0.01% TFA, 60 mL min^{-1}) for 12, 11, 9 and 12 min, respectively, to give hancockiamide A TFA salt (**1**; t_R 10.30 min; 216 mg) and an enriched fraction

(Fr C2; 51 mg). Fr C2 was further purified by preparative HPLC (Alltima C_{18}, isocratic 35% MeCN/H_2O containing 0.01% TFA, 20 mL min^{-1}) to yield hancockiamide E TFA salt (**5**; t_R 19.00 min; 2.0 mg).

Fraction A10 (310 mg) was further fractionated using Sephadex LH-20 size-exclusion chromatography with MeOH as the eluent (3 × 28 cm, 2 mL min^{-1}) and resolved into six fractions (Fr B1 to B6).. Fr B2 (75 mg) was further purified by preparative HPLC (Alltima C_{18}, isocratic 15% MeCN/H_2O containing 0.01% TFA, 20 mL min^{-1}) to give hancockiamide D di-TFA salt (**4**; t_R 10.15 min; 3.0 mg). (see isolation scheme below)

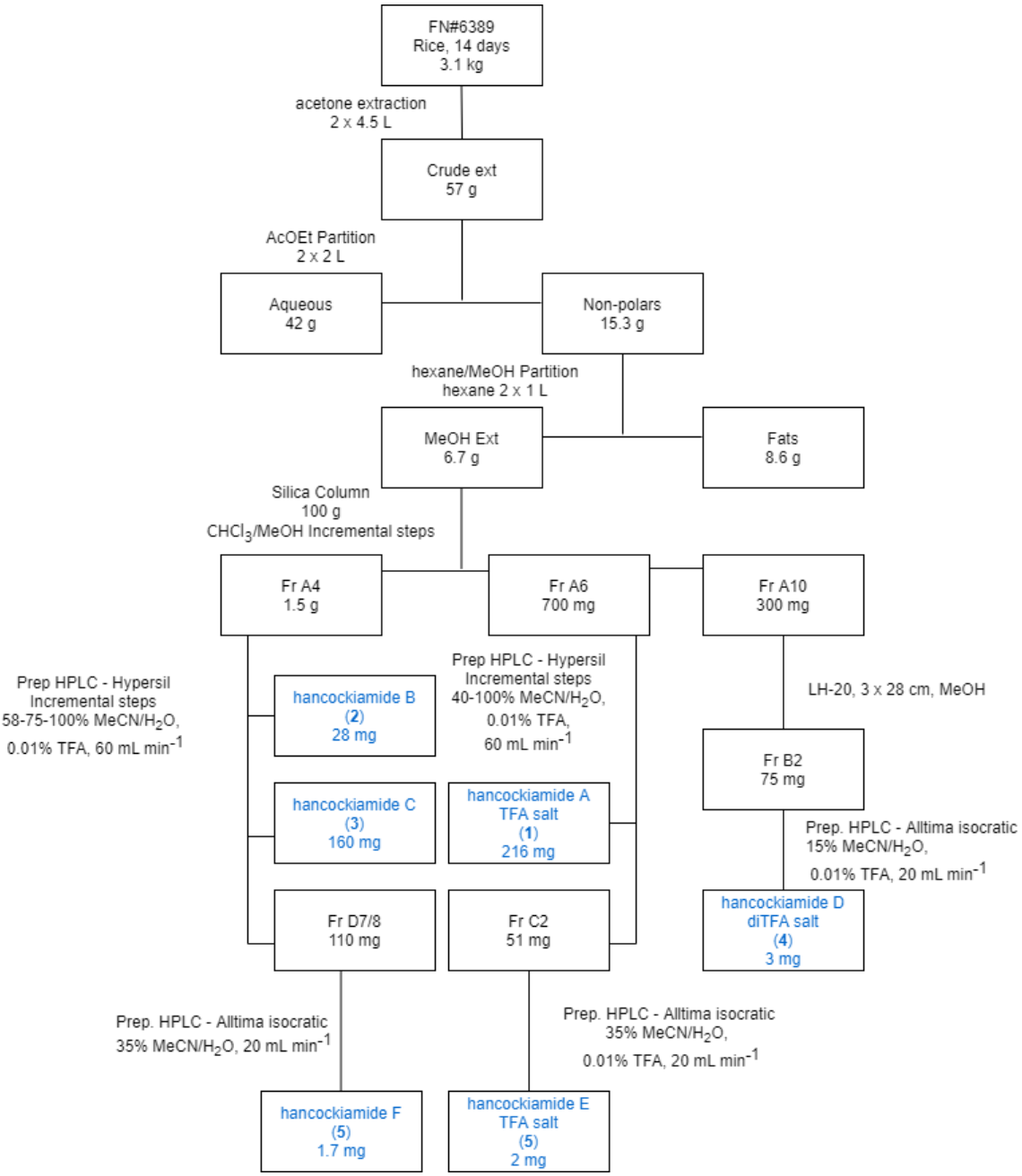

The fungus (A. *hancockii* MST FP2241) was inoculated onto jasmine rice (sterilized at 120 °C

for 40 min) in 60 × 250 mL Erlenmeyer flasks, each containing 50 g of rice, and the flasks were incubated at 24 °C for 14 days. The grains were pooled and extracted with acetone (1 × 5 L), and the extract was evaporated under reduced pressure to give a crude extract (90 g in 1500 mL). The slurry was partitioned against AcOEt (2 × 2 L) and the organic layer reduced *in vacuo* to an oily residue (13.5 g). The non-polar extract was dissolved in AcOEt (1 L) and partitioned against aqueous HCl (2 × 500 mL; 1% *v/v*) to extract the amines. The aqueous layer was then basified to pH 8.9 with NaOH (10 M) solution and partitioned against AcOEt (2 × 500 mL). The combined organic layer was then evaporated *in vacuo* to yield an enriched amine fraction (1.3 g). The amines were further purified by preparative HPLC (Zorbax Si, stepwise in 10% increments from 60% to 100% AcOEt/hexane, 80 mL min^{-1}) for 10 min at each increment to yield hancockiamide A (**1**; t_R 18.65 min; 226 mg) and hancockiamide D (**4**; t_R 44.87 min; 100 mg).

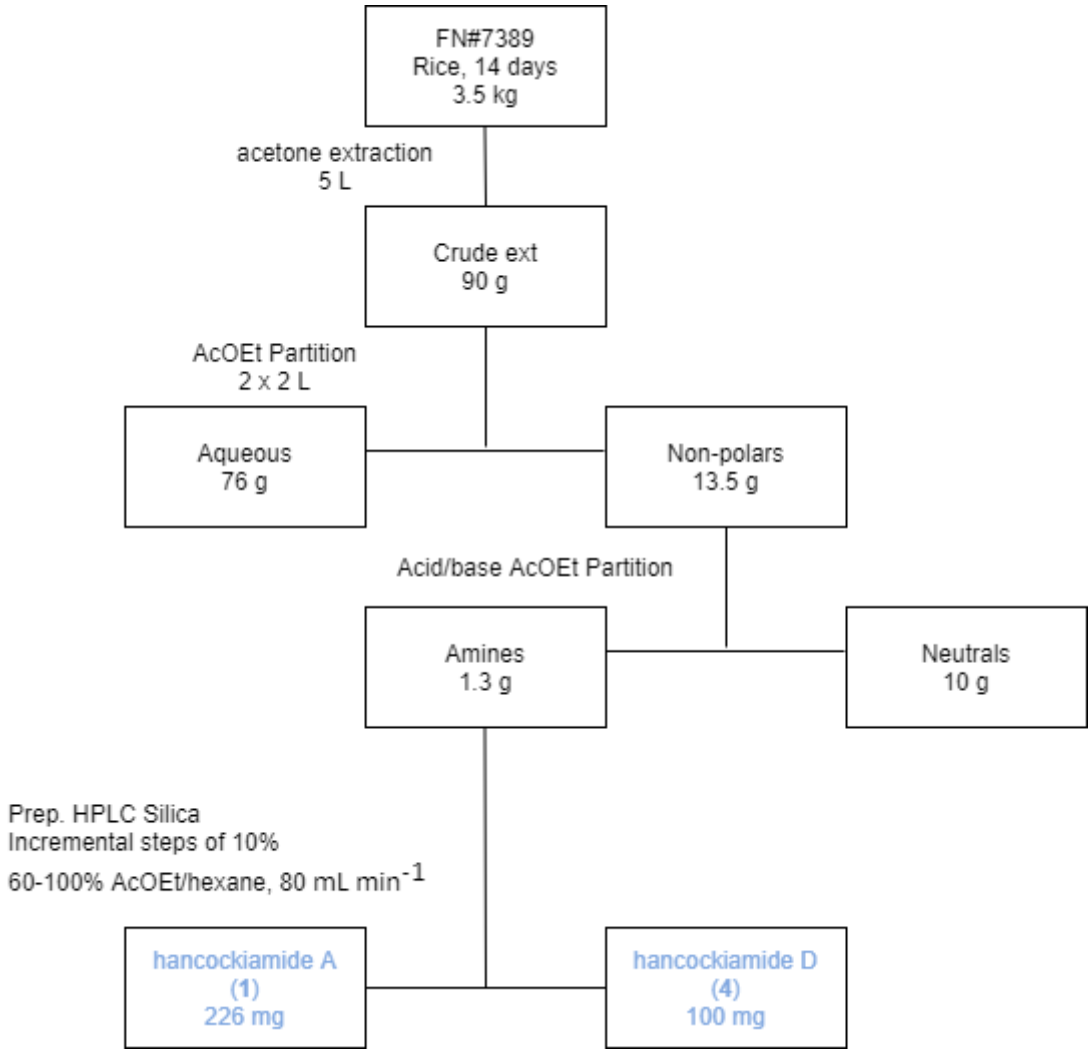

The fungus (*A. nidulans* MST FP2506) was inoculated onto sterile YES agar [yeast extract (40

g), sucrose (300 g), agar (40 g) in distilled water to 2 L autoclaved 120 °C for 40 min], and incubated at 24 °C for 14 days, after which the agars were pooled and extracted with acetone (2 × 4 L). The combined extract was evaporated *in vacuo* to produce a crude extract (43 g in 1600 mL). The slurry was partition against AcOEt (2 × 2 L) and organic layer was reduced *in vacuo* to an oily residue (10 g). The residue was dissolved in MeOH (400 mL), defatted with hexane (2 × 500 mL) and evaporated *in vacuo* to give an enriched methanolic extract (4.8 g).

The methanolic extract was dissolved in $CHCl_3$ (300 mL) and absorbed onto silica gel (30 g) then dried *in vacuo* and loaded onto a silica gel column (100 g, 5 × 30 cm). The column was eluted with hexane, then 50% hexane/$CHCl_3$ and $CHCl_3$, followed by incremental steps of 1, 2, 4, 8, 16, 32, 64 and 100% MeOH/$CHCl_3$ (500 mL each fraction), to yield 11 fractions (Fr A1 to A11).

Fraction A4 (630 mg) was further fractionated by preparative HPLC (Zorbax Si, stepwise in 5% increments from 5% to 25% EtOH/hexane, 80 mL min^{-1}) for 5 min at each increment to give B1 to 22 fractions.

Fraction B9 (6.2 mg) was purified by Sephadex LH-20 size-exclusion chromatography with MeOH as the eluent (3 × 28 cm, 2 mL min^{-1}) to yield xenocockiamide D (**13**; 4 mg). Fraction B11 (14 mg) was further enriched by Sephadex LH-20 size-exclusion chromatography with MeOH as the eluent (3 × 28 cm, 2 mL min^{-1}) to give an enriched fraction (9 mg) which was purified preparative HPLC (Grace Si, incremental steps of 2.5% from 17.5% to 40% AcOEt/hexane, 7 mL min^{-1}) for 5 min at each increment to yield xenocockiamide B (**11**; t_R 32.55 min; 3.3 mg). Fraction B14 (6.7 mg) was enriched by Sephadex LH-20 size-exclusion chromatography with MeOH as the eluent (3 × 28 cm, 2 mL min^{-1}) to yield (6.0 mg) which was purified by preparative HPLC (Grace Silica, stepwise in 2.5% increments from 17.5% to 40% AcOEt/hexane, 7 mL min^{-1}) to yield hancockiamide I (**9**; t_R 35.80 min; 2.3 mg). Fraction B16 (65 mg) was purified by Sephadex LH-20 size-exclusion chromatography with MeOH as the eluent (2 × 55 cm, at 4 mL min^{-1}) to yield xenocockiamide C (**12**; 41 mg). Fraction B19 (25 mg) was purified by Sephadex LH-20 size-exclusion chromatography with MeOH as the eluent (2 × 55 cm, at 4 mL min^{-1}) to yield hancockiamide G (**7**; 8 mg).

Fraction A9 (1 g) was dissolved in AcOEt (200 mL) and partitioned against aqueous HCl (2 × 100 mL; 1% *v/v*) to extract the amines. The aqueous layer was then basified to pH 8.7 with NaOH (10 M) solution and partitioned against AcOEt (2 × 200 mL). The combined organic layer was

evaporated *in vacuo* to yield an enriched amine fraction (123 mg). The amines were further purified by preparative HPLC (Grace Si, stepwise in 5% increments from 5% to 50% EtOH/hexane, 7 mL min^{-1}) for 3 min up until 25% and 6 min increments to 100% to yield xenocockiamide A (**10**; t_R 11.50 min; 47 mg) and hancockiamide H (**8**; t_R 16.75 min; 10.4 mg). (see isolation scheme below)

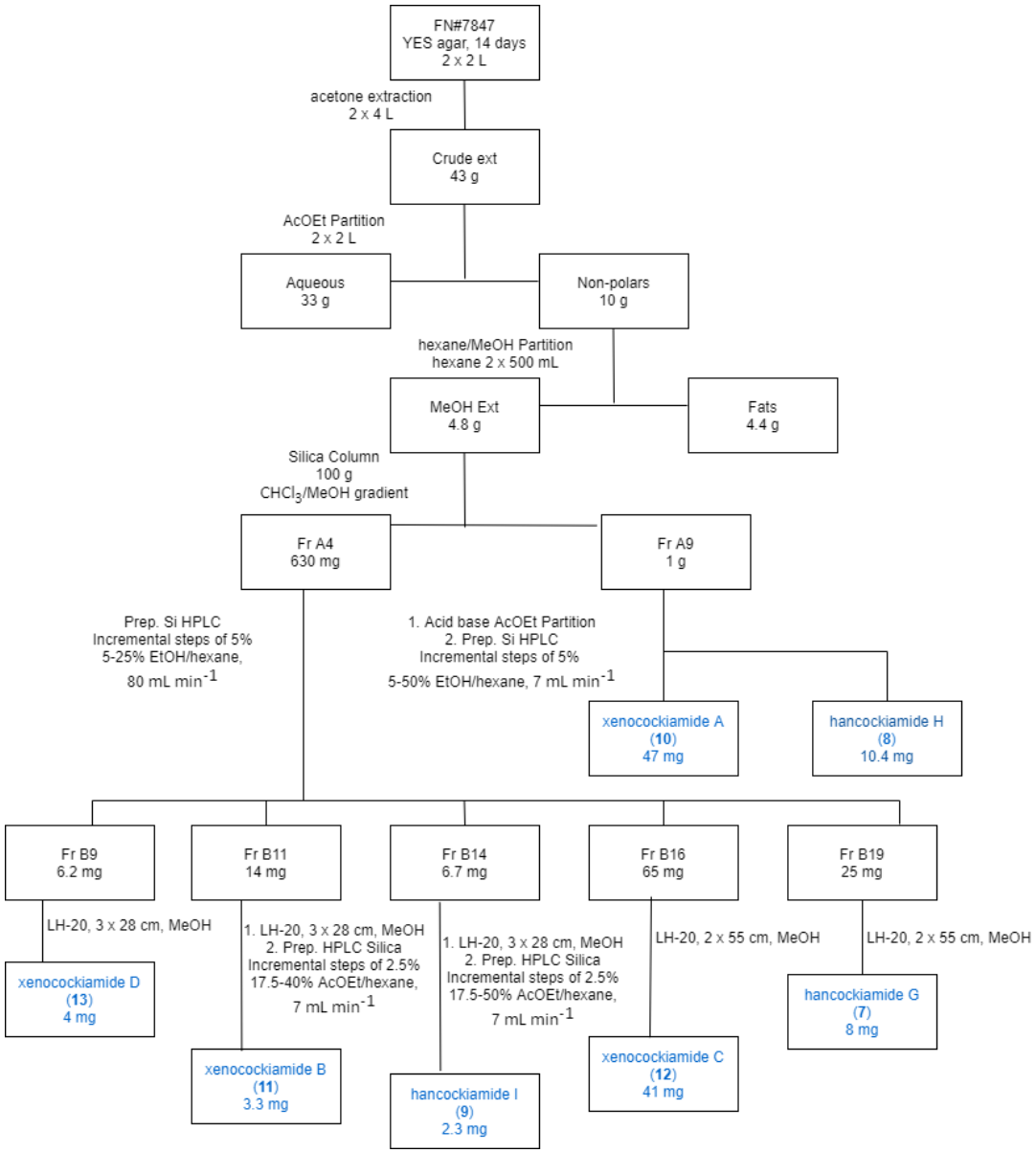

3. Compound characterization

HRESI(+)MS analysis of hancockiamide B (**2**) revealed an adduct ion $[M + Na]^+$ *m/z* 537.2359, indicative of a molecular formula $C_{31}H_{34}N_2O_5$ (Δmmu –0.1) corresponding to an increase of C_2H_2O compared to **1**. The ^1H (Figure S19) and ^{13}C (Figure S20) NMR spectra of **2** in DMSO-d_6 were considerably more complex than those of **1**, with four closely matched sets of signals in a 46:25:16:13 ratio and significant peak broadening observed for many of the resonances. The NMR data for the major conformer (Table S9) were generally consistent with those for **1**, with the main differences being the absence of a signal corresponding to 1-NH and presence of additional resonances for an acetyl group (C-1‴, δ_C 169.5; C-2‴, δ_H 2.03, s, 3H; δ_C 21.9). Detailed analysis of the remaining 2D NMR correlations (Figure S22) confirmed the structure of **2** to be the N^1-acetyl analogue of **1**, as shown in Figure 1.

HRESI(+)MS analysis of hancockiamide C (**3**) revealed an adduct ion $[M + Na]^+$ *m/z* 535.2204, indicative of a molecular formula $C_{31}H_{32}N_2O_5$ (Δmmu 0.1) corresponding to an decrease of H_2 compared to **2**. The ^1H (Figure S25) and ^{13}C (Figure S26) NMR spectra of **3** in DMSO-d_6 were very similar to those of **2**, again with four closely matched sets of signals in a 49:30:12:9 ratio and significant peak broadening. The NMR data for the major conformer (Table S10) were generally consistent with those for **2**, with the only significant differences being the absence of resonances for 7-OH and 8-OMe, a break in symmetry for Ring A, and the presence of an additional deshielded methylene group (δ_H 5.79, br s and 5.58, br s; δ_C 100.9). Diagnostic HMBC correlations (Figure S28) from this methylene group to C-7 and C-8 suggested cyclization between 7-OH and 8-OMe to give a 7,8-methylenedioxy ring. Detailed analysis of the remaining 2D NMR correlations (Figure S28) confirmed the structure of **3** as shown in Figure 1.

HRESI(+)MS analysis of hancockiamide D (**4**) revealed a protonated molecule $[M + H]^+$ *m/z* 343.2017, indicative of a molecular formula $C_{20}H_{26}N_2O_3$ (Δmmu 0.1) corresponding to a decrease of C_9H_6O compared to **1**. The ^1H (Figure S31) and ^{13}C (Figure S32) NMR spectra of **4** in DMSO-d_6 were much simpler than those of **1–3**, with no evidence of peak doubling or broadening. The NMR data for **4** (Table S11) revealed signals corresponding to Rings A and B and the central piperazine ring of **1**, but no signals corresponding to the cinnamoyl group. Detailed analysis of the remaining 2D NMR correlations (Figure S34) confirmed the structure of **4** to be the $N^{1'}$-descinnamoyl analogue of **1**, as shown in Figure 1.

HRESI(+)MS analysis of hancockiamide E (**5**) revealed a protonated molecule $[M + H]^+$ *m/z* 547.2432, indicative of a molecular formula $C_{31}H_{34}N_2O_7$ (Δmmu –0.7) corresponding to an increase of $C_2H_2O_3$ compared to **1**. The ^1H (Figure S43) and ^{13}C (Figure S44) NMR spectra of **5** in DMSO-d_6 were similar to those of **1**, with two closely paired sets of signals in an 80:20 ratio and significant peak broadening. The NMR data for the major conformer (Table S13) were consistent with Rings A, and C, and central piperazine ring of **1**. However, examination of the resonances for Ring B suggested the presence of an asymmetrically 1,3,4,5-tetrasubstituted aromatic ring rather than the monosubstituted aromatic ring in **1**. Additional resonances for a single methoxy group (6′-OMe, δ_H 3.84, s; δ_C 56.3) and a methylenedioxy group (δ_H 5.99, br s, 2H; δ_C 101.2) suggested the same substitution pattern as Ring A in **3**. Detailed analysis of the remaining 2D NMR correlations (Figure S46) confirmed the structure of **5** as shown.

HRESI(+)MS analysis of hancockiamide F (**6**) revealed an adduct ion $[M + Na]^+$ *m/z* 551.2148, indicative of a molecular formula $C_{31}H_{32}N_2O_6$ (Δmmu –0.5) containing one additional oxygen atom compared to **3**. The ^1H (Figure S49) and ^{13}C (Figure S50) NMR spectra of **6** in DMSO-d_6 contained two sets of closely paired signals in a 79:21 ratio, although there was no evidence of the peak

broadening observed in **1**–**3** and **5**. The NMR data for the major conformer (Table S14) were consistent with Rings A, B and C, the *N*-acetyl group and central piperazine ring of **3**. The main differences were the absence of signal for H-2 and the significant deshielding of C-2 (δ_C 204.1), consistent with the presence of a ketone carbonyl group. The presence of HMBC correlations from H_2-1 to C-2′and the absence of corresponding correlations from H_2-1′ to C-2 suggested cleavage of the central piperazine ring between 1′-N and C-2. Detailed analysis of the remaining 2D NMR correlations (Figure S52) confirmed the structure of **6** to be a ring-opened analogue of **3**, as shown in Figure 1. The compound was tentatively assigned a 2′*S* configuration on biosynthetic grounds.

HRESI(+)MS analysis of **7** revealed a protonated molecule $[M + H]^+$ *m/z* 471.2273, indicative of a molecular formula $C_{29}H_{30}N_2O_4$ (Δmmu –0.5) corresponding to a decrease of C_2H_2O compared to **3**. Indeed, the NMR data for **7** (Table S15) were very similar to those for **3**, with the main differences being the absence of signals for the N^1-acetyl group and the presence of an additional exchangeable proton (δ_H 2.20, br s). Detailed analysis of the remaining 2D NMR correlations (Figure S58) confirmed the structure of **7** as the N^1-desacetyl analogue of **1**.

HRESI(+)MS analysis of **8** revealed a protonated molecule $[M + H]^+$ *m/z* 341.1860, indicative of a molecular formula $C_{20}H_{24}N_2O_3$ (Δmmu 0.0) corresponding to one DBE less than **4**. Detailed analysis of the 2D NMR correlations (Figure S64) confirmed the structure of **8** to be the 7,8-methylenedioxy analogue of **4**.

HRESI(+)MS analysis of **9** revealed a protonated molecule $[M + H]^+$ *m/z* 601.2695, indicative of a molecular formula $C_{38}H_{36}N_2O_5$ (Δmmu –0.1) corresponding to an increase of C_9H_6O compared to **7**. The ^{1}H NMR signals for **9** (Figure S67) were broadened to such an extent that few individual peaks could be resolved and virtually no 2D couplings were observed. However, careful inspection and integration of the ^{1}H-^{13}C HSQC NMR spectrum (Figure S69) revealed signals consistent with one methoxy group, one methylenedioxy group and two cinnamoyl groups. Therefore, the structure of **9** was tentatively assigned to be the N^1-cinnamoyl analogue of **7**.

The structure of **10** was confirmed by comparison of spectroscopic data (Figures S70-S73) and HPLC retention time (Figure S7) with an authentic synthetic sample of 2,5-dibenzylpiperazine. The structures of **11**–**12** were also confirmed following mono- and di-derivatisation of synthetic **10** with cinnamoyl chloride. The spectroscopic data (Figures S88-S94) and HPLC retention times (Figures S8-S9) for the synthetic **11**–**12** were identical to those for the natural samples.

HRESI(+)MS analysis of **13** revealed a protonated molecule $[M + H]^+$ *m/z* 501.2539, indicative of a molecular formula $C_{34}H_{32}N_2O_2$ (Δmmu 0.2) corresponding to a decrease of C_2H_4 compared to **12**. The ^{1}H NMR signals for **13** were also significantly broadened and very challenging to interpret. However, careful inspection and integration of the ^{1}H-^{13}C HSQC NMR spectrum (Figure S97) revealed only one isolated double bond, suggesting the presence of only one cinnamoyl group. Given the decrease of C_2H_4 compared to **12**, we hypothesised that **13** may be the corresponding N^1-benzoyl analogue.. This hypothesis was confirmed by derivatisation of synthetic **11** with benzoyl chloride. The spectroscopic data (Figures S98-S99) and HPLC retention time (Figure S10) for the synthetic **13** were identical to those for the natural samples.

Hancockiamide A (1): White solid. $[\alpha]_D^{22}$ +110 (*c* 0.11, MeOH). UV (MeCN) λ_{max} (log ε) 207 (4.86), 242 (4.20), 275 (4.37) nm. HRESI(+)MS *m/z* 495.2252 $[M+Na]^+$ (calcd. for $C_{29}H_{32}N_2O_4Na^+$ 495.2254).

Hancockiamide B (2): White solid. $[\alpha]_D^{22}$ +92 (*c* 0.05, MeOH). UV (MeCN) λ_{max} (log ε) 206

(4.75), 237sh (4.10), 275 (4.28) nm. HRESI(+)MS *m/z* 537.2359 $[M+Na]^+$ (calcd. for $C_{31}H_{34}N_2O_5Na^+$ 537.2360).

Hancockiamide C (3): White solid. $[\alpha]_D^{22}$ +129 (*c* 0.09, MeOH). UV (MeCN) λ_{max} (log ε) 209 (4.79), 253sh (4.20), 277 (4.34) nm. HRESI(+)MS *m/z* 535.2204 $[M+Na]^+$ (calcd. for $C_{31}H_{32}N_2O_5Na^+$ 535.2203).

Hancockiamide D (4): Off-white solid. $[\alpha]_D^{22}$ +2 (*c* 0.04, MeOH). UV (MeCN) λ_{max} (log ε) 208 (4.76), 238sh (3.89), 273 (3.48) nm. HRESI(+)MS *m/z* 343.2017 $[M+H]^+$ (calcd. for $C_{20}H_{27}N_2O_3^+$ 343.2016).

Hancockiamide E (5): Off-white solid. $[\alpha]_D^{22}$ +83 (*c* 0.04, MeOH). UV (MeCN) λ_{max} (log ε) 208 (4.92), 240 (4.20), 275 (4.29) nm. HRESI(+)MS *m/z* 547.2432 $[M+H]^+$ (calcd. for $C_{31}H_{35}N_2O_7^+$ 547.2439).

Hancockiamide F (6): Off-white solid. $[\alpha]_D^{22}$ +84 (*c* 0.10, MeOH). UV (MeCN) λ_{max} (log ε) 207 (4.76), 271 (4.38), 297sh (4.00) nm. HRESI(+)MS *m/z* 551.2148 $[M+Na]^+$ (calcd. for $C_{31}H_{32}N_2O_6Na^+$ 551.2153).

Hancockiamide G (7): White Solid. $[\alpha]_D^{22}$ +70 (*c* 0.20, MeOH). UV (MeCN) λ_{max} (log ε) 207 (4.48), 250sh (3.86), 274 (3.96) nm. HRESI(+)MS *m/z* 471.2273 $[M+H]^+$ (calcd. for $C_{29}H_{31}N_2O_4^+$ 471.2278).

Hancockiamide H (8): Pale yellow oil. $[\alpha]_D^{22}$ –6 (*c* 0.22, MeOH). UV (MeCN) λ_{max} (log ε) 209 (4.62), 238sh (3.75), 277 (3.18) nm. HRESI(+)MS *m/z* 341.1860 $[M+H]^+$ (calcd. for $C_{20}H_{25}N_2O_3^+$ 341.1860).

Hancockiamide I (9): White Solid. $[\alpha]_D^{22}$ +49 (*c* 0.11, MeOH). UV (MeCN) λ_{max} (log ε) 205sh (4.26), 211sh (4.25), 223sh (3.97), 276 (3.96) nm. HRESI(+)MS *m/z* 601.2695 $[M+H]^+$ (calcd. for $C_{38}H_{37}N_2O_5^+$ 601.2697).

Xenocockiamide A (10): Pale yellow oil. $[\alpha]_D^{22}$ –7 (*c* 0.25, MeOH). UV (MeCN) λ_{max} (log ε) 260 (2.89). HRESI(+)MS *m/z* 267.1856 $[M+H]^+$ (calcd. for $C_{18}H_{23}N_2^+$ 267.1856).

Xenocockiamide B (11): Off-white solid. $[\alpha]_D^{22}$ +123 (*c* 0.16, MeOH). UV (MeCN) λ_{max} (log ε) 217sh (4.31), 276 (4.18) nm. HRESI(+)MS *m/z* 397.2271 $[M+H]^+$ (calcd. for $C_{27}H_{29}N_2O^+$ 397.2274).

Xenocockiamide C (12): Off-white solid. $[\alpha]_D^{22}$ +47 (*c* 0.16, MeOH). UV (MeCN) λ_{max} (log ε) 211sh (4.14), 217 (4.10), 277 (4.04) nm. HRESI(+)MS *m/z* 527.2689 $[M+H]^+$ (calcd. for $C_{36}H_{35}N_2O_2^+$ 527.2693).

Xenocockiamide D (13): Pale yellow oil. $[\alpha]_D^{22}$ +42 (*c* 0.17, MeOH). UV (MeCN) λ_{max} (log ε) 216sh (4.02), 275 (3.75) nm. HRESI(+)MS *m/z* 501.2539 $[M+H]^+$ (calcd. for $C_{34}H_{33}N_2O_2^+$ 501.2537).

4. Synthesis of xenocockiamide analogs

Cinnamoyl chloride (200 mg; 1.20 mmol) was dissolved in MeCN (2 mL) and added dropwise to a stirred solution of xenocockiamide A (**10**; 110 mg; 4.0 mmol) in MeCN (20 mL). After 60 min, the reaction mixture was diluted with sat. $NaHCO_3$ (100 mL) and extracted with AcOEt (100 mL). The organic extract was reduced *in vacuo* and purified by preparative HPLC (Zorbax C_{18}, 50% MeCN/H_2O for 12 min increased to 100% MeCN for 8 min, 20 mL min^{-1}) to yield xenocockiamide B (**11**; t_R 8.67 min; 40.2 mg, 36.5%) and xenocockiamide C (**12**; t_R 19.46 min; 14.4 mg, 13.1%). Benzoyl chloride (254 mg; 1.81 mmol) was added dropwise to a stirred solution of xenocockiamide B (**11**; 16.6 mg; 41.9 μmol) in MeCN (5 mL) containing triethylamine (30 μL), which was chilled to –20 °C prior to the reaction. After 18 h, the reaction mixture was recovered by dilution with H_2O (50 mL) and partitioned against AcOEt (50 mL). The organic extract was reduced *in vacuo* and purified by preparative HPLC (Zorbax C_{18}, isocratic 75% MeCN, 20 mL min^{-1}) to yield xenocockiamide D (**13**; t_R 12.87 min; 17.4 mg, 82.7%).

5. Reconstruction *hkm* pathway and heterologous expression in *A. nidulans*

The entire *hkm* gene cluster were cloned as three separate fragments into three AMA1-based episomal vectors with three different auxotrophy markers (*pyrG*, *riboB* and *pyrO*) under the native *hkm* gene promoters and terminators by yeast transformation-assisted recombination. Briefly, full length of *hkm6-11* fragment was amplified by PCR with three sets of primers from *A. hancockii* gDNA (Table S1). Then *S. cerevisiae* strain BJ5464-NpgA competent cells were transformed by the three overlapping DNA fragments and NotI-digested pYFAC-pyrG to generate plasmid pYFAC-CS1 by yeast homologous recombination. *Hkm1-5* whole region and *hkm12* were amplified with the designed primers (Table S1) and ligated into the NotI site of pYFAC-ribo and pYFAC-pyrO, respectively, to get pYFAC-CS2 and pYFAC-CS3 plasmids (see the below diagram). For the partial gene cluster expression plasmids were constructed using the same method only with the difference in the gene fragment that amplified and cloned into the pYFAC vectors (see Table S3). Yeast miniprep of corrected transformants was performed with Zymoprep™ Yeast Plasmid Miniprep I Kit. The resulting heterologous expression plasmids were introduced into *A. nidulans* LO7890 by polyethylene glycol protoplast transformation as described previously.[3]

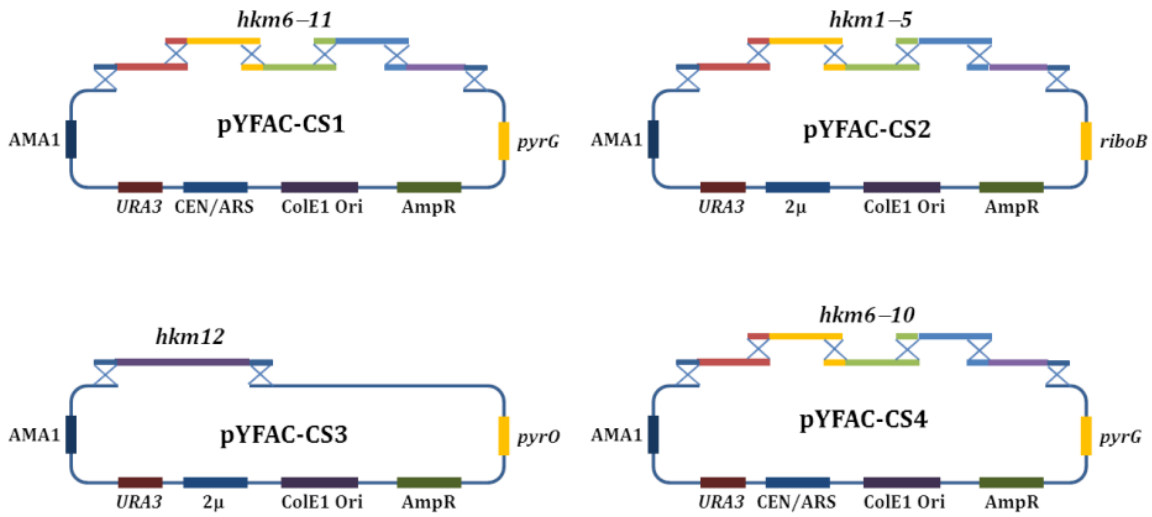

6. Analytical methods

Analytical HPLC was performed on a gradient Agilent 1260 Infinity quaternary HPLC system. Preparative HPLC was performed on a gradient Shimadzu HPLC system comprising two LC-8A preparative liquid pumps with static mixer, SPD-M10AVP diode array detector and SCL-10AVP system controller with Rheodyne 7725i injection port. The columns used in the purification of the metabolites were selected from either a Hypersil C_{18} column (50 × 100 mm, 5 μm; Grace Discovery), or an Alltima C_{18} column (22 × 250 mm, 5 μm, Grace Discovery), eluted as isocratic or incremental stepped gradients with MeCN/water mixtures with or without 0.01% TFA modifier, as described for each separation. Preparative silica chromatography was undertaken using a Zorbax Si column (21.2 × 250 mm, 5 μm; Agilent) or Alltima Si column (10 × 250 mm, 10 μm; Grace) eluting with EtOH/hexane or AcOEt/hexane gradients. LCMS was performed on an Agilent 1260 Infinity series HPLC equipped with an Agilent 6130 Infinity series single quadrupole mass detector in both positive and negative ion modes.

For the *A. nidulans hkm* expressing strains, extracts from both mycelium and media were analyzed. Mycelium was collected by filtration and extracted with acetone. Media was extracted with either ethyl acetate/methanol/acetic acid (89.5:10:0.5). The crude extracts were dried down in vacuo and re-dissolved in methanol for LC-MS analysis. LC-DAD-MS metabolite profiles were performed on an Agilent 1260 liquid chromatography (LC) system coupled to a diode array detector (DAD) andm an Agilent 6130 Quadrupole mass spectrometer (MS) with an ESI source. Chromatographic separation was performed at 40 °C using a Kinetex C18 column (2.6 μm, 2.1 mm

× 100 mm; Phenomenex). Chromatographic separation was achieved with a linear gradient of 5-95% MeCN-H_2O (0.1% (v/v) formic acid) in 10 min followed by 95% MeCN for 3 min then 5% MeCN-H_2O for 3 min, with a flow rate of 0.75 mL/min. The MS data were collected in the *m/z* range 100–1000.

7. Expression and purification of Hkm11 from yeast

As the gene *hkm11* is intro-free, the open reading frame of *hkm11* was directly amplified by PCR with primers of ADH2p-g11-F/ADH2t-g11(HT)-R from gDNA of *A. hancockii*. The PCR product was then inserted into the NdeI/PmlI-digestion site of the backbone vector xw55 by yeast homologous recombination to construct the expression plasmid. Then the plasmid was transformed into *S. cerevisiae* BJ5464-NpgA and dropout without uracil media was used to select the transformants. After growing for 2 days in 3 ml of dropout without uracil liquid media (30 °C, 240 rpm), yeast harboring the expression plasmid was inoculated into a 2 L flask containing 1 L YPD media (20 g peptone, 10 g yeast extract, 50 ml of 20% dextrose). The culture was placed in a shaker set 30 °C, 240 rpm. After 72 h, the cells were harvested by centrifugation (3750 rpm, 20 min, 4 °C) and resuspended in ~30 mL lysis buffer (20 mM Tris-HCl, pH 7.9, 0.5 M NaCl, 10 mM imidazole), and lysed by sonication on ice. Cellular debris was removed by centrifugation (17000 rpm, 30 min, at 4 °C), and Ni-resin was then added to the supernatant (2 mL/liter of culture). The suspension was swirled at 4 °C for over-night and loaded into a gravity column. The protein-bound resin was washed with 10 mM imidazole in wash buffer (50 mM NaH_2PO_4, 300 mM NaCl, 2 mM DTT), check the eluent using qualitative Bradfold assay for every quarter of washing, until Bradfold reagent didn't turn blue. Followed by 20 mM imidazole in wash buffer, when Bradfold reagent didn't turn blue, eluted protein with 250 mM imidazole in wash buffer until Bradfold assay turned negative. Purified Hkm11 was concentrated and exchanged into wash buffer + 10% glycerol with the Amicon filters, aliquoted, and flash frozen with liquid nitrogen.

8. In vitro enzymatic assay of Hkm11

To test the *in vitro* activity of Hkm11, 2 mM of cinnamic acid, 2 mM of hancockiamide D, 6 mM ATP, 4 mM $MgSO_4$ and 5 μM of the purified protein Hkm11 were combined in 50 mM Tris-HCl buffer (pH 7.5) to a total volume of 150 μL. After 12 h incubation at 37 °C, the reaction mixture were quenched and extracted with 150 μL acetonitrile. The organic layer was directly used

for LC-MS analysis.

9. Yeast feeding assay

The plasmid xw55-CS1 was transformed into *S. cerevisiae* BJ5464-NpgA. Yeast strain expressing *hkm11* was initially grown in dropout minus uracil liquid media for 2 days, and then inoculated 300 μL cultures into 100 mL fresh YPD media and shaking cultured for 24 h at 30 °C, 240 rpm. Then the yeast expressing Hkm11 culture was concentrated to 10 mL by centrifugation (800 rpm, 8 min). To facilitate the protein expression, 70 μL 100% ethanol was added into the culture. After that, the yeast culture was fed with different cinnamic acid analogues and shaking cultured for another 48 h. The culture was then extracted with the same volume extract solvents (ethyl acetate/methanol/acetic acid at 89.5:10:0.5 ratio). The organic extracts were dried down *in vacuo* and re-dissolved in methanol for LC-MS analysis.

10. Bioassays

Purified metabolites were dissolved in DMSO to provide stock solutions (10,000 μg/mL). An aliquot of each stock solution was transferred to the first lane of Rows B to G in a 96-well microtiter plate and two-fold serially diluted with DMSO across the 12 lanes of the plate to provide a 2,048-fold concentration gradient. Bioassay medium was added to an aliquot of each test solution to provide a 100-fold dilution into the final bioassay, thus yielding a test range of 100 to 0.05 μg/mL in 1% DMSO. Row A contained no test compound (as a reference for no inhibition) and Row H was uninoculated (as a reference for complete inhibition).

CyTOX: NS-1 (ATCC TIB-18) mouse myeloma cells and Neonatal Foreskin Fibroblast (NFF) cells were inoculated in 96-well microtiter plates (190 μL) at 50,000 cells/mL in DMEM (Dulbecco's Modified Eagle Medium + 10% fetal bovine serum (FBS) + 1% penicillin/streptomycin (10,000 U/mL / 10,000 μg/mL, Life Technologies Cat. No. 15140122) and incubated in 37 °C (5% CO_2) incubator. At 48 h, resazurin (250 μg/mL; 10 μL) was added to each well and the plates were incubated for a further 48 h. Finally, the absorbance of each well at 605 nm was measured using a Spectromax plate reader (Molecular Devices).

ProTOX: *Bacillus subtilis* (ATCC 6633) and *Staphylococcus aureus* (ATCC 25923) were used as indicative species for Gram positive and negative antibacterial activity, respectively. A bacterial suspension (50 mL in 250 mL flask) was prepared in nutrient media by cultivation for 24 h at 250

rpm, 28 °C. The suspension was diluted to an absorbance of 0.01 absorbance units per mL, and 10 μL aliquots were added to the wells of a 96-well microtiter plate, which contained the test compounds dispersed in nutrient broth (Amyl) with resazurin (12.5 μg/mL). The plates were incubated at 28 °C for 48 h during which time the positive control wells change color from a blue to light pink color. MIC end points were determined visually. The absorbance was measured using Spectromax plate reader (Molecular Devices) at 605 nm and the IC_{50} values determined graphically.

EuTOX: *Candida albicans* (ATCC 10231) and *Saccharomyces cerevisiae* (ATCC 9763) were used as indicative species for antifungal activity. A yeast suspension (50 mL in 250 mL flask) was prepared in 1% malt extract broth by cultivation for 24 h at 250 rpm, 24 °C. The suspension was diluted to an absorbance of 0.005 and 0.03 absorbance units per mL for *C. albicans* and S. *cerevisiae,* respectively. Aliquots (20 μL and 30 μL) *of C. albicans* and S. *cerevisiae,* respectively were applied to the wells of a 96-well microtiter plate, which contained the test compounds dispersed in malt extract agar containing bromocresol green (50 μg/mL). The plates were incubated at 24 °C for 48 h during which time the positive control wells change color from a blue to yellow. MIC end points were determined visually. The absorbance was measured using Spectromax plate reader (Molecular Devices) at 620 nm and the IC_{50} determined graphically.

Phytox is a generic bioassay platform for herbicidal discovery. In the present study, *Eragrostis tef* (teff) seed was used as indicative monocotyledon species for herbicidal discovery. 10 to 15 teff seeds were dispensed using LabTIE seed dispenser into the wells of a 96-well microtiter plate containing the test compounds dispersed in 200 μL of agar (1% w/v) per well. The plates were placed in a tray wrapped with semi-opaque bag, exposed to 1600 lux (inside the bag) using Power-GLO (20W) and Sun-GLO (20W) tubes, and incubated for 72 h at 24 °C. *Arabidopsis thaliana* (arabi) seed was used as indicative dicotyledon species for herbicidal discovery. Arabi was sterilized in 70% v/v ethanol containing 0.05% (v/v) Triton-X100 for 5 min. Seeds were allowed to settle, and replaced with 100% (v/v) ethanol briefly to mix, decanted ethanol and allowed ethanol residue to evaporate. Sterilized seeds (15-20) were dispensed using LabTIE seed dispenser into the wells of a 96-well microtiter plate containing the test compounds dispersed in 200uL 0.5 x Murashige and Skoog (MS) medium (Sigma M5524) (pH 5.9 + 0.7% w/v agar) per well. Plates were placed in 4 °C fridge for 48 h to stratify the seeds, then incubated at 24 °C for 72 h in a tray

wrapped with semi-opaque bag, exposed to 1600 lux (inside the bag) using Power-GLO (20W) and Sun-GLO (20W) tubes.

Supplementary Tables

Table S1. Primers used in this study.

Name	Sequence	Description
pKW_hkm_g6-g11-fg1-F	TAGTAACCTCGCGGGTGTTCTTGACGATGGCATCCTGCCATCAGGCTACTATTGGATACT	For the construction of pYFAC-CS1 plasmid
hkm_g6-g11-fg1-R	GGAGCCGTGGACTTCGTT	
hkm_g6-g11-fg2-F	CTTAGTAACCTCGCGGGTGTTCTTGACGATGGCATCCTGCCTATCACCAGCCCGCATCAG	
hkm_g6-g11-fg2-R	CTGAGTCACCCCGTTGAACA	
hkm_g6-g11-fg3-f	CAGGTTTTGTTGAGAGGCGC	
pKW_hym-g6-g11-fg3-R	GAGCTACCGCACAACCGAA	
pKW-hkmg1_g5-F	CTTAGTAACCTCGCGGGTGTTCTTGACGATGGCATCCTGCCGGCTCGGTCTAATTGGGAA	For the construction of pYFAC-CS2 plasmid
hkm_g1-g5-frag1-R	TGTGGTTCGCGAGCTTC	
hkm_g1-g5-frag2-F	ACTGTGATGGCAAAGGAAAT	
hkm_g1-g5-frag2-R	GGGTGAGATAGCAAGGGACA	
hkm_g1-g5-frag3-F	CCCGAACCATCCAATGTTAATC	
ribo-hkm_g1_g5-R	ACTTCTGCTAAAGGGTATCATCGAAAGGGAGTCATCCAGCCAGCCAGAGTTTGCCTGACT	
pKW-g12-F	CTTAGTAACCTCGCGGGTGTTCTTGACGATGGCATCCTGCGGGTTTCCGTGAGTAGAGAA	For the construction of pYFAC-CS3 plasmid
pyrO-g12-R	AGGAGTGATGAGACCCAACAACCATGATACCAGGGGGCGAAAACCGAACCTCTCCATTCG	

pyrG-g10-R	ACTTCAACACAGTGGAGGACATACCCGTAATTTTCTGGGCCGATCTCACCCACCCTTACA	For the construction of pYFAC-CS4 plasmid
pKW-hkm_g4_g5-F	TAGTAACCTCGCGGGTGTTCTTGACGATGGCATCCTGCCCGGAACAGAAAAGATGTGAAG	For the construction of pYFAC-CS5 plasmid with the primer ribo-hkm_g1_g5-R
PalcA-hkmg5-F	GTTAATTAGAACTCTTCCAATCCTATCACCTCGCCTTAATATGGAGACACCAACCCCTCC	For the construction of pYFAC-CS6 plasmid
pyrG-hkmg5-R	AACACAGTGGAGGACATACCCGTAATTTTCTGGGCTTAATCTAGGCCTTCCGGAATCCGA	
pKW-hkmg3_g5-F	CTTAGTAACCTCGCGGGTGTTCTTGACGATGGCATCCTGTGCTGACAAGTTACTGTTCC	For the construction of pYFAC-CS7 plasmid with the primers hkm_g1-g5-frag2-R, hkm_g1-g5-frag3-F and ribo-hkm_g1_g5-R
ADH2p-g11-F	ACAATCAACTATCAACTATTAACTATATCGTAATACCATATGACAGTGCCTGCTACTACG	For the construction of xw55-CS1 plasmid
ADH2t-g11(HT)-R	AATTTGTCATTTAAATTAGTGATGGTGATGGTGATGCACCCCACAAGTCGAAATCGAACA	

Table S2. Putative functions of *hkm* genes.

Gene	NCBI locus	Description/conserved domain	Putative function
hkm1	BBP40_009487	Phytanoyl-CoA dioxygenase	Unknown*
hkm2	BBP40_009486	Cellobiose dehydrogenase-like cytochrome	Unknown*
hkm3	BBP40_009485	Acetyltransferase	*N*-acetyltransferase
hkm4	BBP40_009484	2OG-Fe(II) dioxygenase	Putative hydroxylation
hkm5	BBP40_009483	P450 monooxygenase	Methylenedioxy formation
hkm6	BBP40_009482	Tyrosinase	Putative hydroxylation
hkm7	BBP40_009481	FAD-dependent phenol hydroxylase	Putative hydroxylation
hkm8	BBP40_009480	*O*-methyltransferase	*O*-methyltransferase
hkm9	BBP40_009479	NmrA-like, reductase/epimerase	Pyrazine reductase
hkm10	BBP40_009478	NRPS (A-T-R)	NRPS (A-T-R)
hkm11	BBP40_009477	NRPS (A-T-C)	NRPS (A-T-C)
hkm12	BBP40_009476	Phenylalanine ammonia lyase	*trans*-cinnamic acid synthetase

*Note: Both *hkm1* and *hkm2* do not appear to be required for biosynthesis of hancockiamides as *hkm4–12* (without acetyltransferase gene *hkm3*) was able to produce hancockiamide G (**7**), desacetylated derivative of the most advanced metabolite in the pathway hancockiamide C (**3**) (see main manuscript). Upon closer inspection and comparison with its closet BLASTP homolog *Penicillium arizonense* PENARI_c033G11888 (XP_022483527.1), we noticed that the predicted coding sequence of *hkm1* is truncated due to a nonsense mutation at the N-terminal (24th codon from the translational start site ATG correspond to PENARI_c033G11888) and a frameshift mutation in the middle region (see Figure S130). The translated protein sequence including the nonsense mutation is >80% identical to PENARI_c033G11888. Therefore, *hkm1* has likely lost its function in *A. hancockii* but the homologs in other fungi, such as in *P. arizonense* and other species listed in cblaster result (Figure S5), are likely to be functional and could contribute to additional oxidation step(s) on the benzylpiperazine scaffold.

Table S3. Plasmids used in this study.

Name	**Backbone**	**Description**
pYFAC-CS1	pKW-pyrG	*Aspergillus nidulans* expression vector containing *hkm6, hkm7, hkm8, hkm9, hkm10* and *hkm11* under native their promoters and terminators.
pYFAC-CS2	pKW-ribo	*Aspergillus nidulans* expression vector containing *hkm1, hkm2, hkm3, hkm4* and *hkm5* under their native promoters.
pYFAC-CS3	pKW-pyrO	*Aspergillus nidulans* expression vector containing *hkm12* under their native promoter and terminators.
pYFAC-CS4	pKW-pyrG	*Aspergillus nidulans* expression vector containing *hkm6, hkm7, hkm8, hkm9* and *hkm10* under their native promoters and terminators.
pYFAC-CS5	pKW-ribO	*Aspergillus nidulans* expression vector containing *hkm4* and *hkm5* under their native promoters.
pYFAC-CS6	pKW-ribO	*Aspergillus nidulans* expression vector containing *hkm5* under the alchol-inducible *PalcA* promoter.
pYFAC-CS7	pKW-ribO	*Aspergillus nidulans* expression vector containing hkm3, hkm4 and *hkm5* under their native promoters and terminators.
xw55-CS1	xw55	*S. cerevisiae* expression vector containing the gene *hkm11* under the promter *ADH2*.

Table S4. Strains used in this study.

Strain name	Organism	Description
A. nidulans_hkm1-12	*A.nidulans* LO7890	*A. nidulans* expressing plasmids pYFAC-CS1, pYFAC-CS2 and pYFAC-CS3.
A. nidulans_hkm1-11	*A. nidulans* LO7890	*A. nidulans* expressing plasmids pYFAC-CS1and pYFAC-CS2.
A. nidulans_hkm1-10	*A. nidulans* LO7890	*A. nidulans* expressing plasmids pYFAC-CS2 and pYFAC-CS4.
A. nidulans_hkm4-12	*A. nidulans* LO7890	*A. nidulans* expressing plasmids pYFAC-CS1, pYFAC-CS3 and pYFAC-CS5.
A. nidulans_hkm3-12	*A. nidulans* LO7890	*A. nidulans* expressing plasmids pYFAC-CS1, pYFAC-CS3 and pYFAC-CS7.
A. nidulans_hkm5	*A. nidulans* LO7890	*A. nidulans* expressing plasmid pYFAC-CS6.
*S. cerevisiae*_Hkm11	*S. cerevisiae* BJ5464-NpgA	*S. cerevisiae* expressing plasmid xw55-CS1

Table S5. Orthologous gene clusters identified in other fungal species.

A. hancockii *hkm* gene cluster	Putative function	*P. brasilianum* WZXY-M122-9 *brs* gene cluster (% id*)	*Uncinocarpus reesii* 1704 (% id*)	*Penicillium brasilianum* (% id*)	*Neosartorya fischeri* NRRL 181 (% id*)	*Trichophyton interdigitale* H6 (% id*)
hkm1	Phytanoyl-CoA dioxygenase	*PEBR_04673* (32.3%)[a]	*UREG_04217* (41%)	*PMG11_03964* (32%)	*NFIA_045530* (43%)	
hkm2	cellobiose dehydrogenase cytochrome	*brsF* (47.3%)	*UREG_04225* (54%)	*PMG11_03959* (47%)	*NFIA_045610* (49%)	
hkm3	*N*-acetyltransferase	*brsE* (48.6%) *brsI* (37.4%)	*UREG_04224* (51%)	*PMG11_03958* (48%) *PMG11_03962* (37%)		
hkm4	2OG-Fe(II) dioxygenase	*PEBR_04673* (52.1%)[a]	*UREG_04217* (37%)	*PMG11_03964* (52%)	*NFIA_045530* (37%)	
hkm5	Cytochrome P450	*brsH* (49.7%)		*PMG11_03961* (60%)	*NFIA_045580* (57%)	*H101_00666* (2%)
hkm6	Tyrosinase	*brsD* (61.8%)	*UREG_04223* (71%)	*PMG11_03957* (54%)	*NFIA_045560* (43%)	
hkm7	FAD-dependent hydroxylase	*brsC*** (57.8%)	*UREG_04222* (55%)	*PMG11_03956* (54%)	*NFIA_045600* (48%)	
hkm8	*O*-methyltransferase	*brsG* (55.4%)	*UREG_04216* (60%)	*PMG11_03960* (70%)	*NFIA_045570* (63%)	
hkm9	NmrA-like reductase	*brsB* (54.0%)	*UREG_04221* (68%)	*PMG11_03955* (65%)	*NFIA_045620* (66%)	*H101_00667* (66%)
hkm10	NRPS (A-T-R)	*brsA* (61.8%)	*UREG_04220* (55%)	*PMG11_03954* (61%)	*NFIA_045590* (60%)	*H101_00668* (59%)
hkm11	NRPS (A-T-C)		*UREG_04218* (44%)			*H101_00665* (30%)
hkm12	*trans*-Cinnamic acid synthetase		*UREG_04219* (60%)			

* indicates the encoding protein similarity. ** based on nucleotide MK887347.1 on NCBI assumed to be *brsC* (not annotated by the sequence author). [a] based on *P. brasilianum* LaBioMMi136 which should share the identical/similar nucleotide sequence with *P. brasilianum* WZXY-M122-9 which whole genome sequence is not available.

Table S6. Cinnamic acid homologues used for yeast feeding experiments together with hancockiamide D.

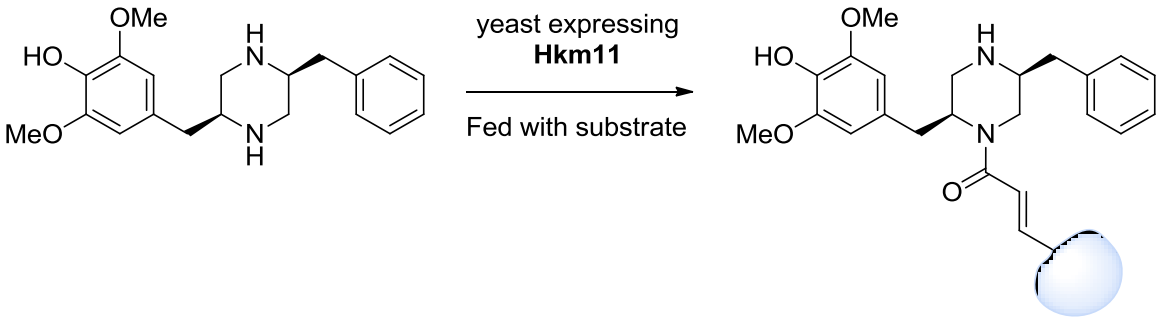

Substrate	Target MS data	Detectable	Substrate	Target MS data	Detectable
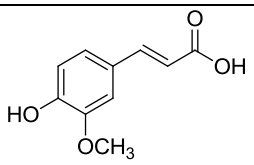 ferulic acid	$[M+H]^+$ 519	**N**	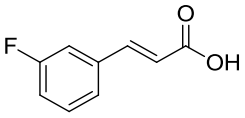 3-fluorocinnamic aicd	$[M+H]^+$ 491	**N**
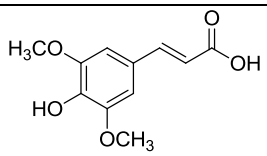 sinapic acid	$[M+H]^+$ 549	**N**	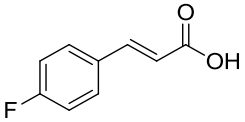 4-fluorocinnamic aicd	$[M+H]^+$ 491	**N**
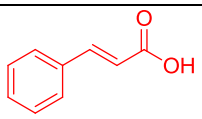 cinnamic aicd	$[M+H]^+$ 473	**Y**	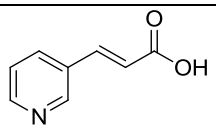 3-(2-pyridyl)acrylic aicd	$[M+H]^+$ 474	**N**
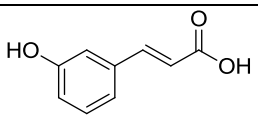 coumaric aicd	$[M+H]^+$ 489	**N**	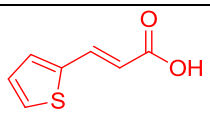 3-(2-thienyl)acrylic aicd	$[M+H]^+$ 479	**Y**
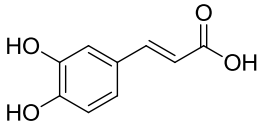 caffeic aicd	$[M+H]^+$ 505	**N**	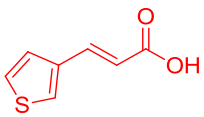 3-(3-thienyl)acrylic aicd	$[M+H]^+$ 479	**Y**
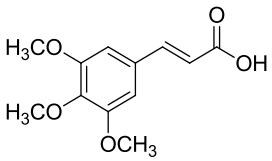 3,4,5-trimethoxy-cinnamic aicd	$[M+H]^+$ 563	**N**	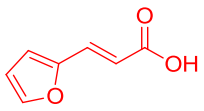 3-(2-furyl)acrylic aicd	$[M+H]^+$ 463	**Y**
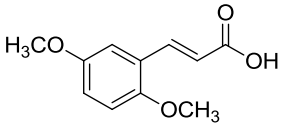 2,5-dimethoxy-cinnamic aicd	$[M+H]^+$ 533	**N**	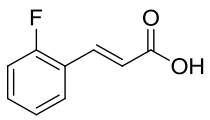 2-fluorocinnamic aicd	$[M+H]^+$ 491	**N**

Table S7. ^{1}H (500 MHz) and ^{13}C (125 MHz) NMR data for hancockiamide A (**1**) in DMSO-d_6

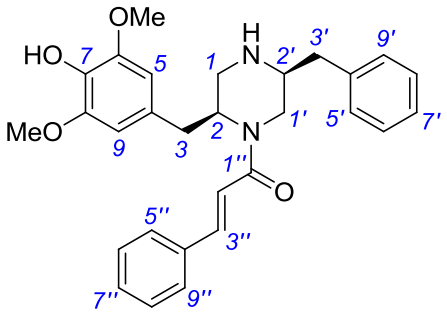

Pos.	δ_C[a], type	δ_H[a] (*J* in Hz)	HMBC	COSY	ROESY
1a	49.2, CH_2	2.93, d (12.4)	3, 2′	1b	1b, 2
1b		2.76[b]	3, 2′	1a, 2a	1a, 2
2	54.1, CH	4.31, m		1b, 3a/b	1a/b, 5/9, 2″
3a	35.6, CH_2	3.05, dd (13.5, 9.3)	2, 4, 5/9	2, 3b	3b, 5/9
3b		2.75[b]	2, 4, 5/9	2, 3a	3a
4	128.7, C				
5/9	106.7, CH	6.43, s	3, 4, 6/8, 7		2, 3a/b, 6/8-OMe
6/8	147.7, C				
7	133.9, C				
1-NH		2.30, br s			
6/8-OMe	55.8, CH_3	3.61, s	6/8		5/9,
7-OH		7.97, br s	6/8, 7		
1′a	42.1, CH_2	4.22, dd (13.1, 2.3)	2, 2′, 1″	1′b	1′b
1′b		2.61, dd (13.1, 10.4)	2′, 3′	1′a	1′a
2′	56.8, CH	2.70[b]	4′		
3′	40.1, CH_2	2.73[b]	2′, 4′, 5′/9′		
4′	138.7, C				
5′/9′	129.2, CH	7.27, dd (7.4, 1.5)	5′/9′, 7′		
6′/8′	128.6, CH	7.31[c]	4′		7′
7′	126.1, CH	7.21, tt (7.2, 1.5)	5′/9′, 6′/8′		6′/8′
1″	165.0, C				
2″	119.2, CH	6.72, d (15.4)	1″, 4″	3″	2, 5″/9″
3″	139.6, CH	7.08, d (15.4)	1″, 5″/9″	2″	5″/9″
4″	135.3, C				
5″/9″	127.5, CH	7.47, dd (7.7, 1.7)	3″, 7″	6″/8″	6″/8″ 2″, 3″
6″/8″	128.3, CH	7.31[c]	4″, 7″	5″/9″	5″/9″
7″	128.4, CH	7.31[c]	5″/9″ , 6″/8″		

[a] Major conformer; [b-c] Overlapping resonances

Table S8. ^{1}H (600 MHz) and ^{13}C (150 MHz) NMR data for hancockiamide A (**1**) TFA salt in DMSO-d_6

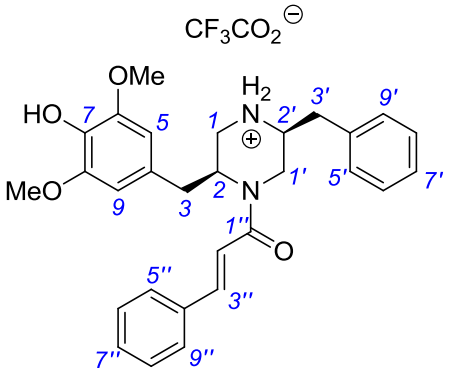

Pos.	δ_C[a], type	δ_H[a] (*J* in Hz)	HMBC	COSY	NOESY
1a	45.9, CH_2	3.39, d (12.6)	3, 2′	1b, 2, 1-NHa/b	
1b		3.31, dd (12.6, 12.4)	3, 2′	1a, 2, 1-NHa/b	
2	51.4, CH	4.77, m	1, 3, 4, 1′, 1″	1a/b, 3a/b	5/9, 2″
3a	35.2, CH_2	3.09, dd (13.8, 10.7)	1, 2, 4, 5/9	2, 3b	5/9
3b		2.83, dd (13.8, 4.8)	1, 2, 4, 5/9	2, 3a	5/9
4	127.0, C				
5/9	106.8, CH	6.46, s	3, 4, 6/8, 7		2, 3a/b, 6/8-OMe
6/8	147.8, C				
7	134.4, C				
1-NHa		9.41, br s		1a/b, 1-NHb	
1-NHb		9.11, br m		1a/b, 1-NHa, 2′	
6/8-OMe	55.8, CH_3	3.62, s	6		5/9, 7-OH
7-OH		8.08, br s			6/8-OMe
1′a	37.5, CH_2	4.45, dd (14.5, 3.1)	2, 1″	1′b, 2′	
1′b		3.04, dd (14.5, 11.9)	1″	1′a, 2′	
2′	55.7, CH	3.43, br s		1′a/b, 1-NHb, 3′a/b	
3′a	36.2, CH_2	3.07, d (13.8)	1′, 2′, 4′, 5′/9′	2′, 3′b	
3′b		2.98, dd (13.8, 9.3)	1′, 2′, 4′, 5′/9′	2′, 3′a	
4′	135.5, C				
5′/9′	129.3, CH	7.33[b]			
6′/8′	128.8, CH	7.39, t (7.5)	4′, 8′	7′	
7′	127.2, CH	7.31, t (7.5)	5′/9′	6′/8′	
1″	165.0, C				
2″	117.9, CH	6.67, d (15.4)	1″, 3″, 4″	3″	2, 5″/9″
3″	140.9, CH	7.09, d (15.4)	1″, 2″, 4″, 5″/9″	2″	5″/9″
4″	135.0, C				
5″/9″	127.7, CH	7.46, dd (7.5, 1.3)	3″, 7″	6″/8″	2″, 3″
6″/8″	128.6, CH	7.33[b]		5″/9″	
7″	129.5, CH	7.33[b]			

[a] Major conformer; [b] Overlapping resonances

Table S9. ^{1}H (600 MHz) and ^{13}C (150 MHz) NMR data for hancockiamide B (**2**) in DMSO-d_6

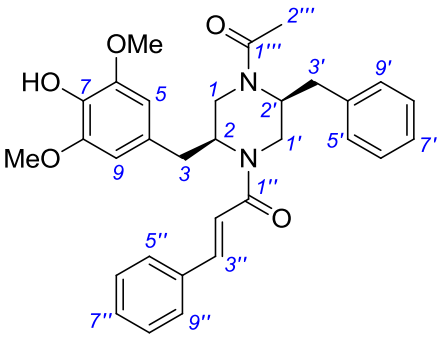

Pos.	δ_C[a], type	δ_H[a] (*J* in Hz)	HMBC	COSY	NOESY
1a	44.1, CH_2	3.77, m		1b, 2	
1b		3.10, m		1a, 2	
2	55.5, CH	4.49, br m		1a/b, 3b	2′
3a	37.9, CH_2	2.88[b]			
3b		2.69[c]		2	
4	129.5, C				
5/9	106.8, CH	6.46[d]	3, 5/9, 6/8, 7		
6/8	147.9, C				
7	134.3, C				
6/8-OMe	55.9, CH_3	3.72, s	6/8		
7-OH		8.12, s	6/8, 7		
1′a	38.4, CH_2	4.16, br		1′b, 2′	
1′b		2.86[b]		1′a, 2′	
2′	52.6, CH	4.26, br		1′a/b, 3′a/b	2
3′a	36.3, CH_2	2.83[b]		2′	
3′b		2.72[c]		2′	
4′	137.5, C				
5′/9′	128.7, CH	7.27[e]	7′		
6′/8′	128.4, CH	7.39	4′, 6′/8′		
7′	126.6, CH	7.24[e]	5′/9′		
1″	165.4, C				
2″	118.6, CH	6.44[d]	1″	3″	
3″	140.8, CH	7.25[e]	1″, 5″/9″	2″	
4″	137.3, C				
5″/9″	127.7, CH	7.39[e]	7″		
6″/8″	128.4, CH	7.33[e]	4″, 6″/8″		
7″	129.1, CH	7.22[e]			
1‴	169.0, C				
2‴	21.8, CH_3	2.03, s	1‴		

[a] Major conformer; [b-e] Overlapping resonances

Table S10. ^{1}H (600 MHz) and ^{13}C (150 MHz) NMR data for hancockiamide C (**3**) in DMSO-d_6

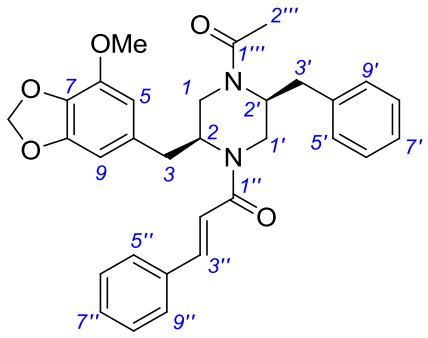

Pos.	δ_C[a], type	δ_H[a] (*J* in Hz)	HMBC	COSY	NOESY
1a	44.2, CH_2	3.81, m	2′, 1‴	1b, 2	
1b		3.09, dd (15.4, 11.3)	2′, 1‴	1a, 2	3b
2	55.4, CH	4.53, br s		1a/b	2′
3a	37.6, CH_2	2.88, m		3b	3b
3b		2.72, m		3a	1b, 3a
4	131.9, C				
5	109.2, CH	6.42, s	3, 7, 9		
6	143.1, C				
7	133.4, C				
8	148.3, C				
9	103.3, CH	6.47, s	3, 5, 7, 8		
6-OMe	56.2, CH_3	3.72, s	6		
7/8-OCH_2O	100.9, CH_2	5.79, br s	7, 8	OCH_2Ob	
		5.58, br s	7, 8	OCH_2Oa	
1′a	38.2, CH_2	4.18, m	2, 1″	1′b ,2′	
1′b		2.89, m	2′, 3′, 1″	1′a	
2′	52.6, CH	4.25, br m		3′a/b	2
3′a	36.7, CH_2	2.84, br m	1′, 2′, 4′, 5′, 9′	2′, 3′b	3′b
3′b		2.73, br m	1′, 2′, 4′, 5′, 9′	2′, 3′a	3′a
4′	137.4, C				
5′/9′	129.4, CH	7.23, br m	3′, 7′	6′/8′	6′/8′
6′/8′	128.5, CH	7.32, br m	4′	5′/9′, 7′	5′/9′, 7′
7′	126.6, CH	7.25, br m	5′/9′	6′/8′	6′/8′
1″	165.1, C				
2″	118.1, CH	6.41, d (15.7)	1″, 3″, 4″	3″	3″
3″	140.3, CH	7.18, d (15.7)	1″, 2″, 4″, 5″, 9″	2″	2″
4″	135.0, C				
5″/9″	127.7, CH	7.40, br m	7″	6″/8″	6″/8″
6″/8″	129.2, CH	7.33, br m	4″, 5″/9″	5″/9″, 7″	5″/9″
7″	129.5, CH	7.27, br m	6″/8″	6″/8″	
1‴	169.1, C				
2‴	21.8, CH_3	2.05, s	1‴		

[a] Major conformer, [b-e] Overlapping resonances

Table S11. ^{1}H (600 MHz) and ^{13}C (150 MHz) NMR data for hancockiamide D (**4**) in DMSO-d_6

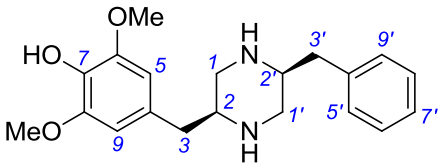

Pos.	δ_C[a], type	δ_H[a] (*J* in Hz)	HMBC	COSY	ROESY
1a	47.1, CH_2	2.61[b]	2, 3		5/9
1b		2.57[c]	3		
2	55.6, CH	2.72, ddd (12.9, 6.8, 3.4)			5/9
3	38.3, CH_2	2.62[b]	1, 2, 3, 5/9	5/9	5/9
4	129.8, C				
5/9	106.4, CH	6.43, s	3, 4, 5/9, 6/8, 7	3, 6/8-OMe	1a, 2, 3, 6/8-OMe
6/8	147.8, C				
7	133.6, C				
1-NH		2.13, br s			
6/8-OMe	55.9, CH_3	3.72, s	6/8	5/9	5, 9
7-OH		8.04, br s			
1′a	47.3, CH_2	2.61[b]	2′, 3′		5′/9′
1′b		2.57[c]	2′		5′/9′
2′	55.2, CH	2.75[d]	1′, 3′, 4′		5′/9′
3′	38.0, CH_2	2.76[d]	1′, 2′, 4′, 5′/9′	5′/9′	5′/9′
4′	140.1, C				
5′/9′	129.1, CH	7.19, dd (7.4, 1.3)	3′, 5′/9′,7′	3′,6′	1′a/b, 2′, 3′
6′/8′	128.4, CH	7.26, t (7.4)	4′, 5′/9′, 6′/8′	5′/9′, 7′	
7′	125.7, CH	7.16, tt (7.4, 1.3)	5′/9′	6′/8′	
1′-NH		2.13, br s			

[a] Major conformer, [b-d] Overlapping resonances

Table S12. ^{1}H (600 MHz) and ^{13}C (150 MHz) NMR data for hancockiamide D (**4**) di-TFA salt in DMSO-d_6

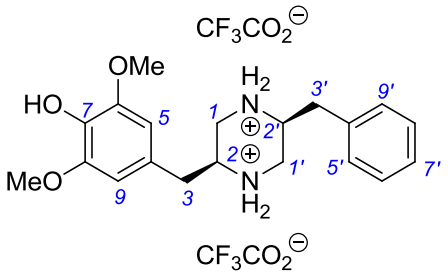

Pos.	δ_C[a], type	δ_H[a] (*J* in Hz)	HMBC	COSY	ROESY
1	41.2, CH_2	3.12[c], br s			5/9
2	52.11[b], CH	3.64[d], br s			5/9
3a	34.1, CH_2	3.07[e], br s	5/9		5/9
3b		2.93[f], br s	5/9		5/9
4	125.4, C				
5/9	106.7, CH	6.55, s	3, 4, 6/8, 7		1, 2, 3a/b,6/8-OMe
6/8	148.1, C			5,9	
7	134.7, C				
1-NH_2		9.26, br s			
6/8-OMe	55.9, CH_3	3.75, s	6/8	6,8	5, 9
7-OH		8.30, br s			
1′	41.2, CH_2	3.12[c], br s			5′/9′
2′	52.25[b], CH	3.64[d], br s			5′/9′
3′a	34.1, CH_2	3.07[e], br s	5′/9′		5′/9′
3′b		2.93[f], br s	5′/9′		
4′	135.8, C				
5′/9′	129.3, CH	7.31, d (7.3)	3′, 7′	6′	1′, 2′, 3′a
6′/8′	128.8, CH	7.37, t (7.3)	4′	5′/9′, 7′	
7′	127.1, CH	7.27, t (7.3)	5′/9′	6′/8′	
1′-NH_2		9.26, br s			

[a] Major conformer, [b] Assignments interchangeable, [c-f] Overlapping resonances

Table S13. ^{1}H (600 MHz) and ^{13}C (150 MHz) NMR data for hancockiamide E (**5**) TFA salt in DMSO-d_6

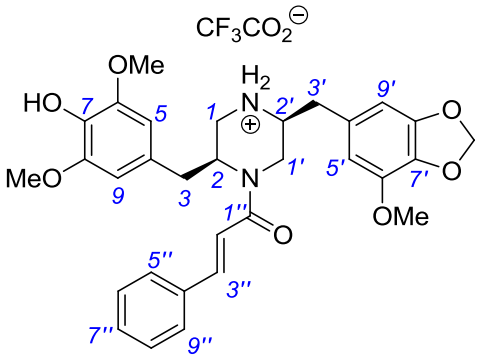

Pos.	δ_C[a], type	δ_H[a] (*J* in Hz)	HMBC	COSY	ROESY
1a	46.1, CH_2	3.36[b]	2′	1b	
1b		3.26[b]		1a, 2,	
2	51.4, CH	4.77, m		1b, 3a/b	5/9, 2″
3a	35.2, CH_2	3.07, dd (13.6, 11.0)	2, 4, 5/9	2, 3b	5/9
3b		2.82, dd (13.6, 4.5)	4, 5/9	2, 3a	5/9
4	127.1, C				
5/9	106.8, CH	6.45, s	3, 4, 5, 6, 7, 9		2, 3a/b, 6′-OMe
6/8	147.9, C				
7	134.4, C				
1-NHa		9.05, br s		1-NHb	
1-NHb		8.90, br m		1-NHa	
6/8-OMe	55.8, CH_3	3.62, s	6, 8		5″/9″, 6″/8″
7-OH		8.08, br s	6, 7, 8		
1′a	37.7, CH_2	4.52, br d (14.6)		1′b, 2′	1′b
1′b		3.00, dd (14.6, 11.9)	2′	1′a,	1′a
2′	55.9, CH	3.41[b]		1′a, 3′	
3′	36.1, CH_2	2.92, d (7.3)	1′, 2′, 4′, 5/9′	2′	5′, 9′
4′	127.9, C				
5′	109.0, CH	6.61, s	3′, 6′,7′, 9′,		3′
6′	143.3, C				
7′	133.9, C				
8′	148.6, C				
9′	103.2, CH	6.60, s	3′, 5′, 7′, 8′,		3′, 6′-OMe
6′-OMe	56.3, CH_3	3.84, s	6′		9′,
7′/8′-OCH_2O	101.2, CH_2	5.99, s	7′, 8′		
1″	165.1, C				
2″	117.9, CH	6.67, d (15.3)	1″, 4″	3″	2, 5/9″
3″	140.8, CH	7.11, d (15.3)	1″, 2″, 4″, 5/9″	2″	
4″	135.0, C				
5″/9″	127.7, CH	7.46, dd (7.5, 1.3)	3″, 5″,7″, 9″	6″/8″	2″, 6/8-OMe
6″/8″	128.6, CH	7.33[c]	4″, 5/9″	5″/9″	6/8-OMe
7″	129.5, CH	7.33[c]	5/9″		

[a] Major conformer, [b] Obscured by water signal; [c] Overlapping resonances

Table S14 ^{1}H (600 MHz) and ^{13}C (150 MHz) NMR data for hancockiamide F (**6**) in DMSO-d_6

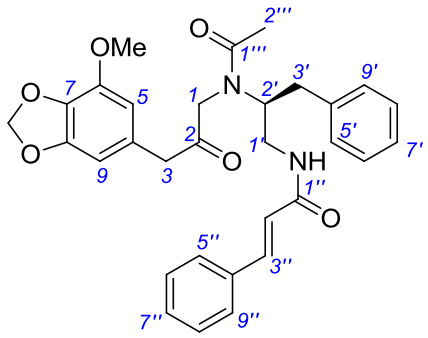

Pos.	δ_C [a], type	δ_H [a] (*J* in Hz)	HMBC	COSY	ROESY
1	50.0, CH_2	4.12, s	2, 2′, 1‴		3, 2″
2	204.1, C				
3	45.9, CH_2	3.70, s	2, 4, 5, 9		1, 9
4	128.7, C				
5	109.3, CH	6.47, d (1.5)	3, 4, 6, 7, 9	9	
6	142.9, C				
7	133.4, C				
8	148.9, C				
9	103.7, CH	6.44, d (1.5)	3, 5, 6, 7, 8	5	3, 6-OMe
6-OMe	56.2, CH_3	3.79, s	6		9
7/8-OCH_2O	101.0, CH_2	5.94, s	7, 8		
1′a	40.7, CH_2	3.37, ddd (14.1, 6.9, 5.4)	2′, 3′, 1″	2′, 1′b, 1′-NH	1′b, 2′
1′b		3.21, ddd (14.1, 8.0, 5.4)	2′, 3′, 1″	2′, 1′a, 1′-NH	1′a, 2′
2′	59.0, CH	4.14, m	1, 1′, 3′	1′a/b, 3′a/b	1′a/b, 3′a/b, 5′/9′, 1′-NH
3′a	36.5, CH_2	2.80, dd (13.9, 6.0)	1′, 2′, 4′, 5′/9′	2′, 3′b	2′
3′b		2.75, dd (13.9, 8.5)	1′, 2′, 4′, 5′/9′	2′, 3′a	2′, 5′/9′
4′	138.3, C				
5′/9′	129.0, CH	7.26, br m	3′, 4′, 5′/9′, 7′	6′/8′	2′, 3′b
6′/8′	128.4, CH	7.30, br m	4′, 6′/8′	5′/9′, 7′	
7′	126.4, CH	7.21, br m	5′/9′	6′/8′	
1′-NH		8.02, t (5.8)	1′, 1″	1′a/b	2′, 2″
1″	165.2, C				
2″	121.7, CH	6.64, d (15.8)	1″, 3″, 4″	3″	1, 5″/9″, 1′-NH
3″	139.2, CH	7.41, d (15.8)	1″, 2″, 4″, 5″/9″	2″	
4″	134.7, C				
5″/9″	127.6, CH	7.57, br m	3″, 5″/9″, 7″	6″/8″	2″, 6″/8″
6″/8″	128.9, CH	7.39, br m	4″, 5″/9″ ,6″/8″	5″/9″, 7″	5″/9″
7″	129.5, CH	7.36, br m	5″/9″	6″/8″	
1‴	169.9, C				
2‴	20.7, CH_3	1.69, s	1‴		

[a] Major conformer

Table S15. ^{1}H (600 MHz) and ^{13}C (150 MHz) NMR data for hancockiamide G (**7**) in DMSO-d_6

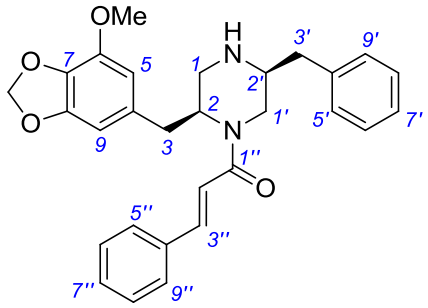

Pos.	δ_C [a], type	δ_H [a] (*J* in Hz)	HMBC	COSY	ROESY
1a	49.5, CH_2	2.93, br d (12.1)	2′, 3	1b, 2	1b, 2
1b		2.79, dd (12.1, 4.3)	3	1a, 2	1a, 2
2	54.3, CH	4.30, m	1, 4, 1′, 1″	1a/b, 3a/b	1a/b, 5, 9, 2′, 2″
3a	35.6, CH_2	3.11, dd (13.4, 10.0)	1, 2, 4, 5, 9	2, 3b	3b, 5, 9
3b		2.70[b]	1, 2, 4, 5, 9	2, 3a	3a, 5, 9
4	133.2, C				
5	108.9, CH	6.41, d (1.4)	3, 6, 7, 9	6-OMe	2, 3a/b, 6-OMe
6	143.0, C				
7	133.4, C				
8	148.1, C				
9	103.3, CH	6.42, d (1.4)	5, 7, 8		2, 3a/b
6-OMe	56.0, CH_3	3.65, s	6	5	5
7/8-OCH_2Oa	100.6,	5.79, d (1.1)	7, 8	7/8-OCH_2Ob	7/8-OCH_2Ob
7/8-OCH_2Ob	CH_2	5.49, br s	7, 8	7/8-OCH_2Oa	7/8-OCH_2Oa
1-NH		2.20, br s			
1′a	42.1, CH_2	4.21, br dd (12.7, 2.5)	2, 2′, 1″	1′b ,2′	1′b, 2′
1′b		2.63, dd (12.7, 10.6)	2′, 1″	1′a	1′a
2′	56.8, CH	2.68[b]	1′, 4′	1′a, 3′	2, 1′a
3′	40.1, CH_2	2.72[b]	1′, 4′, 5′/9′	2′	5′/9′
4′	138.6, C				
5′/9′	129.2, CH	7.26[c]	3′, 5′/9′, 7′	6′/8′	3′
6′/8′	128.5, CH	7.31[c]	4′, 6′/8′	5′/9′, 7′	
7′	126.1, CH	7.22, t (7.5)	5′/9′	6′/8′	
1″	165.2, C				
2″	118.6, CH	6.68, d (15.4)	1″, 3″, 4″	3″	2, 5″/9″ 3″
3″	139.4, CH	7.04, d (15.4)	1″, 2″, 4″, 5″/9″	2″	5″/9″
4″	135.2, C				
5″/9″	127.5, CH	7.47, dd (8.0, 1.8)	3″, 5″/9″, 7″	6″/8″	2″, 3″, 6″/8″
6″/8″	128.3, CH	7.32[c]	4″	5″/9″, 7″	5″/9″
7″	129.2, CH	7.27[c]		6″/8″	

[a] Major conformer; [b-c] Overlapping resonances

Table S16. ^{1}H (600 MHz) and ^{13}C (150 MHz) NMR data for hancockiamide H (**8**) in DMSO-d_6

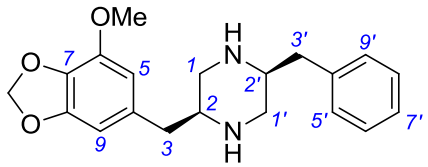

Pos.	δ_C [a], type	δ_H [a] (*J* in Hz)	HMBC	COSY	ROESY
1a	47.2, CH_2	2.60[a], m	2′, 1‴	1b, 2	
1b		2.55[b], dd (15.4, 11.3)	2′, 1‴	1a, 2	3b
2	55.3, CH	2.73[c], br s		1a/b	2′
3	38.06, CH_2	2.65, m		3b	3b
4	134.5, C				
5	108.4, CH	6.45, d (1.2)	3, 7, 9		
6	143.0, C				
7	132.8, C				
8	148.2, C				
9	102.8, CH	6.44, d (1.2)	3, 5, 7, 8		
6-OMe	56.2, CH_3	3.79, s	6		
7/8-OCH_2O	102.8, CH_2	5.91, br s	7, 8		
1′a	47.2, CH_2	2.60[a], m	2, 1″	1′b ,2′	
1′b		2.55[b], m	2′, 3′, 1″	1′a	
2′	55.3, CH	2.73[c], br m		3′a/b	2
3′	38.11, CH_2	2.72[c], br m	1′, 2′, 4′, 5′, 9′	2′, 3′b	3′b
4′	140.0, C				
5′/9′	129.1, CH	7.18, br d (7.6)	3′, 7′	6′/8′	6′/8′
6′/8′	128.1, CH	7.26, br dd (7.6, 7.3)	4′	5′/9′, 7′	5′/9′, 7′
7′	125.7, CH	7.16, br dd (7.3, 7.3)	5′/9′	6′/8′	6′/8′
1-NH_2		2.25, br s			
1′-NH_2		2.25, br s			

[a-c] Overlapping resonances

Table S17. ^{1}H (600 MHz) and ^{13}C (150 MHz) NMR data for hancockiamide I (**9**) in DMSO-d_6

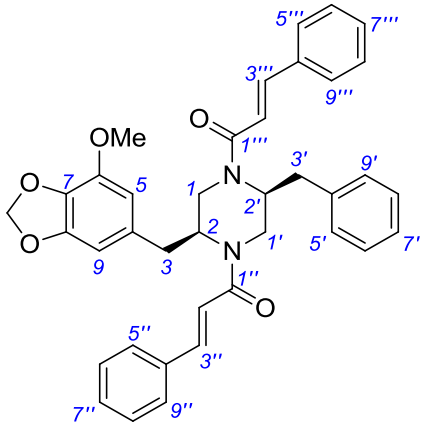

Pos.	δ_C [a,b], type	δ_H [a,b] (*J* in Hz)
1a	43.3, CH_2	4.37[c], br
1b		3.12[d], br
2	54.7, CH	4.43[c], br
3	37.6, CH_2	2.75[e], br
4	133.5, C	
5	109.2, CH	6.47[f], br
6	143.1, C	
7	131.8, C	
8	148.3, C	
9	103.4, CH	6.45 [f], br
6-OMe	54.8, CH_3	3.75, s
7/8-OCH_2O	100.8, CH_2	5.98, br s
		5.80, br s
1′a	43.3, CH_2	4.37[c], br
1′b		3.12 [d], br
2′	55.6, CH	4.49 [c], br
3′a	37.6 CH_2	2.91 [e], br
4′	137.3, C	
5′/9′	129.6, CH	7.32[f], br
6′/8′	128.4, CH	7.32 [f], br
7′	126.5, CH	7.17 [f], br
1″	165.5, C	
2″	118.0, CH	6.49[f], br
3″	141.5, CH	7.49[f], br
4″	134.9, C	
5″/9″	128.0, CH	7.46[f], br
6″/8″	128.7, CH	7.40[f], br
7″	128.6, CH	7.32[f], br
1‴	165.5, C	
2‴	118.0, CH	6.49[f], br
3‴	141.5, CH	7.49[f], br
4‴	134.9	
5‴/9‴	128.0, CH	7.46[f], br
6‴/8‴	128.7, CH	7.40[f], br
7‴	128.4, CH	7.32[f], br

[a] Major conformer; [b] Assignments based on comparison with related metabolites and HSQCs
[c-f] Overlapping resonances. [g] Due to extreme peak broadening, no useful 2D correlations could be obtained

Table S18. ^{1}H (600 MHz) and ^{13}C (150 MHz) NMR data xenocockiamide A (**10**) DMSO-d_6

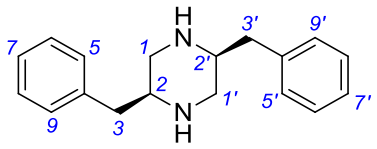

Pos.	δ_C, type	δ_H (*J* in Hz)	HMBC	COSY	ROESY
1a/1′a	47.2, CH_2	2.62, ddd, (11.6, 5.1, 2.5)	3, 2′	1b, 2	
1b/1′b		2.55, br dd (11.6, 2.5)	2, 3	1a, 2	2
2/2′	55.4, CH	2.74, br s	3, 1′	1a/1b	1b
3/3′	38.1, CH_2	2.74, br s	2, 4, 5/9,	5/9	5/9
4/4′	140.0, C				
5/5′/9/9′	129.1, CH	7.19, dd, (8.2, 1.5)	3, 5/9, 7	3, 6/8, 7	3
6/6′/8/8′	128.2, CH	7.26, ddd, (8.2, 7.5, 1.5)	4, 6/8	5/9, 7	
7/7′	125.7, CH	7.16, ddd, (7.5, 7.5, 1.5)	5/9	5/9, 6/8	
1/1′-NH_2		2.06, br s			

Table S19. ^{1}H (600 MHz) and ^{13}C (150 MHz) NMR data for xenocockiamide B (**11**) in DMSO-d_6

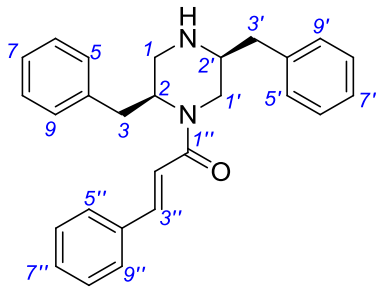

Pos.	δ_C[a], type	δ_H[a] (*J* in Hz)	HMBC	COSY	ROESY
1a	49.3, CH_2	2.93, br d (12.5)	3, 2′	1b, 2	1b
1b		2.76[b]	3	1a	1a, 2
2	54.0, CH	4.34, m,		1a, 3a/b	1b, 3b, 5/9, 2″
3a	35.5, CH_2	3.17, dd (13.5, 9.5)	1, 2, 4, 5/9	2, 3b	3b
3b		2.88, dd (13.5, 5.5)	1, 2, 4, 5/9	2, 3a	3a
4	138.9, C				
5/9	129.3, CH	7.21	3, 5/9, 7	6/8	2, 3a/b, 6/8
6/8	128.3, CH	7.31	4, 6/8	5/9, 7	5/9, 7
7	126.1 C	7.22		6/8	6/8
1-NH		2.26, br s			
1′a	42.1, CH_2	4.23, br d	2, 2′, 1″	1′b, 2′	1′b
1′b		2.65 [b]	2′, 1″	1′a	1′a
2′	56.8, CH	2.66[b]	4′	1′a, 3′	
3′	40.1, CH_2	2.73[b]	1′, 4′, 5′/9′	2′	5′/9′
4′	138.6, C				
5′/9′	129.2, CH	7.27,	3′, 5′/9′, 7′		3′
6′/8′	128.1, CH	7.17[c]	4′, 6′/8′	7′	
7′	126.2, CH	7.06, tt (7.2, 1.4)	5′/9′	6′/8′	
1″	164.8, C				
2″	118.7, CH	6.62, d (15.5)	1″, 3″, 4″	3″	2, 5″/9″
3″	139.9, CH	7.04, d (15.5)	1″, 2″, 4″, 5″/9″	2″	5″/9″
4″	135.2, C				
5″/9″	127.6, CH	7.44, dd (7.7, 1.7)	3″, 5″/9″, 7″	6″/8″	6″/8″ 2″, 3″
6″/8″	128.6, CH	7.35[c]	4″, 6″/8″	5″/9″	5″/9″
7″	129.2, CH	7.27[c]	5″/9″		

[a] Major conformer; [b-c] Overlapping resonances

Table S20. ^{1}H (600 MHz) and ^{13}C (150 MHz) NMR data for xenocockiamide C (**12**) in DMSO-d_6

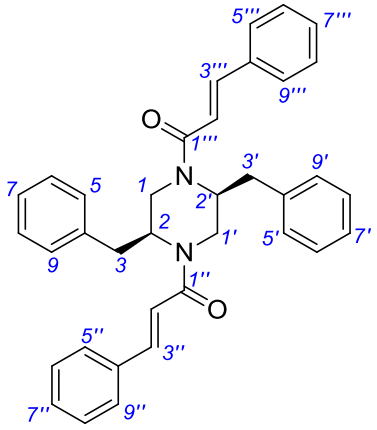

Pos.	δ_C[a/b], type	δ_H[a/b] (*J* in Hz)
1a/1′a	43.3, CH_2	4.37[c]
1b/1′b		3.15
2/2′	53.1, CH	4.41[c]
3/3′	37.8, CH_2	2.90, br s
4/4′	137.4, C	
5/9/5′/9′	128.4, CH	7.30[d]
6/8/6′/8′	129.6, CH	7.25[d]
7/7′	126.5, CH	7.15[d]
1″/1‴	165.4, C	
2″/2‴	118.0, CH	6.23, br s
3″/3‴	141.5, CH	7.18[d]
4″/4‴	137.3, C	
5″/9″/5‴/9‴	128.0, CH	7.45[d]
6″/8″/6‴/8‴	128.7, CH	7.38[d]
7″/7‴	128.4, CH	7.30[d]

[a] Major conformer; [b] Assignments based on comparison with related metabolites and HSQCs

[c-d] Overlapping resonances. [e] Due to extreme peak broadening, no useful 2D correlations could be obtained.

Table S21. ^{1}H (600 MHz) and ^{13}C (150 MHz) NMR data for xenocockiamide D (**13**) in DMSO-d_6

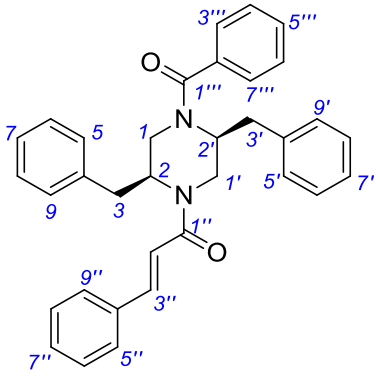

Pos.	δ_C [a/b], type	δ_H [a/b] (*J* in Hz)
1a/1′a	43.3, CH_2	4.36[c]
1b/1′b		3.09
2/2′	53.5, CH	4.48[c]
3/3′	37.4, CH_2	2.90, br s
4/4′	137.1, C	
5/9/5′/9′	128.3, CH	7.31[d]
6/8/6′/8′	129.6, CH	7.23[d]
7/7′	126.5, CH	7.17[d]
1″	165.7, C	
2″	118.1, CH	6.43, br s
3″	141.3, CH	7.16[d]
4″	137.0, C	
5″/9″	128.4, CH	7.49[d]
6″/8″	128.7, CH	7.38[d]
7″	128.4, CH	7.30[d]
1‴	170.3	
2‴	137.0, C	
3‴/7‴	128.0, CH	7.49[d]
4‴/6‴	128.3, CH	7.40[d]
5‴	129.3, CH	7.30[d]

[a] Major conformer; [b] Assignments based on comparison with related metabolites and HSQCs
[c-d] Overlapping resonances. [e] Due to extreme peak broadening, no useful 2D correlations could be obtained.

Table S22. *In vitro* bioassay results for **1-13** identified in this study.

Compd.	Minimum inhibitory concentration (μg/mL)								
	Bs[a]	*Sa*[b]	*Ca*[c]	*Sc*[d]	*Mm*[e]	*Nff*[f]	*Tf*[g]	*Teff*[h]	*Arabi*[i]
1	50	–	–	–	3.1	–	–	–	–
2	50	–	–	–	25	–	–	–	–
3	–	–	–	–	25	–	–	–	6.3
4	–	–	–	–	1.6	–	–	–	50
5	–	–	–	–	13	–	–	–	–
6	–	–	–	–	100	–	–	–	–
7	6.3	25	100	–	13	100	–	–	100
8	–	–	–	–	50	–	–	–	–
9	–	–	–	–	–	–	–	–	–
10	–	–	–	–	50	–	–	–	–
11	6.3	25	50	100	6.3	50	50	–	–
12	–	–	–	–	–	–	–	–	–
13	–	–	–	–	13	–	–	–	–
control	0.4[j]	0.8[j]	1.6[k]	1.6[k]	0.4[l]	3.1[l]	1.6[m]	3.1[n]	0.2[n]

[a] *Bacillus subtilis* (ATCC 6633). [b] *Staphylococcus aureus* (ATCC 25923). [c] *Candida albicans* (ATCC 10231). [d] *Saccharomyces cerevisiae* (ATCC 9763); [e] Murine myeloma NS-1 (ATCC TIB-18). [f] Neonatal foreskin fibroblast. [g] *Tritrichomonas foetus* (KV-1). [h] *Eragrostis tef*. [i] *Arabidopsis thaliana*. [j] tetracycline hydrochloride. [k] blasticidin S hydrochloride. [l] staurosporine. [m] metronidazole. [n] cyclohexamide. – indicates no activity detected at 100 μg/mL.

Supplementary Figures

A)

```
Identities = 215/294 (73%),
Positives = 235/294 (79%), Gaps = 32/294 (10%)

Hkm1 with nonsense stopcodon     1 MTIPPTPKPQIKQVPYTTDPEAI*-KVVEDGAVIVEGFLSPDTLQLFNHDLDEIAKVVPT  59
                                   MTIP T KPQI++VP TTDPEAI   V EDGAVI+EGFLSP+TLQ FN DLD IAKVVPT
PENARI_c033G11888                1 MTIPSTSKPQIRRVPNTTDPEAIWNIVEEDGAVIIEGFLSPNTLQRFNQDLDGIAKVVPT  60

Hkm1 with nonsense stopcodon    60 GRQLLHYDDPMPKTLRWISYLPVLSKTFRHDILNNITLHSVCEDAFRETGDYWMITGTAM 119
                                   GR+ L++DDPMPKTLRW+SYLP+LSKTFRHDILNN TLH VCE AF+ETGDYWMITGTAM
PENARI_c033G11888               61 GRKFLYFDDPMPKTLRWMSYLPILSKTFRHDILNNTTLHRVCETAFKETGDYWMITGTAM 120

Hkm1 with nonsense stopcodon    120 EDHPGDNGQPLHRDEATHPVIHHMPS----------------------------CRKWAE 151
                                   EDHPGD+GQ LHRDEATHPVI HMP                                KWAE
PENARI_c033G11888               121 EDHPGDDGQVLHRDEATHPVIRHMPLGAPLLSISWITAVTDFTEENGATRLILGSHKWAE 180

Hkm1 with nonsense stopcodon    152 KGDPPEELTVRATMTAGDTLLMHQGMVHGGGVHRGEGVRRLLLTQMASCQLAPTETFMSA 211
                                   KGDP EELTV+ATM AGD+LLM+QGMVHGGGVHRGE  RRLLLTQMASCQLA TETFMSA
PENARI_c033G11888               181 KGDPLEELTVQATMKAGDSLLMNQGMVHGGGVHRGEEARRLLLTQMASCQLAHTETFMSA 240

Hkm1 with nonsense stopcodon    212 PRPLVETMTPLAQKMIGWRTTRPLPTNISGLMNVELGRLEDDLNLKSNQPE--- 262
                                   PR +VETMTPLAQKMIGWRTTRPLPTNISGLMN++LG LED++ L SNQP+
PENARI_c033G11888               241 PRSIVETMTPLAQKMIGWRTTRPLPTNISGLMNLKLGCLEDEIELLSNQPDIFA 294
```

B)

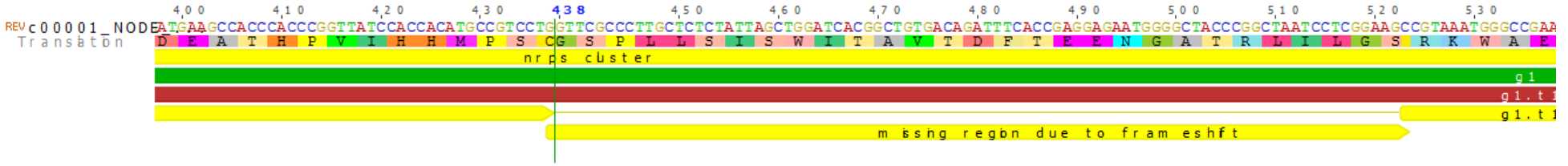

Figure S1. Detailed analysis of Hkm1. (A) protein sequence alignment of the revised Hkm1 with nonsense stop codon and PENARI_c033G11888 from *Penicillium arizonense*. (B) the missing region in predicted Hkm1 due to frameshift mutation.

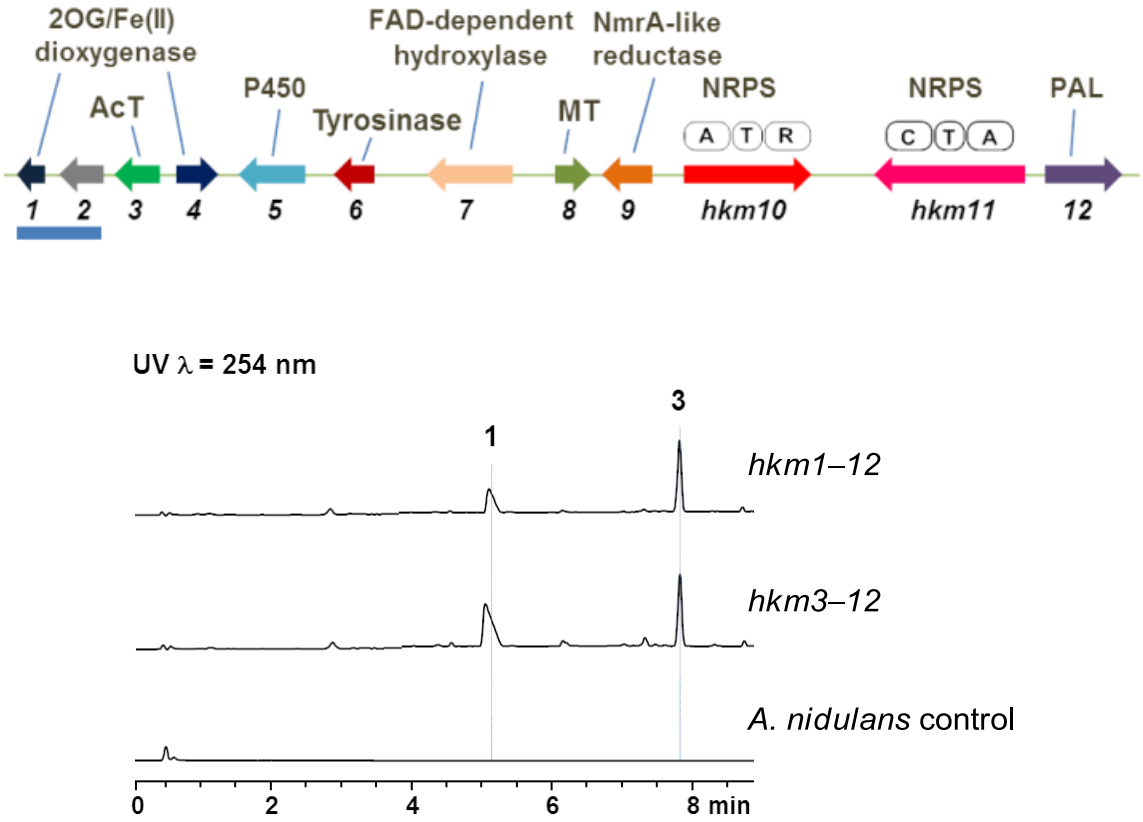

Figure S2. HPLC metabolite profile of *Aspergillus nidulans* expressing *hkm3–12*.

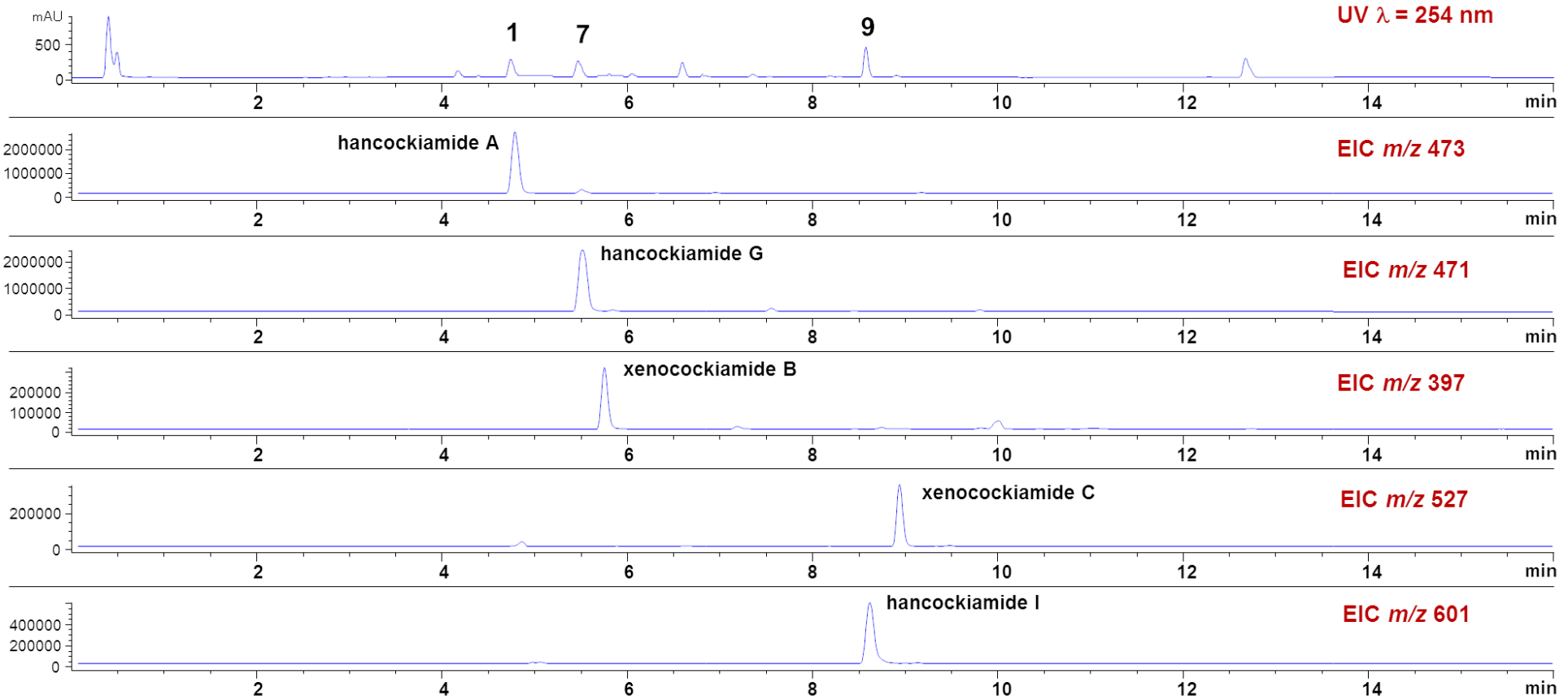

Figure S3. LCMS metabolite profile of the extracts from small scale culture (50 mL) of *Aspergillus nidulans* expressing *hkm4–12* grown on GMM liquid media.

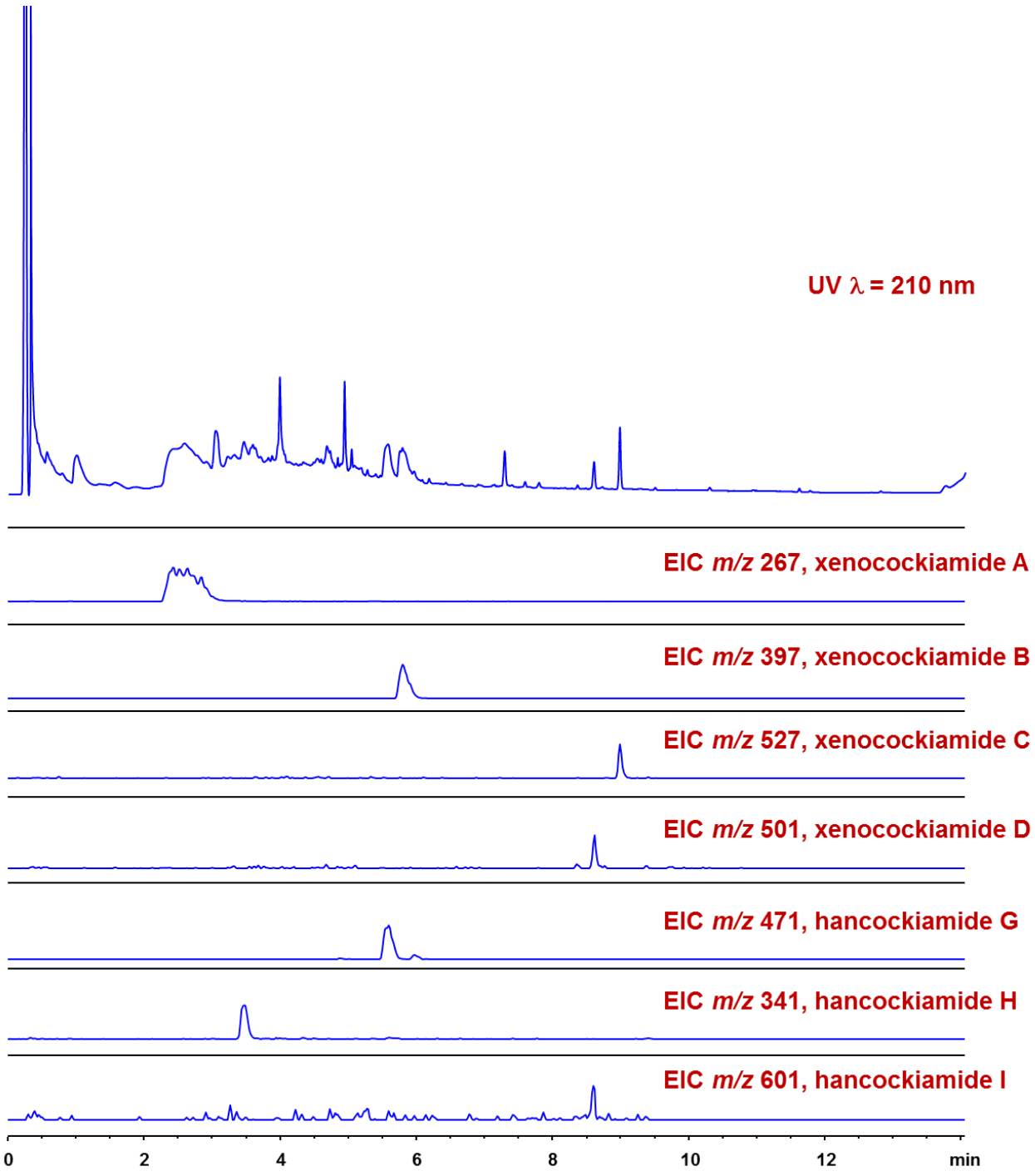

Figure S4. LCMS metabolite profile of the extracts *Aspergillus nidulans* expressing *hkm4–12* grown on YES media.

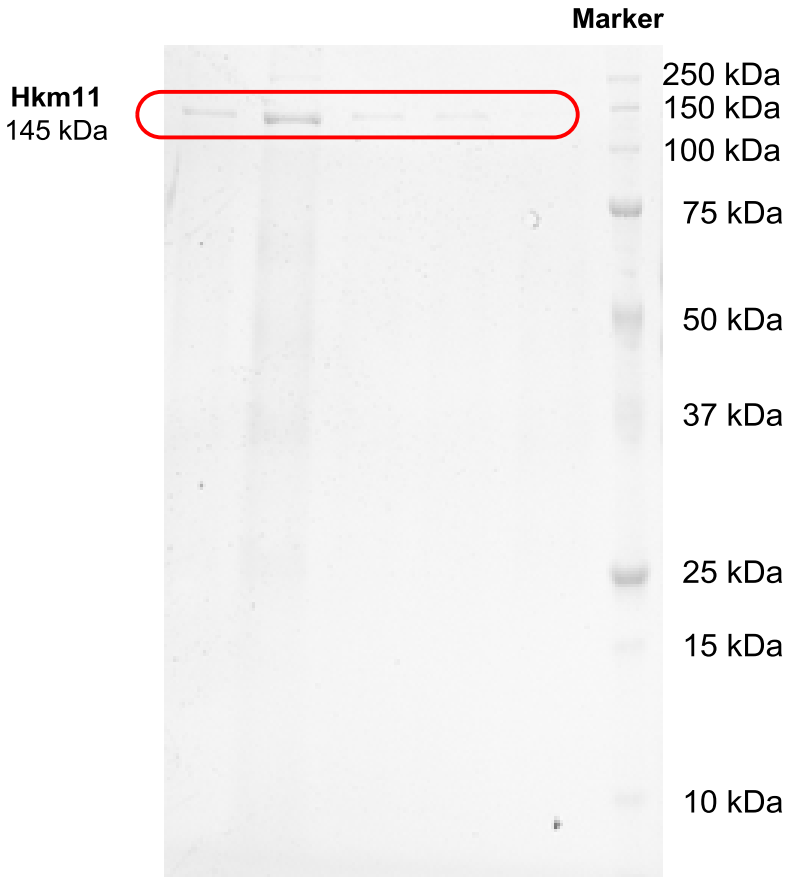

Figure S5. SDS-PAGE analysis of the C-terminal His-tagged recombinant Hkm11.

Note: Precision Plus ProteinTM Dual Color Standard (BIO-RAD) was used as ladder.

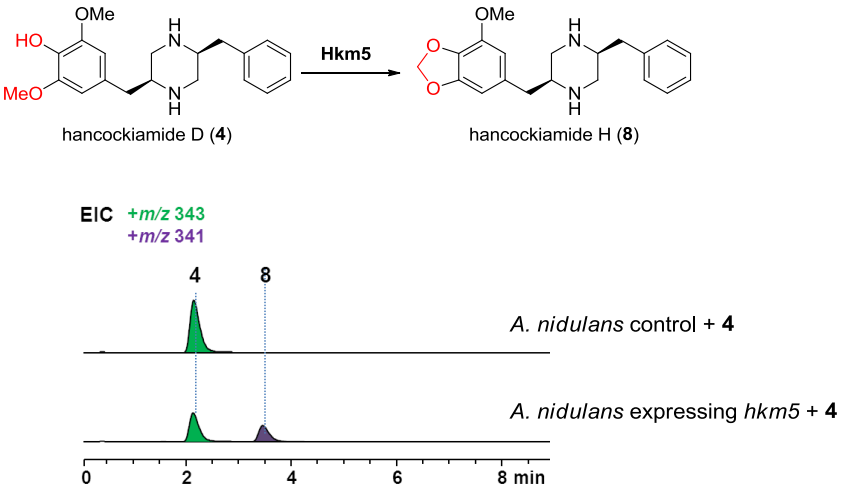

Figure S6. In vivo verification of the function of Hkm5 by *Aspergillus nidulans* feeding experiments.

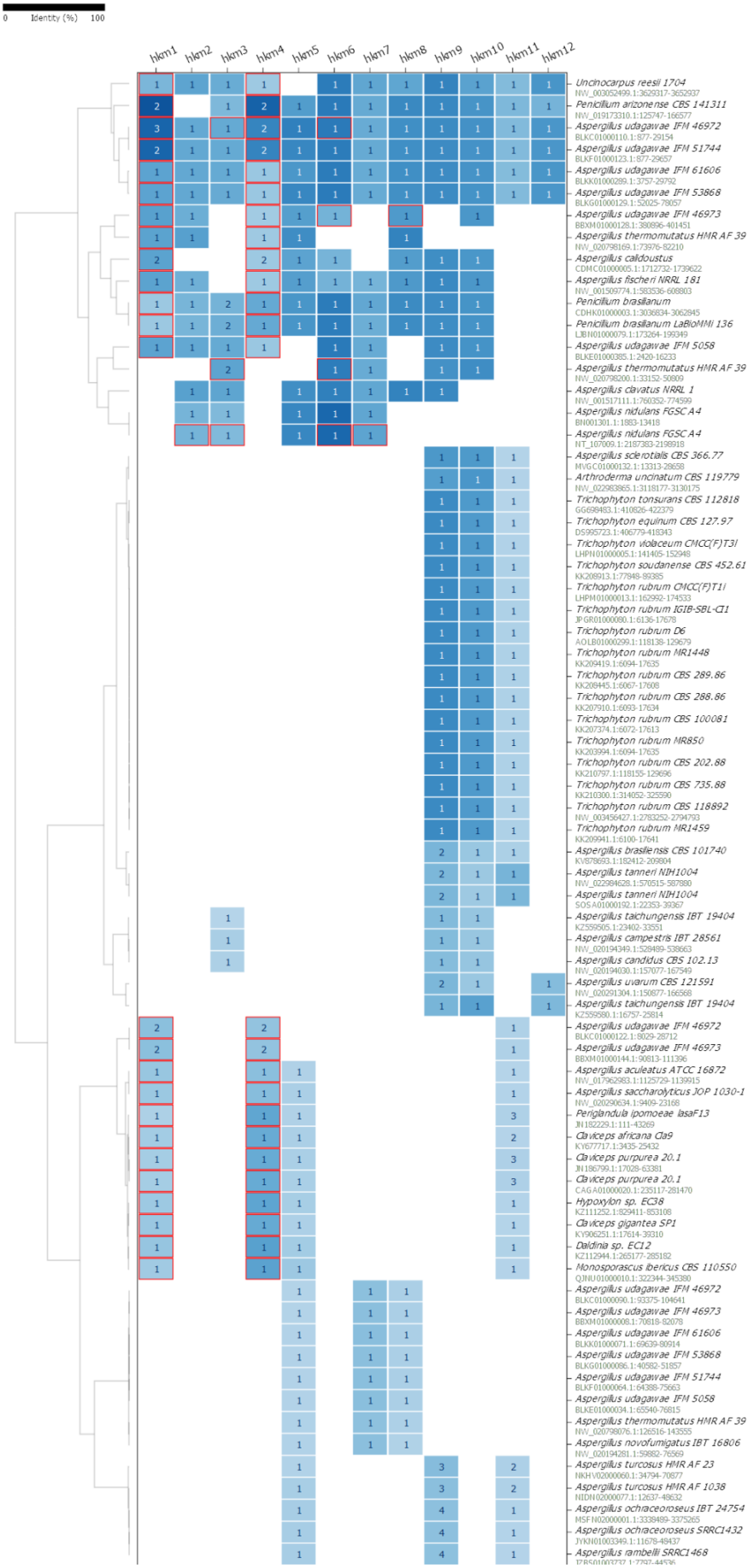

Figure S7. Homologous gene clusters identified in public genome databases using *hkm* cluster as query sequence via cblaster (https://zenodo.org/record/3660769) tool.

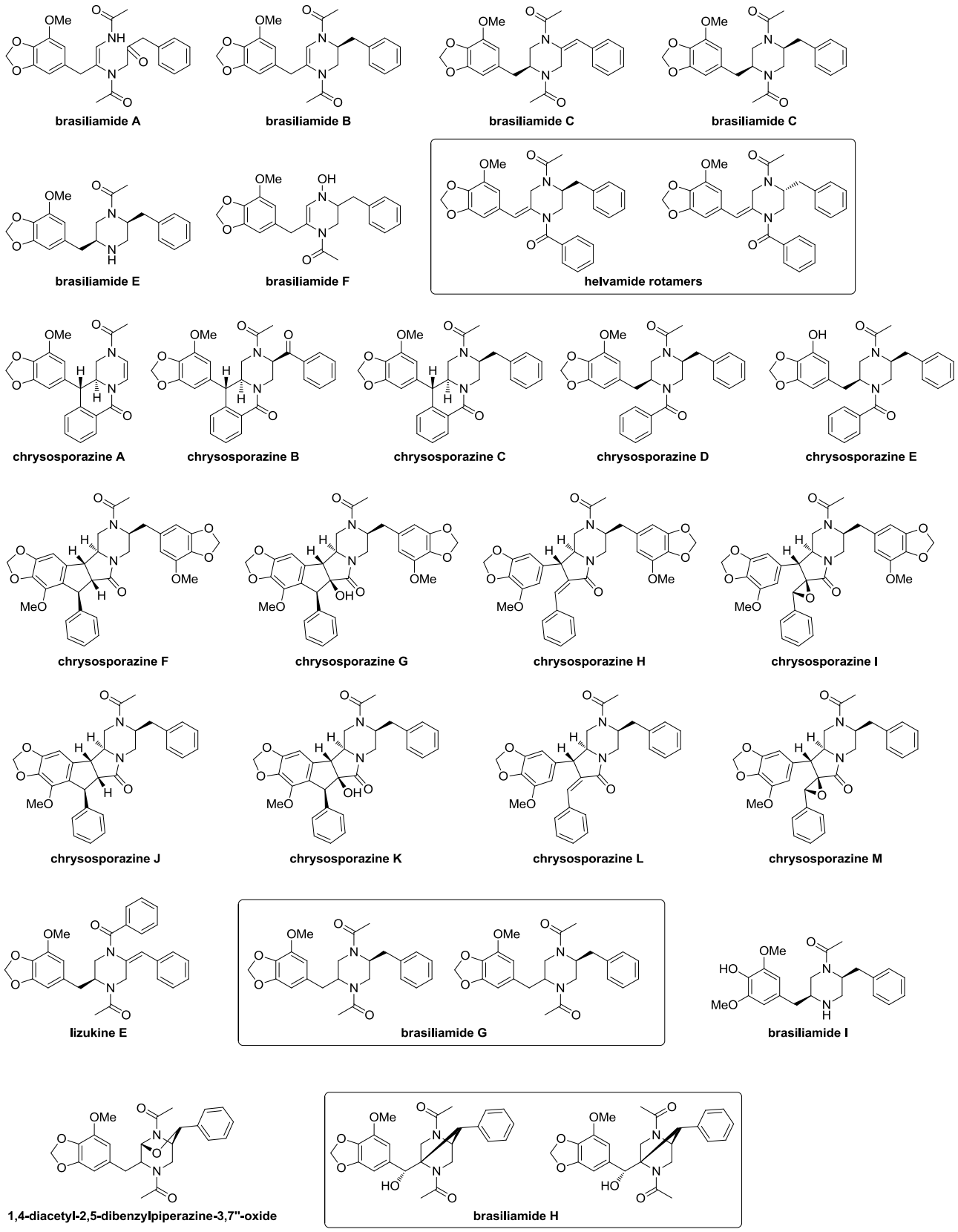

Figure S8. Phenylpropanoid piperazines isolated from fungi.

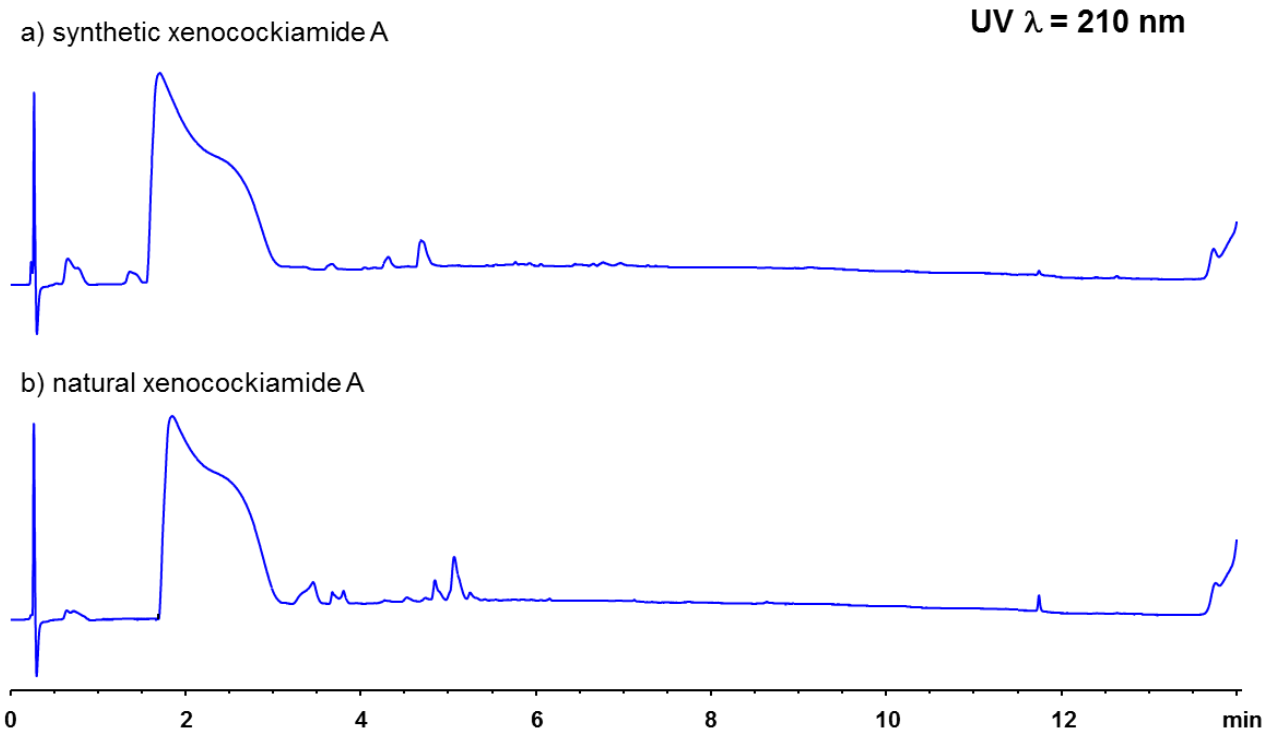

Figure S9. HPLC chromatograms of synthetic and natural xenocockiamide A (**10**).

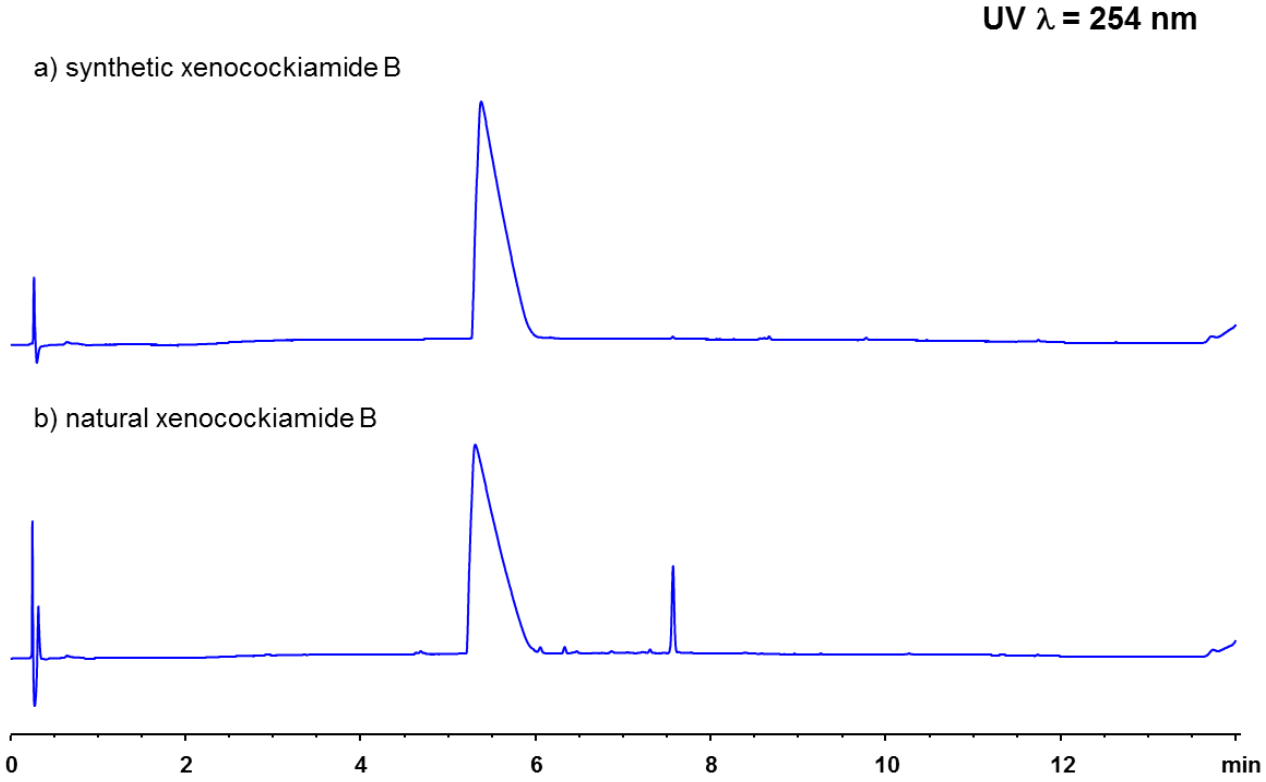

Figure S10. HPLC chromatograms of synthetic and natural xenocockiamide B (**11**).

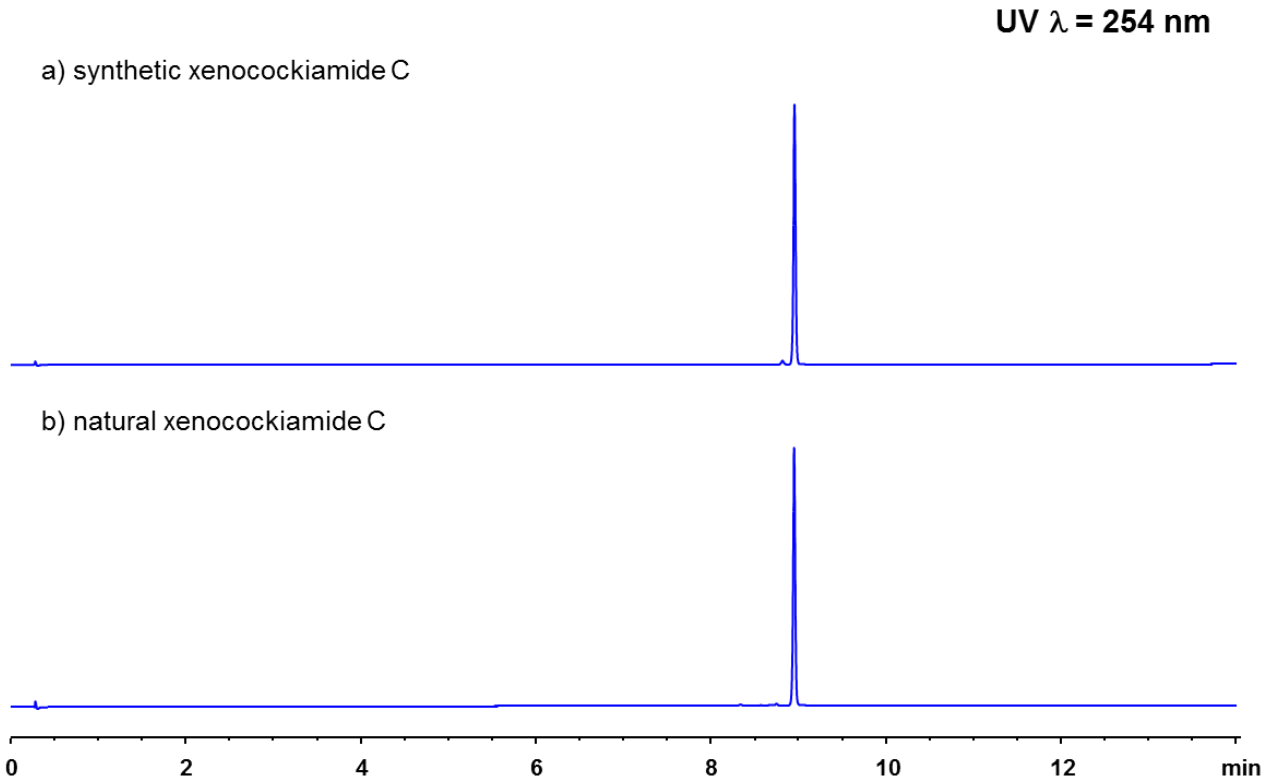

Figure S11. HPLC chromatograms of synthetic and natural xenocockiamide C (**12**).

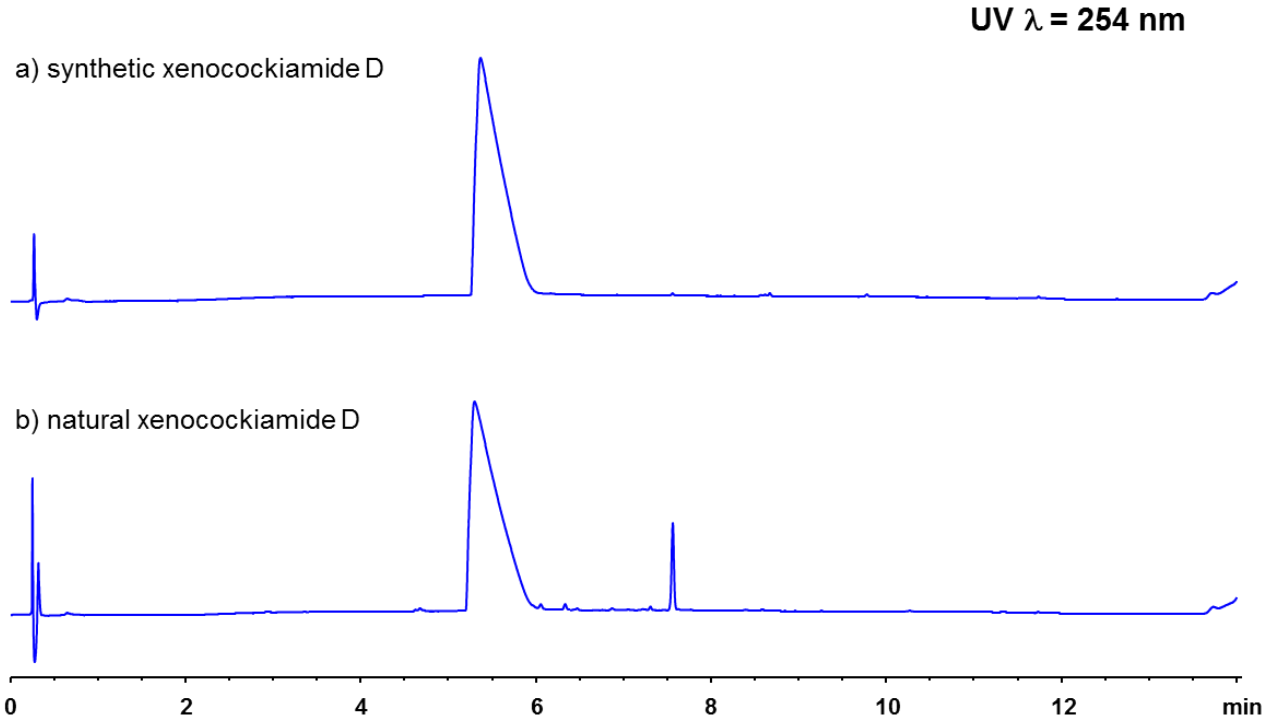

Figure S12. HPLC chromatograms of synthetic and natural xenocockiamide D (**13**).

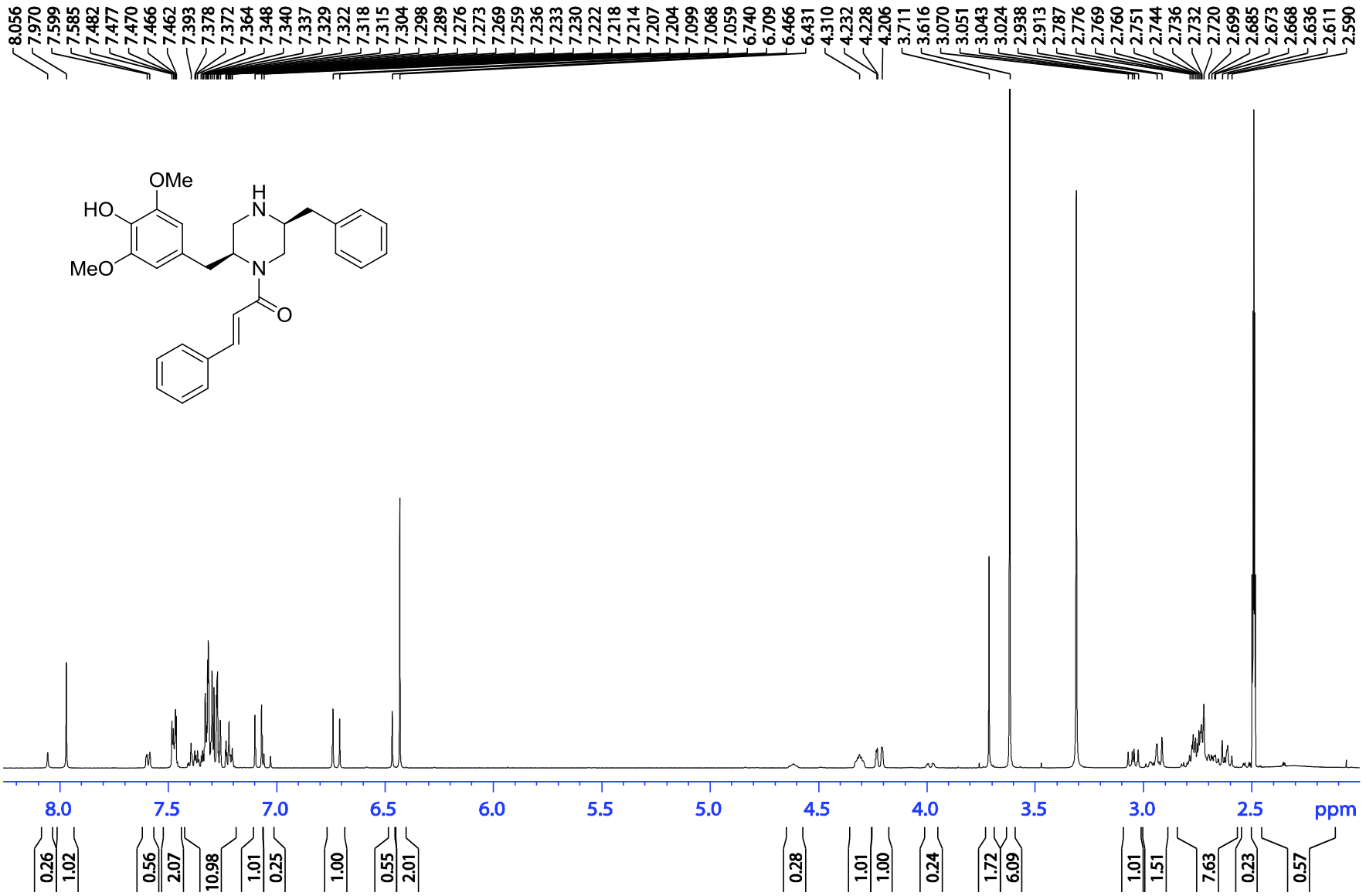

Figure S13. ^{1}H NMR spectrum (500 MHz, DMSO-d_6) of hancockiamide A (**1**)

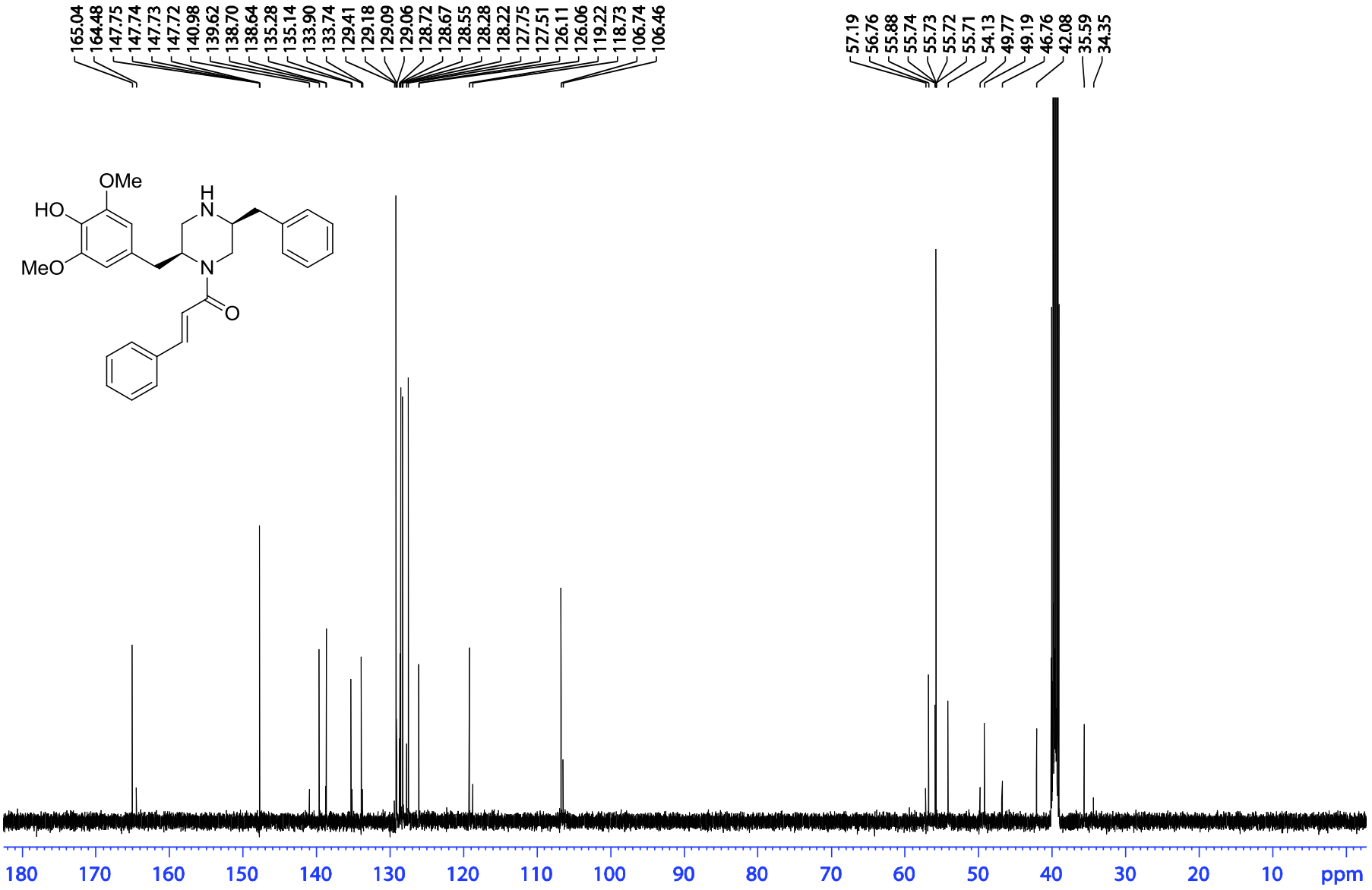

Figure S14. ^{13}C NMR spectrum (125 MHz, DMSO-d_6) of hancockiamide A (**1**)

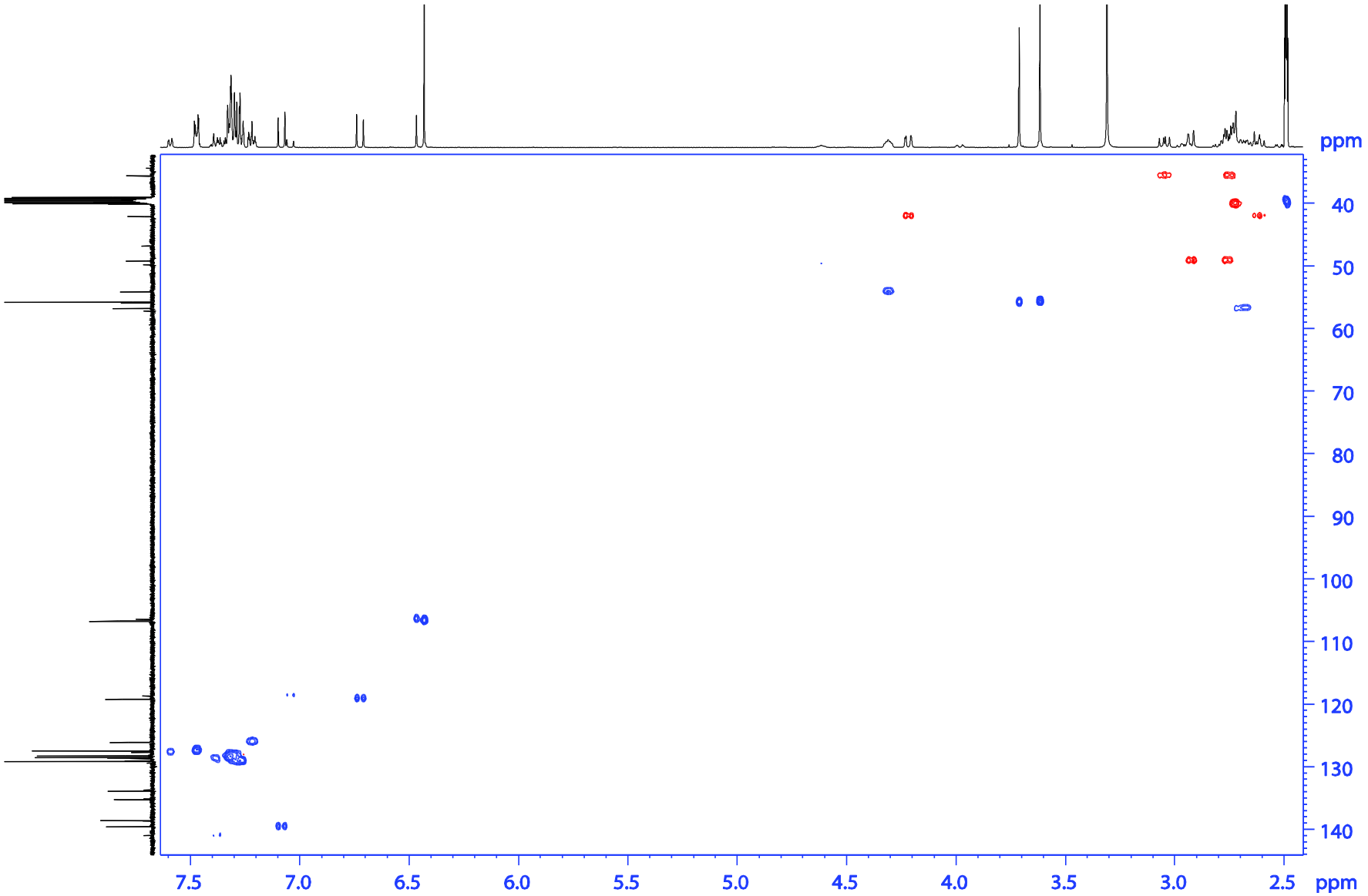

Figure S15. ^{1}H-^{13}C HSQC spectrum (500 MHz, DMSO-d_6) of hancockiamide A (**1**)

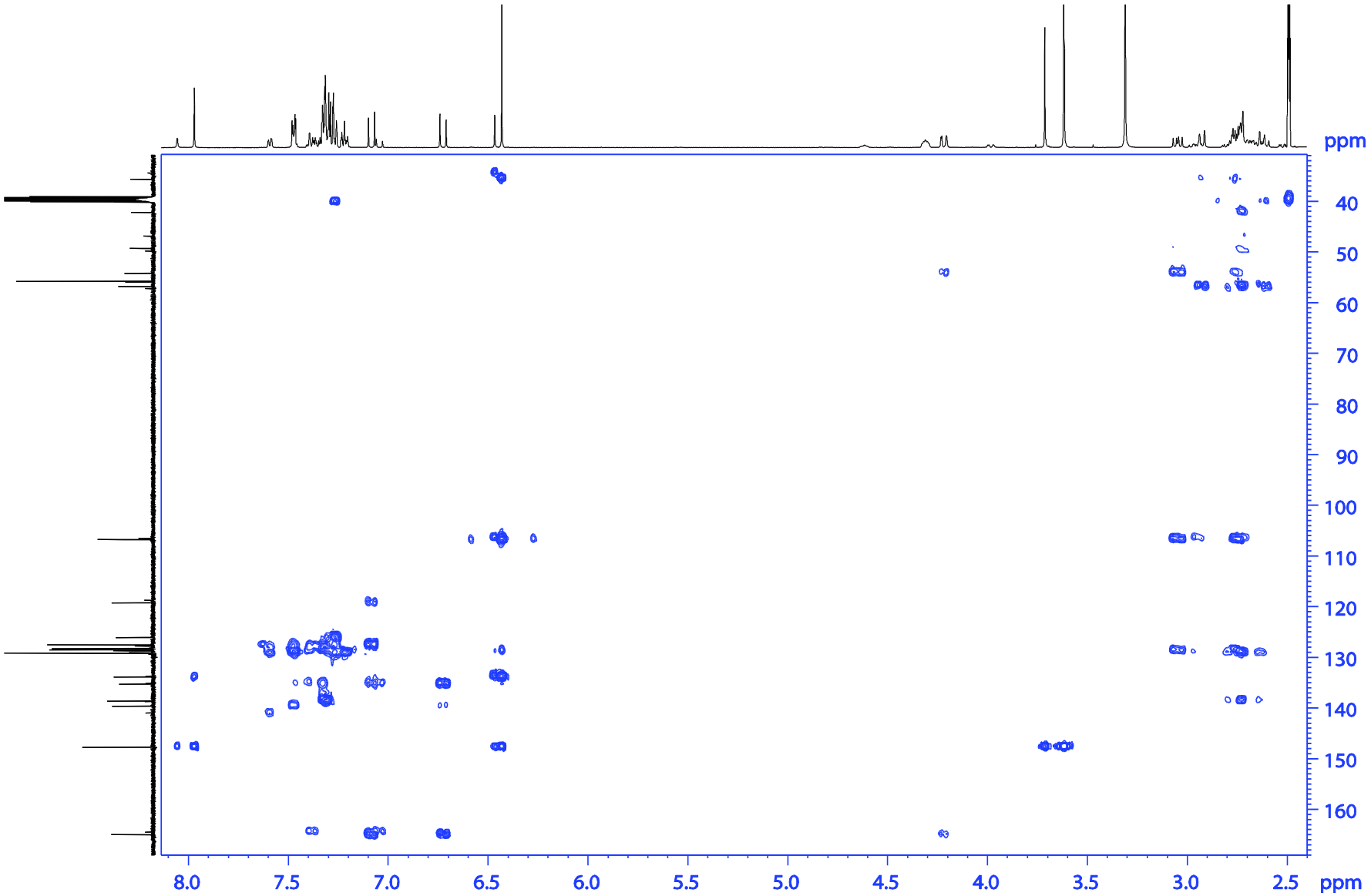

Figure S16. ^{1}H-^{13}C HMBC NMR spectrum (500 MHz, DMSO-d_6) of hancockiamide A (**1**)

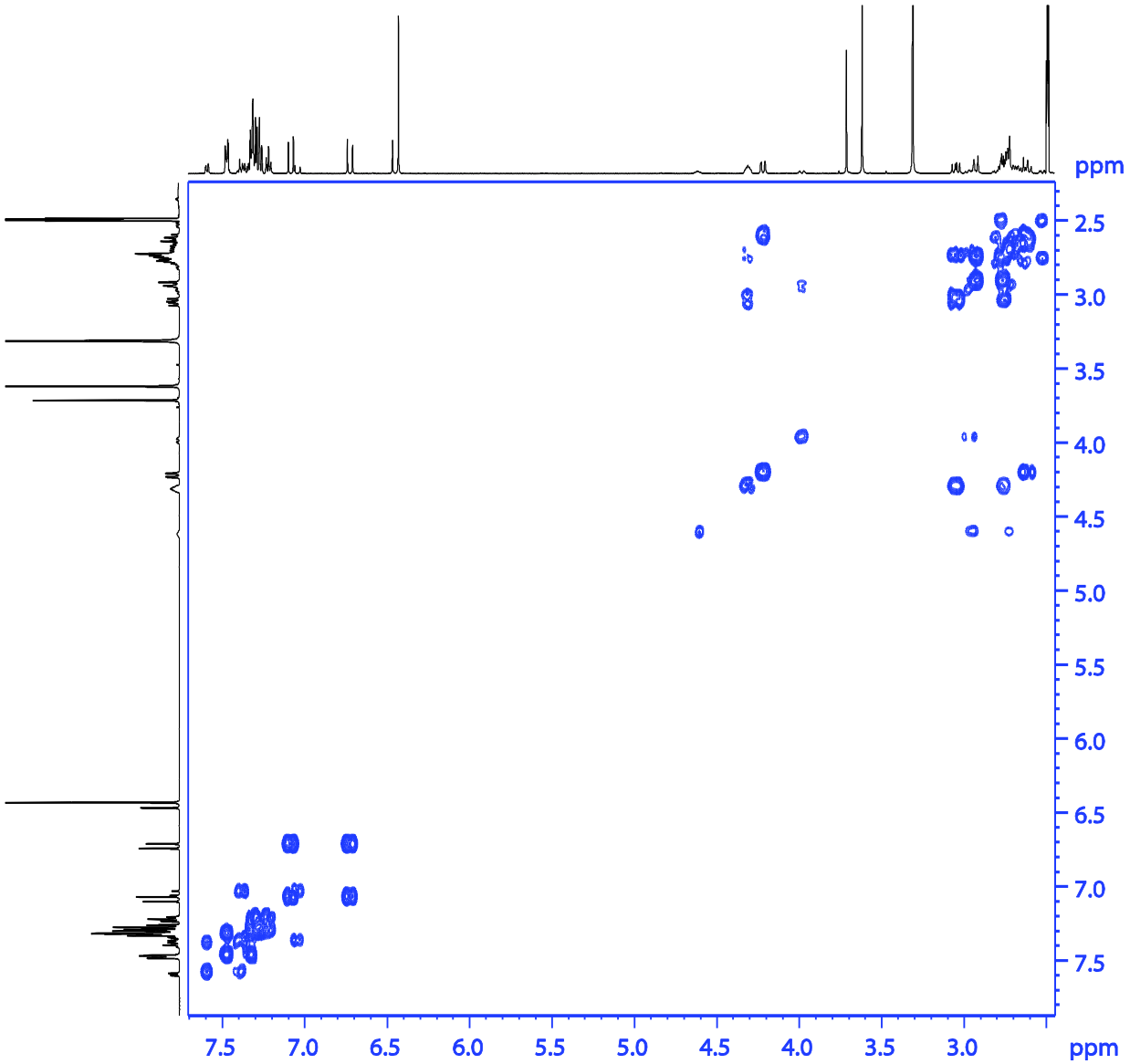

Figure S17. COSY NMR spectrum (500 MHz, DMSO-d_6) of hancockiamide A (**1**)

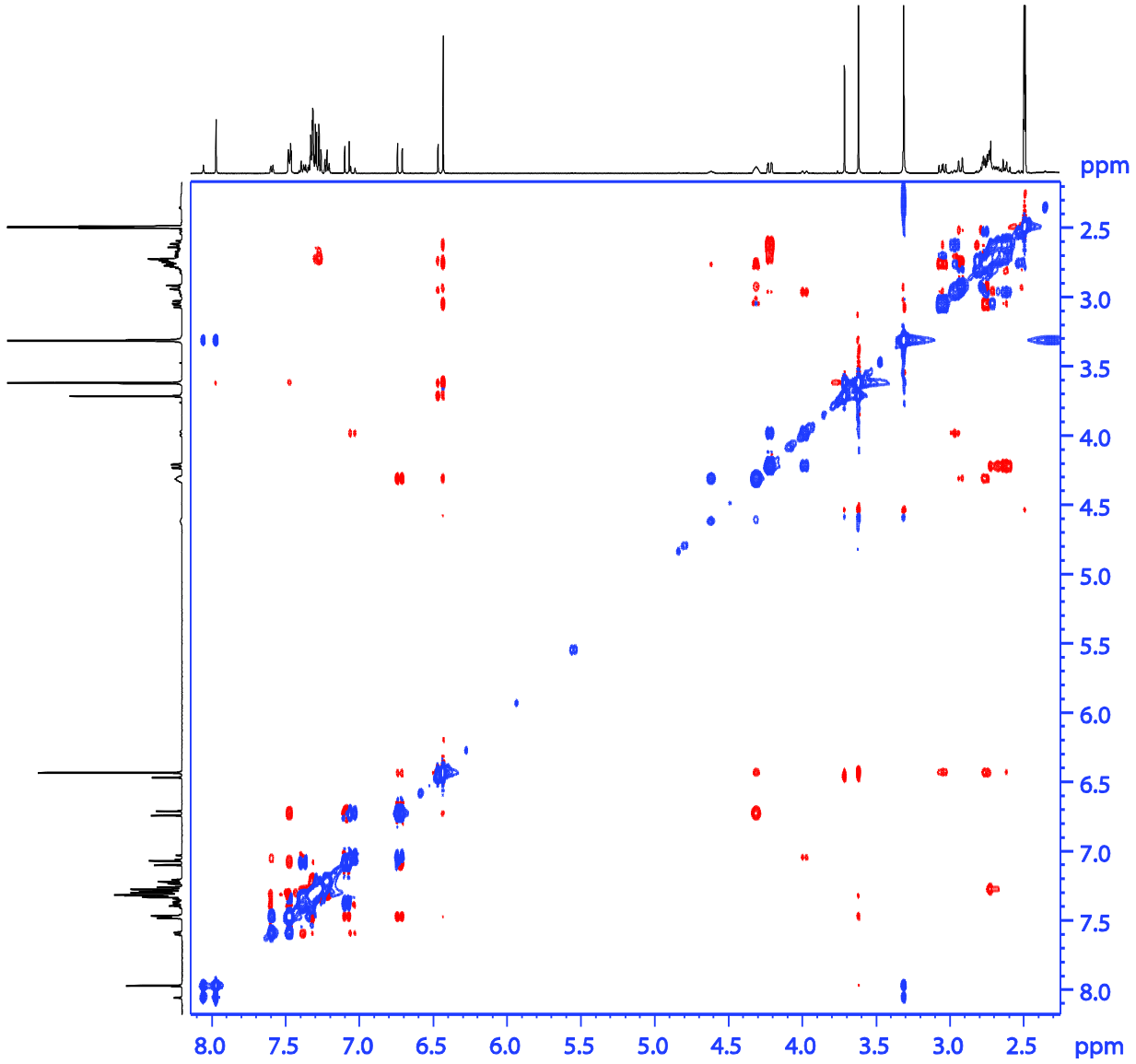

Figure S18. ROESY NMR spectrum (500 MHz, DMSO-d_6) of hancockiamide A (**1**)

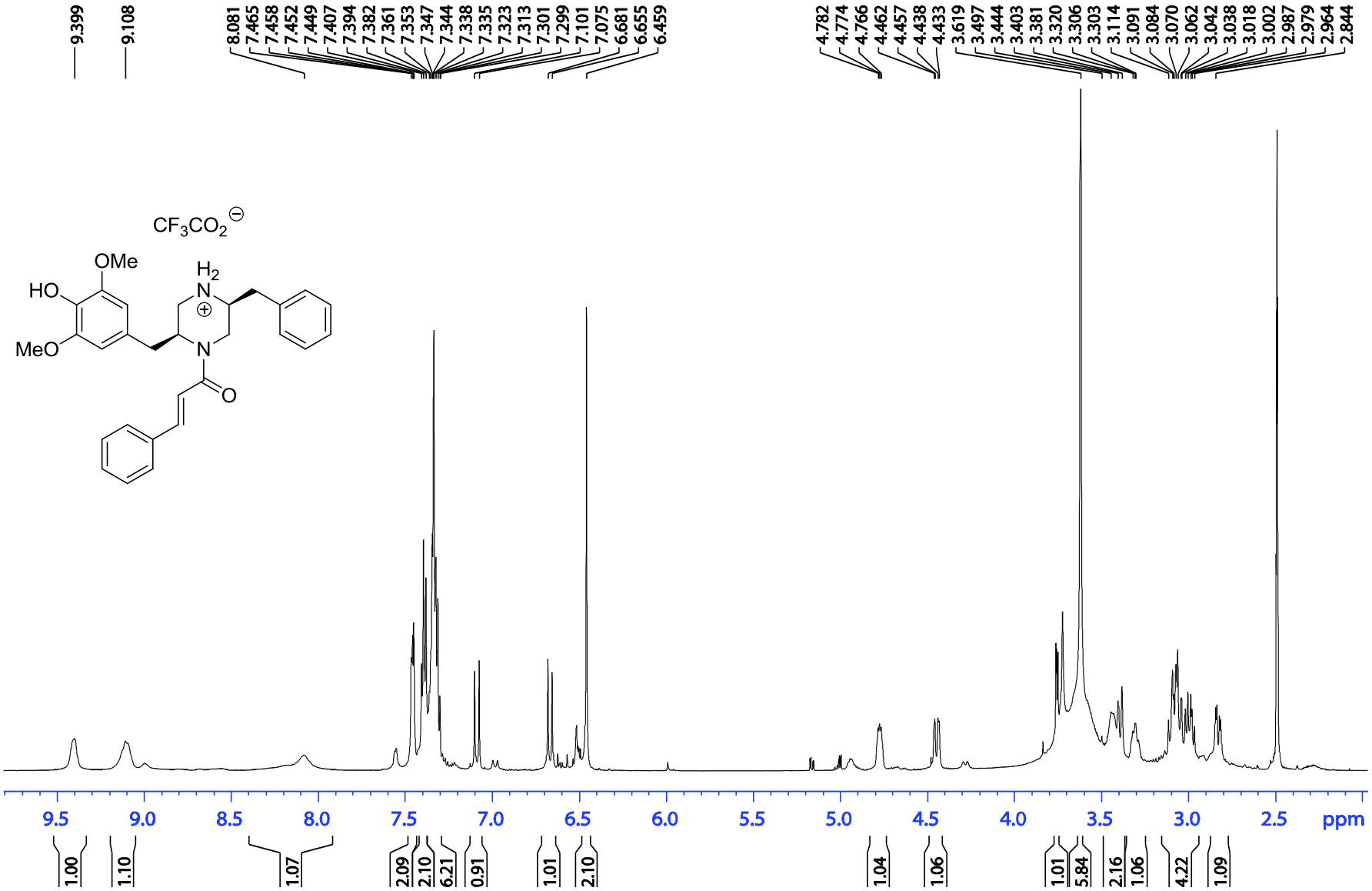

Figure S19. ^{1}H NMR spectrum (600 MHz, DMSO-d_6) of hancockiamide A (**1**) TFA salt

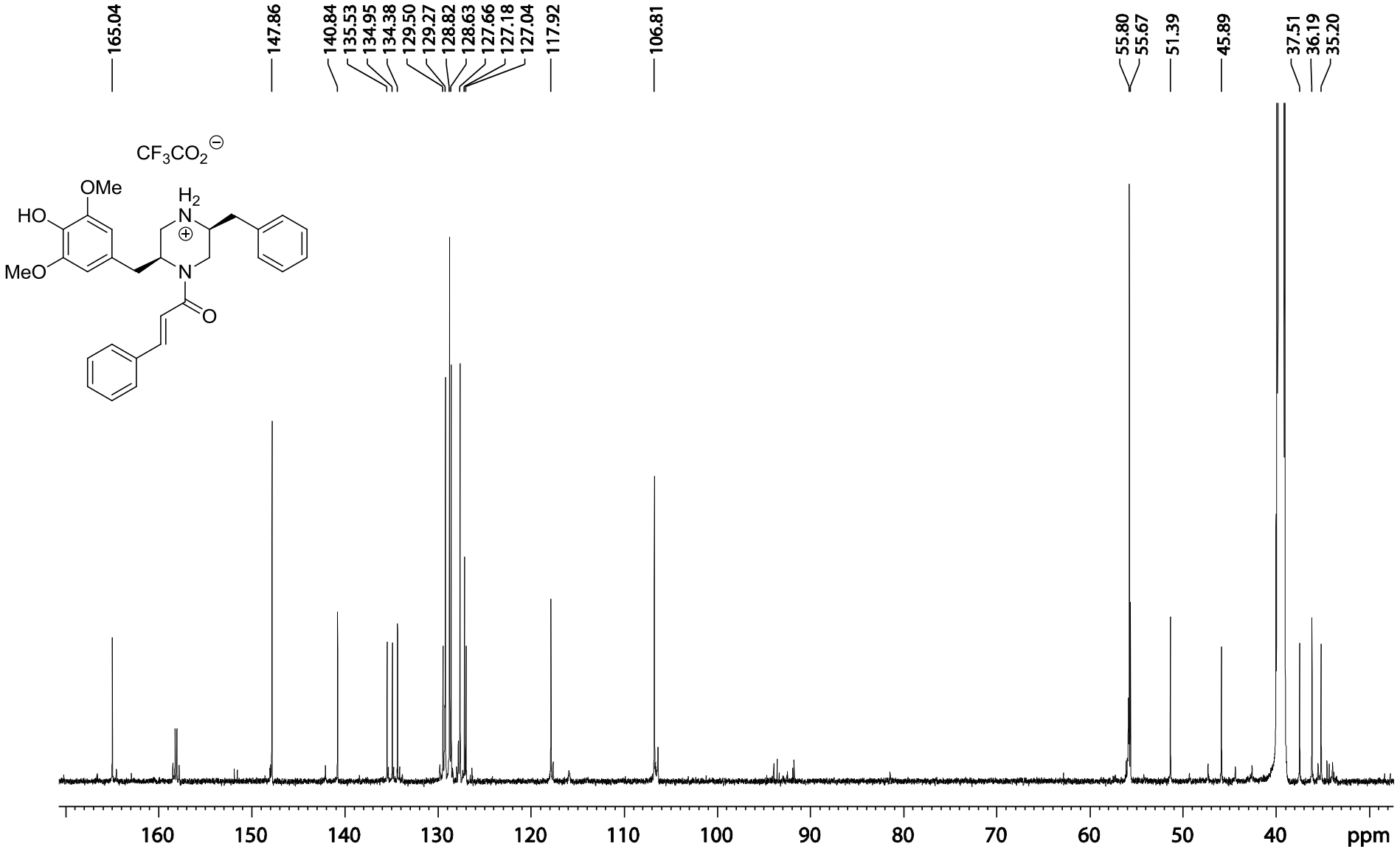

Figure S20. ^{13}C NMR spectrum (150 MHz, DMSO-d_6) of hancockiamide A (**1**) TFA salt

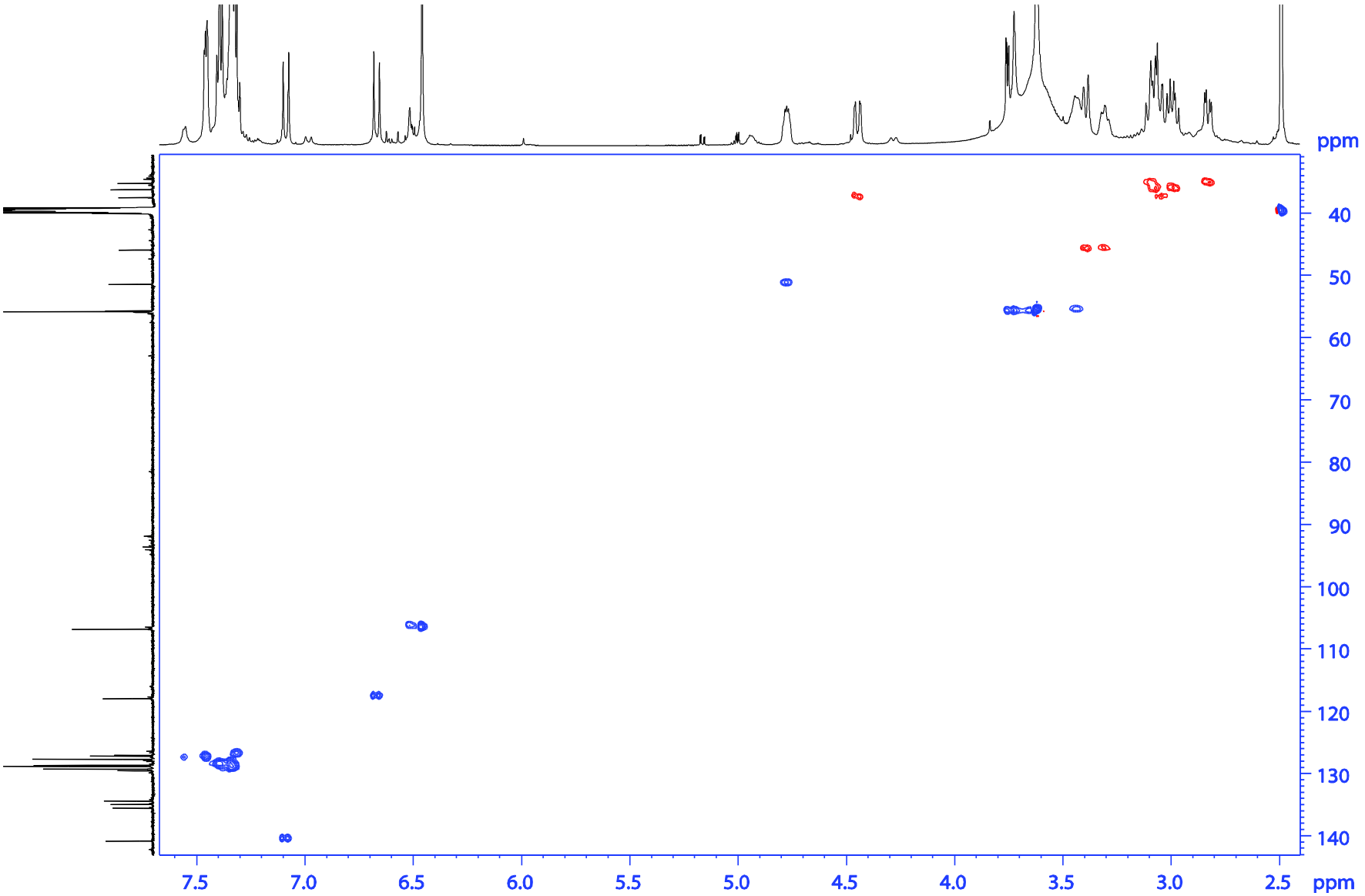

Figure S21. ^{1}H-^{13}C HSQC spectrum (600 MHz, DMSO-d_6) of hancockiamide A (**1**) TFA salt

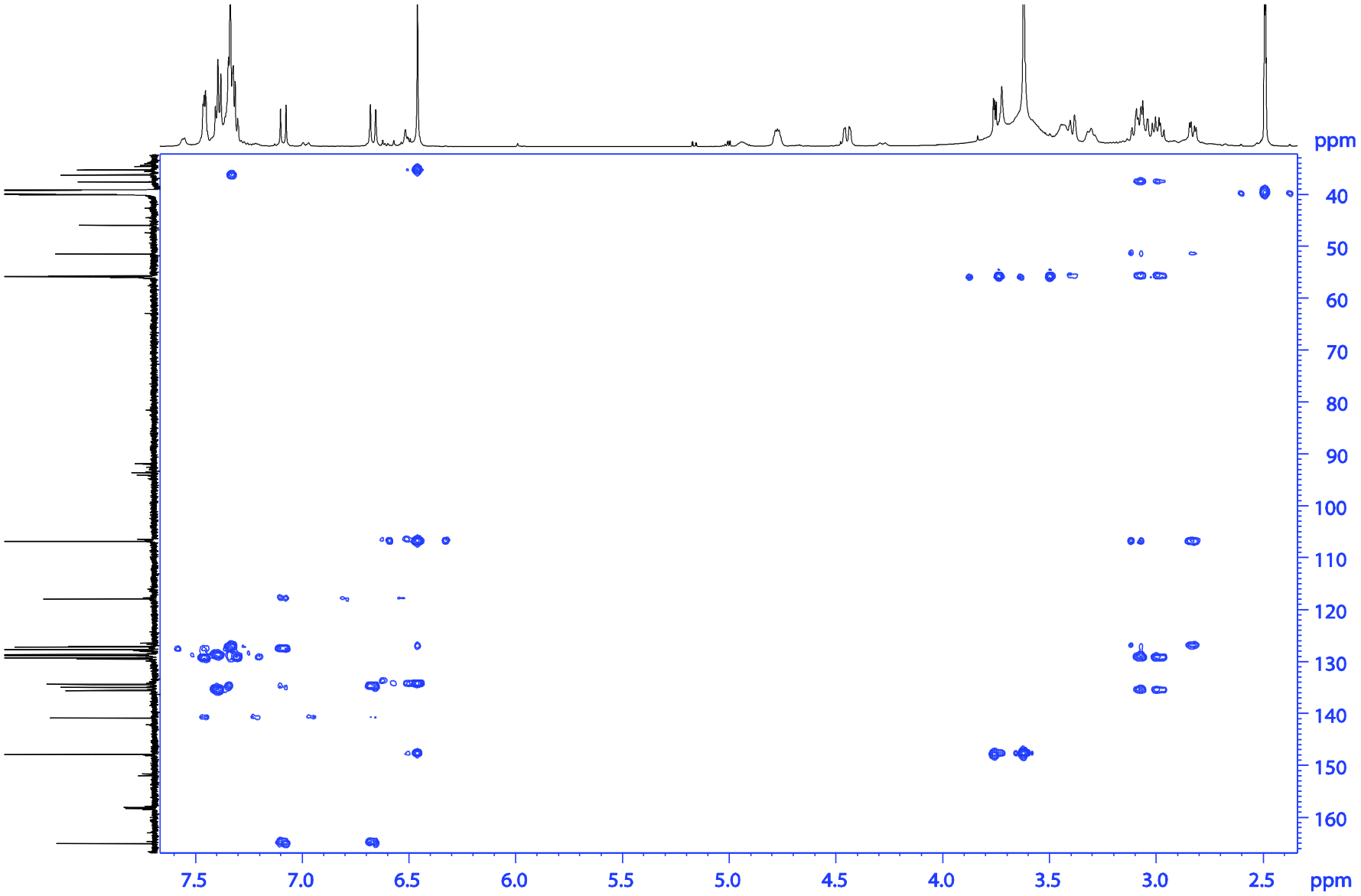

Figure S22. ^{1}H-^{13}C HMBC NMR spectrum (600 MHz, DMSO-d_6) of hancockiamide A (**1**) TFA salt

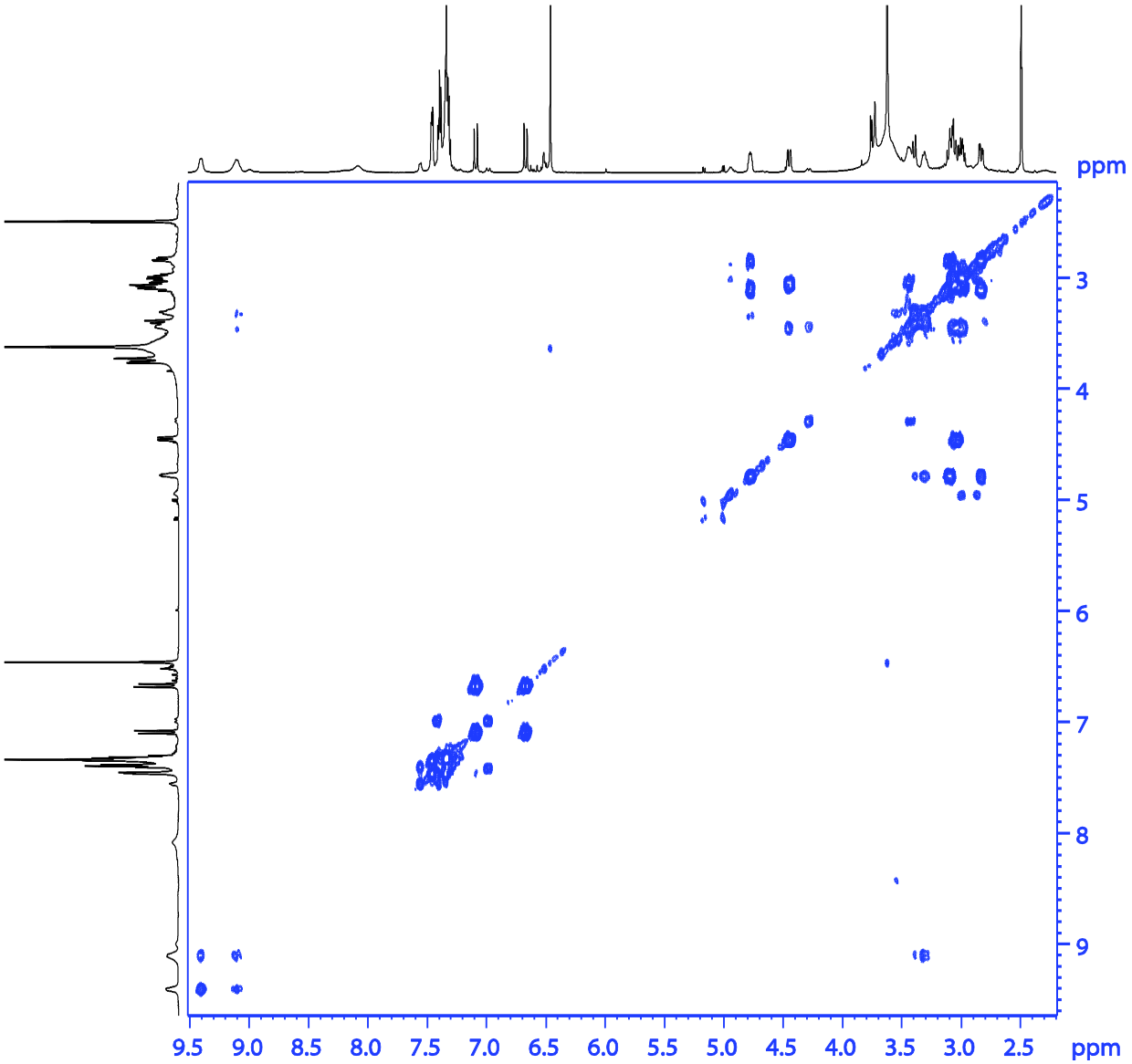

Figure S23. COSY NMR spectrum (600 MHz, DMSO-d_6) of hancockiamide A (**1**) TFA salt

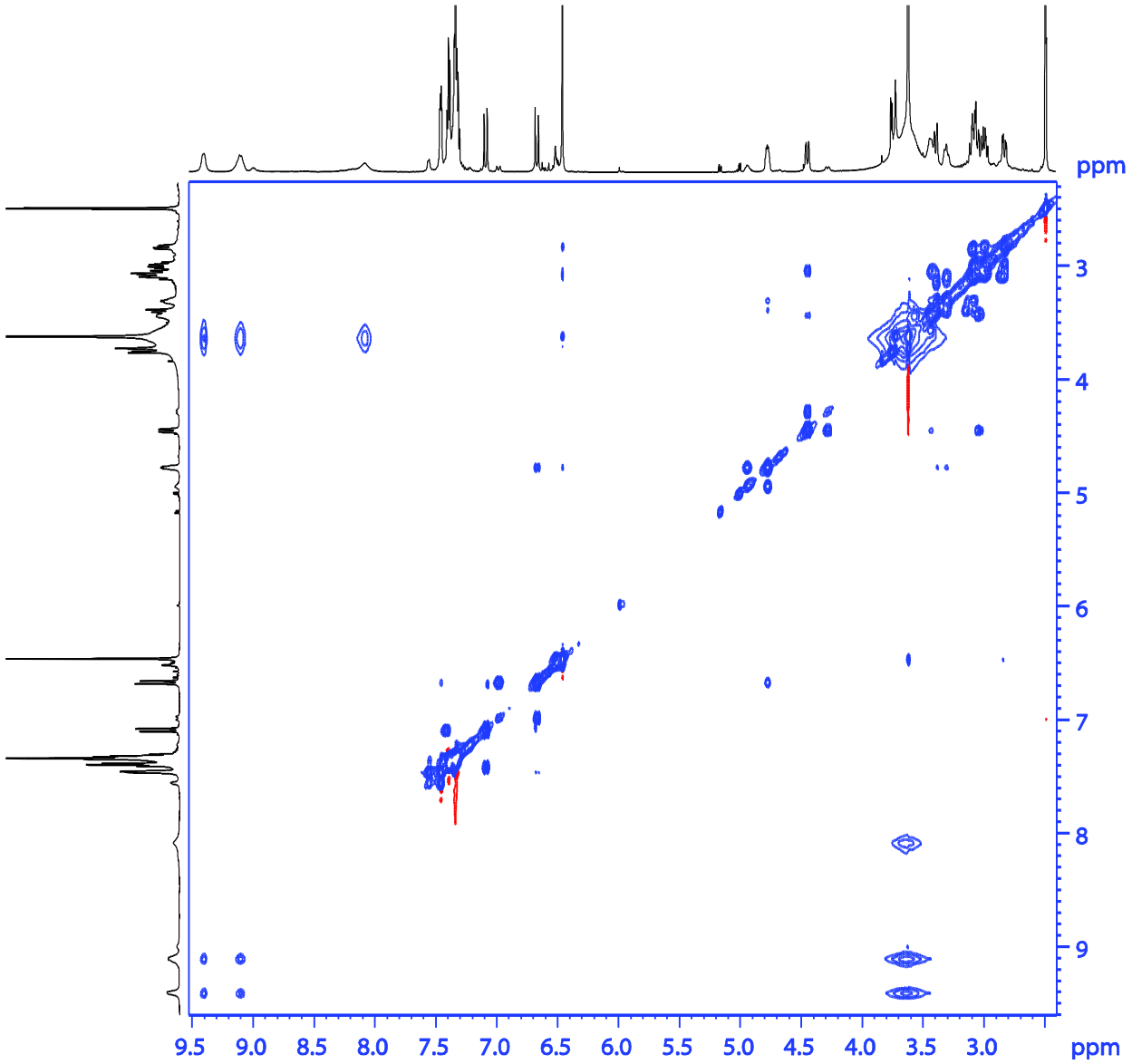

Figure S24. NOESY NMR spectrum (600 MHz, DMSO-d_6) of hancockiamide A (**1**) TFA salt

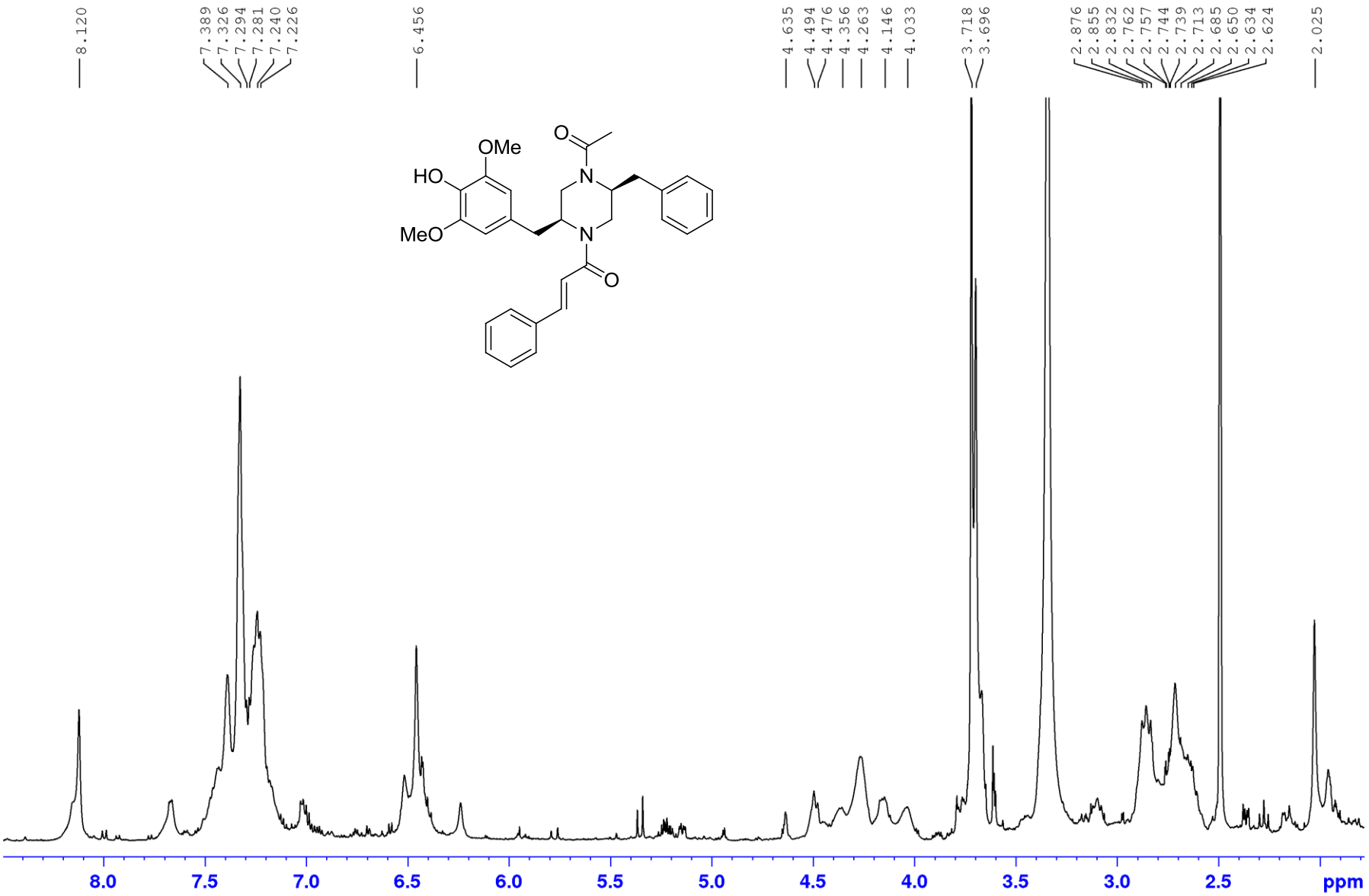

Figure S25. ^{1}H NMR spectrum (600 MHz, DMSO-d_6) of hancockiamide B (**2**)

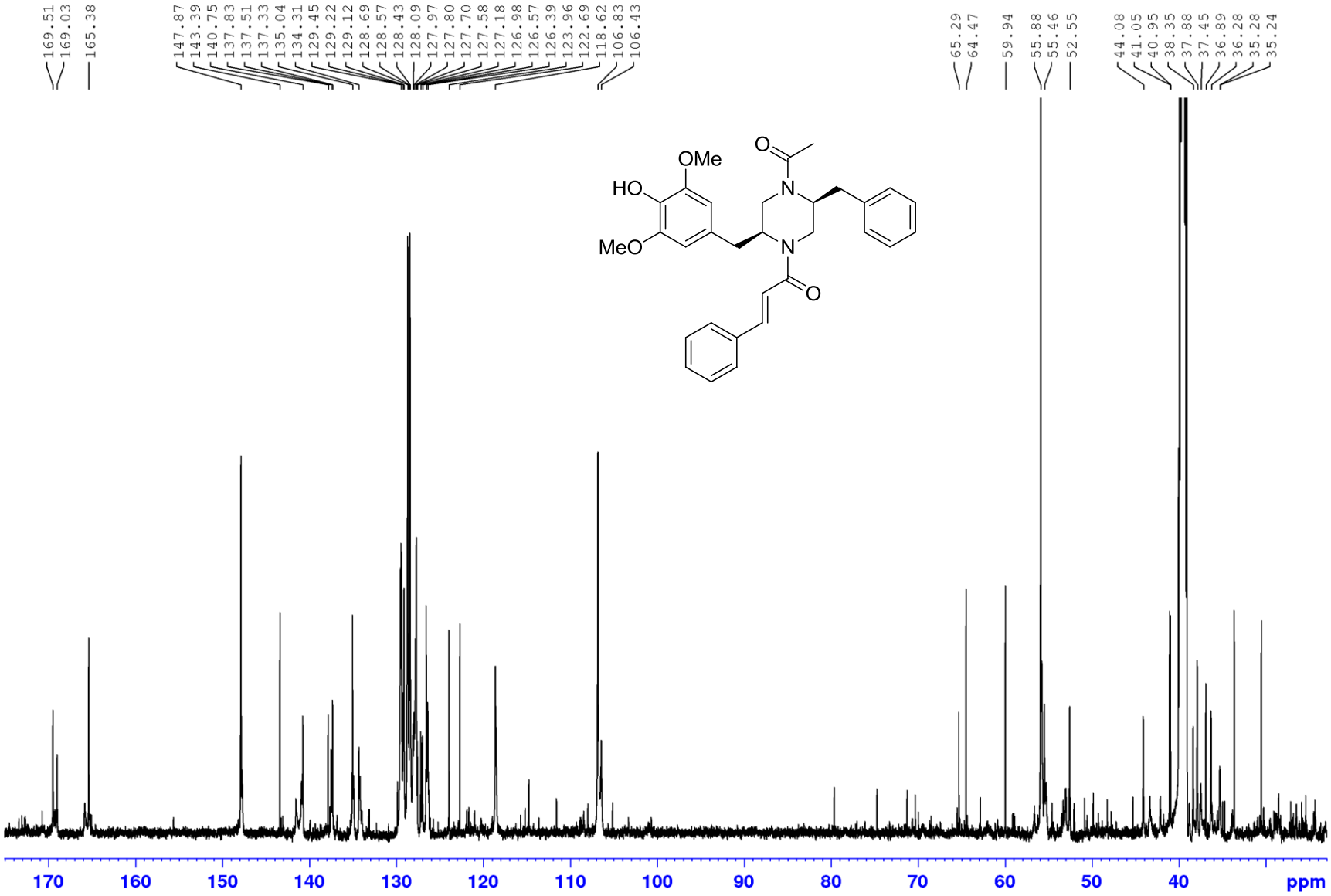

Figure S26. ^{13}C NMR spectrum (150 MHz, DMSO-d_6) of hancockiamide B (**2**)

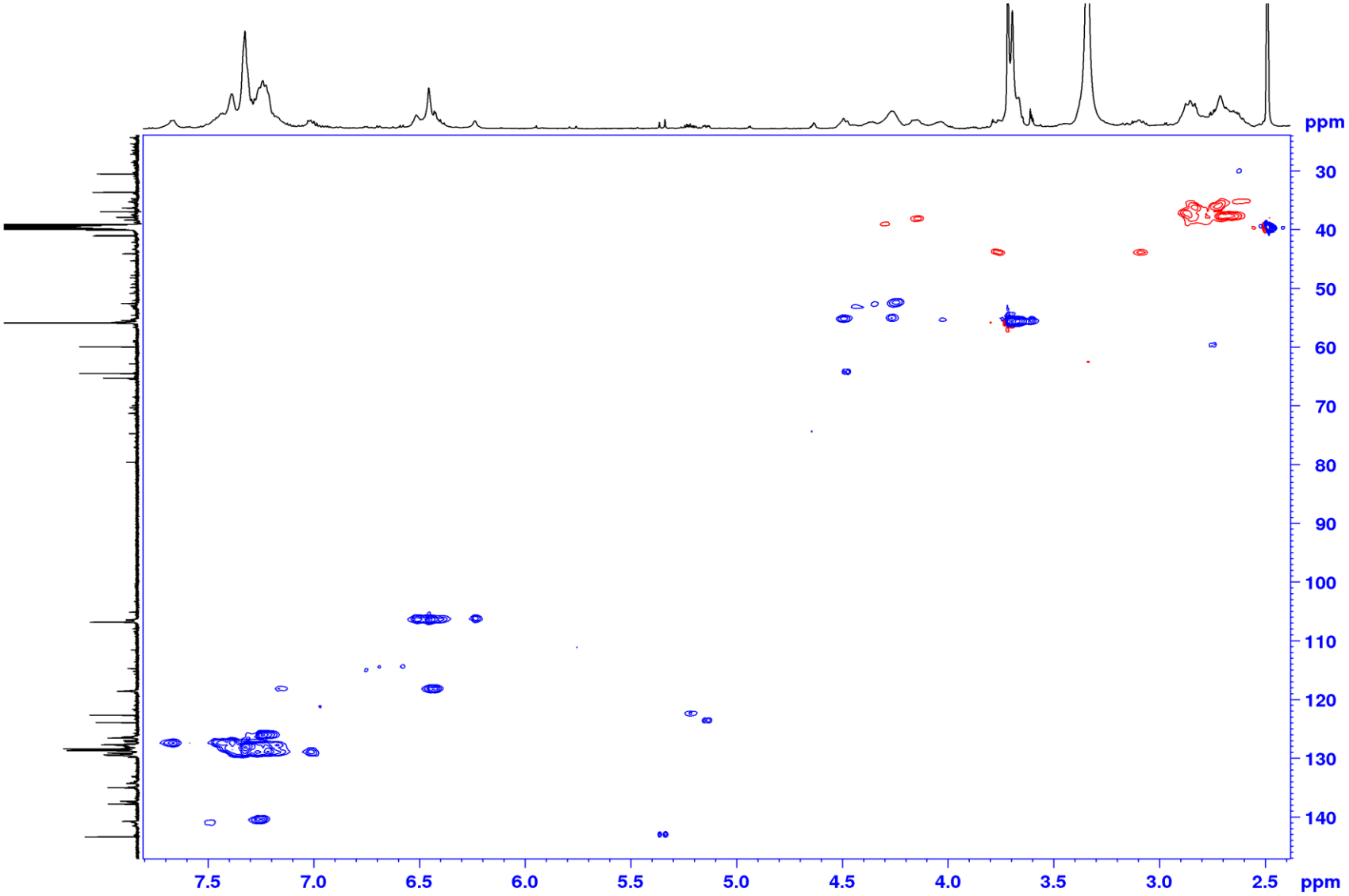

Figure S27. ^{1}H-^{13}C HSQC spectrum (600 MHz, DMSO-d_6) of hancockiamide B (**2**)

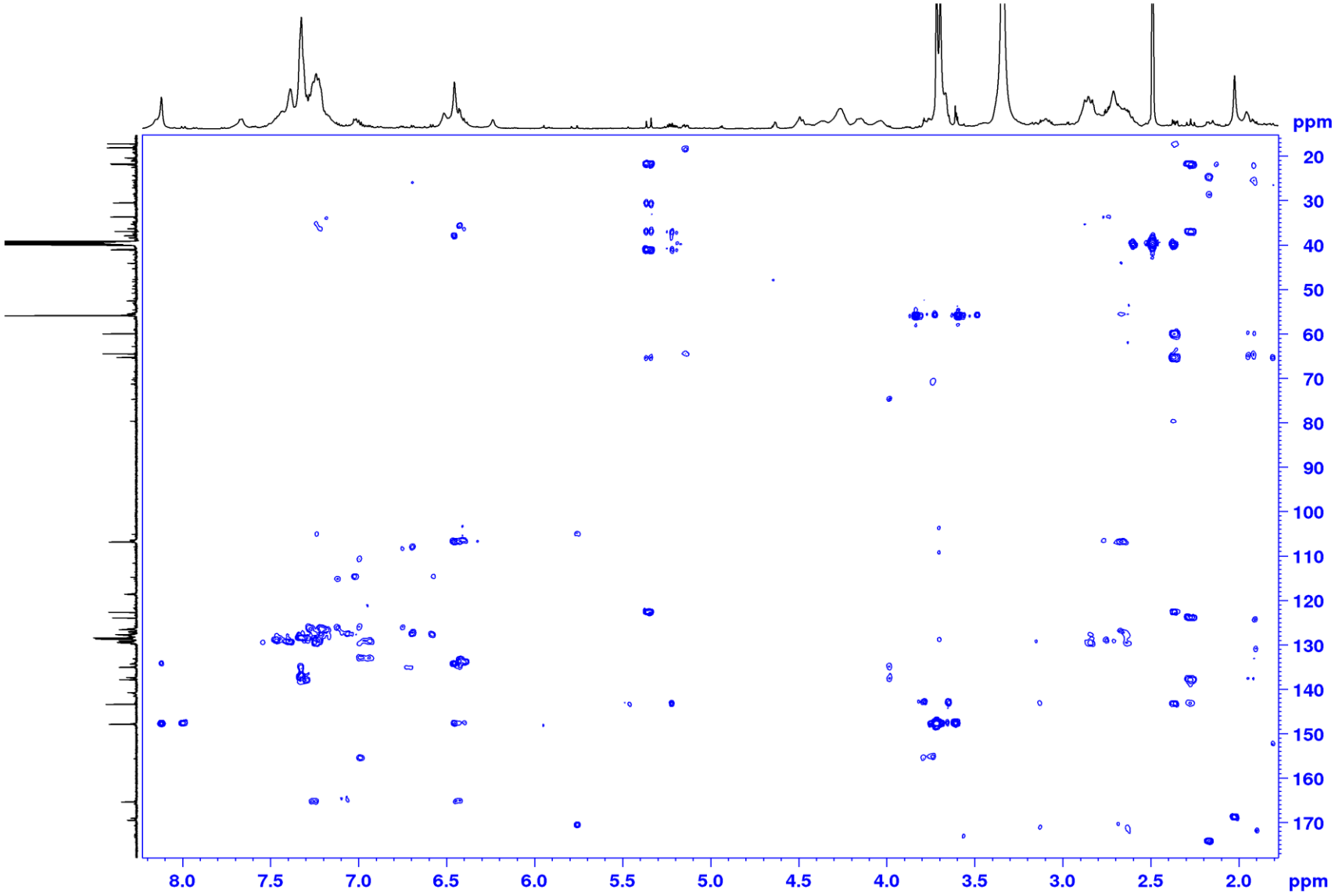

Figure S28. ^{1}H-^{13}C HMBC spectrum (600 MHz, DMSO-d_6) of hancockiamide B (**2**)

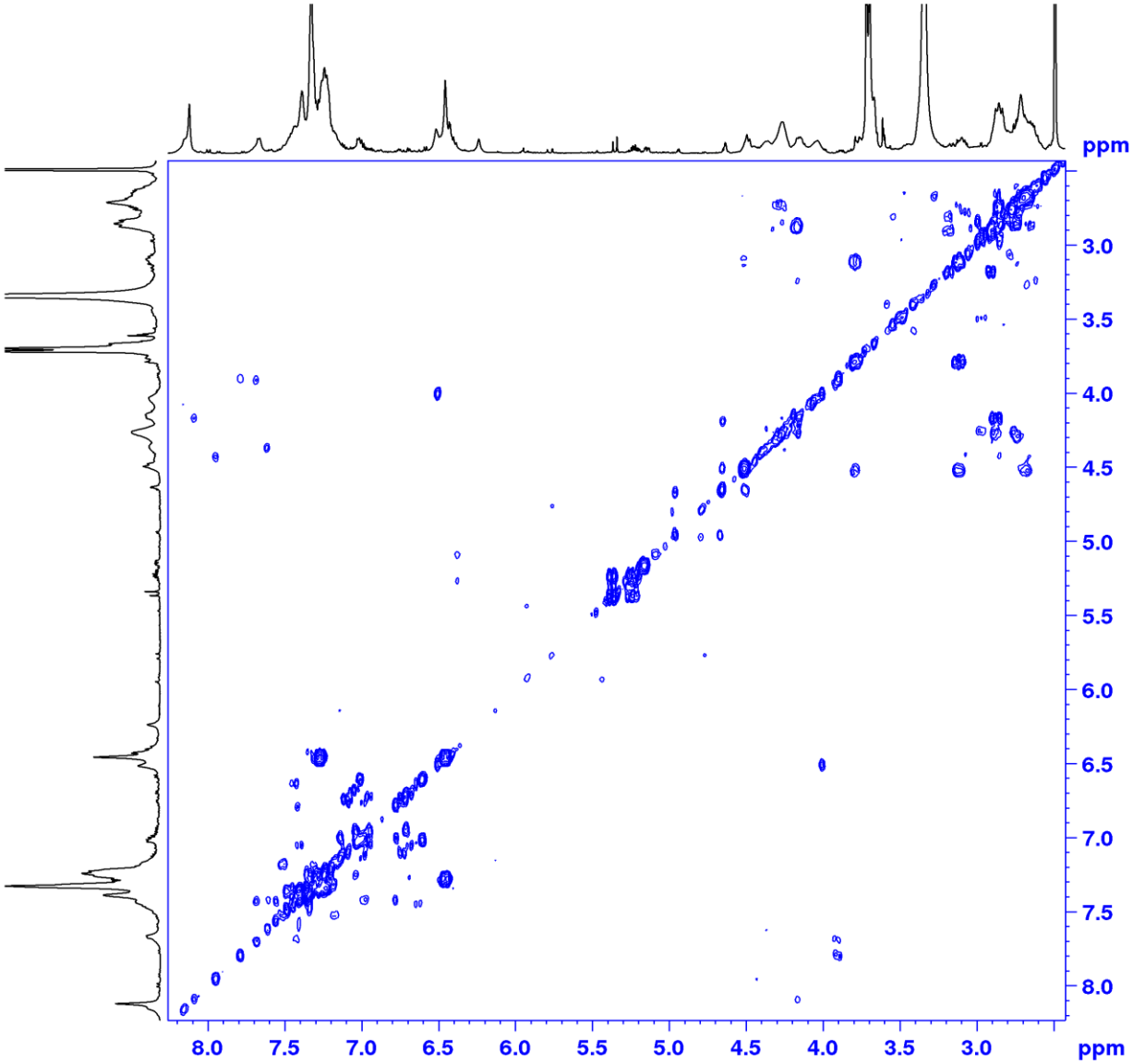

Figure S29. COSY spectrum (600 MHz, DMSO-d_6) of hancockiamide B (**2**)

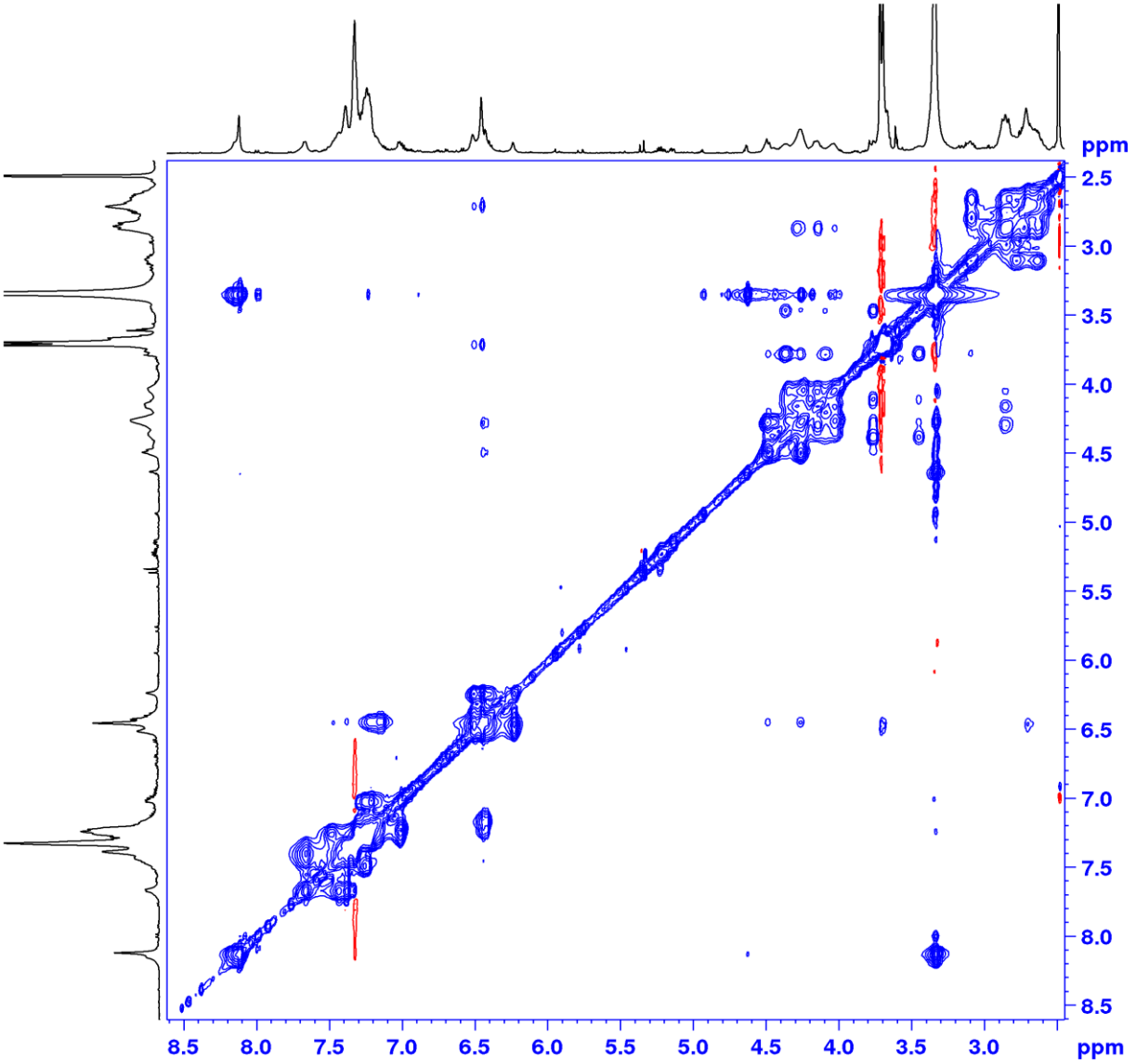

Figure S30. NOESY spectrum (600 MHz, DMSO-d_6) of hancockiamide B (**2**)

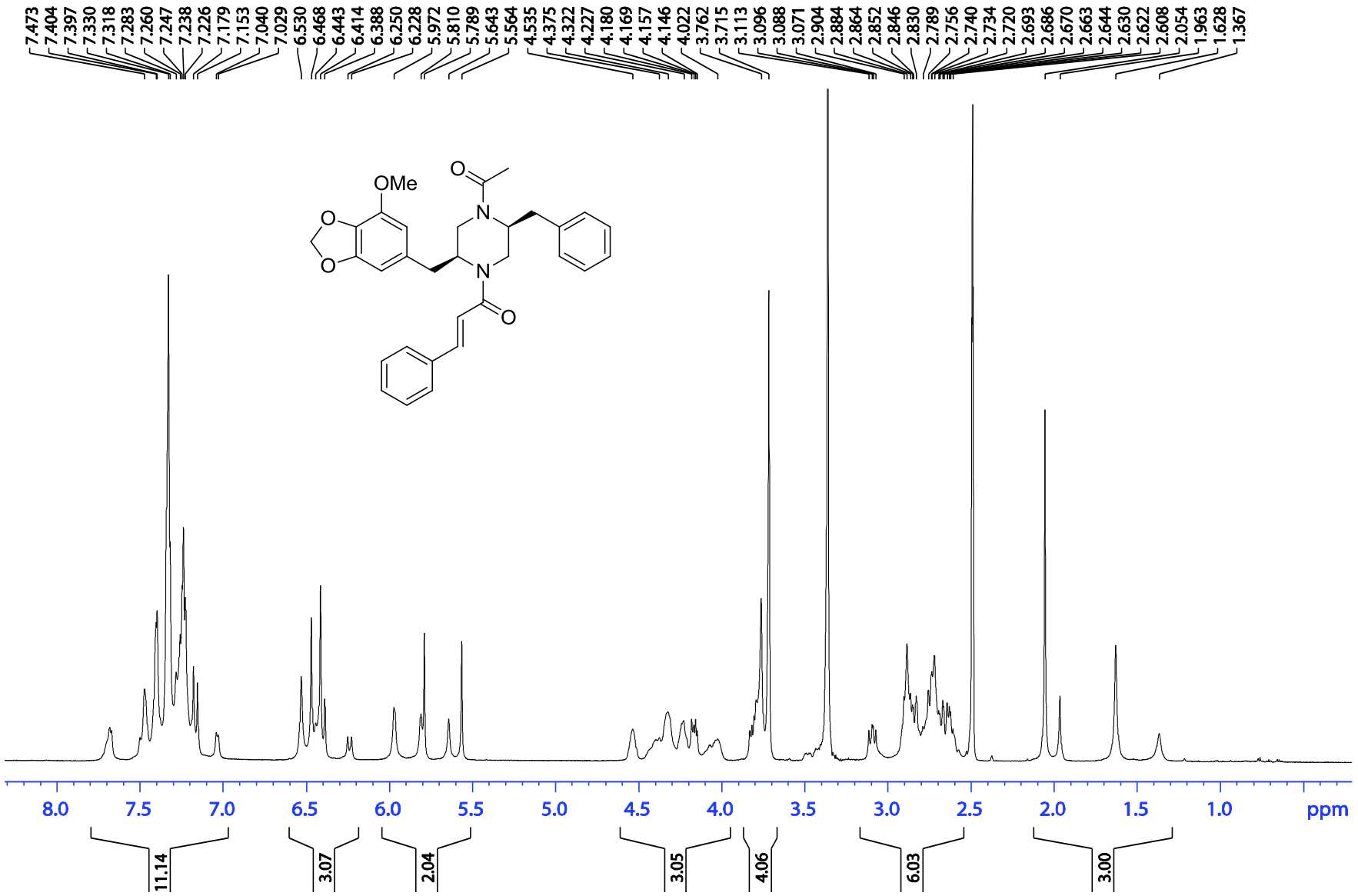

Figure S31. ^{1}H NMR spectrum (600 MHz, DMSO-d_6) of hancockiamide C (**3**)

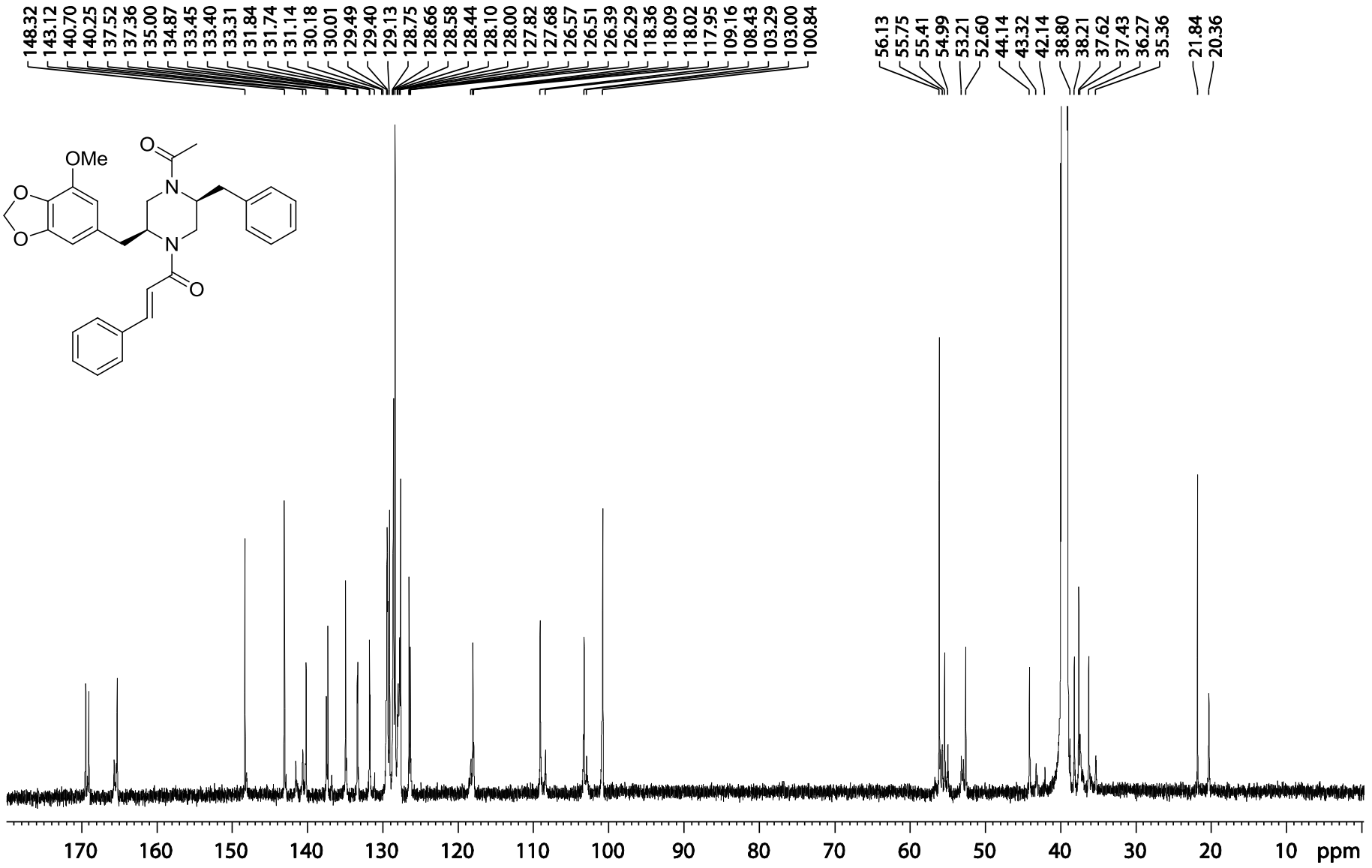

Figure S32. ^{13}C NMR spectrum (150 MHz, DMSO-d_6) of hancockiamide C (**3**)

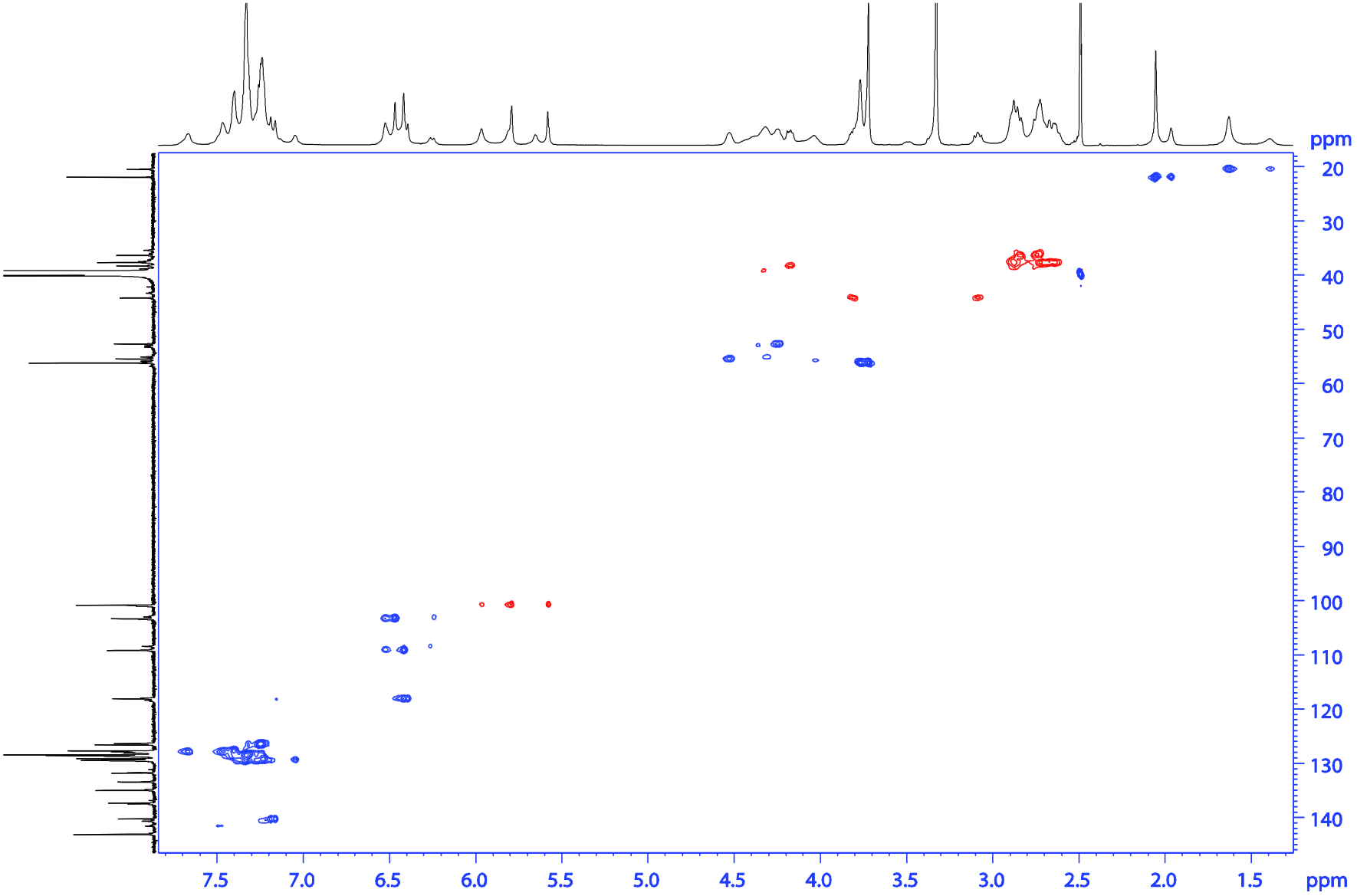

Figure S33. ^{1}H-^{13}C HSQC spectrum (600 MHz, DMSO-d_6) of hancockiamide C (**3**)

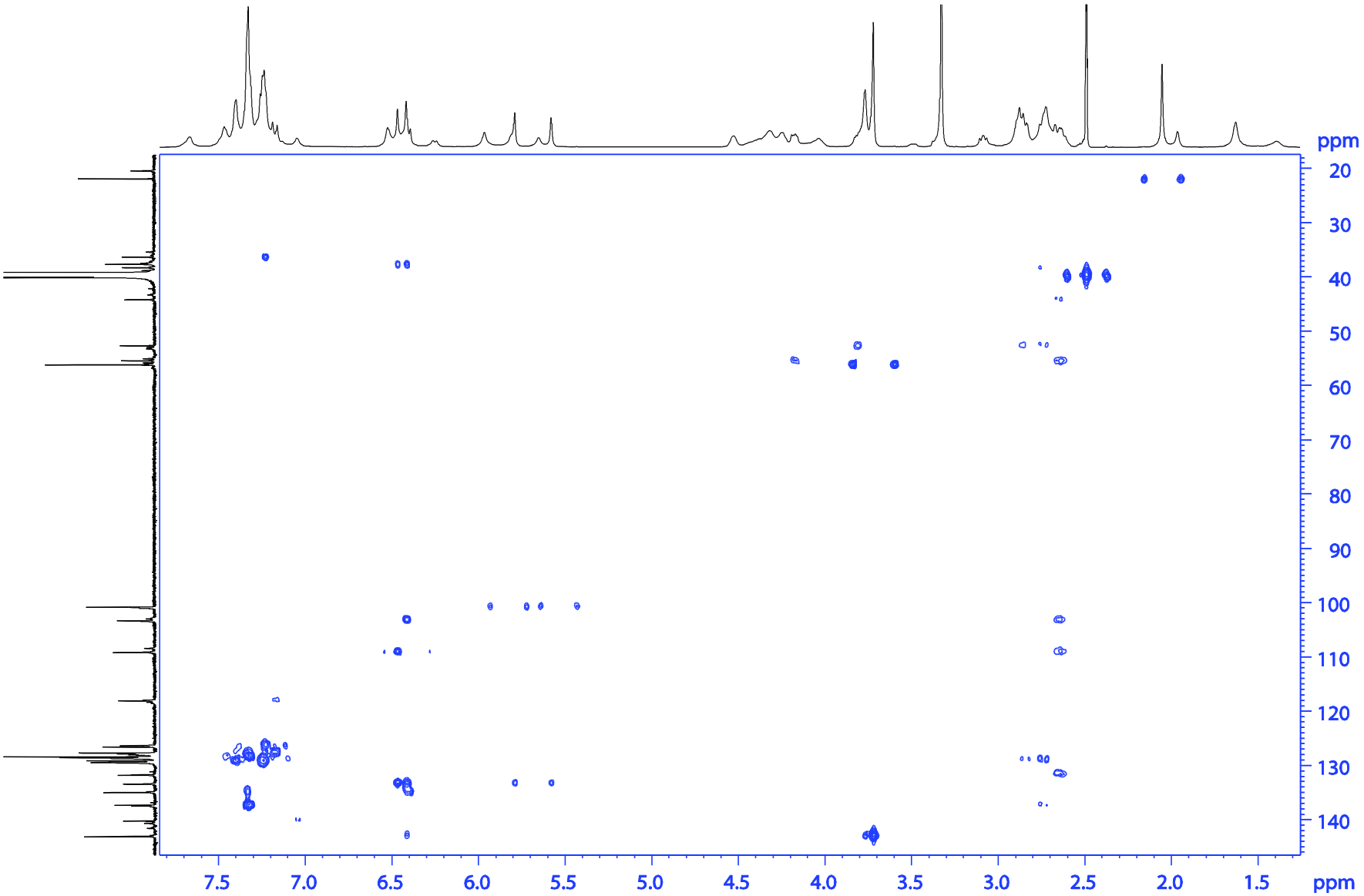

Figure S34. ^{1}H-^{13}C HMBC spectrum (600 MHz, DMSO-d_6) of hancockiamide C (**3**)

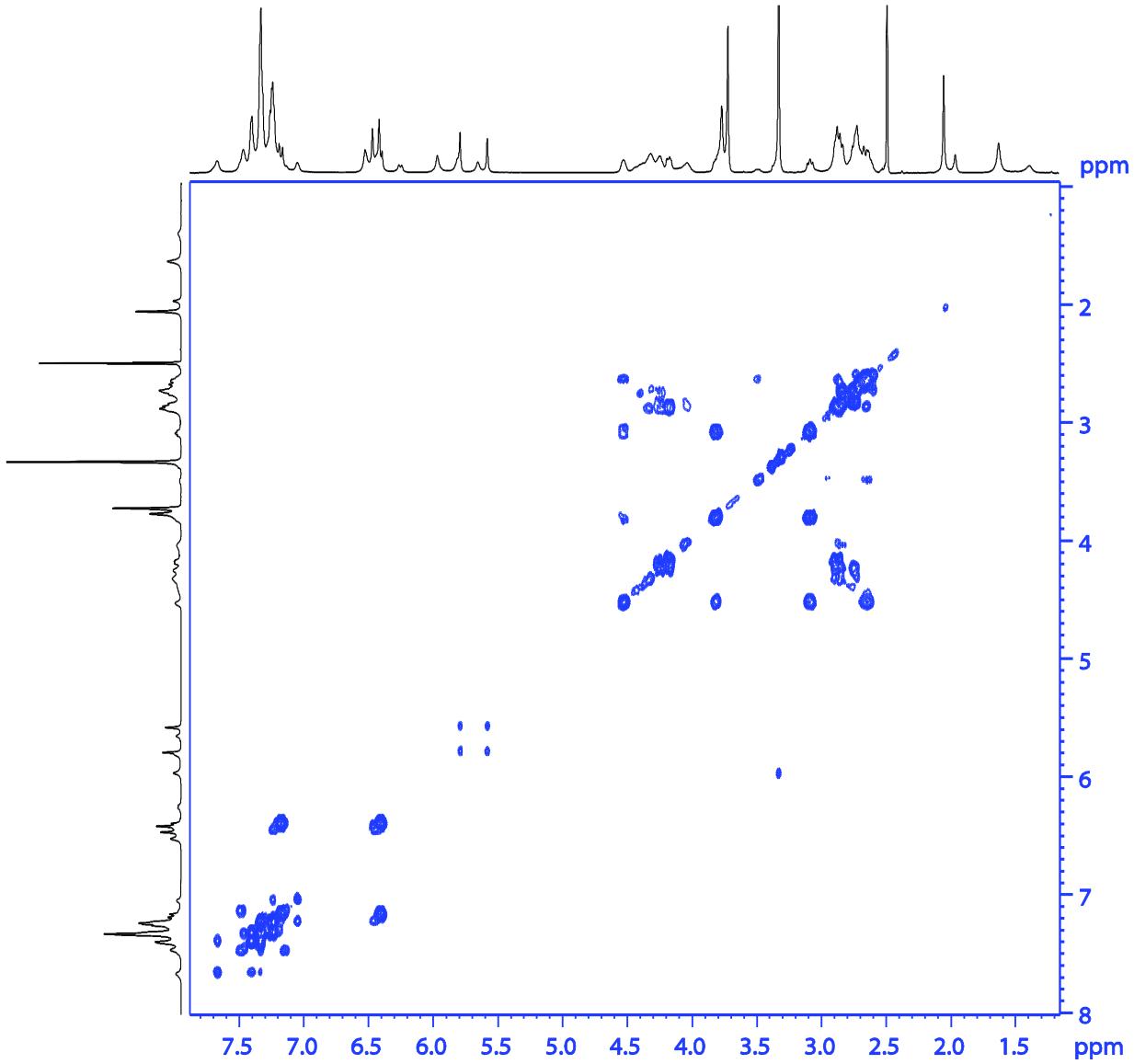

Figure S35. COSY spectrum (600 MHz, DMSO-d_6) of hancockiamide C (**3**)

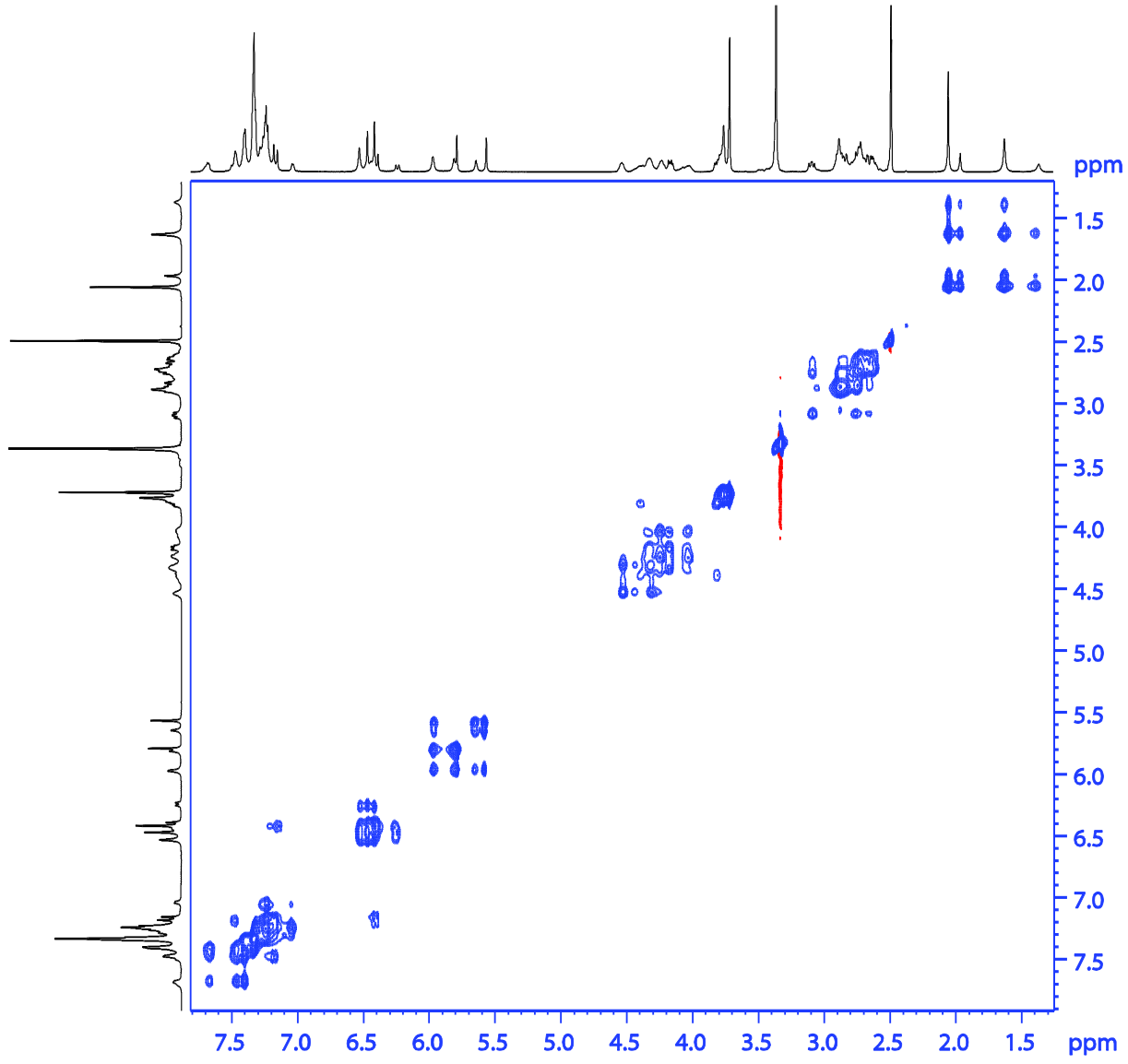

Figure S36. NOESY spectrum (600 MHz, DMSO-d_6) of hancockiamide C (**3**)

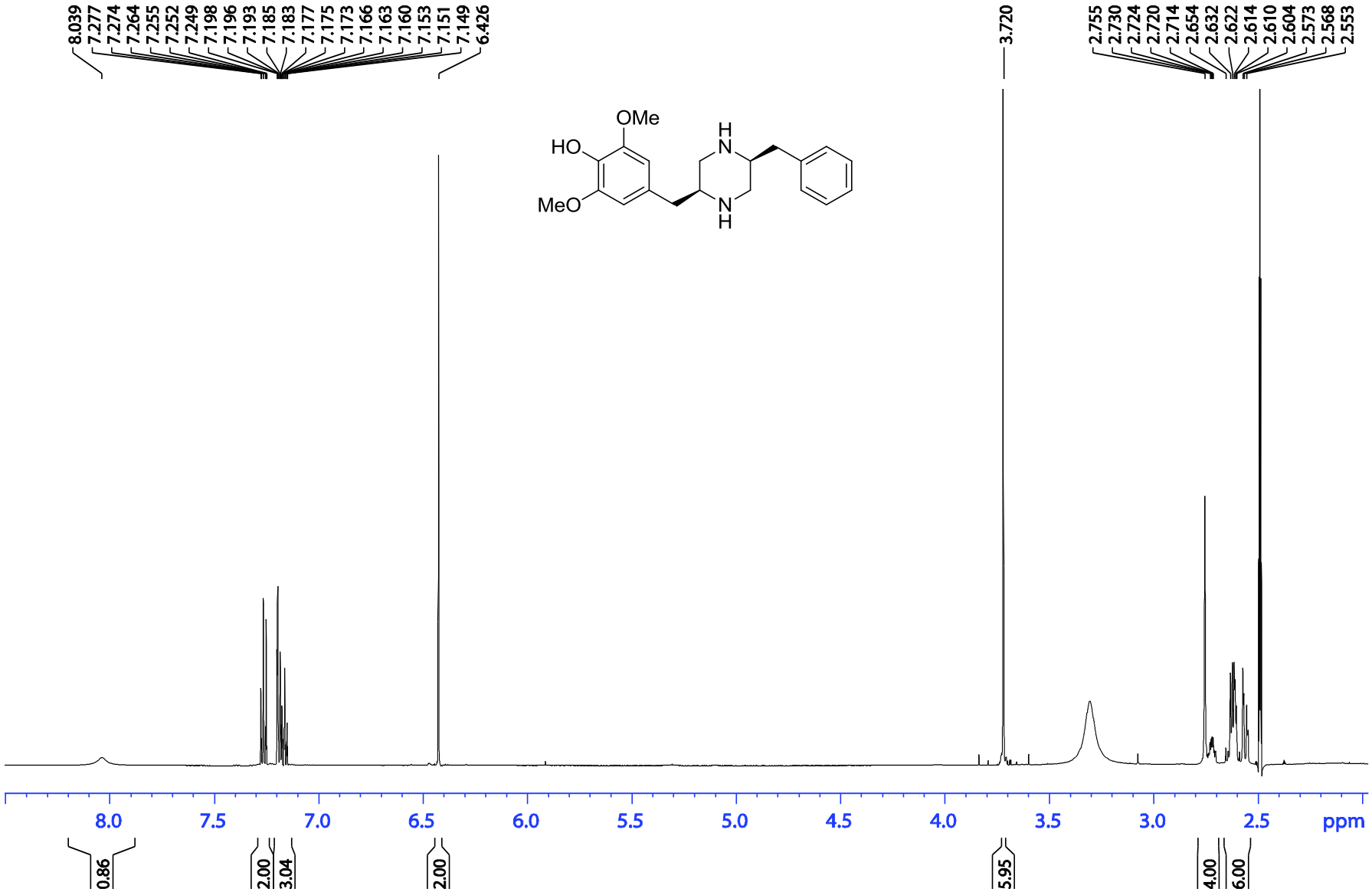

Figure S37. ^{1}H NMR spectrum (600 MHz, DMSO-d_6) of hancockiamide D (**4**)

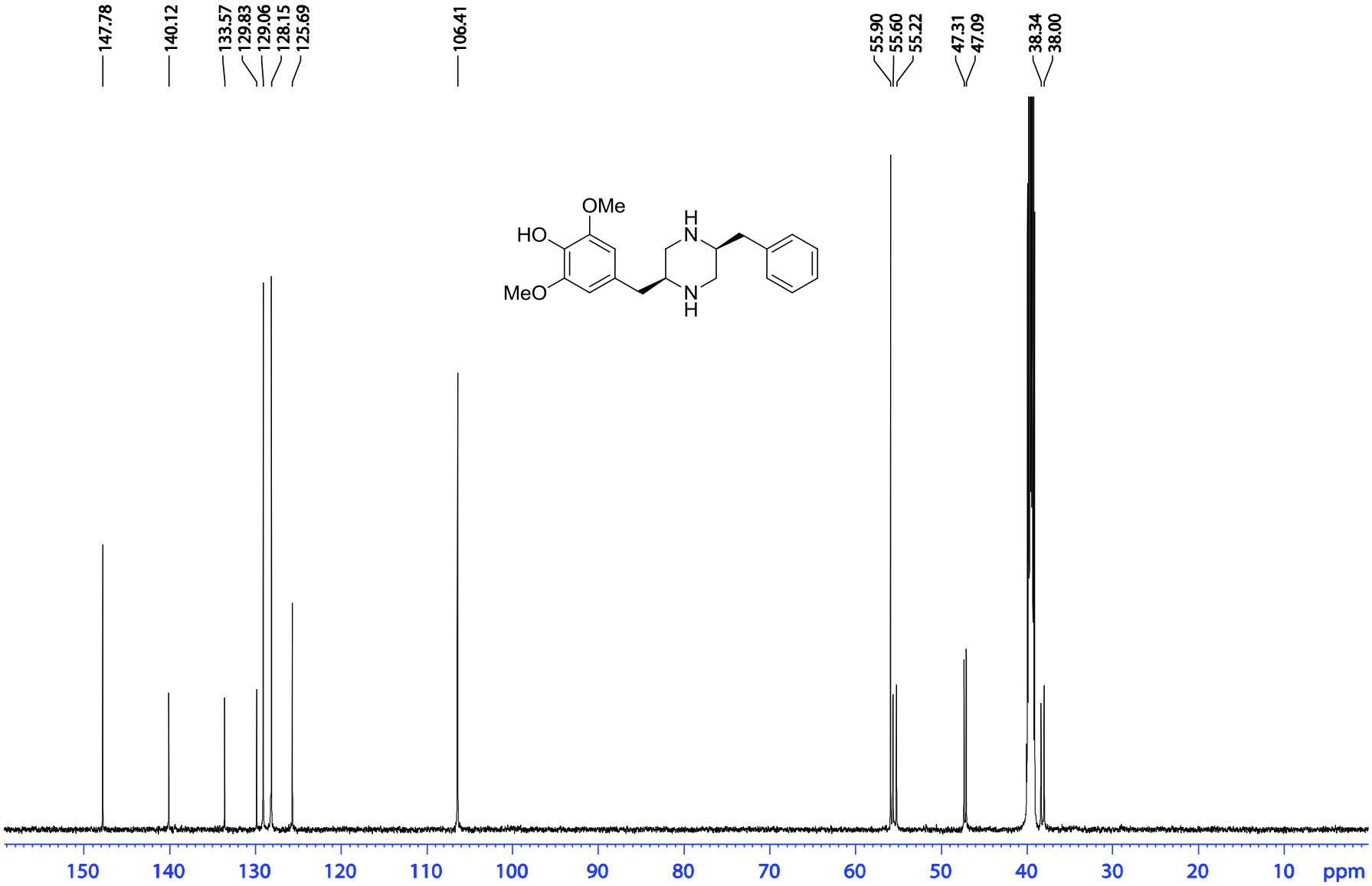

Figure S38. ^{13}C NMR spectrum (150 MHz, DMSO-d_6) of hancockiamide D (**4**)

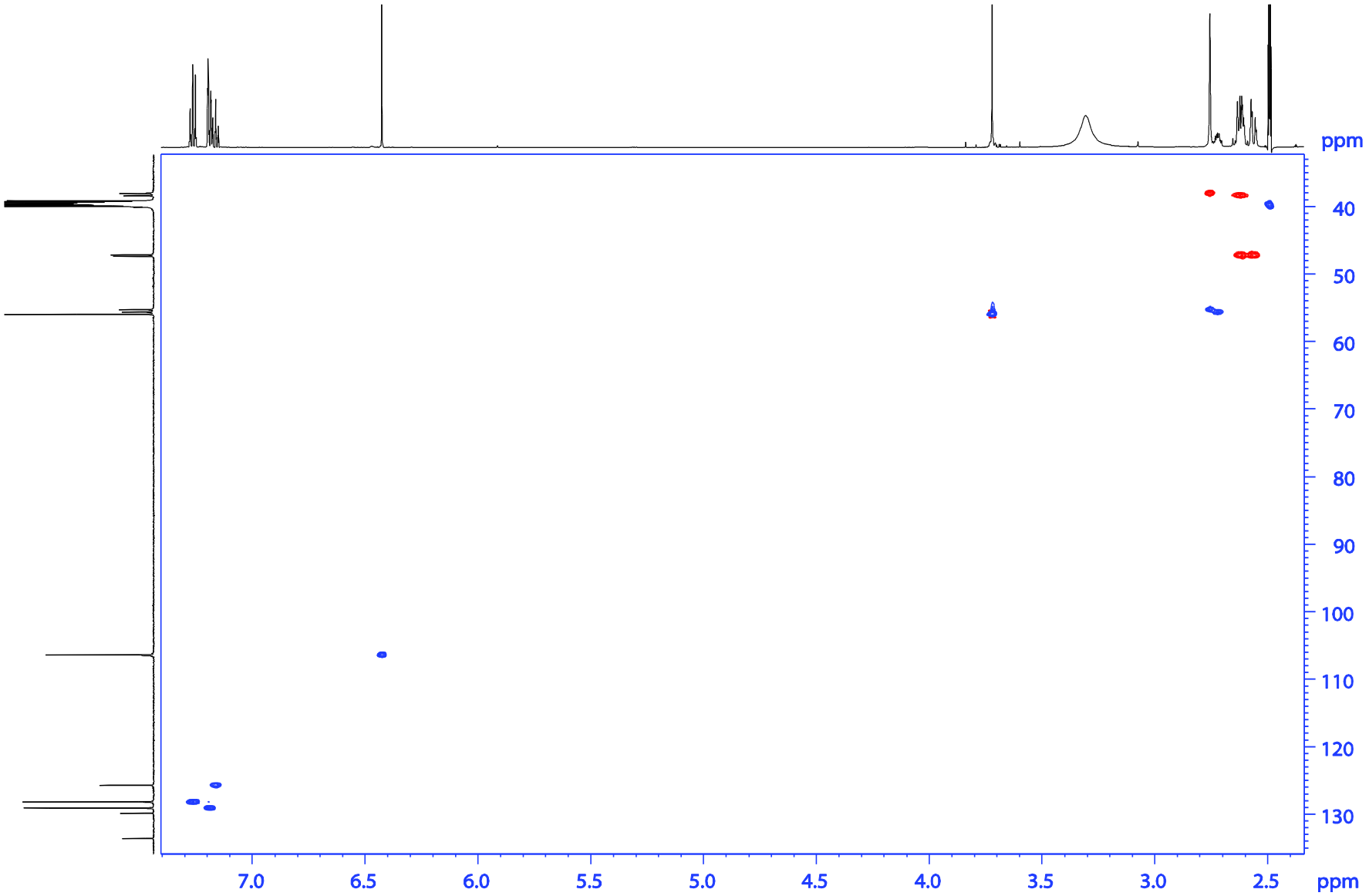

Figure S39. ^{1}H-^{13}C HSQC spectrum (600 MHz, DMSO-d_6) of hancockiamide D (**4**)

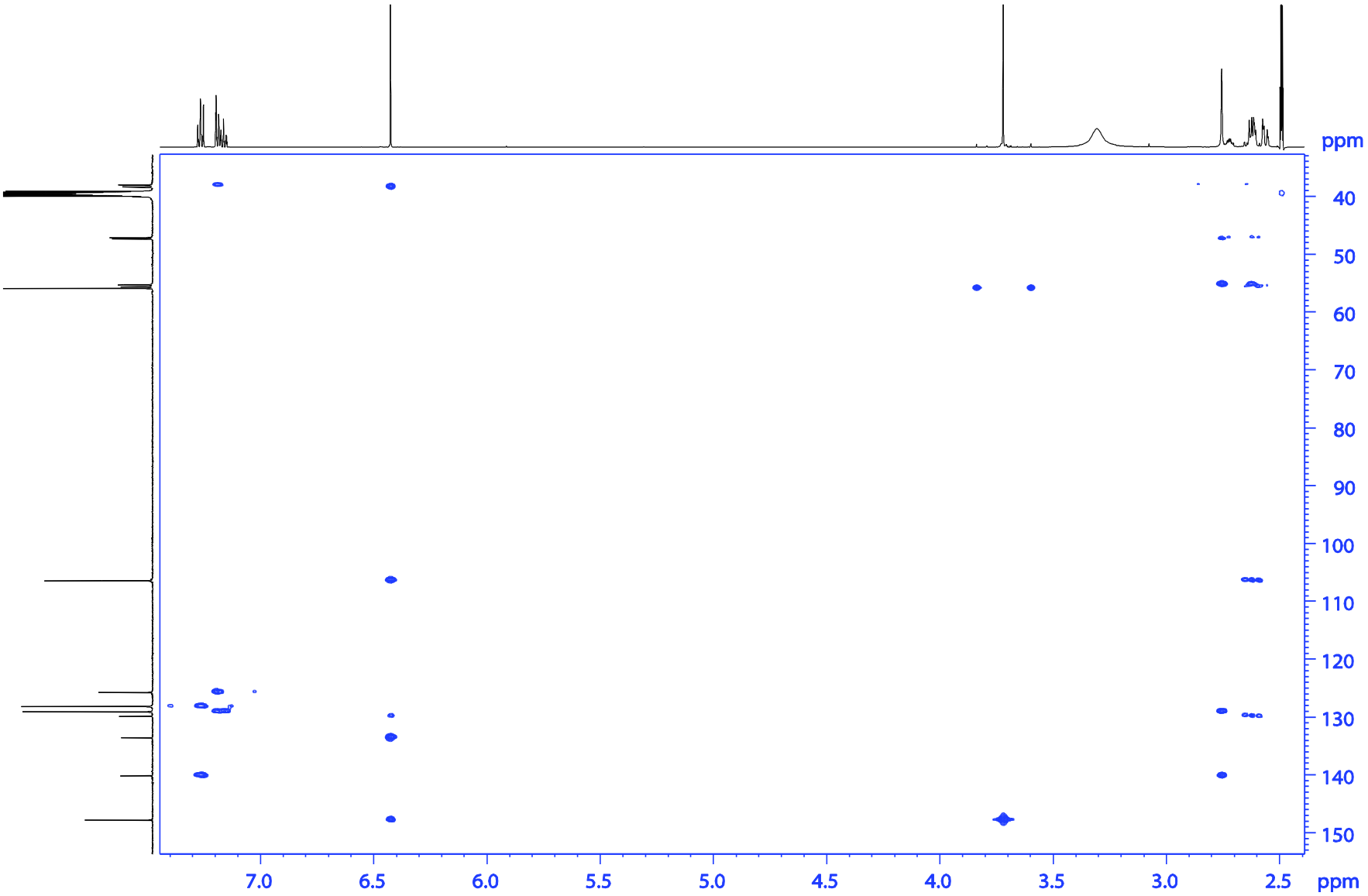

Figure S40. ^{1}H-^{13}C HMBC spectrum (600 MHz, DMSO-d_6) of hancockiamide D (**4**)

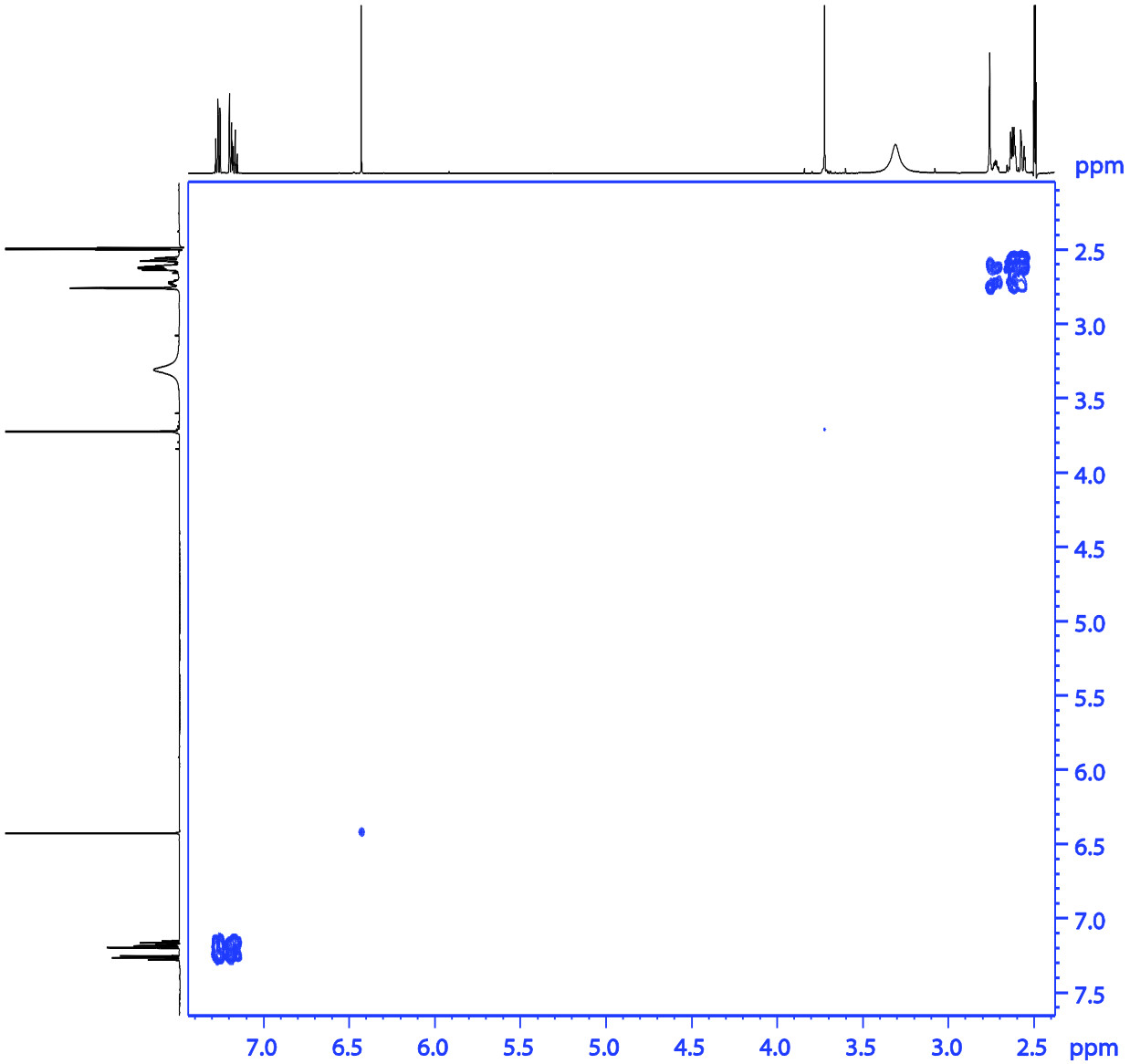

Figure S41. COSY spectrum (600 MHz, DMSO-d_6) of hancockiamide D (**4**)

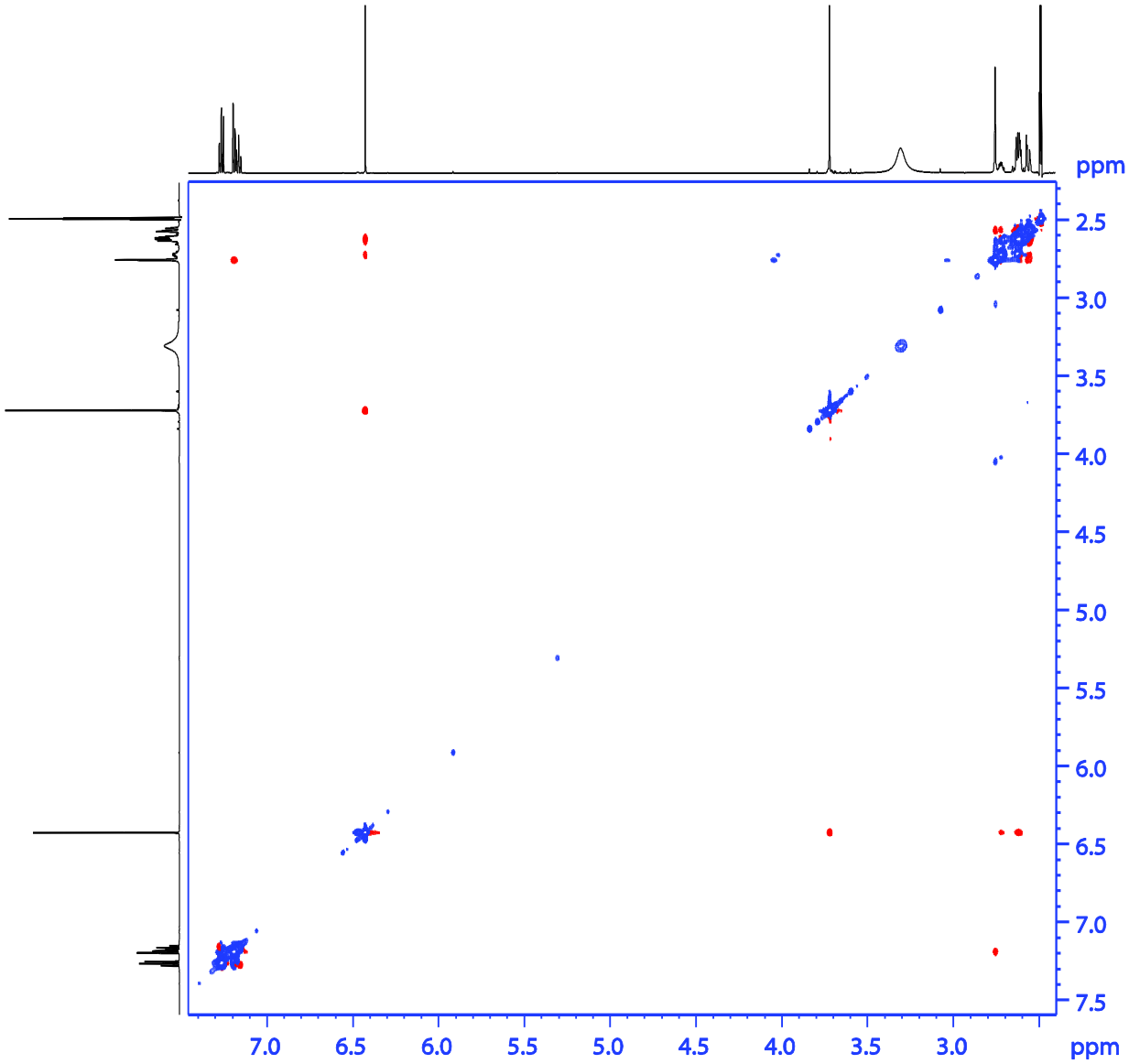

Figure S42. ROESY spectrum (600 MHz, DMSO-d_6) of hancockiamide D (**4**)

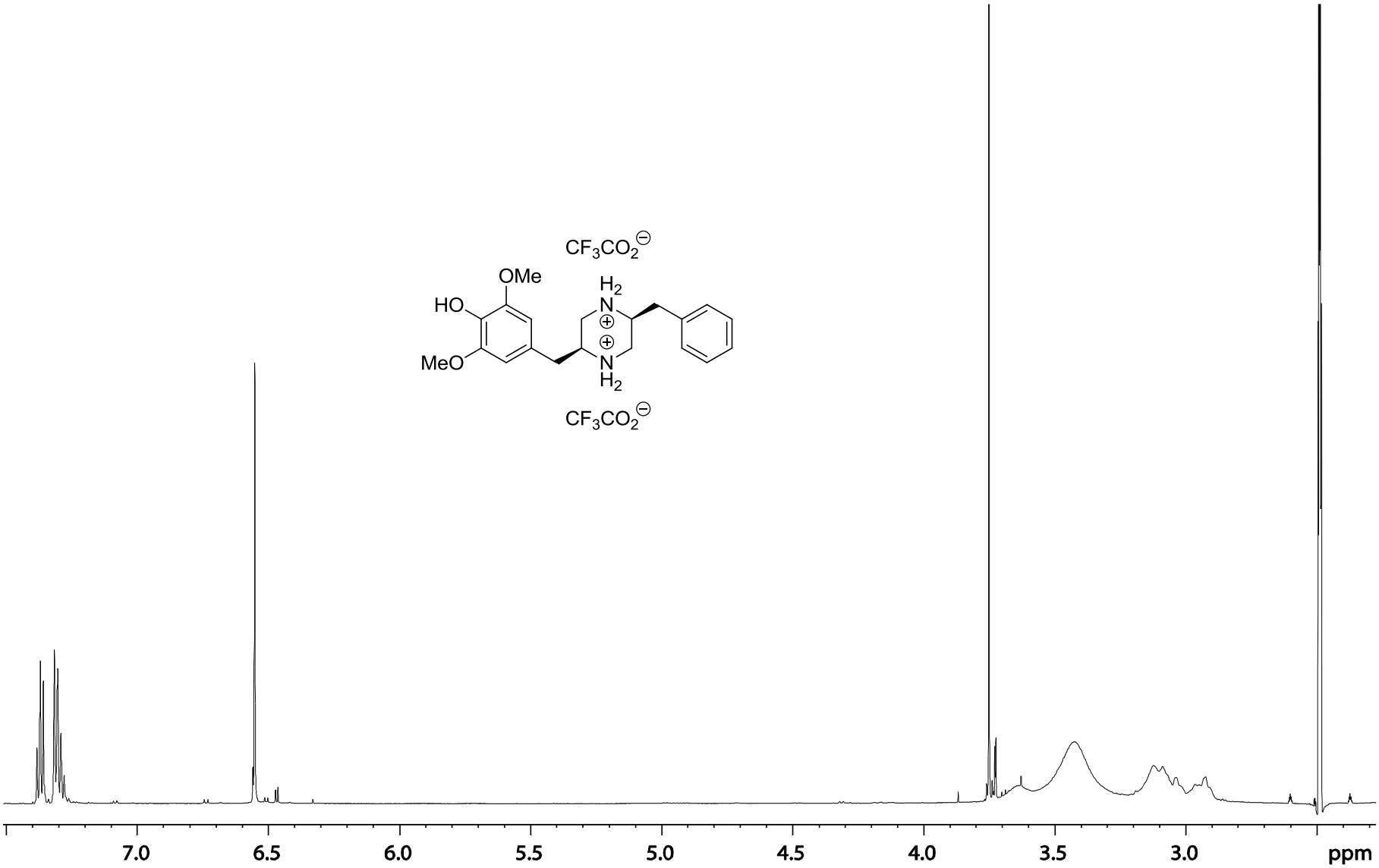

Figure S43. ^{1}H NMR spectrum (600 MHz, DMSO-d_6) of hancockiamide D di-TFA salt (**4**)

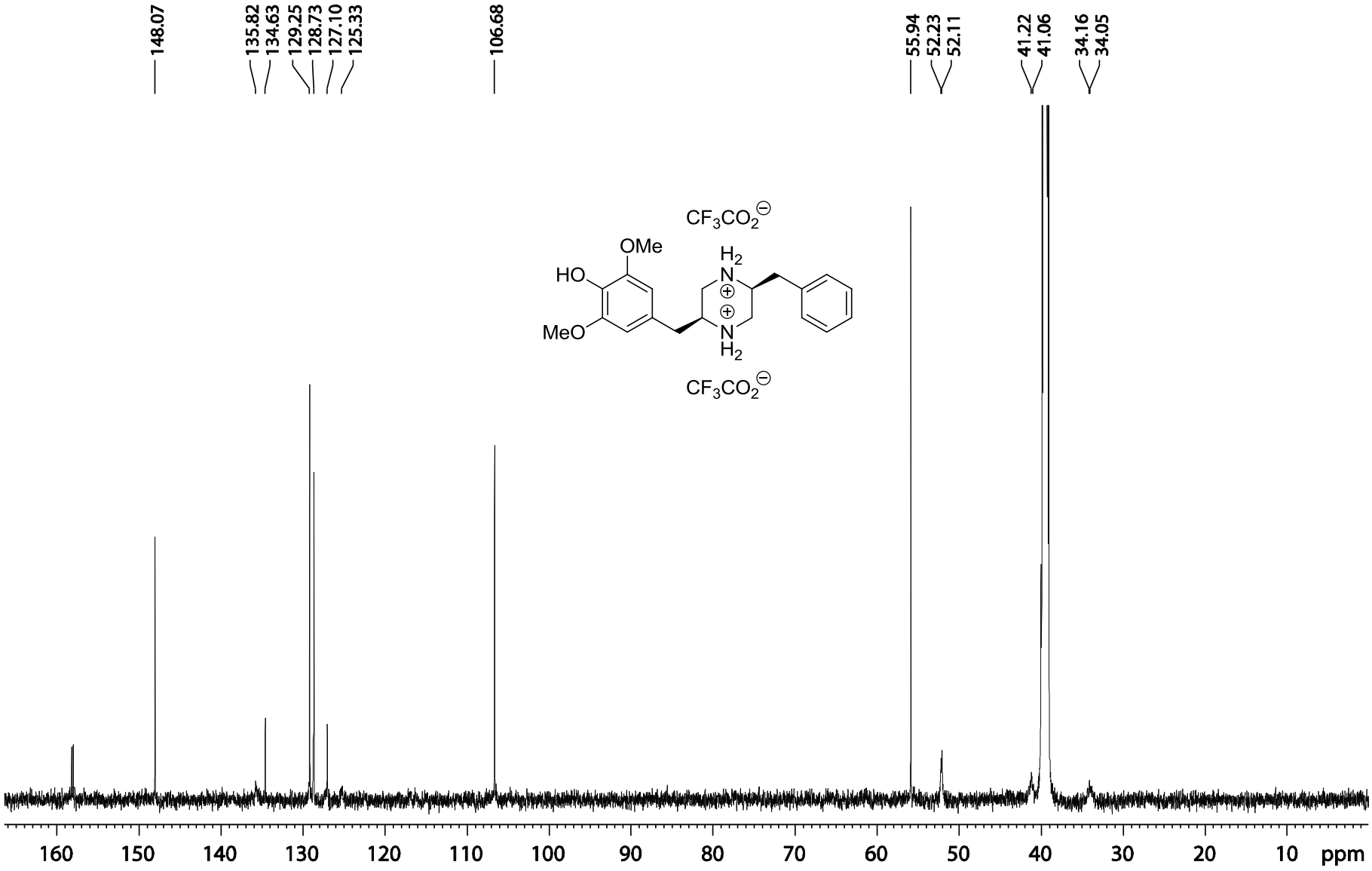

Figure S44. ^{13}C NMR spectrum (150 MHz, DMSO-d_6) of hancockiamide D di-TFA salt (**4**)

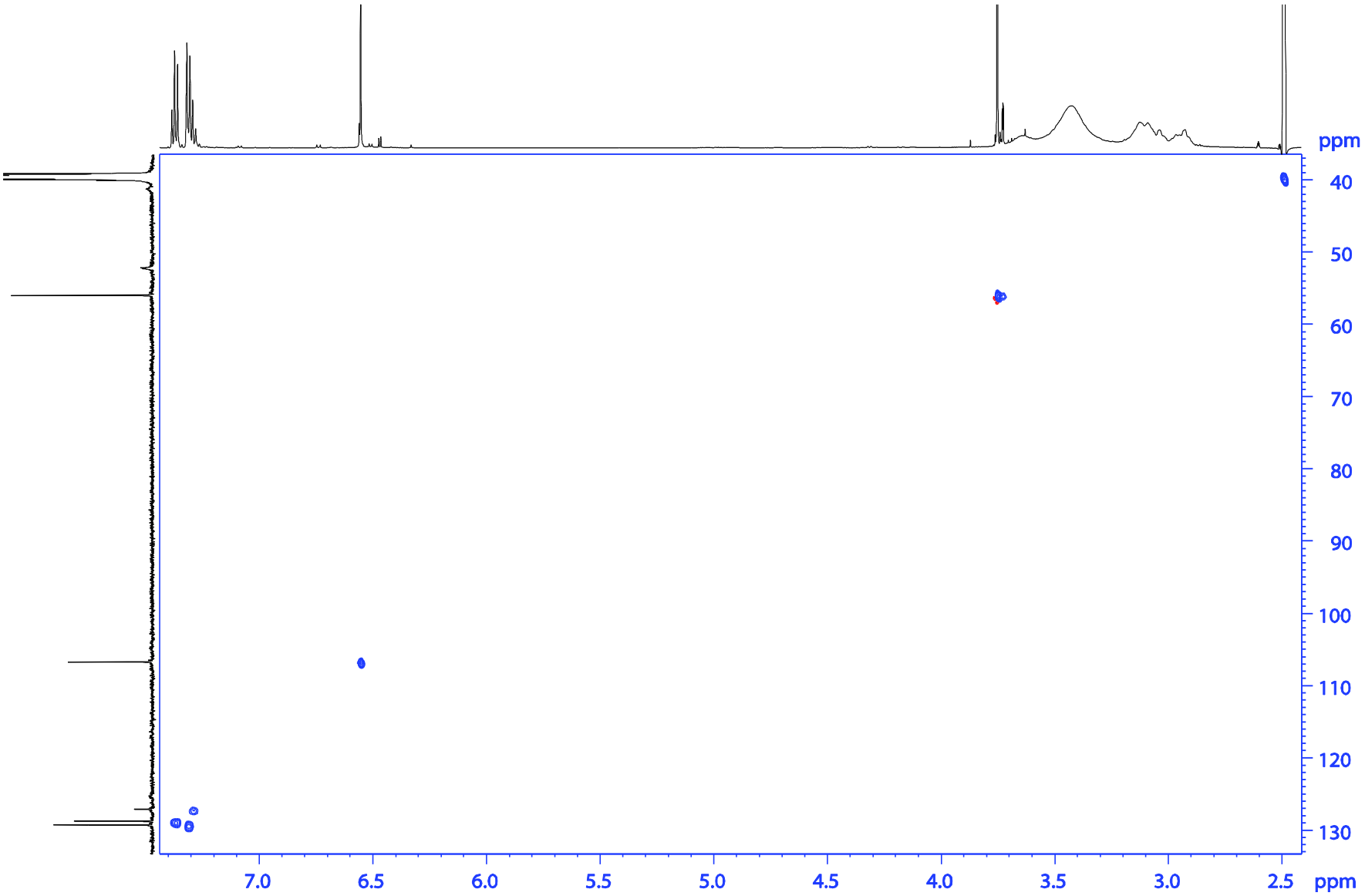

Figure S45. ^{1}H-^{13}C HSQC spectrum (600 MHz, DMSO-d_6) of hancockiamide D di-TFA salt (**4**)

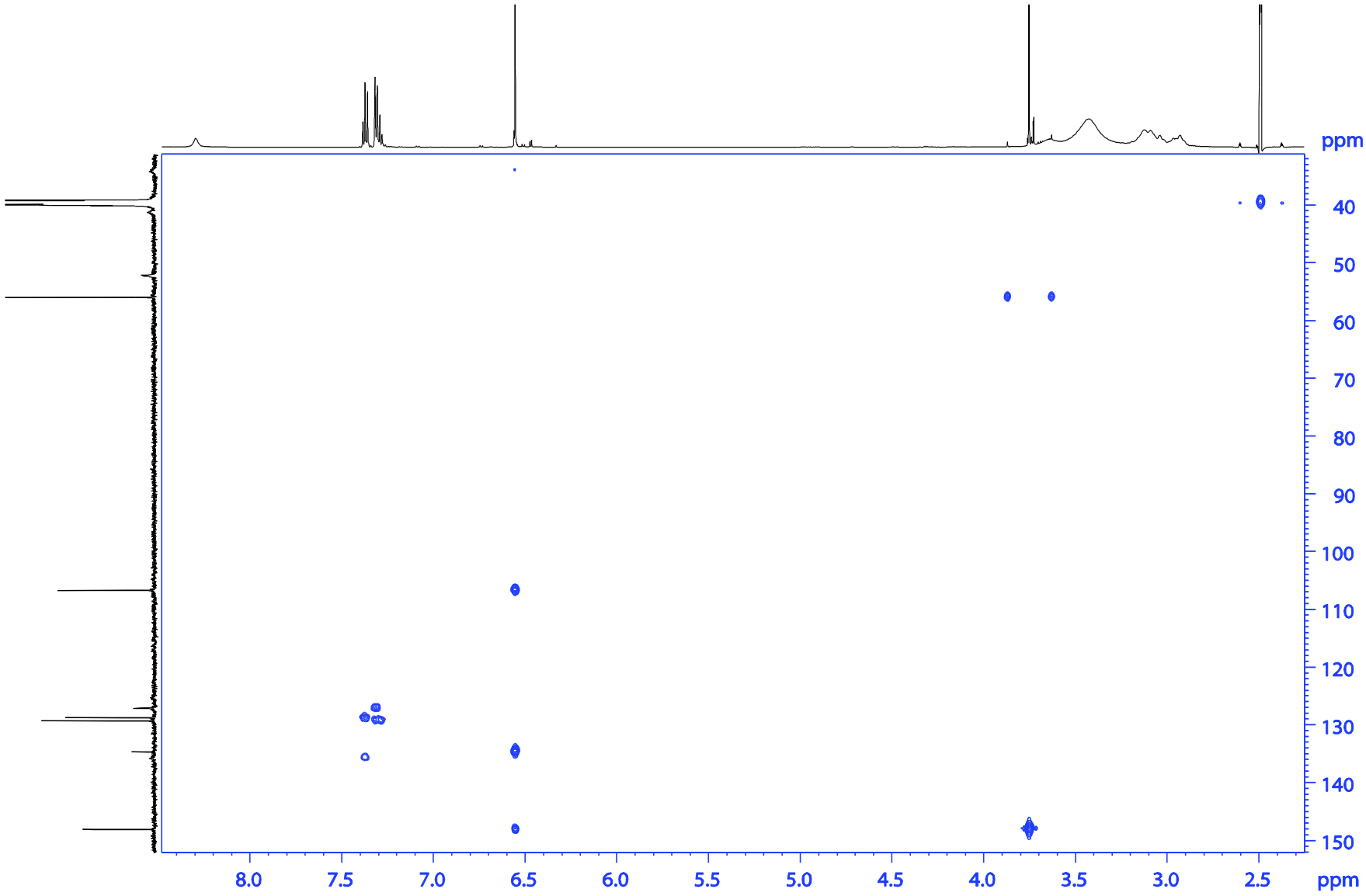

Figure S46. ^{1}H-^{13}C HMBC spectrum (600 MHz, DMSO-d_6) of hancockiamide D di-TFA salt (**4**)

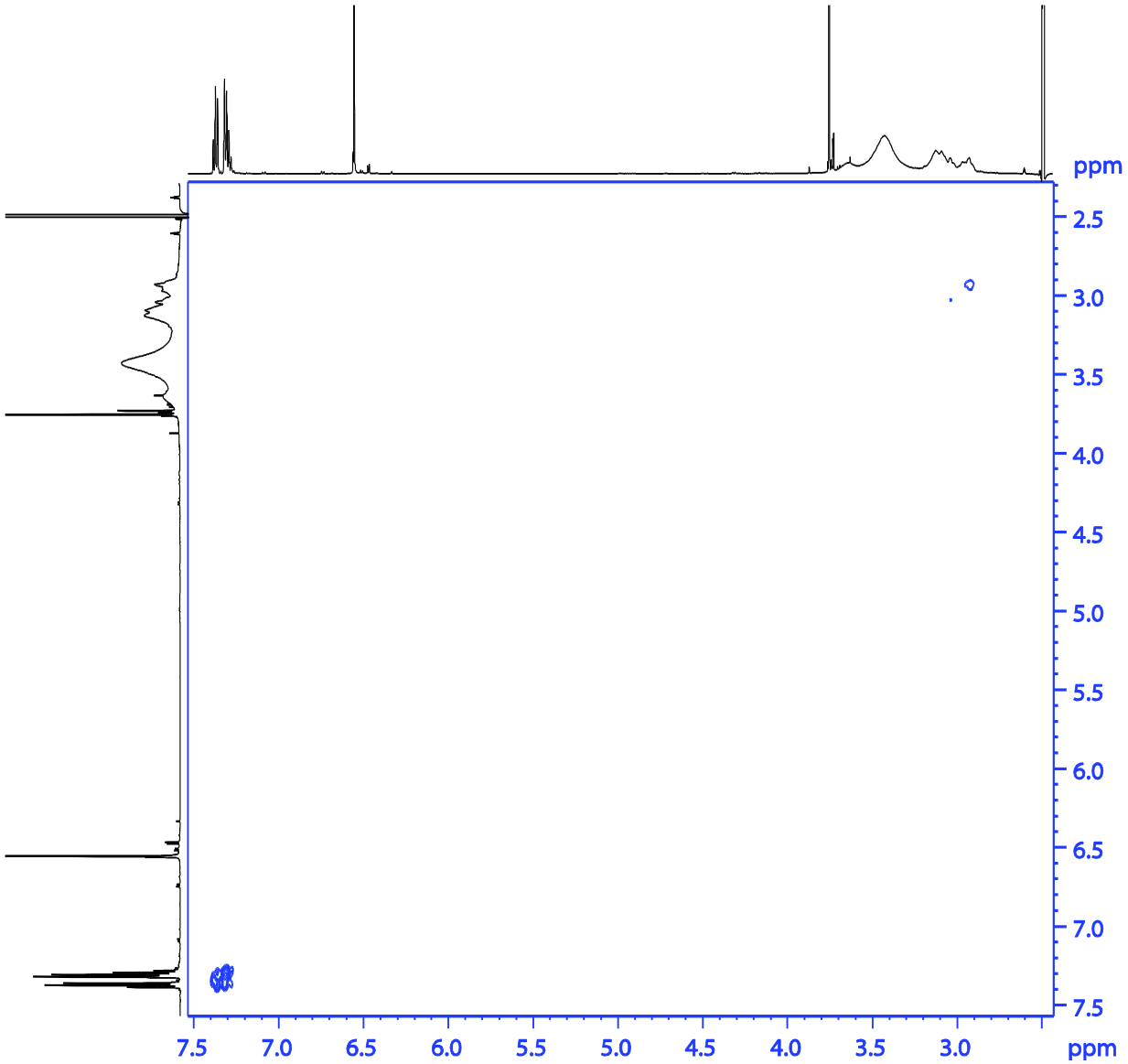

Figure S47. COSY spectrum (600 MHz, DMSO-d_6) of hancockiamide D di-TFA salt (**4**)

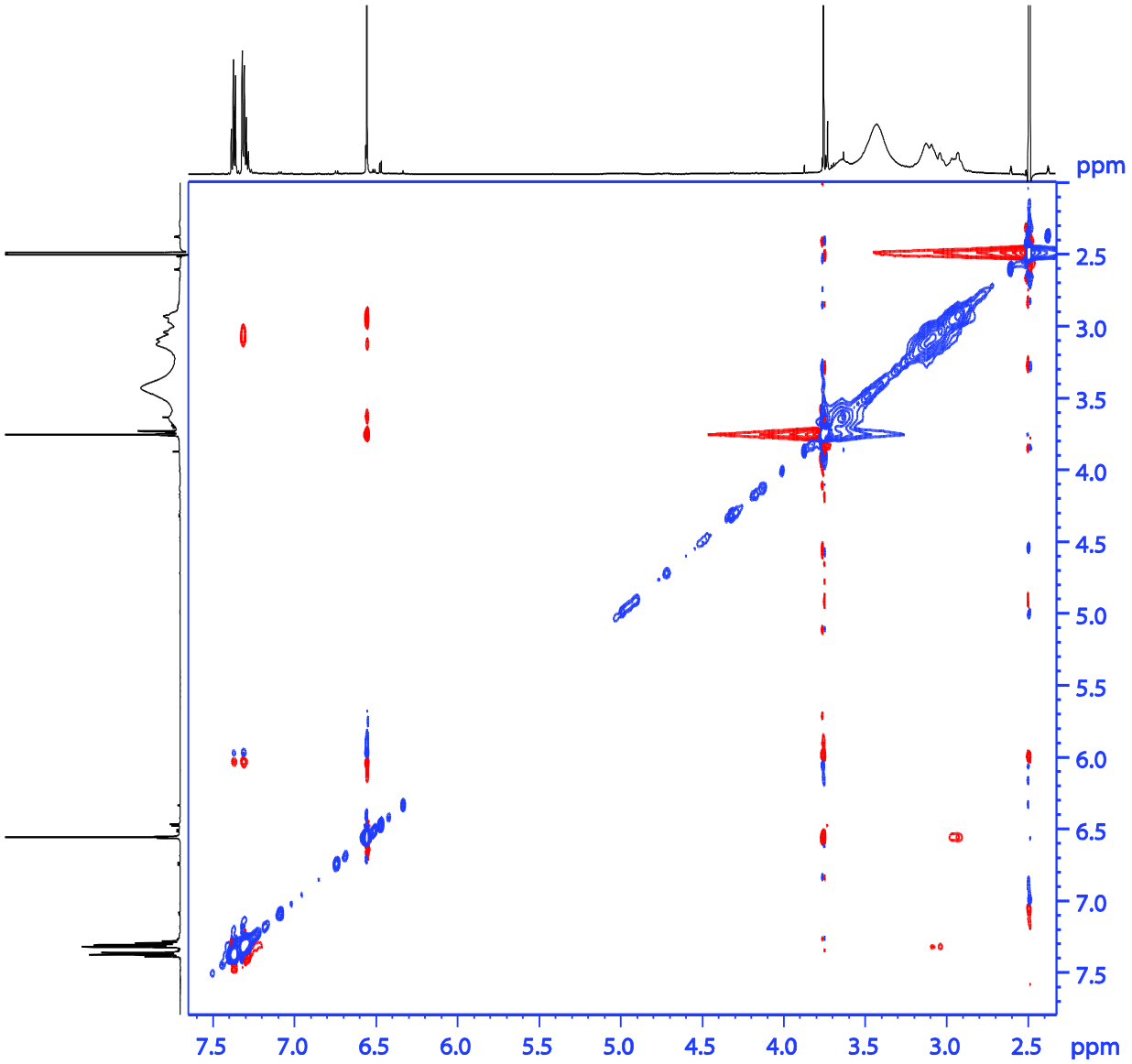

Figure S48. ROESY spectrum (600 MHz, DMSO-d_6) of hancockiamide D di-TFA salt (**4**)

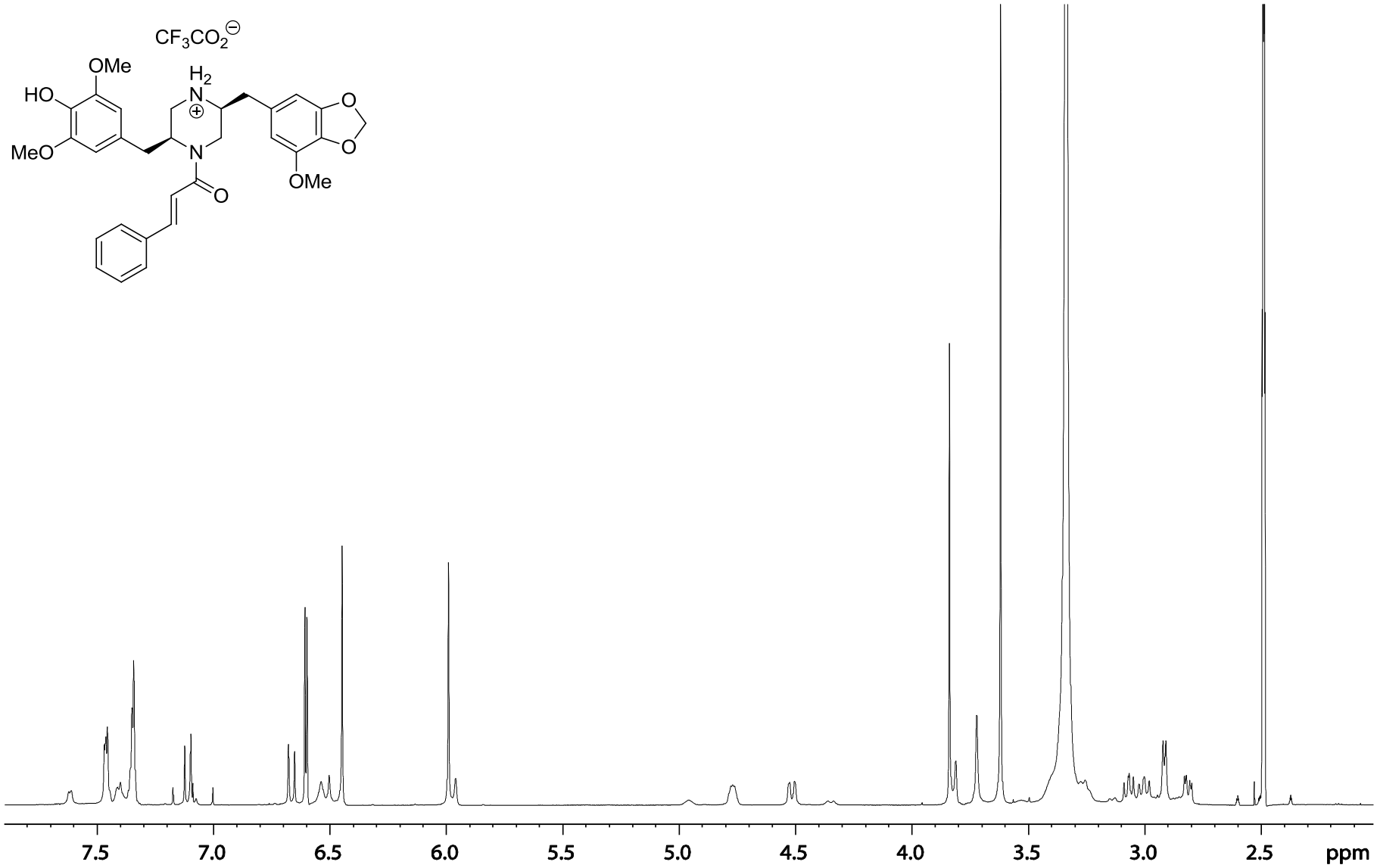

Figure S49. ^{1}H NMR spectrum (600 MHz, DMSO-d_6) of hancockiamide E TFA salt (**5**)

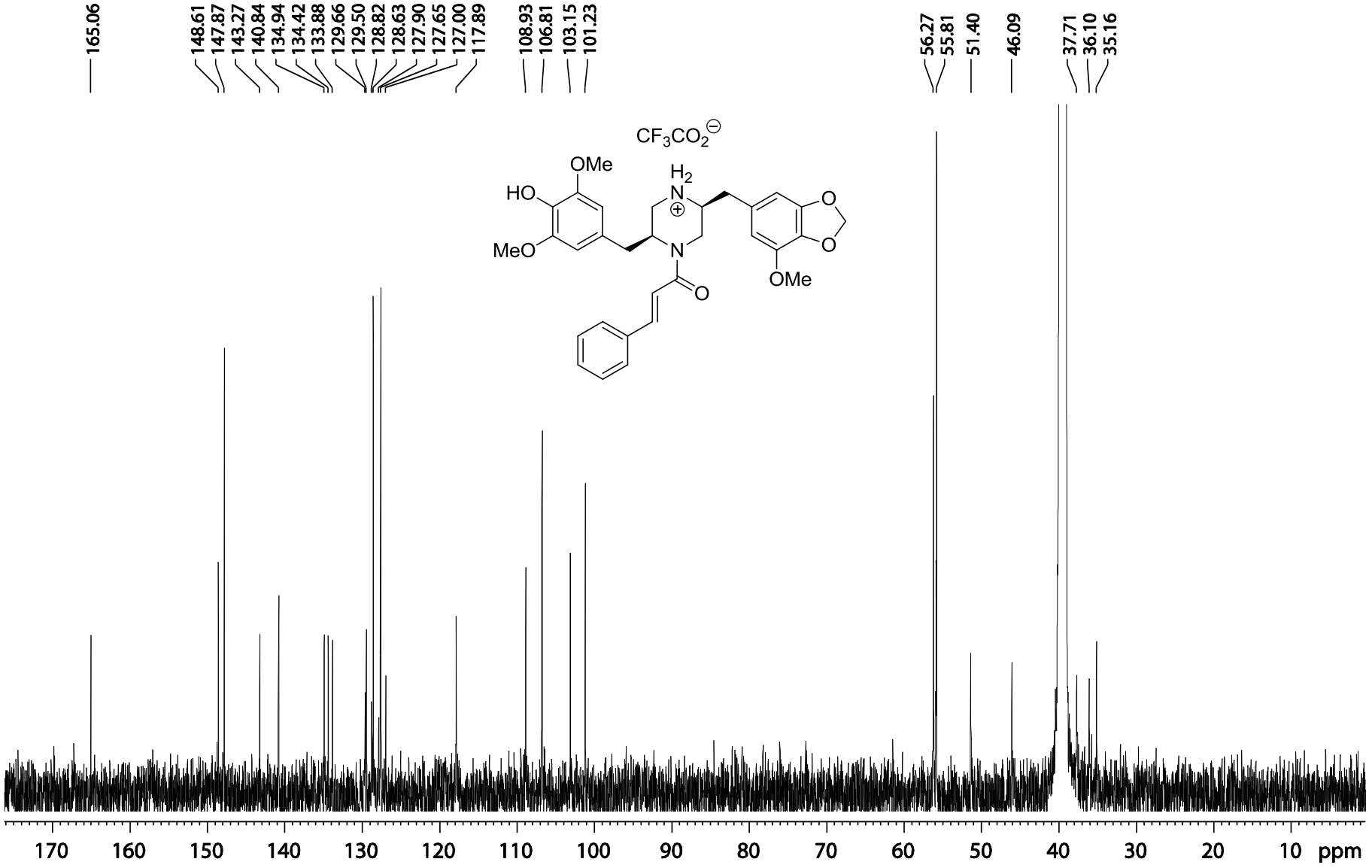

Figure S50. ^{13}C NMR spectrum (150 MHz, DMSO-d_6) of hancockiamide E TFA salt (**5**)

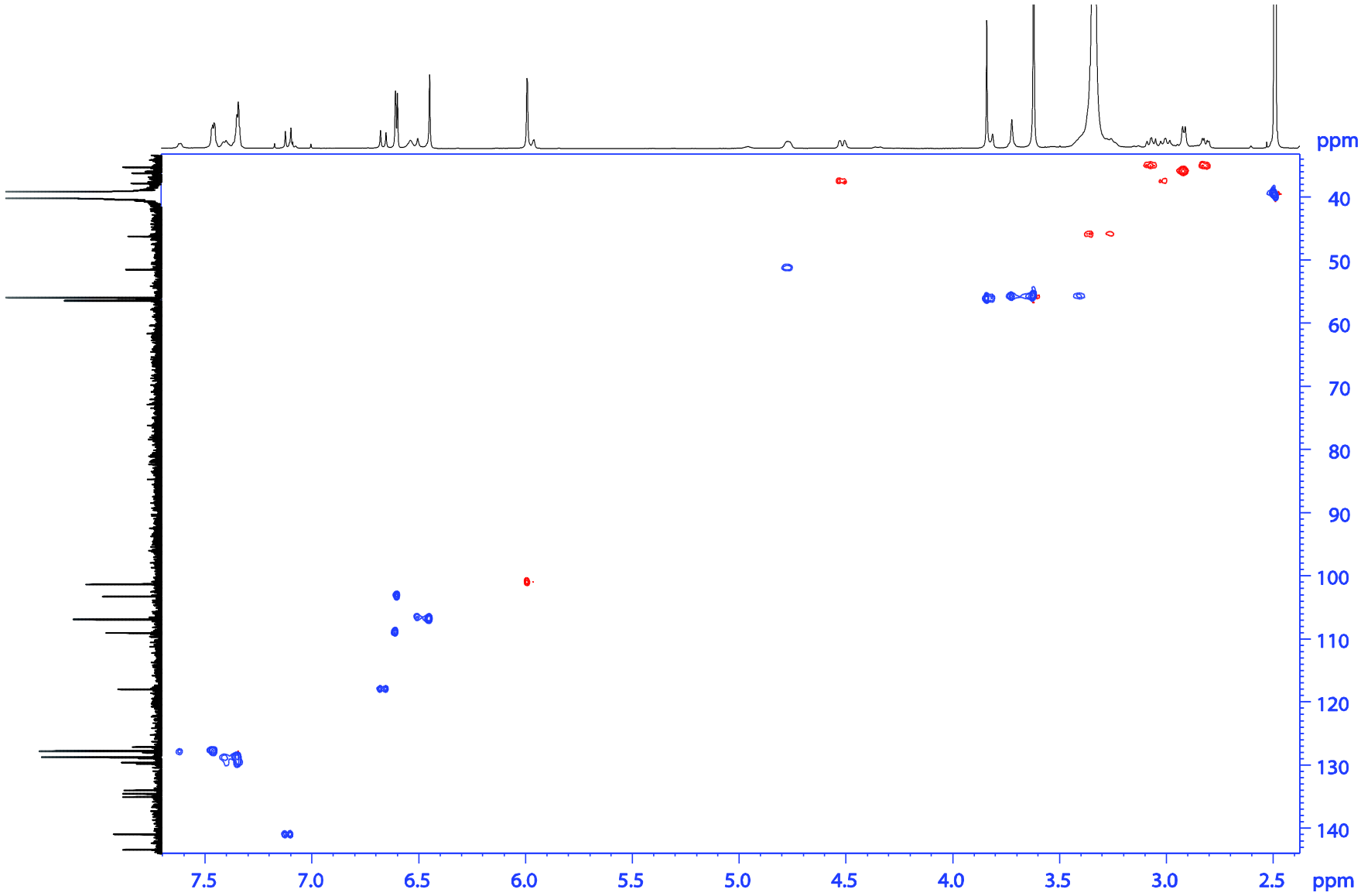

Figure S51. ^{1}H-^{13}C HSQC spectrum (600 MHz, DMSO-d_6) of hancockiamide E TFA salt (**5**)

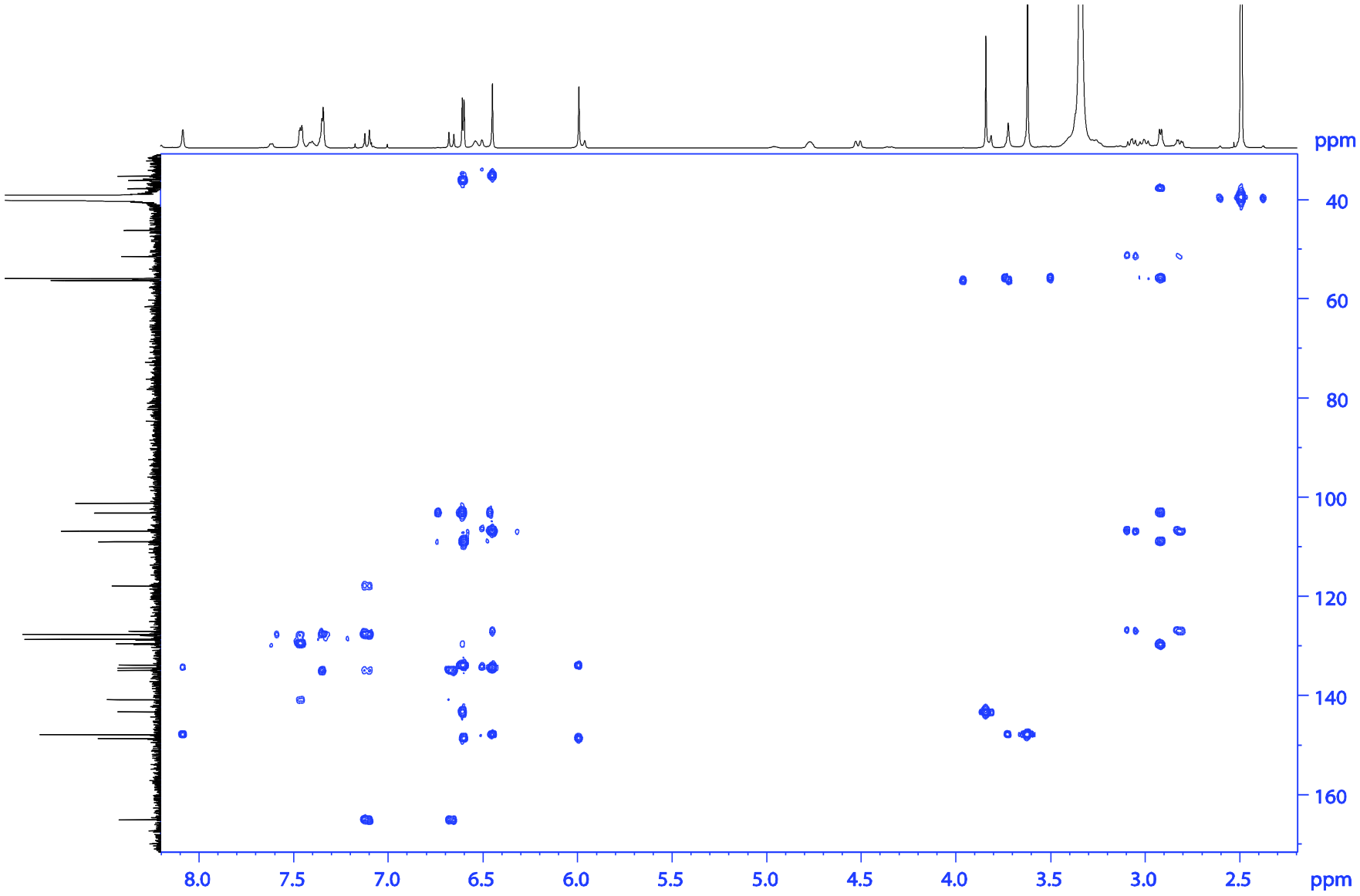

Figure S52. ^{1}H-^{13}C HMBC spectrum (600 MHz, DMSO-d_6) of hancockiamide E TFA salt (**5**)

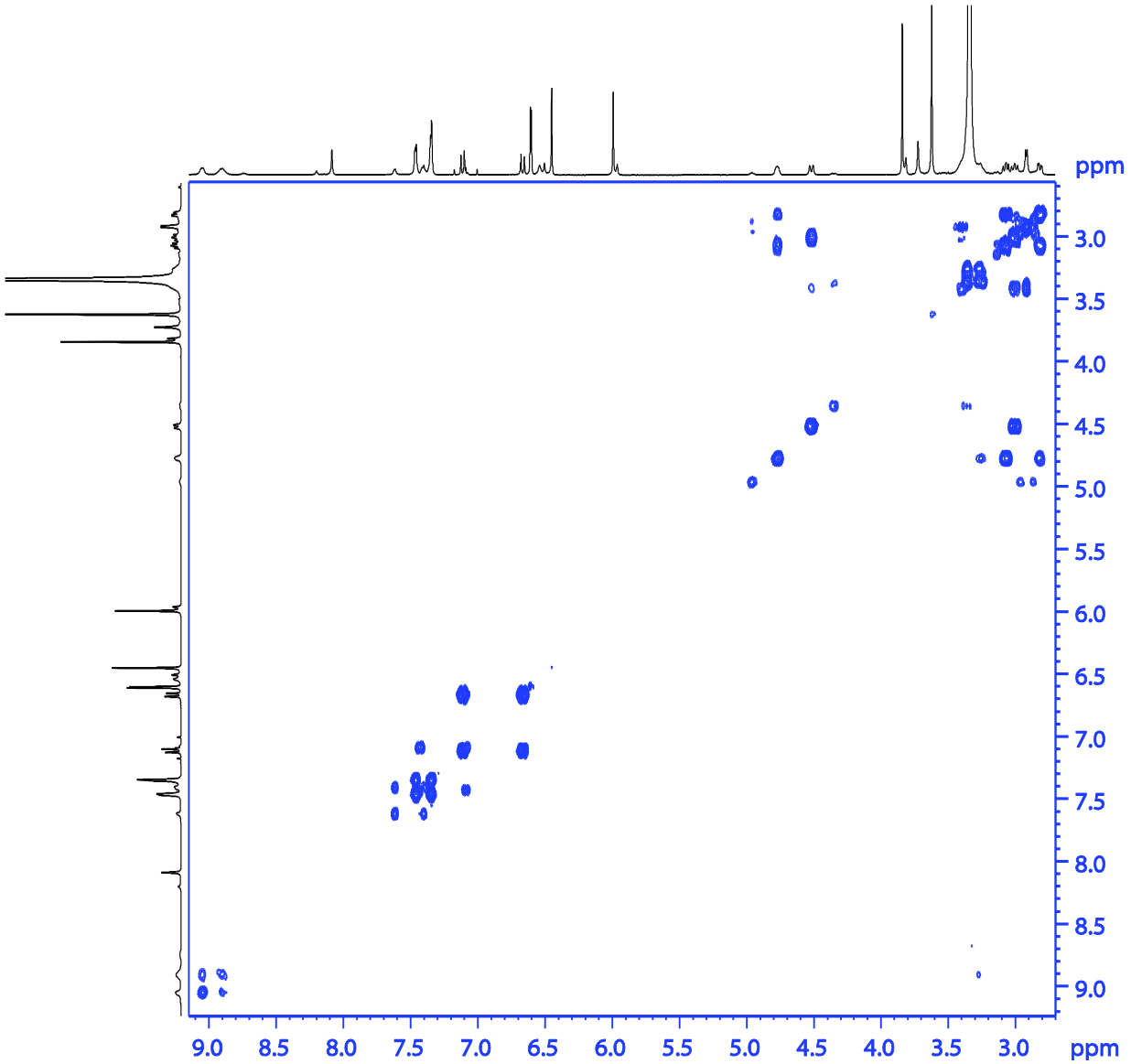

Figure S53. COSY spectrum (600 MHz, DMSO-d_6) of hancockiamide E TFA salt (**5**)

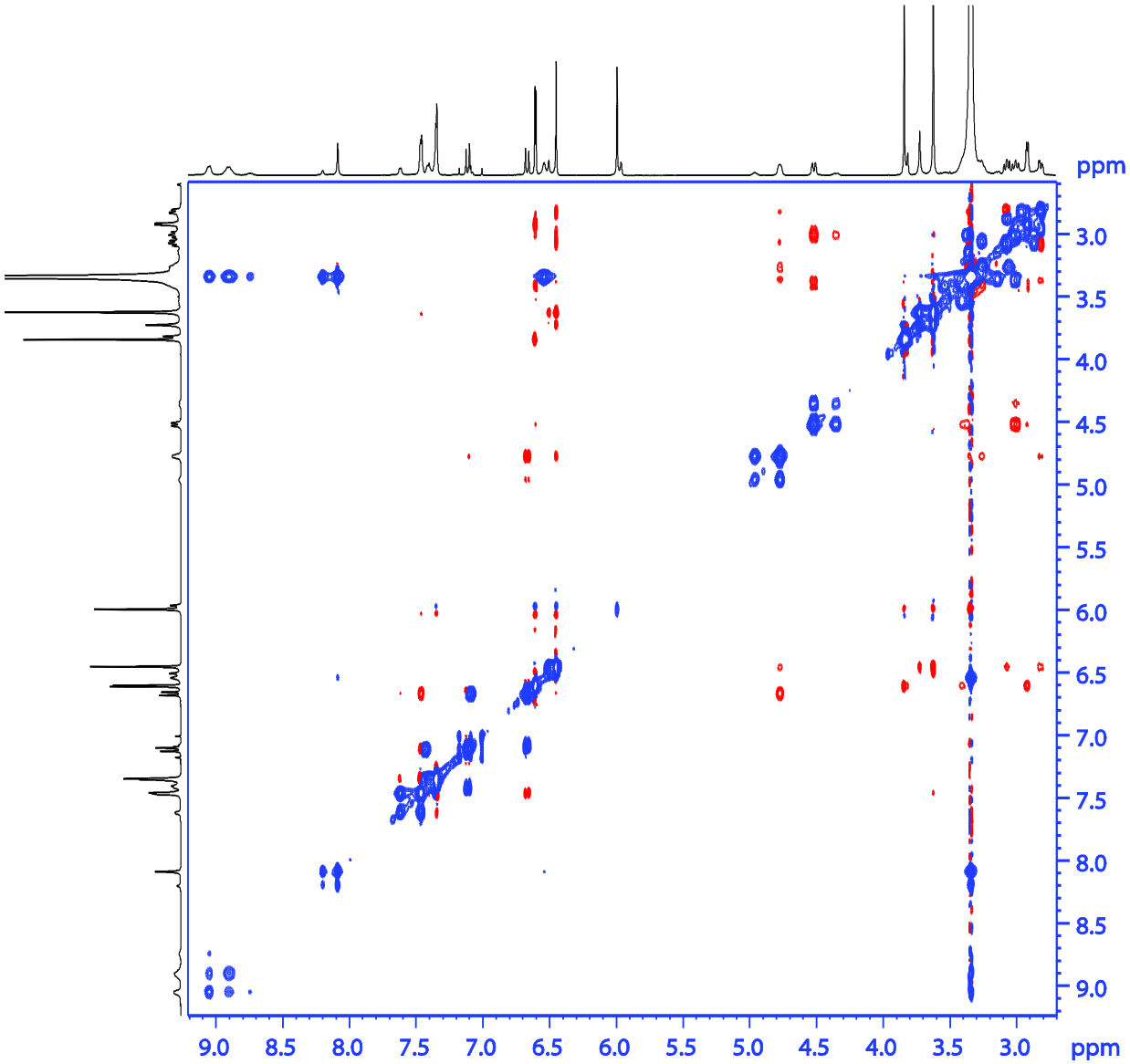

Figure S54. ROESY spectrum (600 MHz, DMSO-d_6) of hancockiamide E TFA salt (**5**)

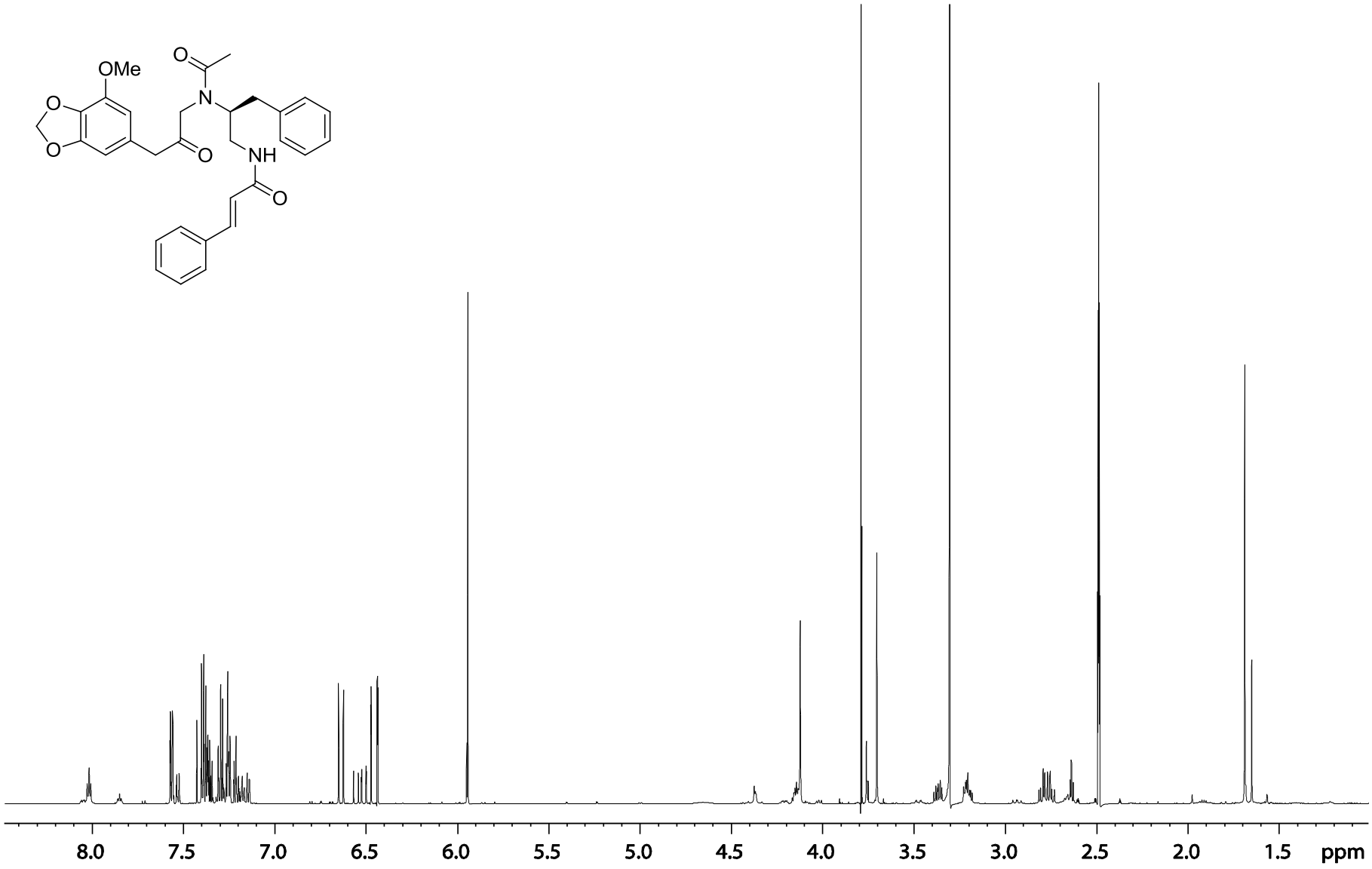

Figure S55. ^{1}H NMR spectrum (600 MHz, DMSO-d_6) of hancockiamide F (**6**)

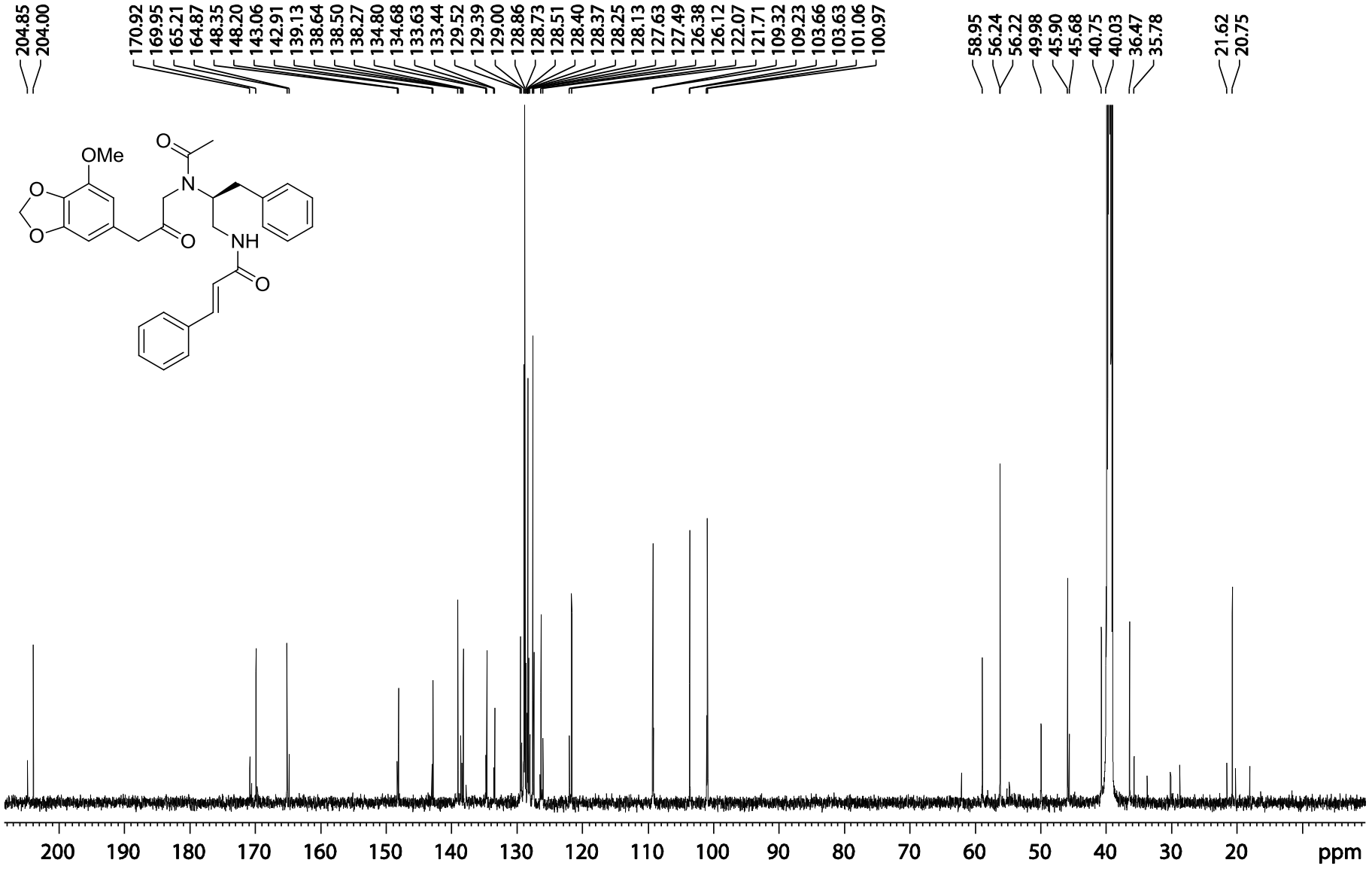

Figure S56. ^{13}C NMR spectrum (150 MHz, DMSO-d_6) of hancockiamide F (**6**)

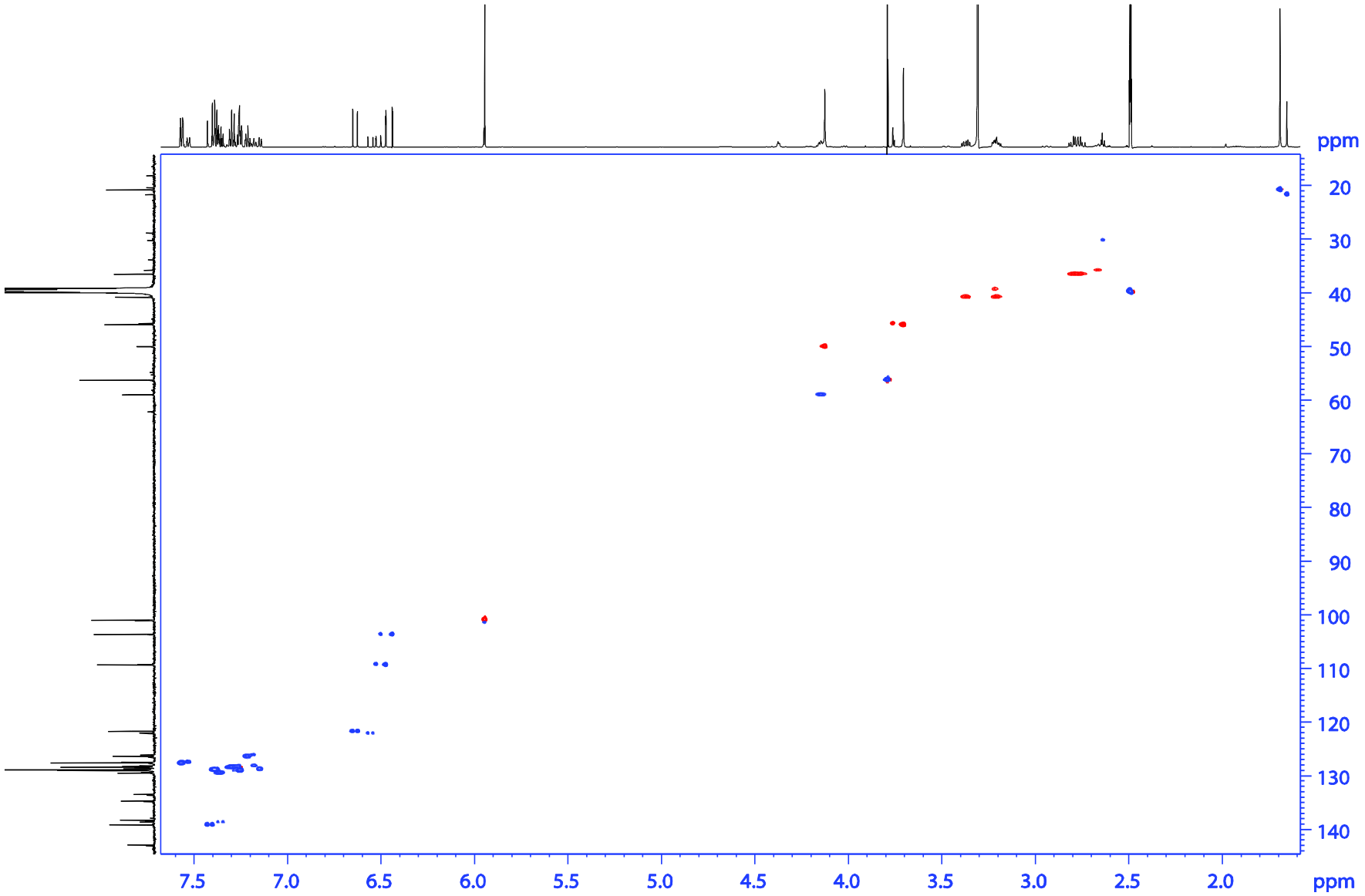

Figure S57. ^{1}H-^{13}C HSQC spectrum (600 MHz, DMSO-d_6) of hancockiamide F (**6**)

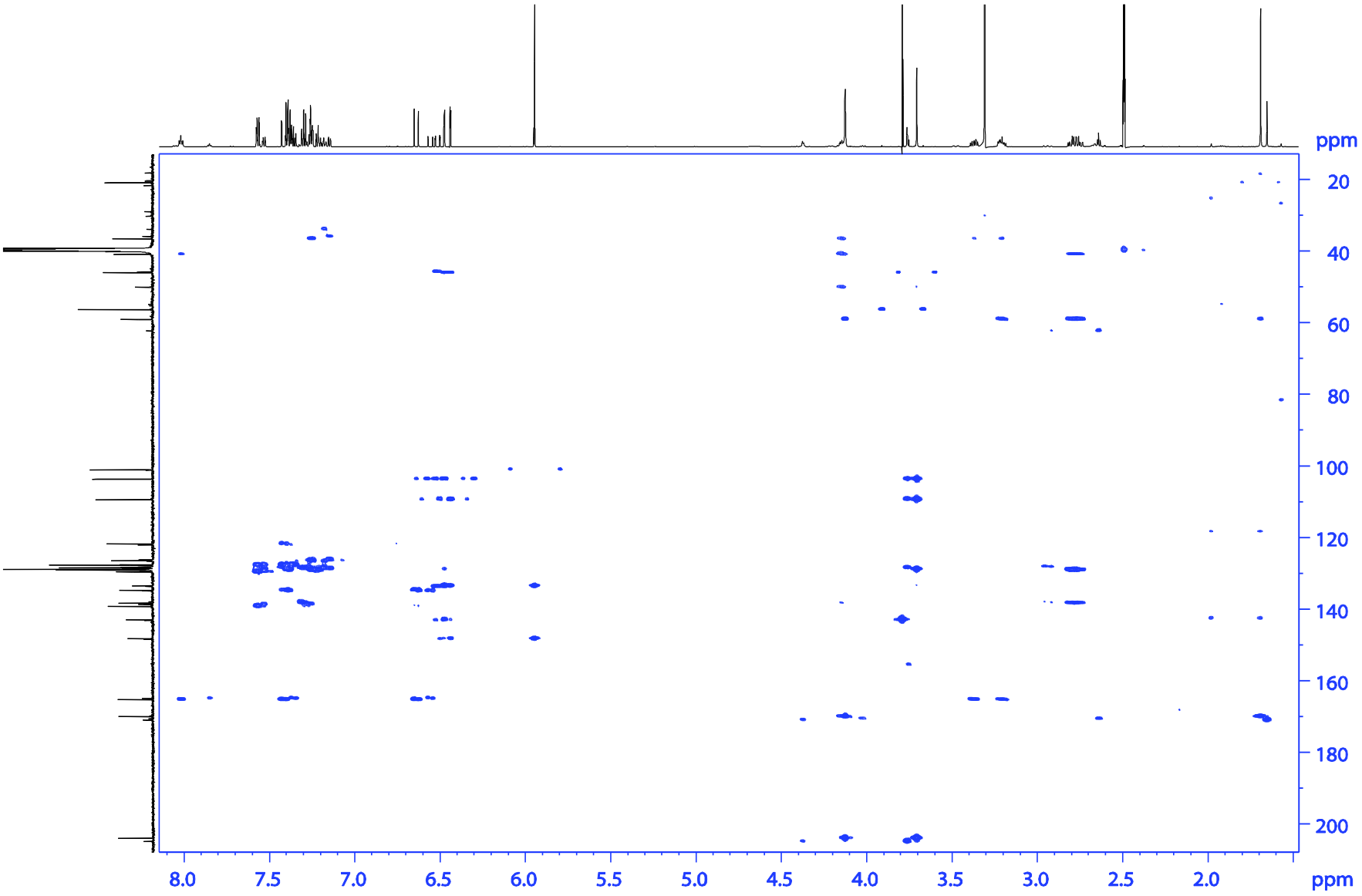

Figure S58. ^{1}H-^{13}C HMBC spectrum (600 MHz, DMSO-d_6) of hancockiamide F (**6**)

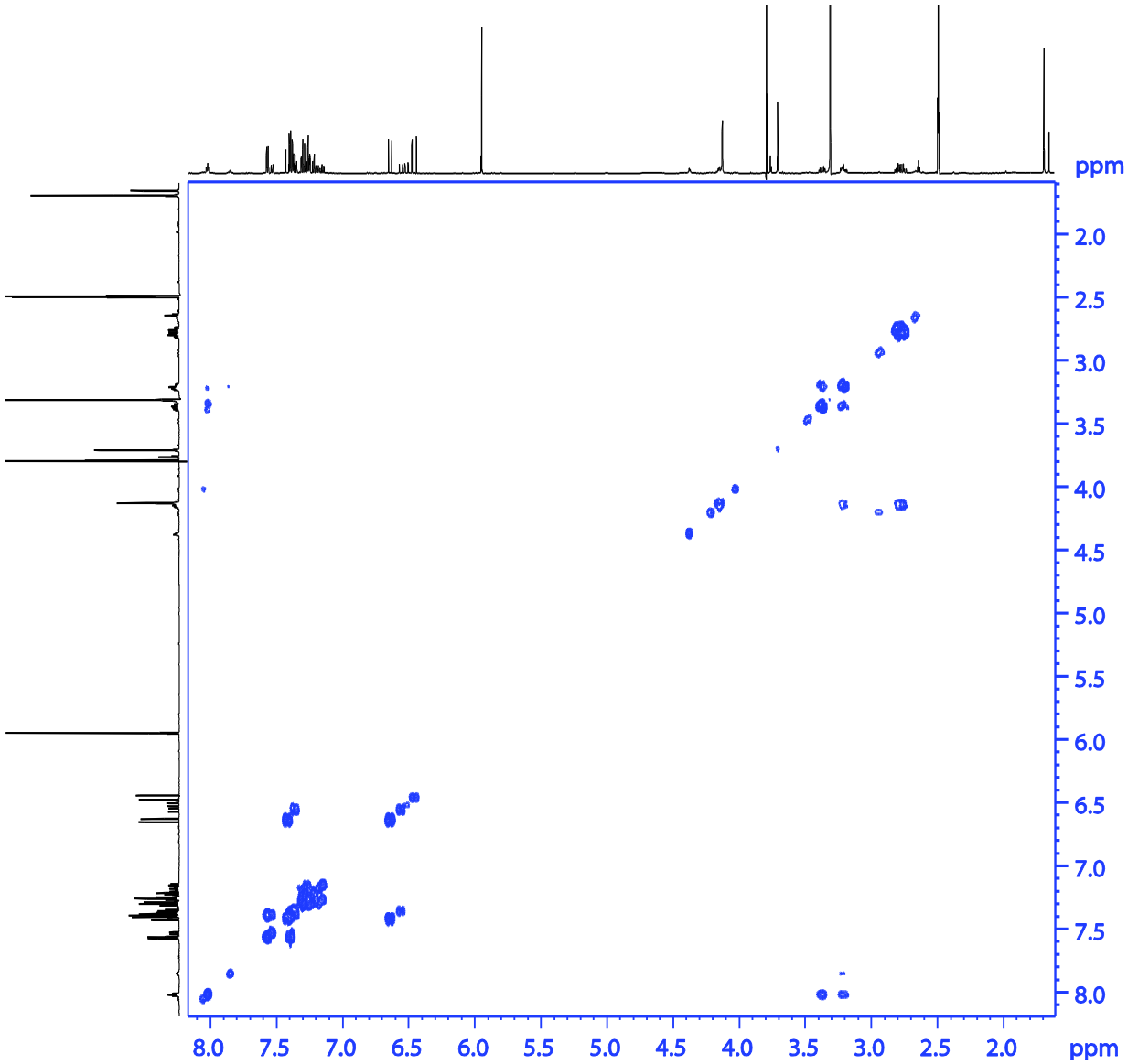

Figure S59. COSY spectrum (600 MHz, DMSO-d_6) of hancockiamide F (**6**)

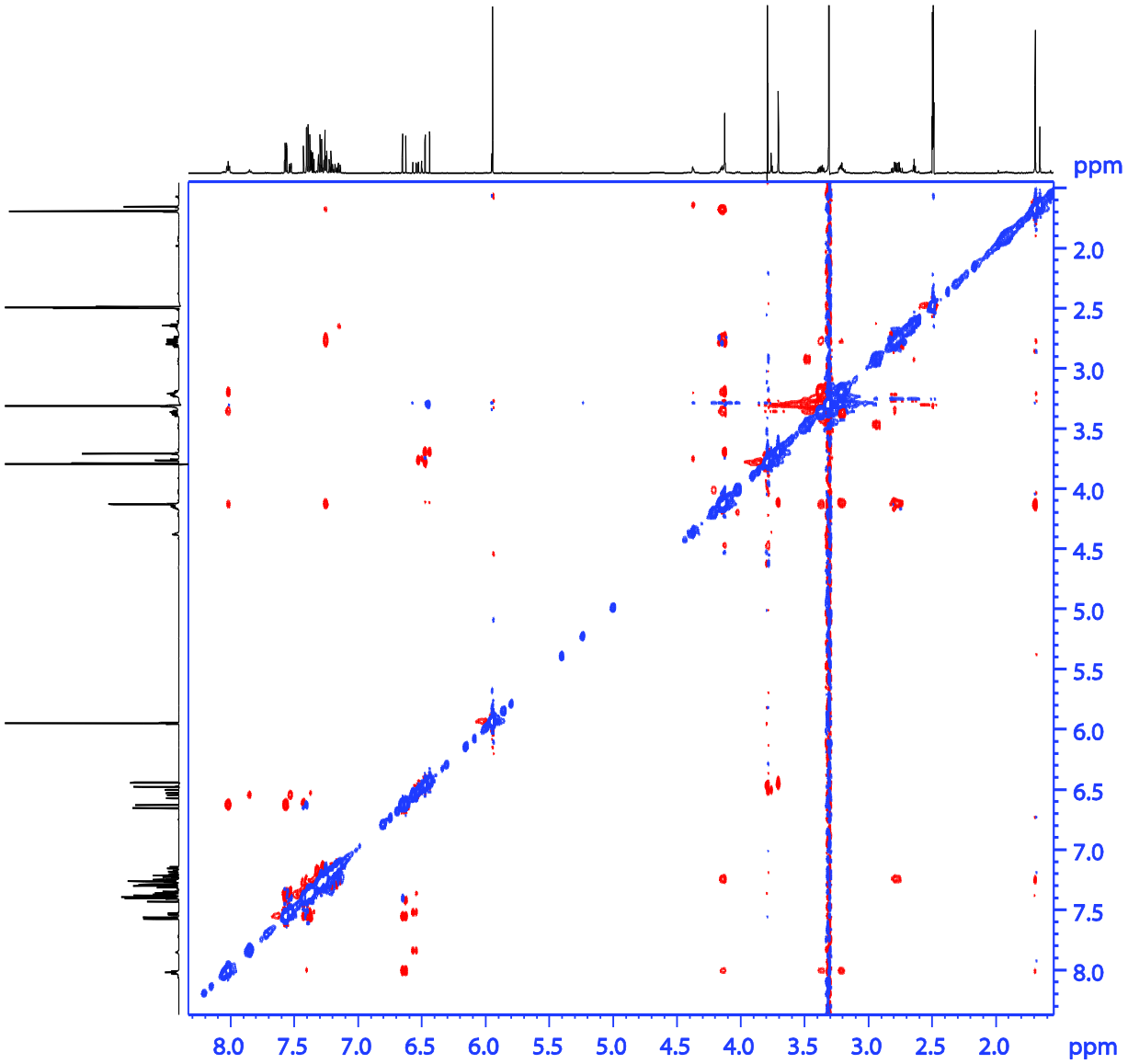

Figure S60. ROESY spectrum (600 MHz, DMSO-d_6) of hancockiamide F (**6**)

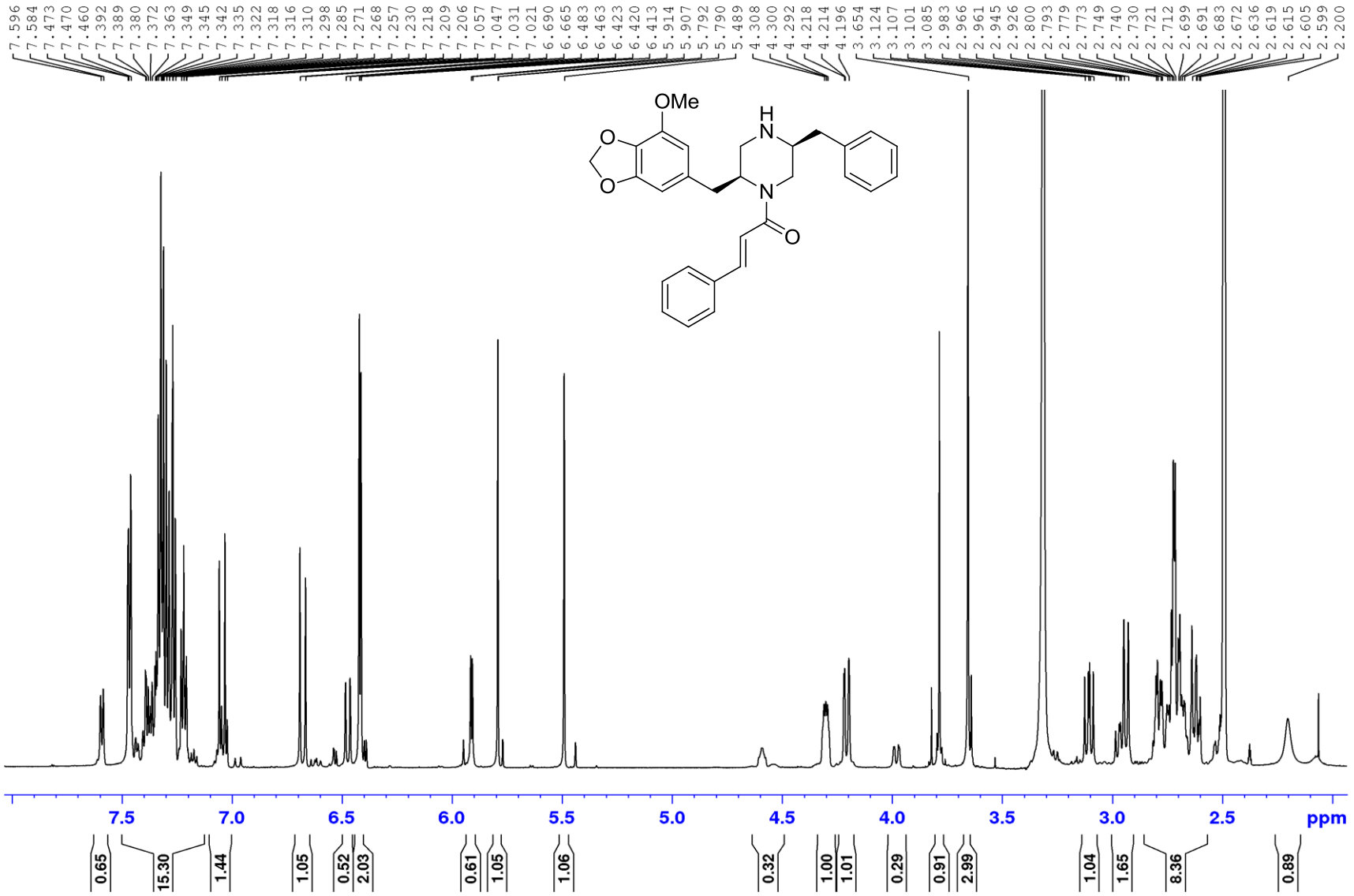

Figure S61. ^{1}H NMR spectrum (600 MHz, DMSO-d_6) of hancockiamide G (**7**)

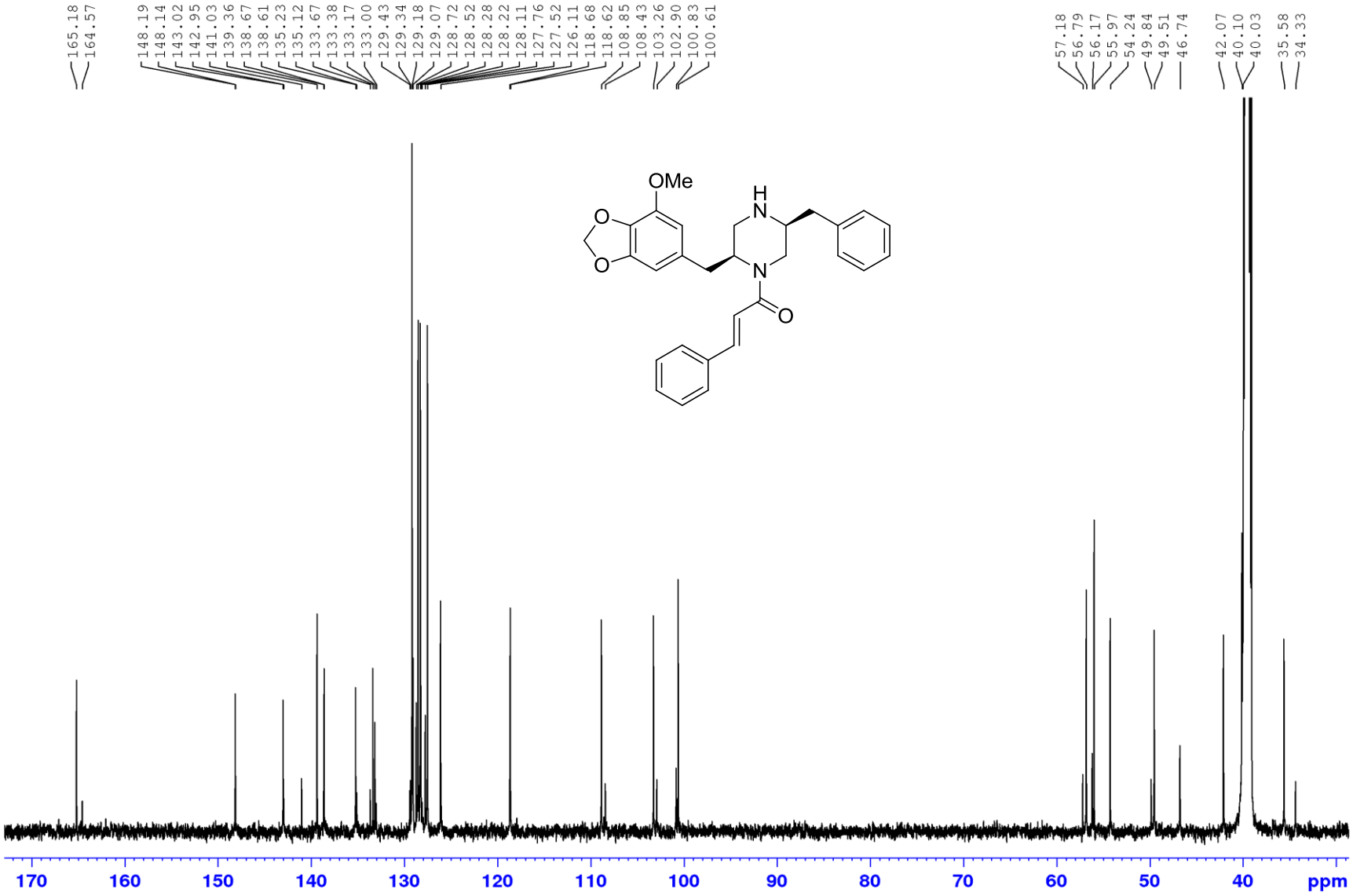

Figure S62. ^{13}C NMR spectrum (150 MHz, DMSO-d_6) of hancockiamide G (**7**)

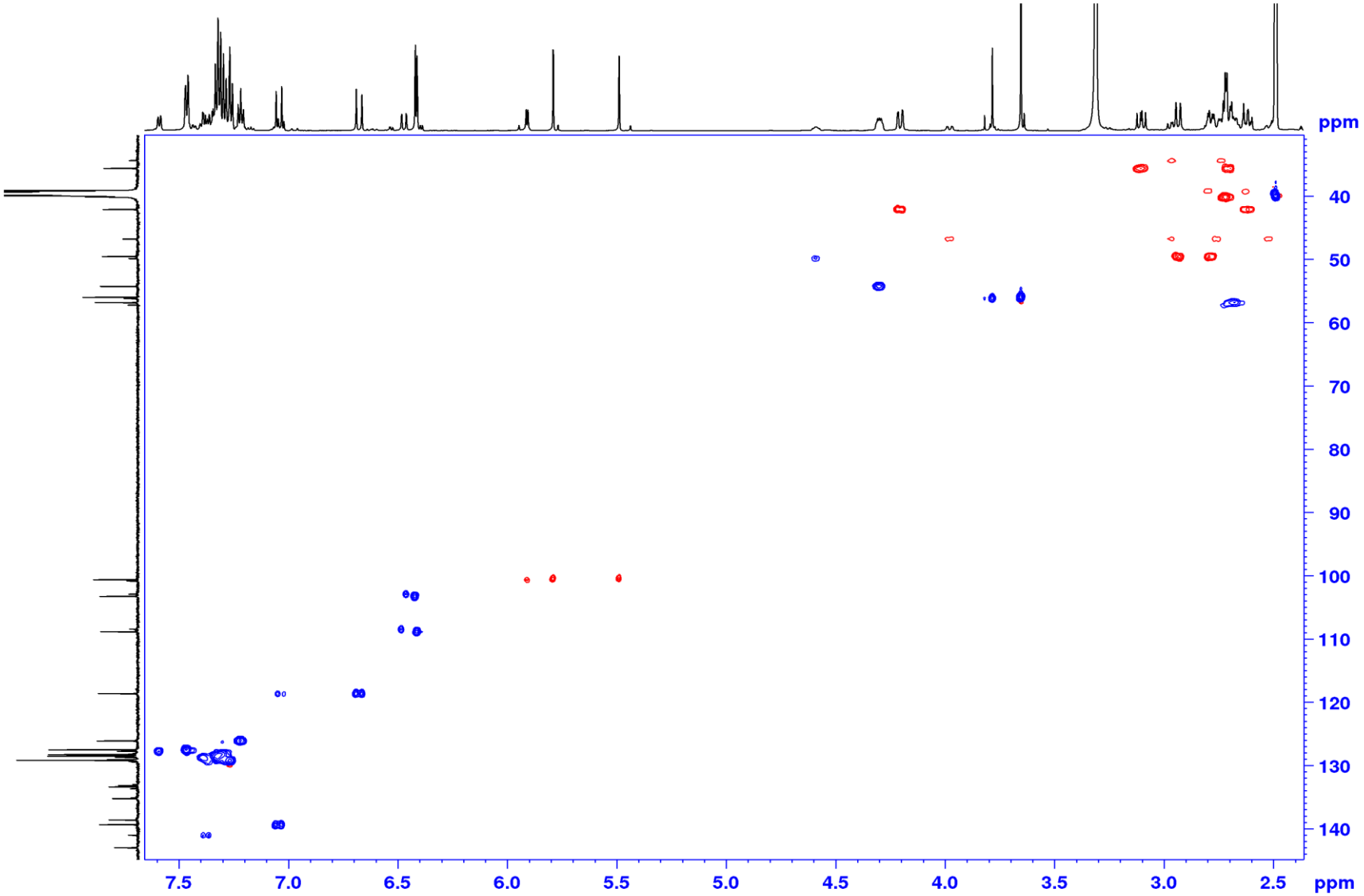

Figure S63. ^{1}H-^{13}C HSQC spectrum (600 MHz, DMSO-d_6) of hancockiamide G (**7**)

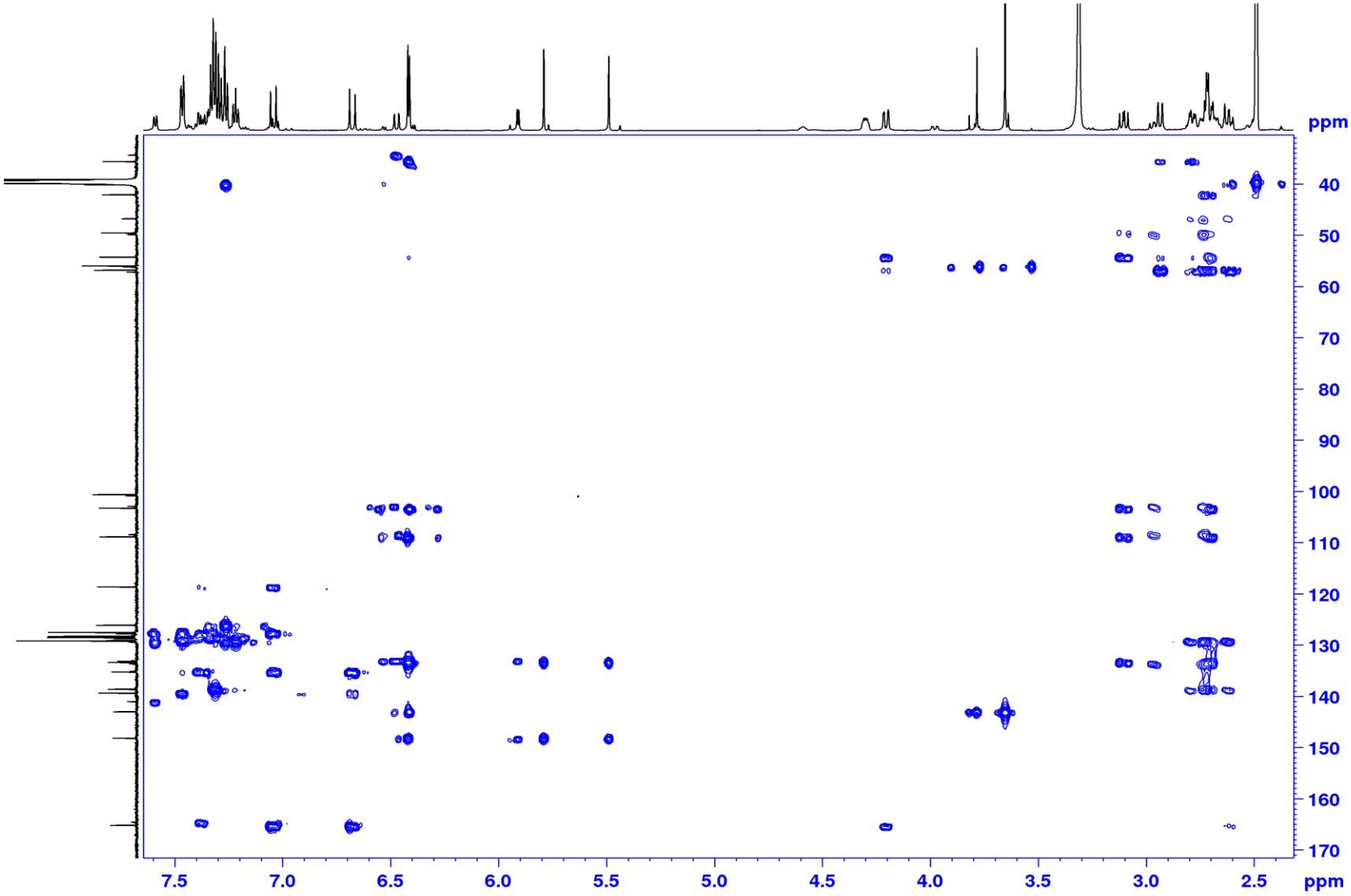

Figure S64. ^{1}H-^{13}C HMBC spectrum (600 MHz, DMSO-d_6) of hancockiamide G (**7**)

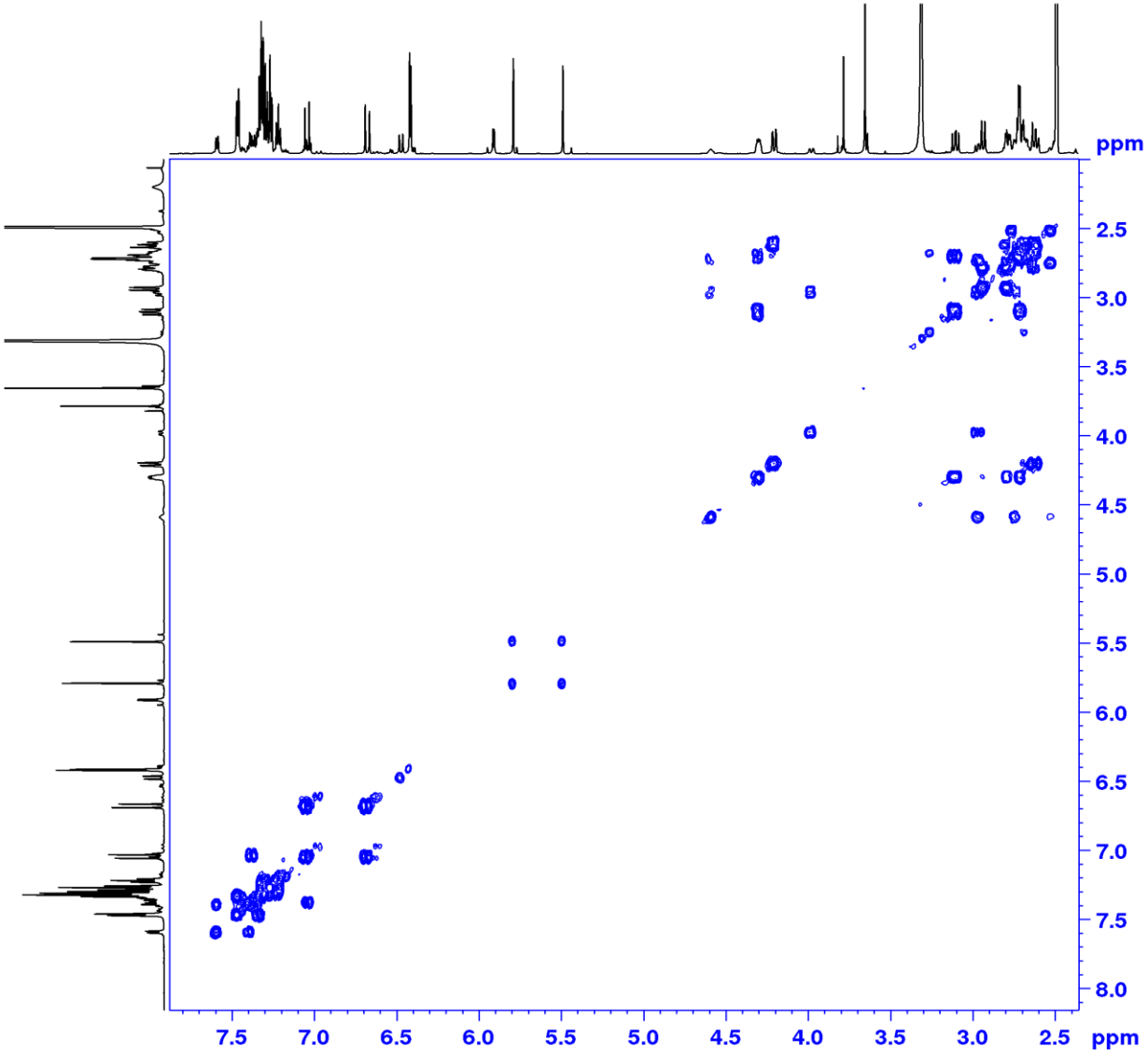

Figure S65. COSY spectrum (600 MHz, DMSO-d_6) of hancockiamide G (**7**)

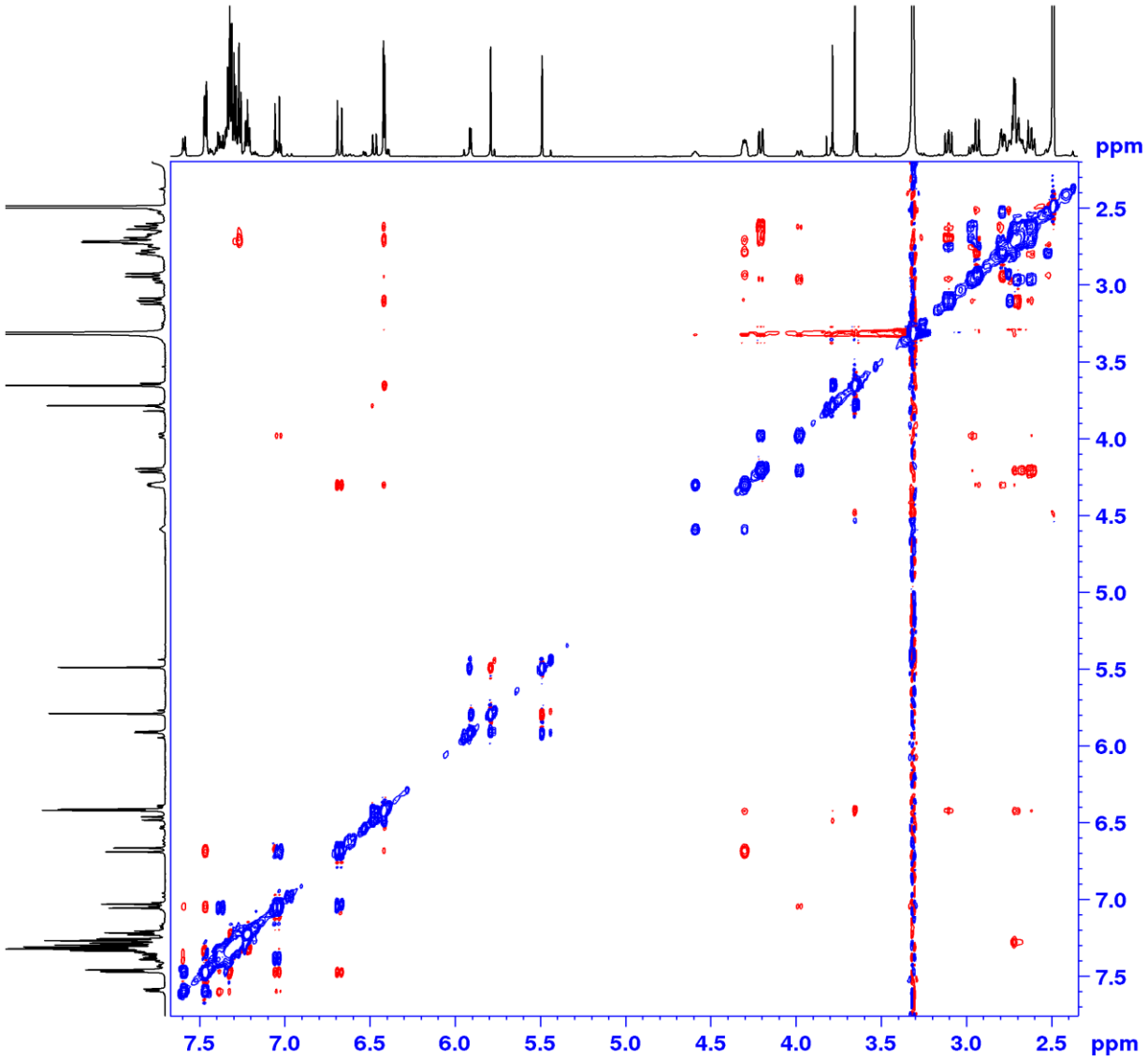

Figure S66. ROESY spectrum (600 MHz, DMSO-d_6) of hancockiamide G (**7**)

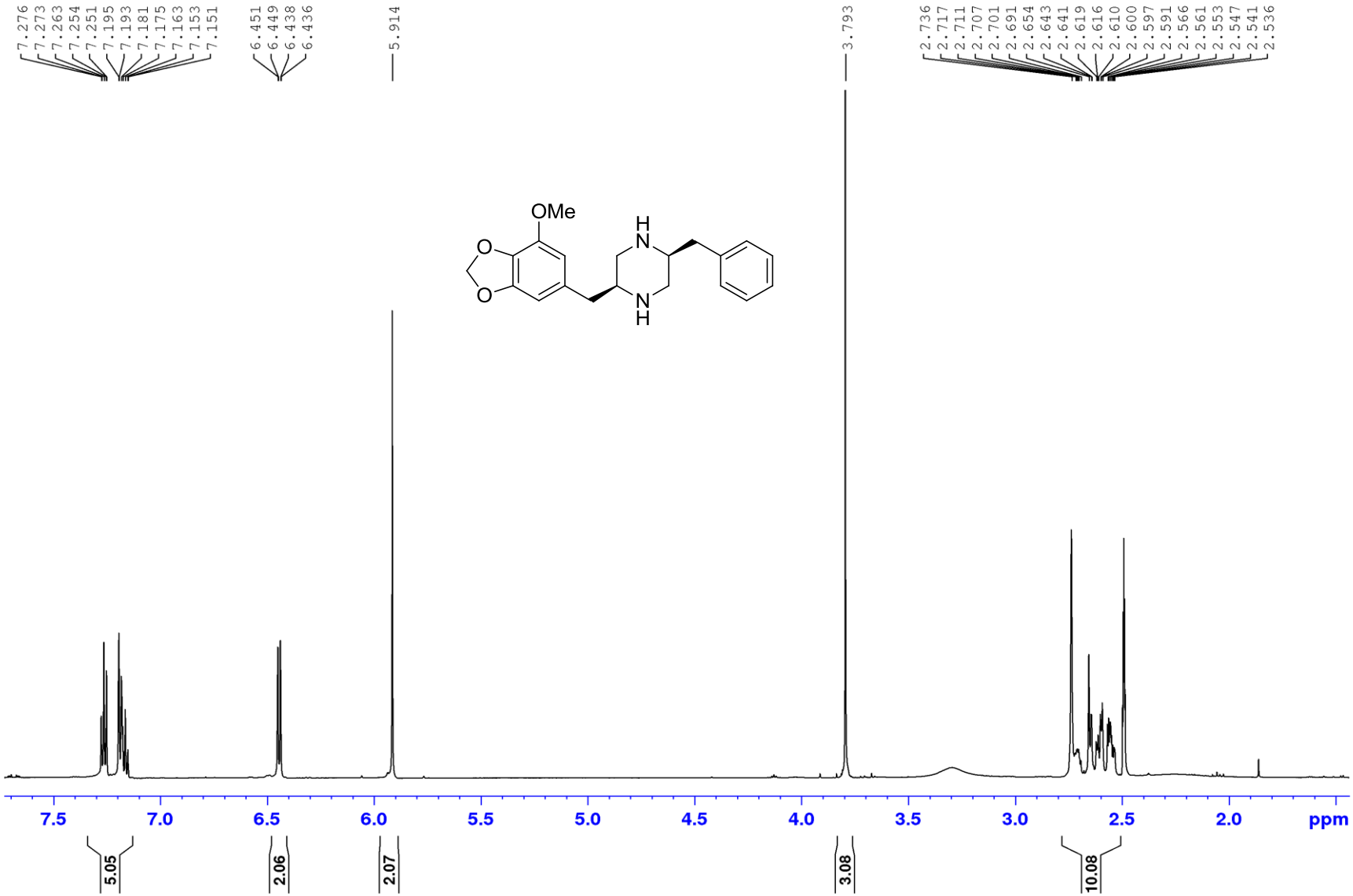

Figure S67. ^{1}H NMR spectrum (600 MHz, DMSO-d_6) of hancockiamide H (**8**)

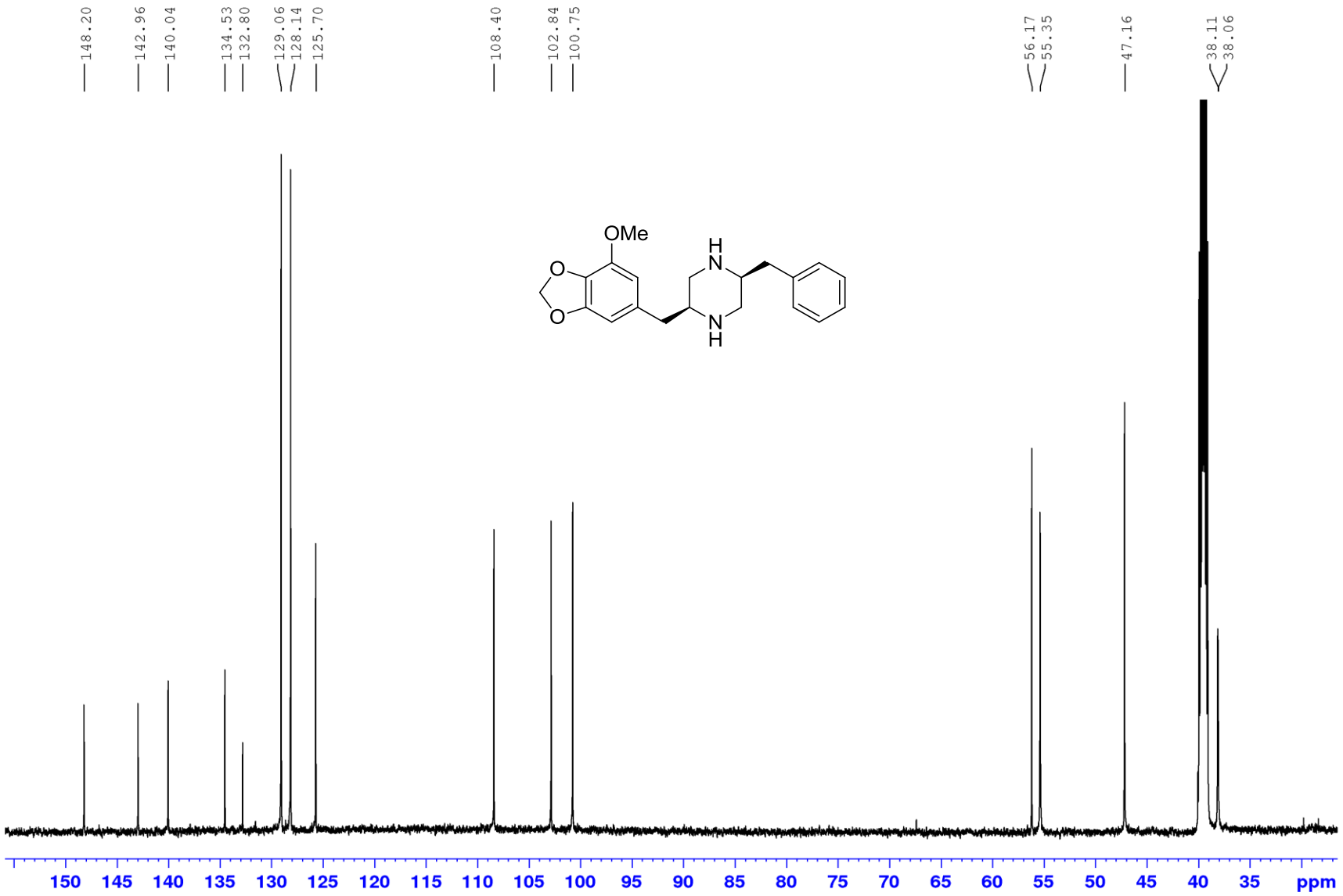

Figure S68. ^{13}C NMR spectrum (150 MHz, DMSO-d_6) of hancockiamide H (**8**)

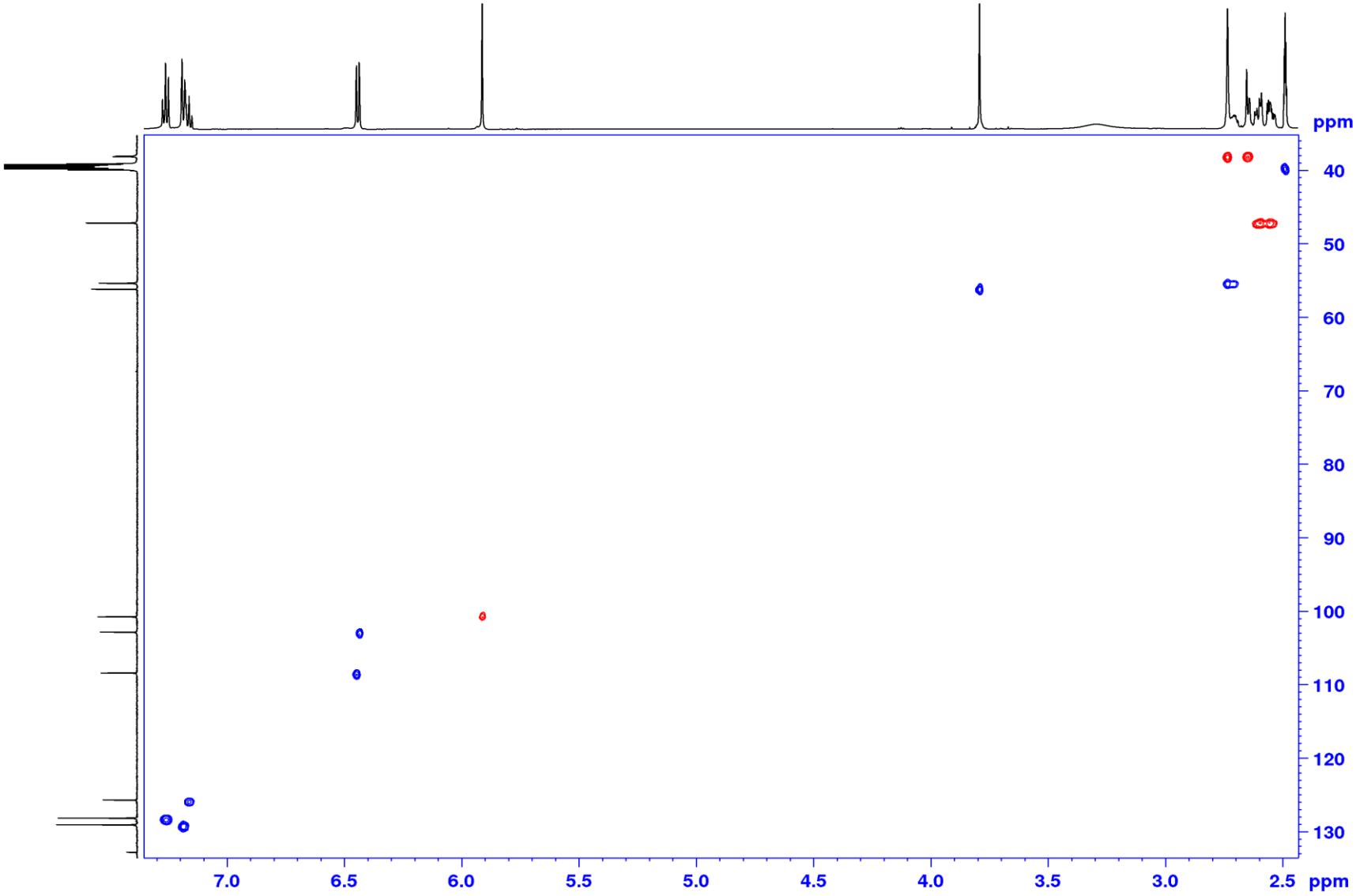

Figure S69. ^{1}H-^{13}C HSQC spectrum (600 MHz, DMSO-d_6) of hancockiamide H (**8**)

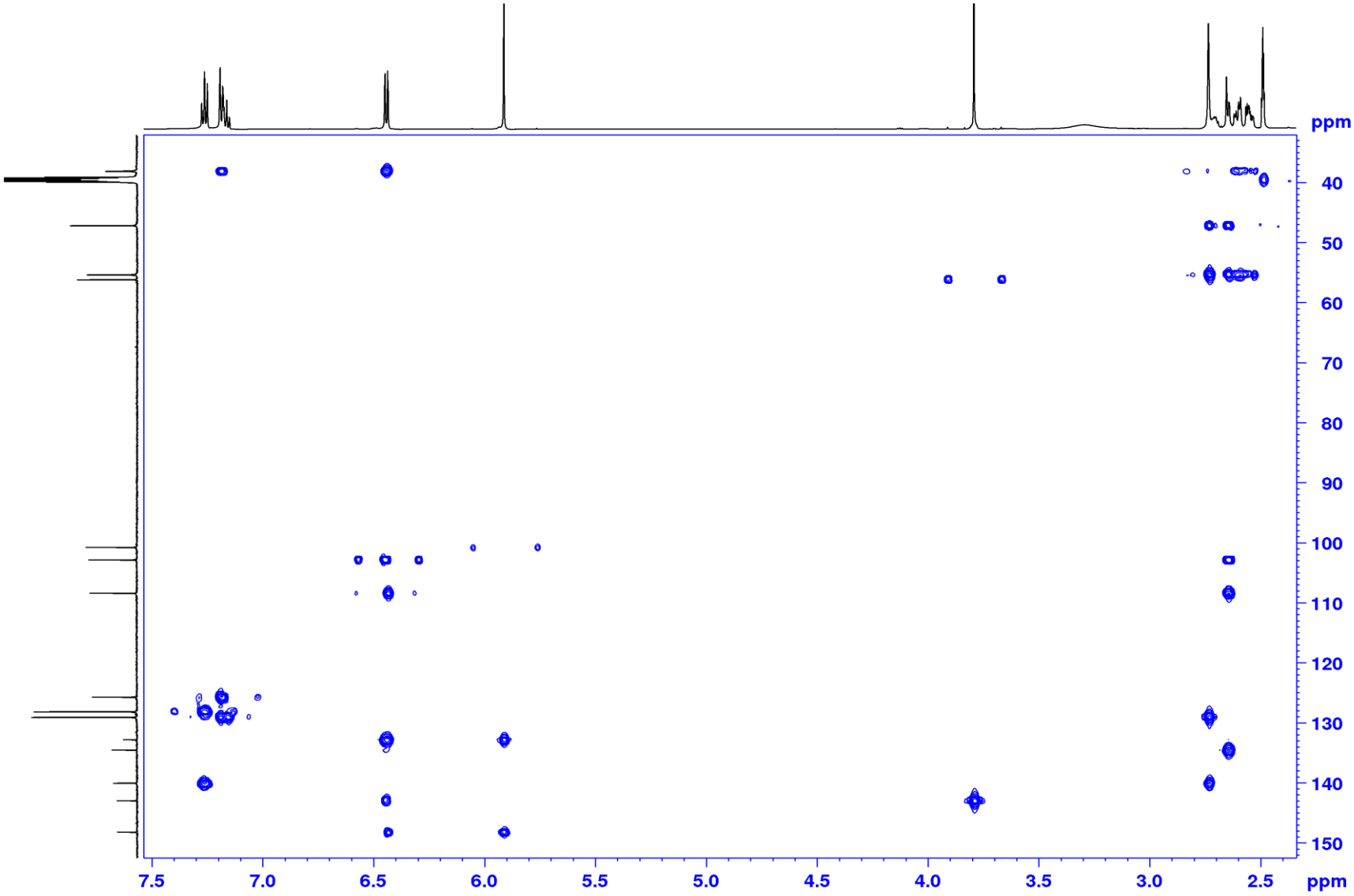

Figure S70. ^{1}H-^{13}C HMBC spectrum (600 MHz, DMSO-d_6) of hancockiamide H (**8**)

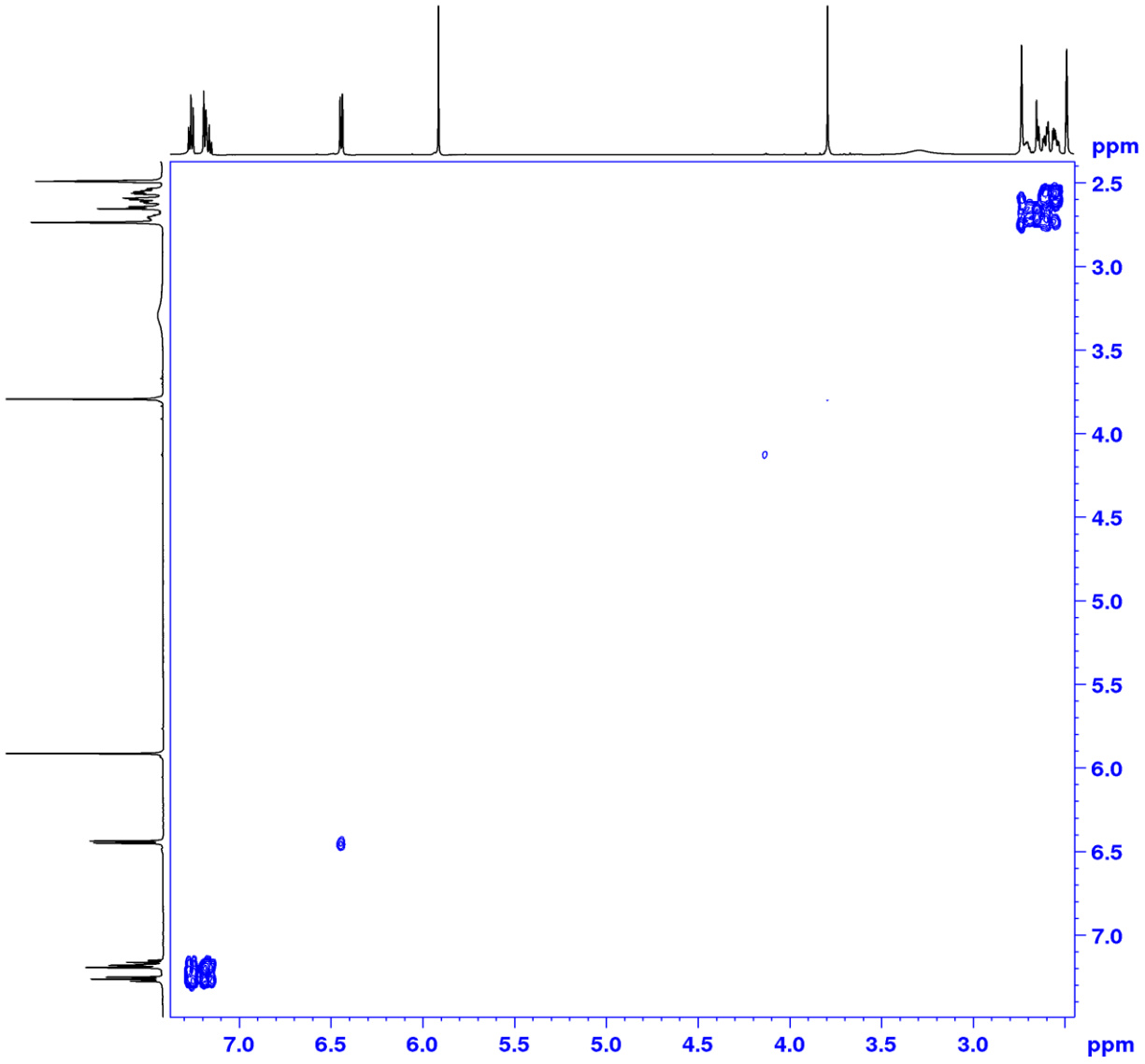

Figure S71. COSY spectrum (600 MHz, DMSO-d_6) of hancockiamide H (**8**)

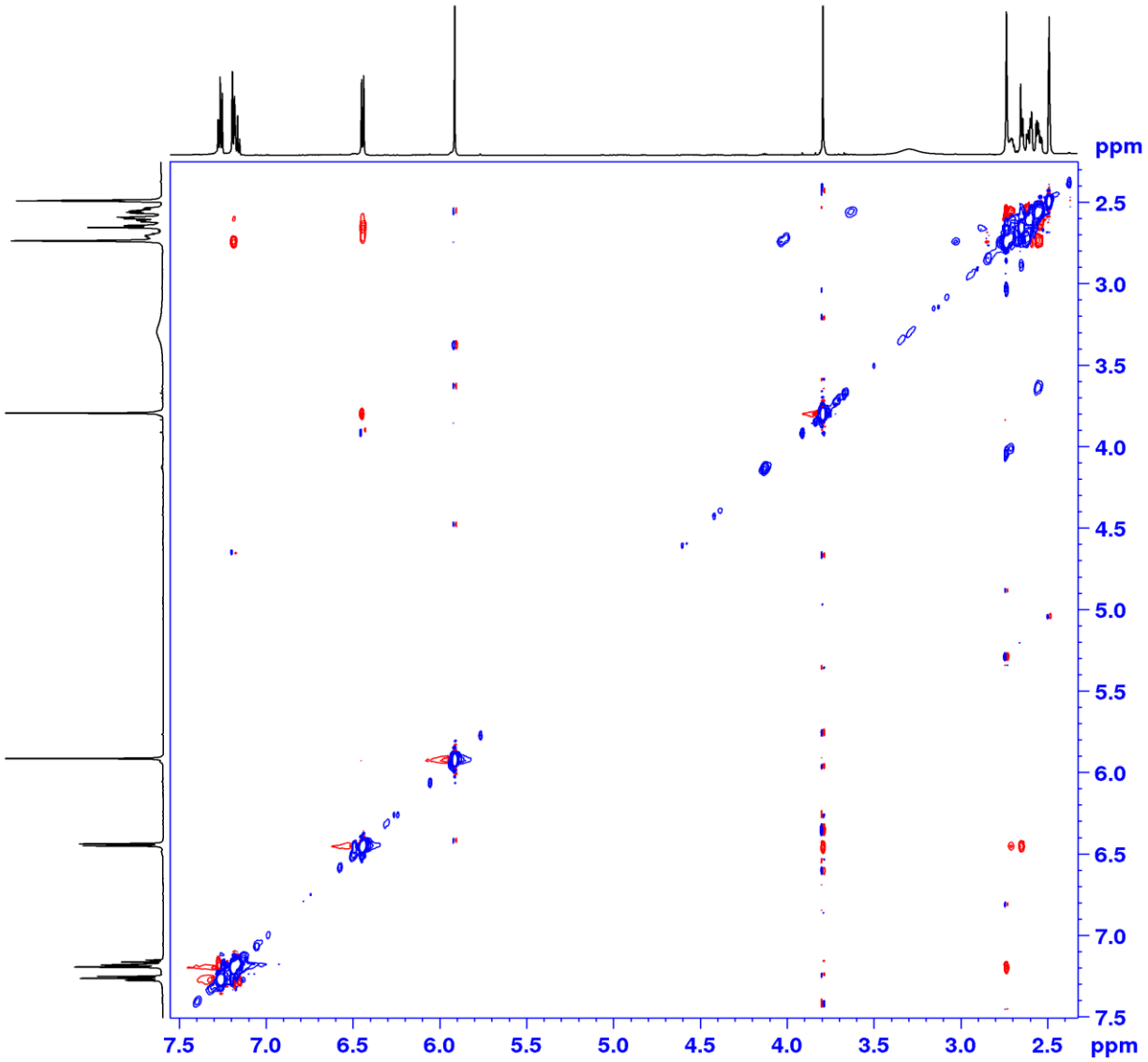

Figure S72. ROESY spectrum (600 MHz, DMSO-d_6) of hancockiamide H (**8**)

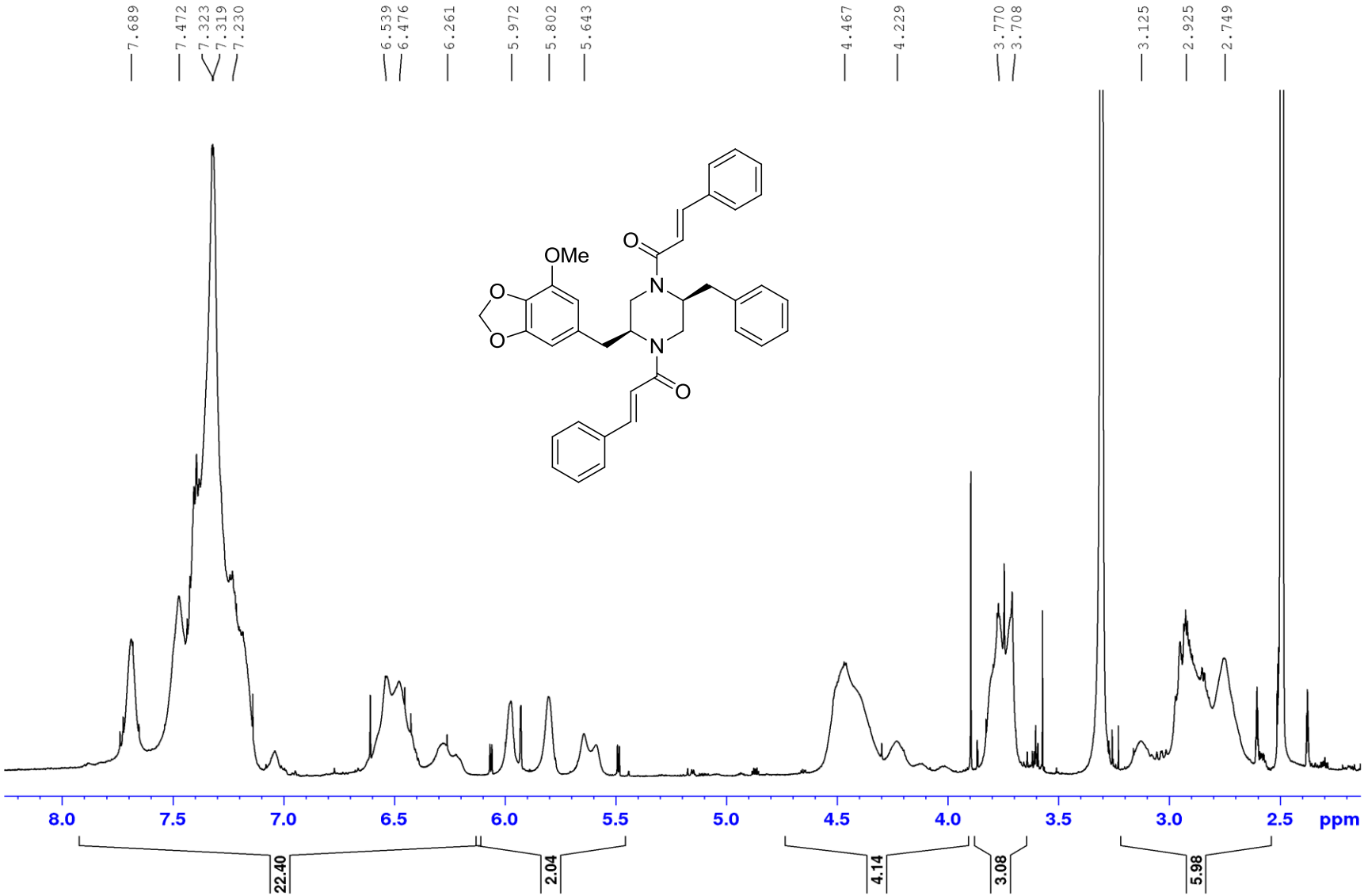

Figure S73. ^{1}H NMR spectrum (600 MHz, DMSO-d_6) of hancockiamide I (**9**)

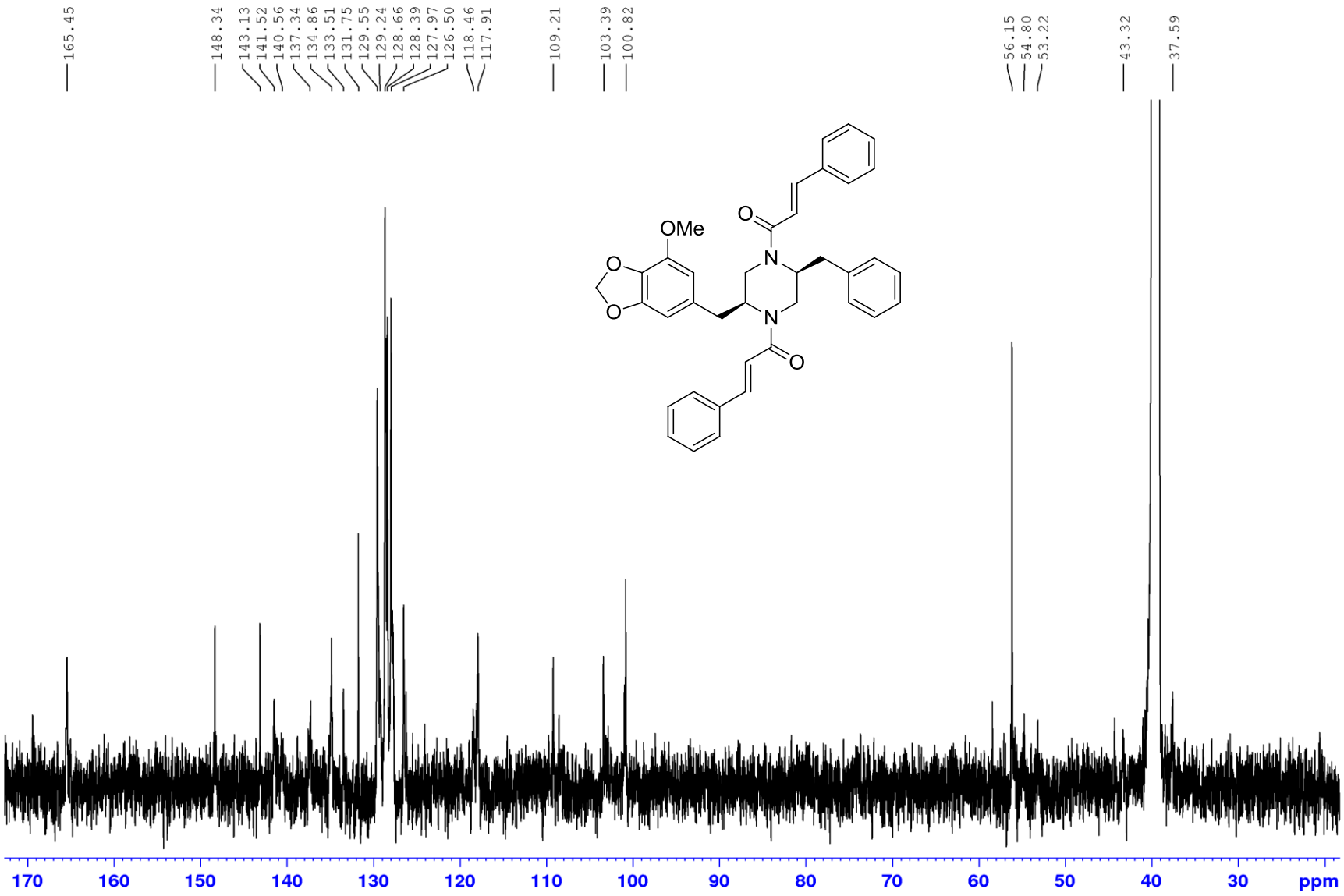

Figure S74. ^{13}C NMR spectrum (150 MHz, DMSO-d_6) of hancockiamide I (**9**)

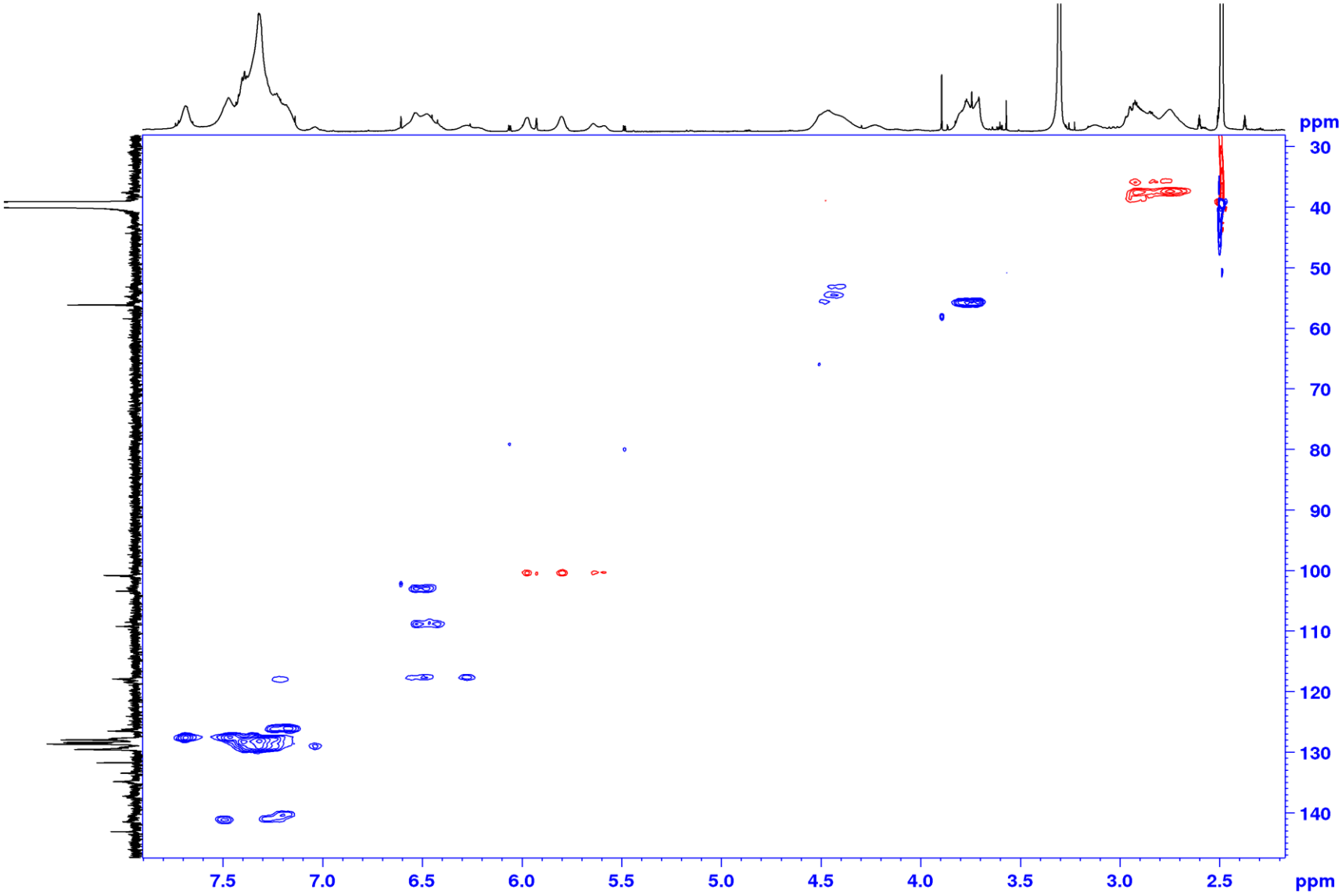

Figure S75. ^{1}H-^{13}C HSQC spectrum (600 MHz, DMSO-d_6) of hancockiamide I (**9**)

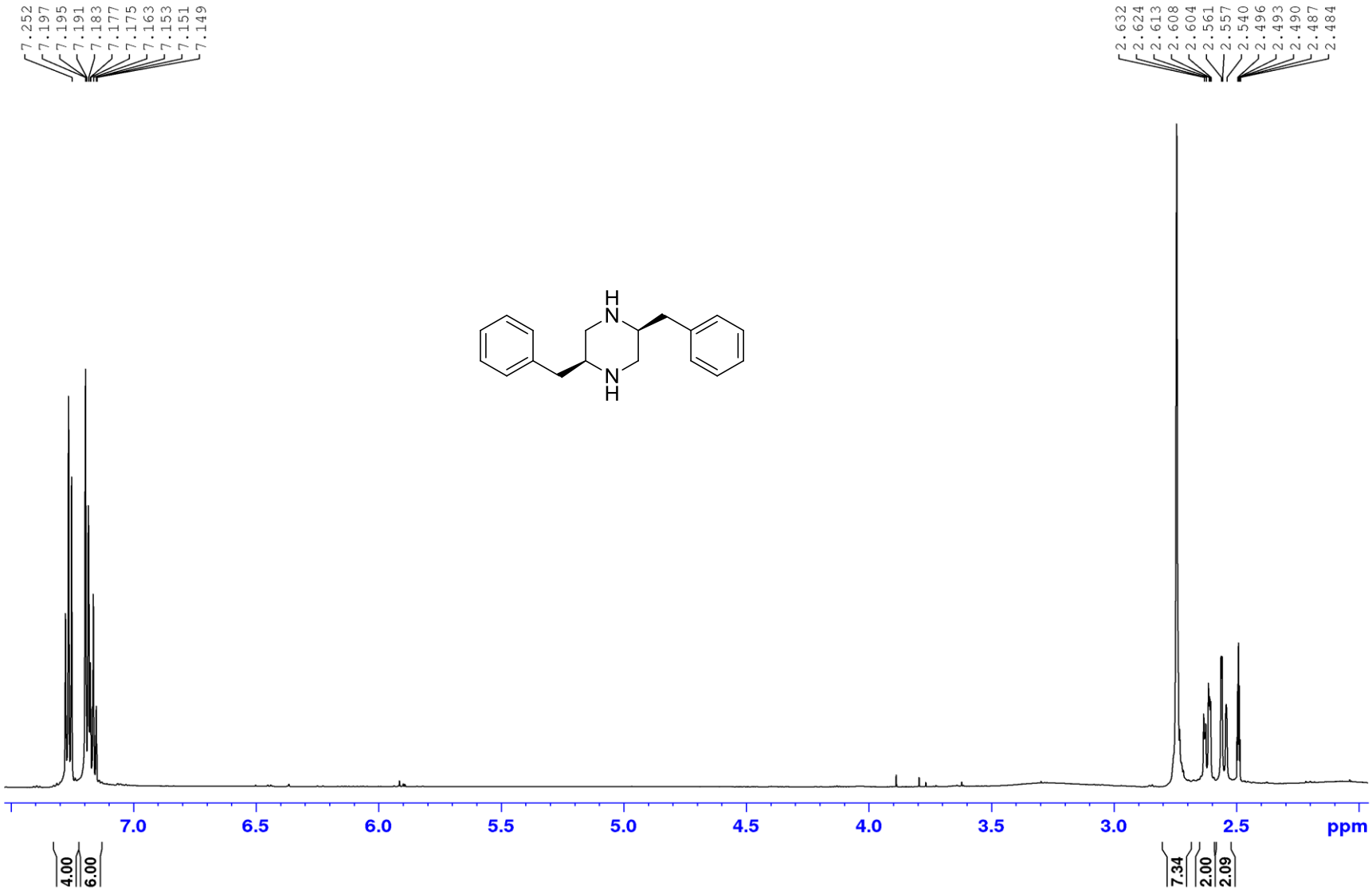

Figure S76. ^{1}H NMR spectrum (600 MHz, DMSO-d_6) of xenocockiamide A (**10**)

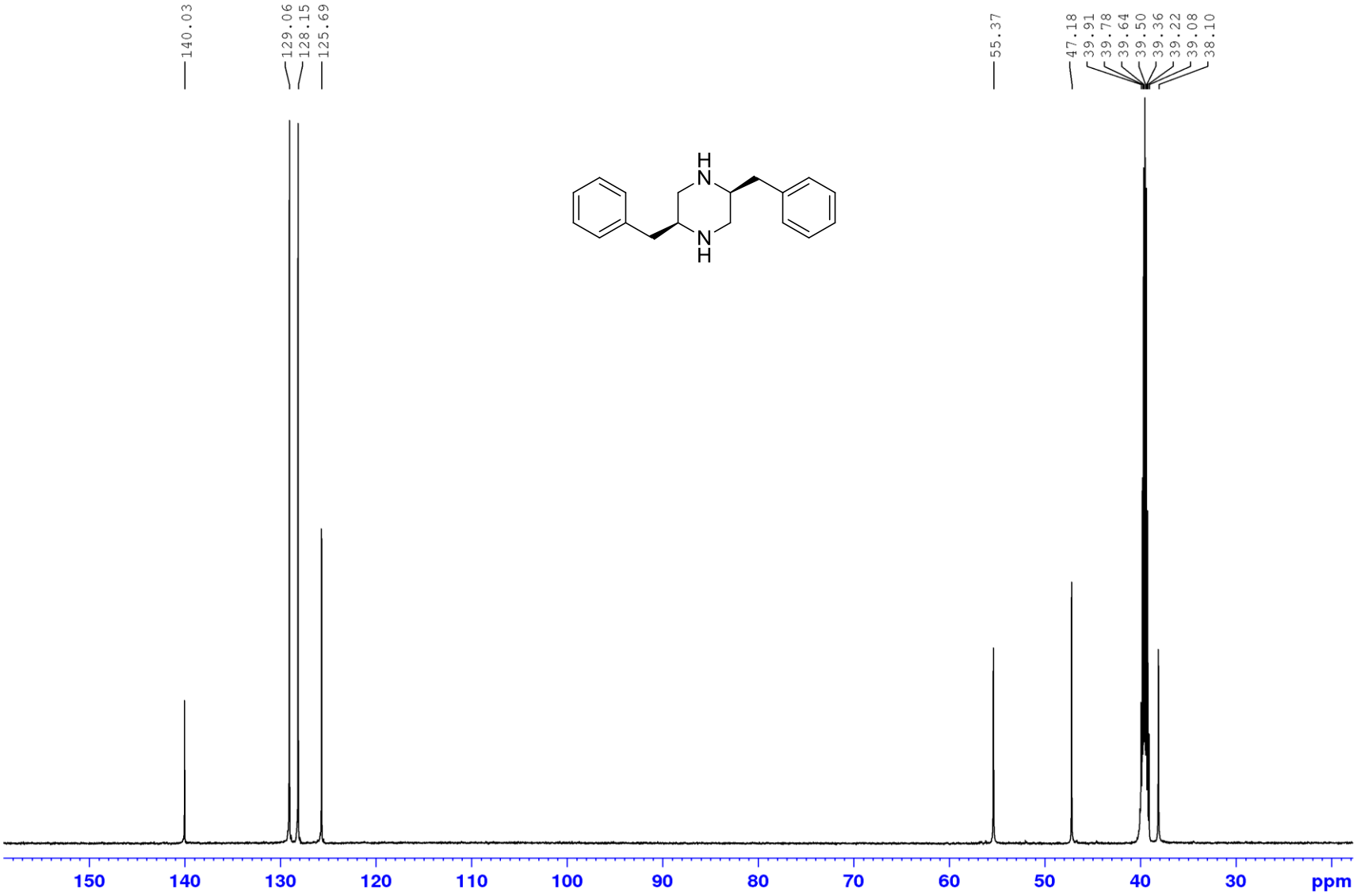

Figure S77. ^{13}C NMR spectrum (150 MHz, DMSO-d_6) of xenocockiamide A (**10**)

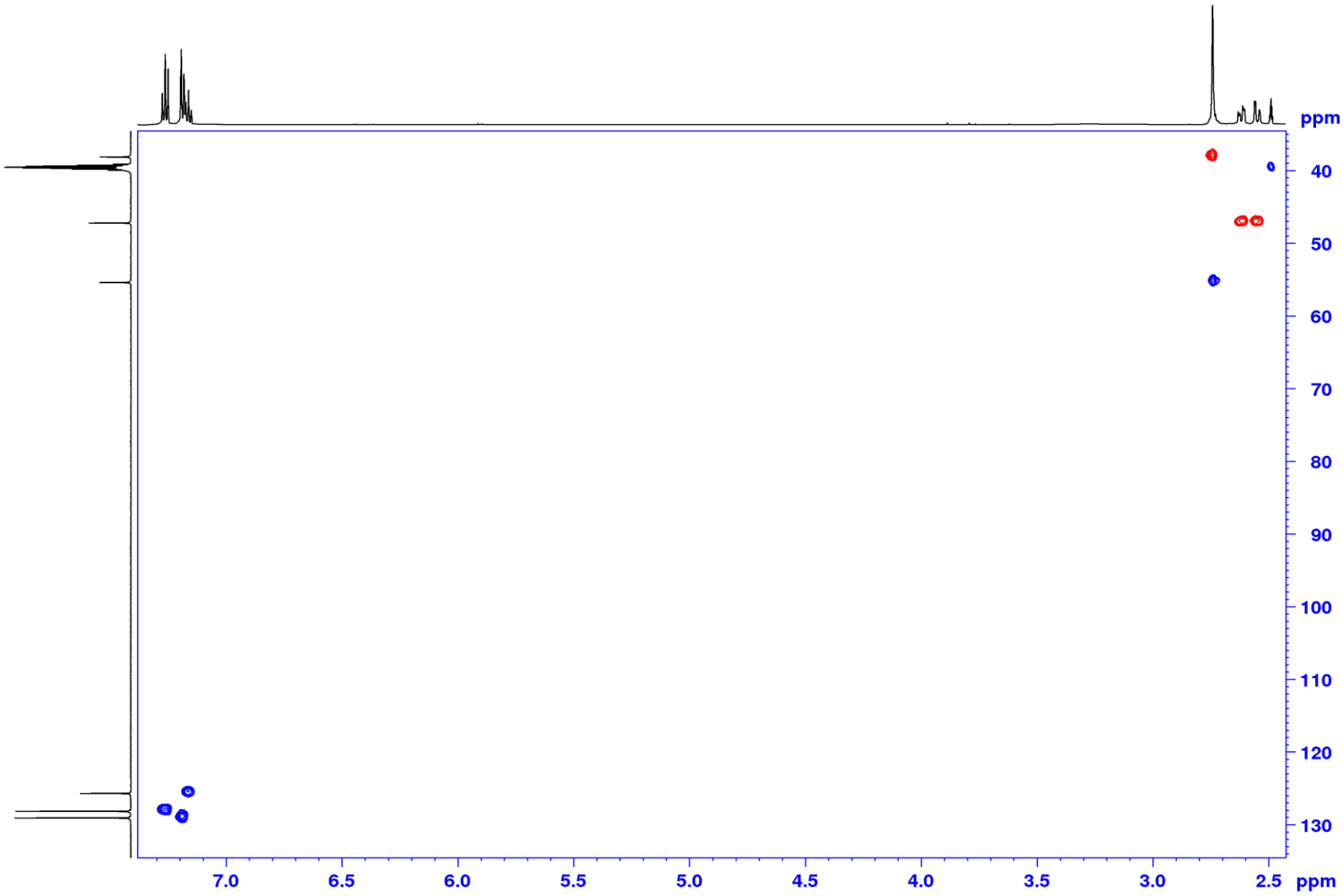

Figure S78. ^{1}H-^{13}C HSQC spectrum (600 MHz, DMSO-d_6) of xenocockiamide A (**10**)

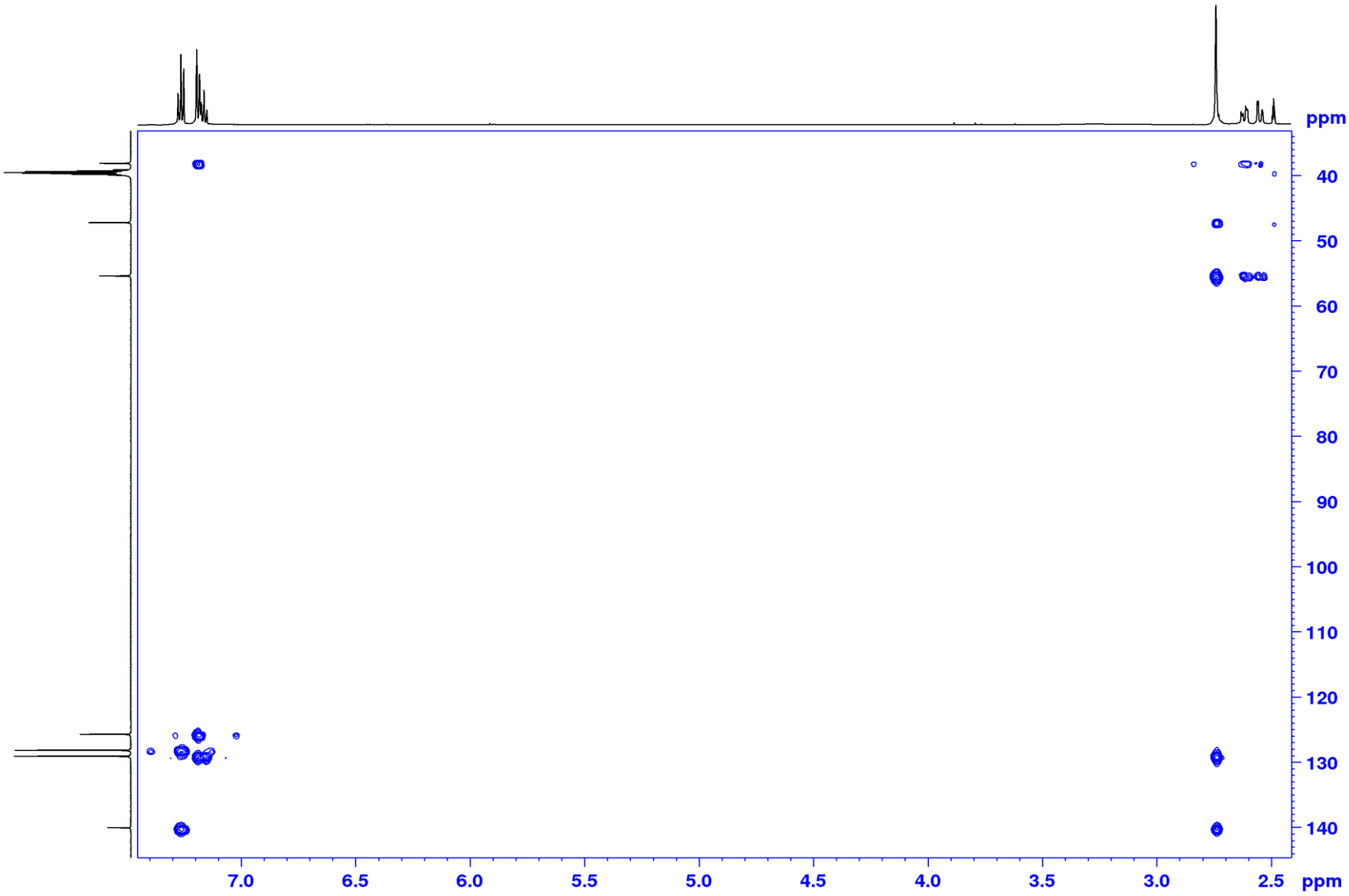

Figure S79. ^{1}H-^{13}C HMBC spectrum (600 MHz, DMSO-d_6) of xenocockiamide A (**10**)

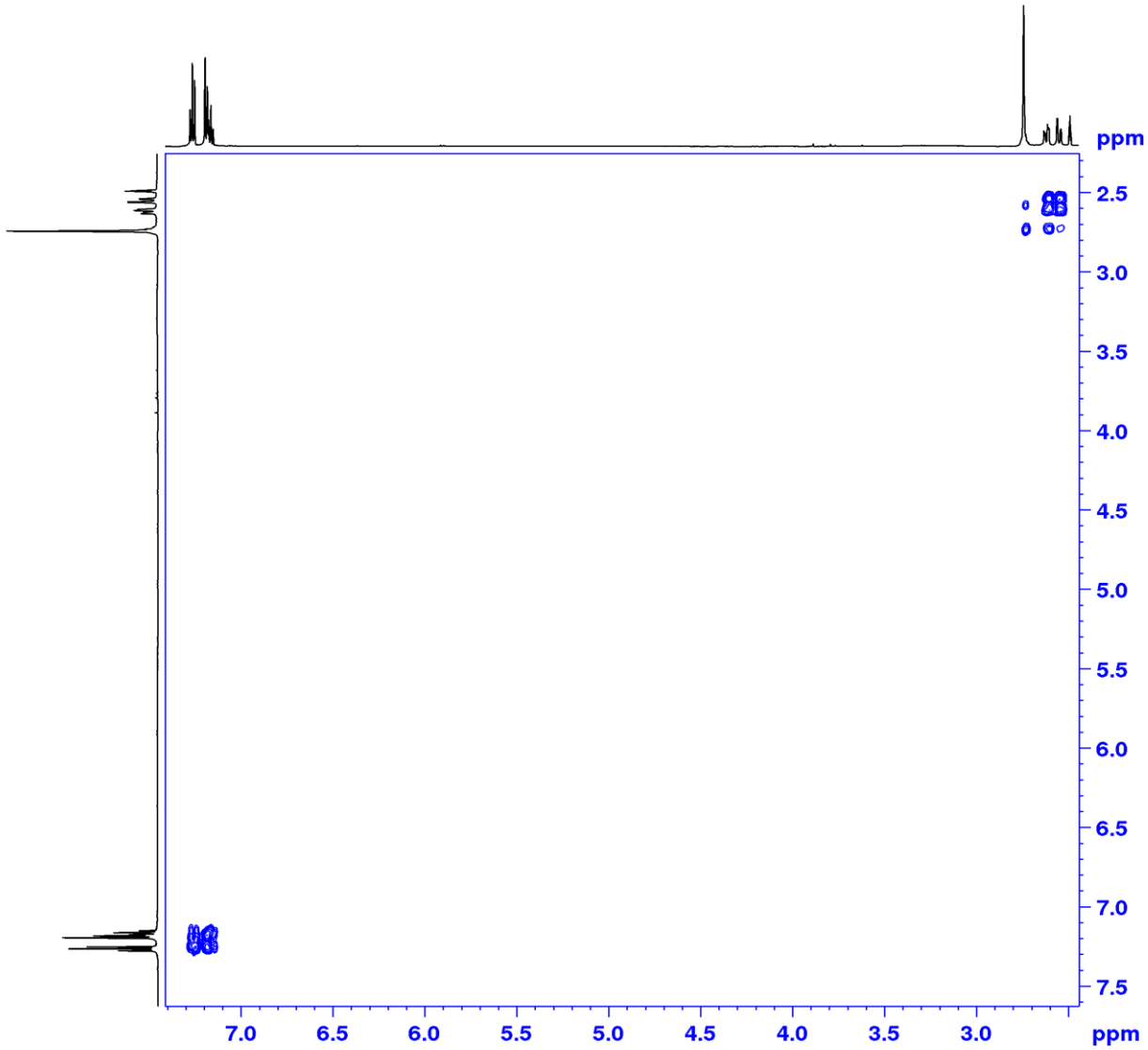

Figure S80. COSY spectrum (600 MHz, DMSO-d_6) of xenocockiamide A (**10**)

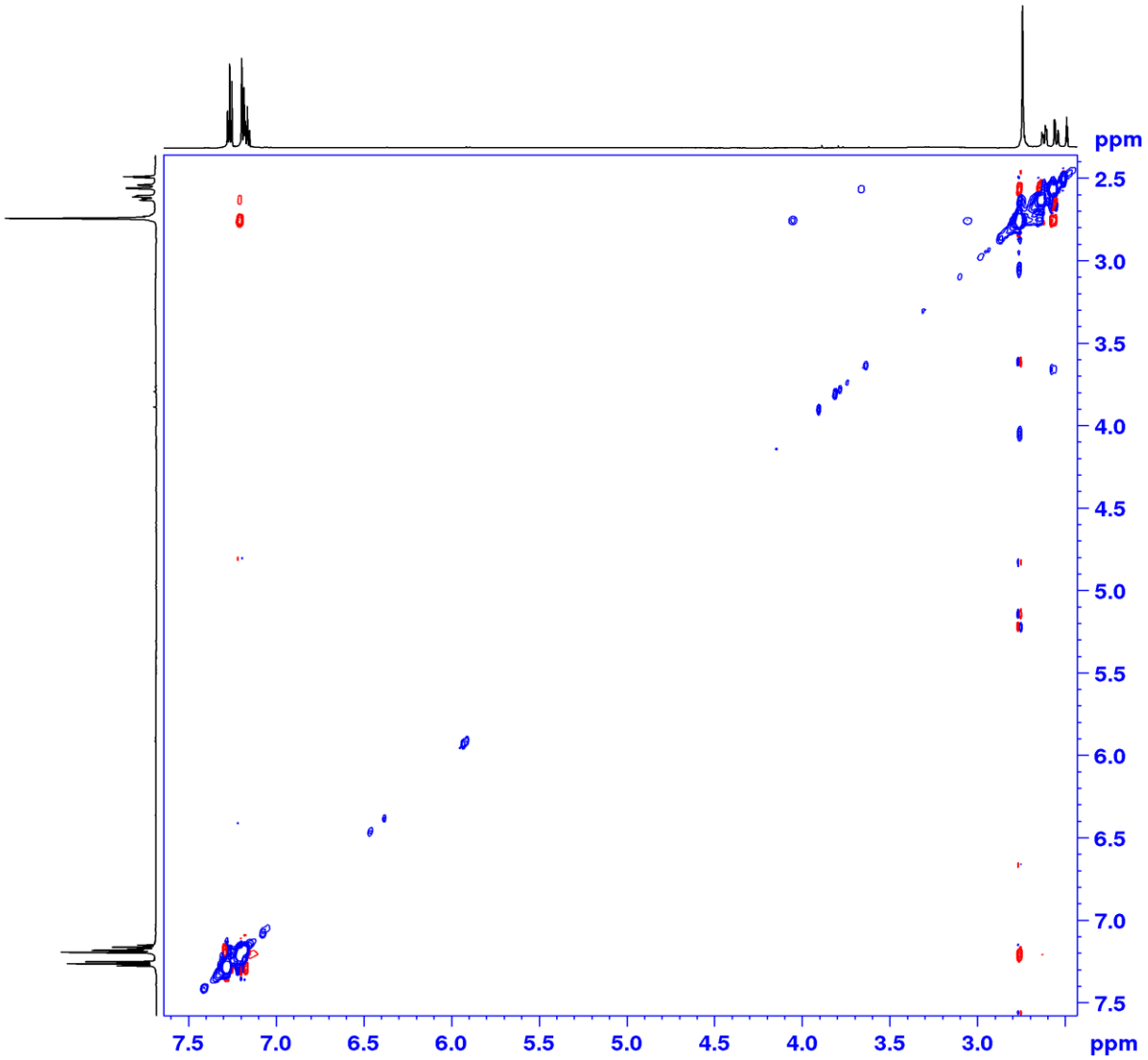

Figure S81. ROESY spectrum (600 MHz, DMSO-d_6) of xenocockiamide A (**10**)

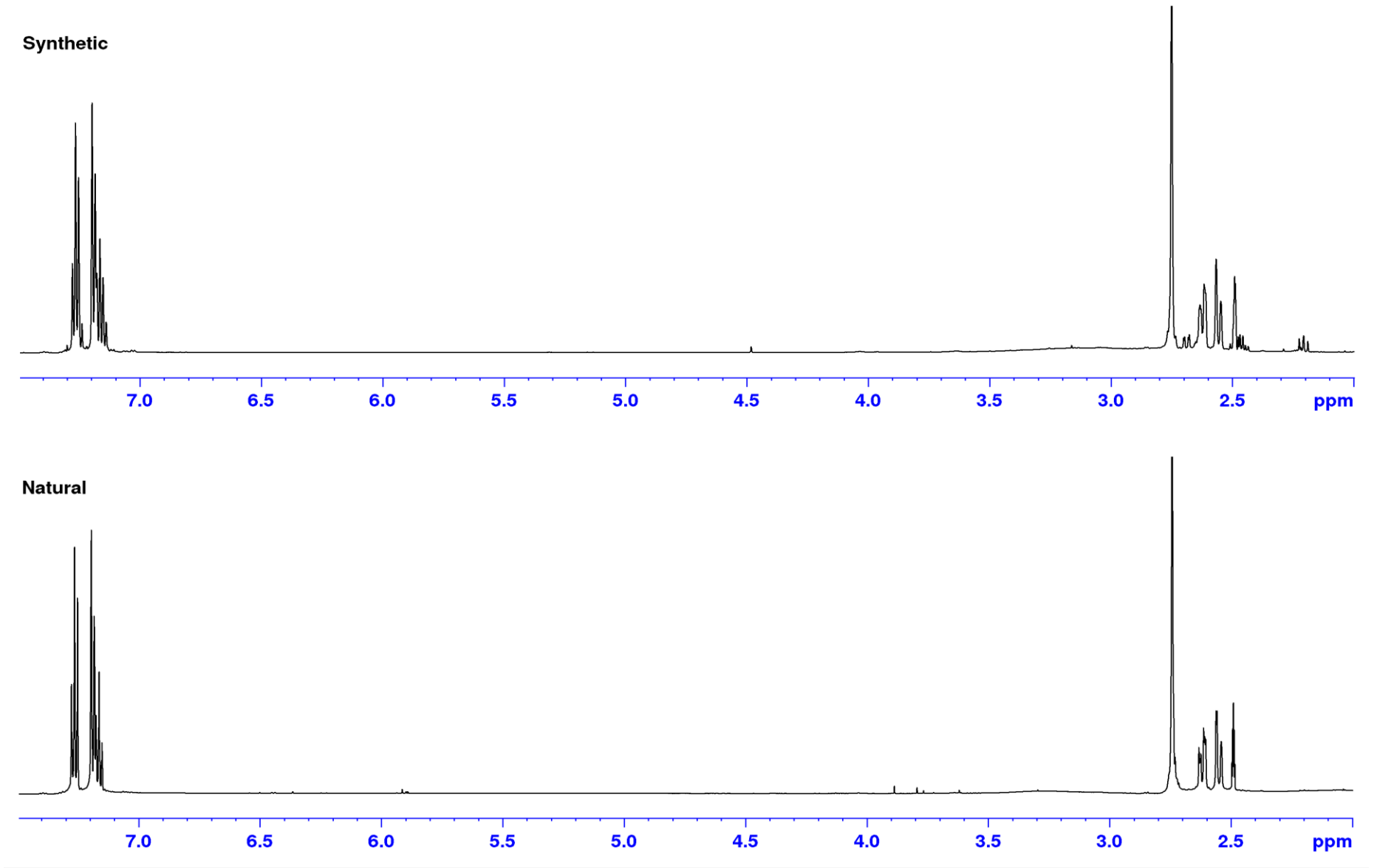

Figure S82. Comparison of ^{1}H NMR spectra (600 MHz, DMSO-d_6) of natural and synthetic xenocockiamide A (**10**)

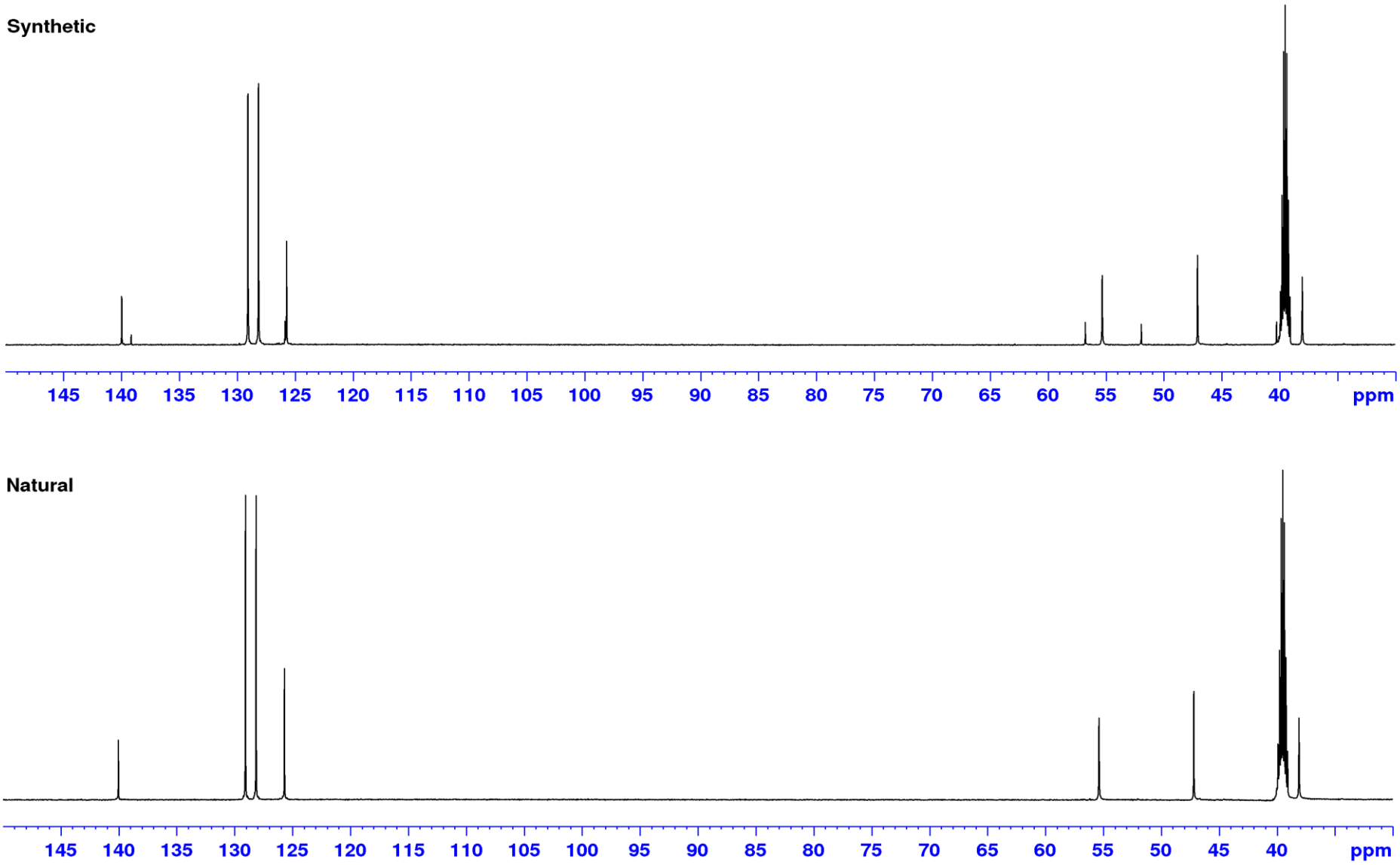

Figure S83. Comparison of ^{13}C NMR spectra (150 MHz, DMSO-d_6) of natural and synthetic xenocockiamide A (**10**)

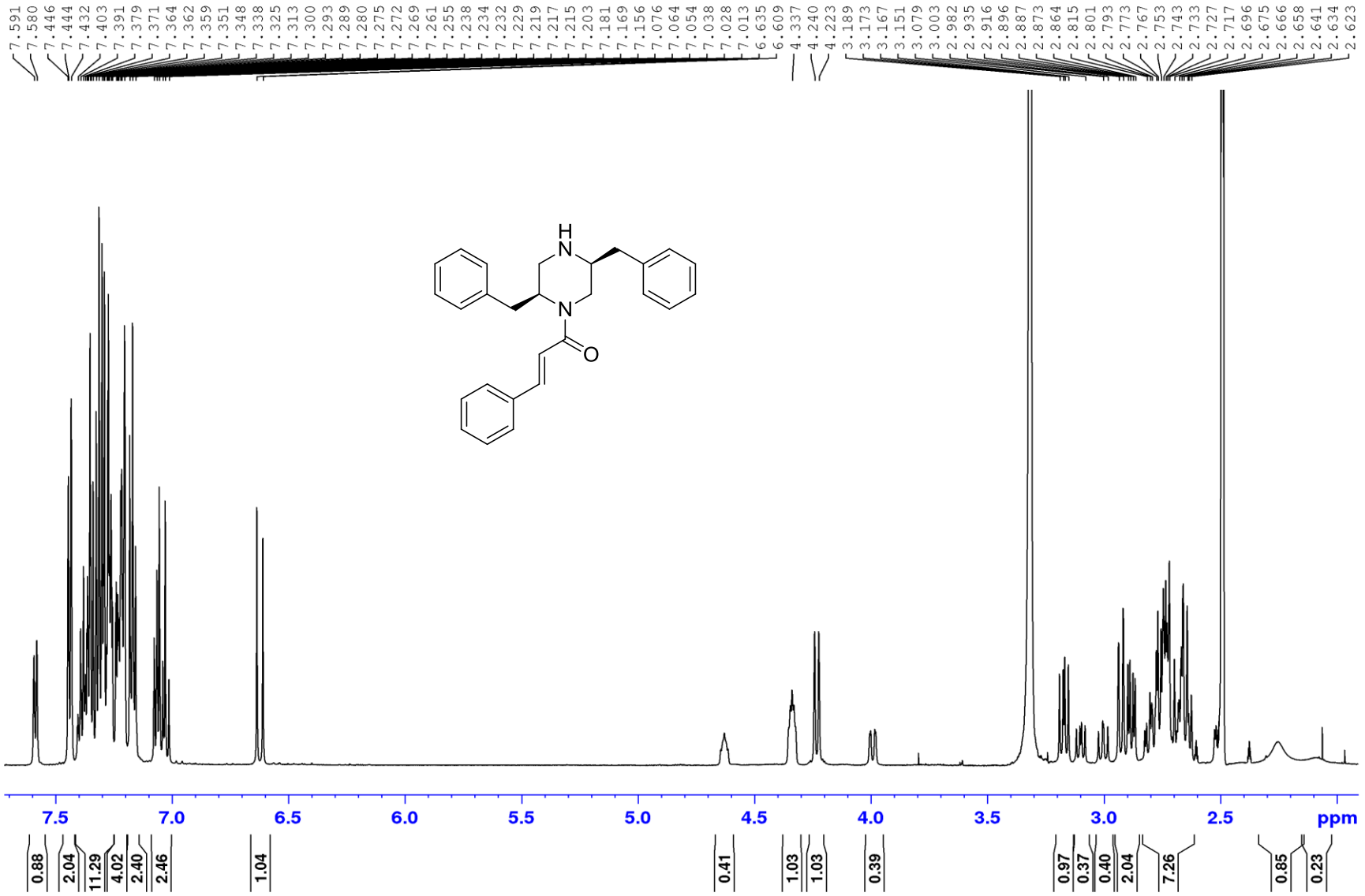

Figure S84. ^{1}H NMR spectrum (600 MHz, DMSO-d_6) of xenocockiamide B (**11**)

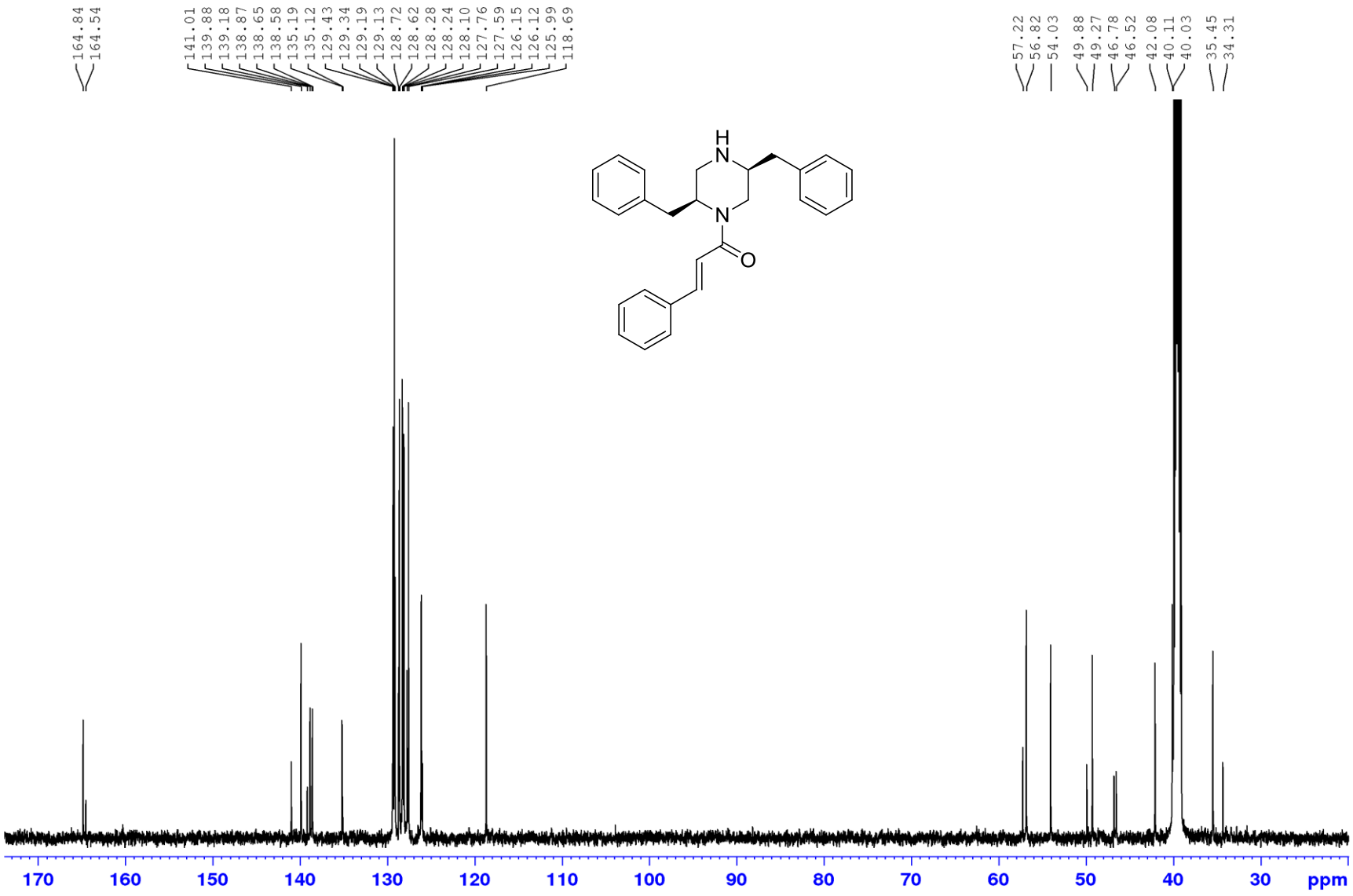

Figure S85. ^{13}C NMR spectrum (150 MHz, DMSO-d_6) of xenocockiamide B (**11**)

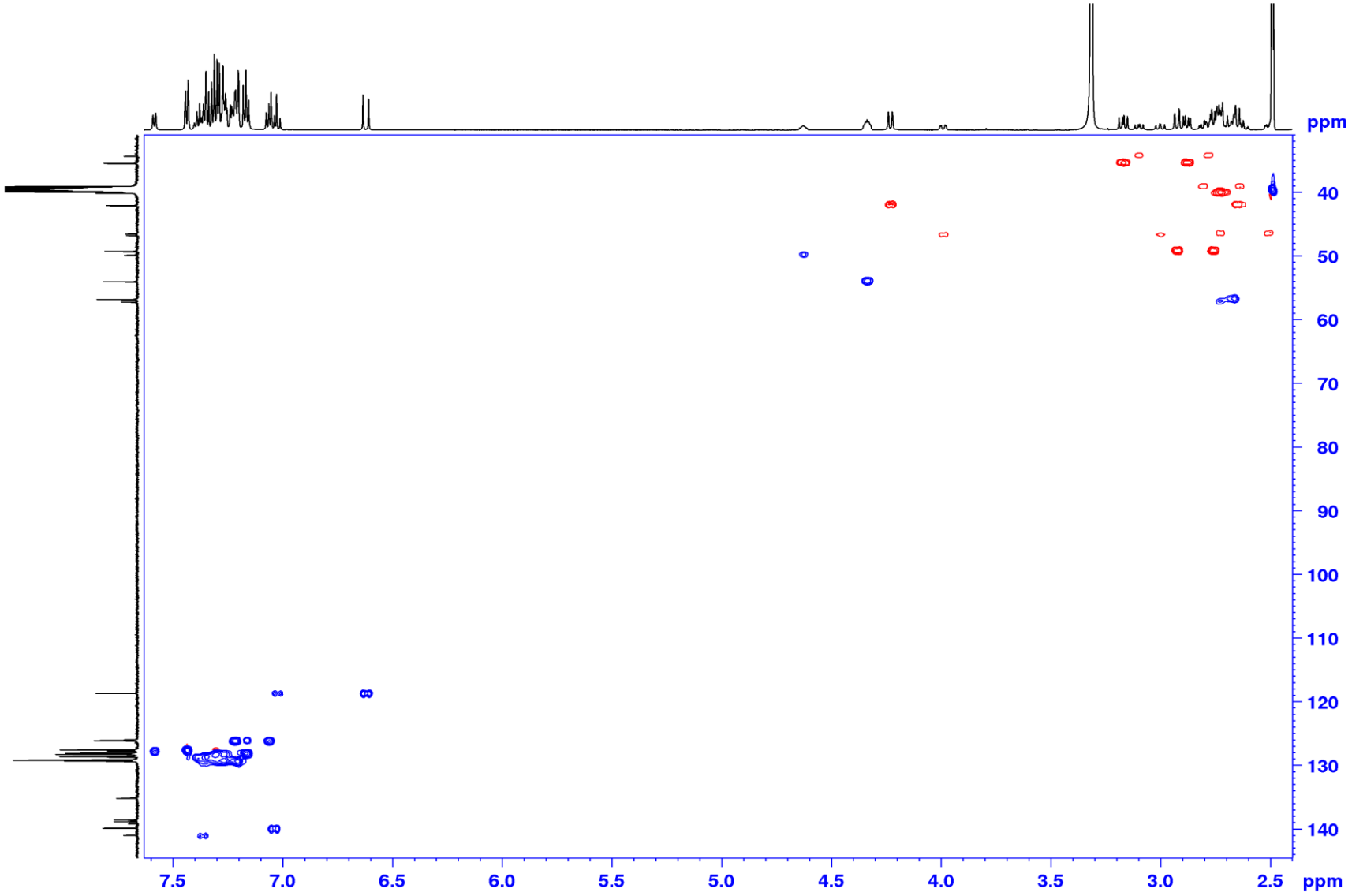

Figure S86. ^{1}H-^{13}C HSQC spectrum (600 MHz, DMSO-d_6) of xenocockiamide B (**11**)

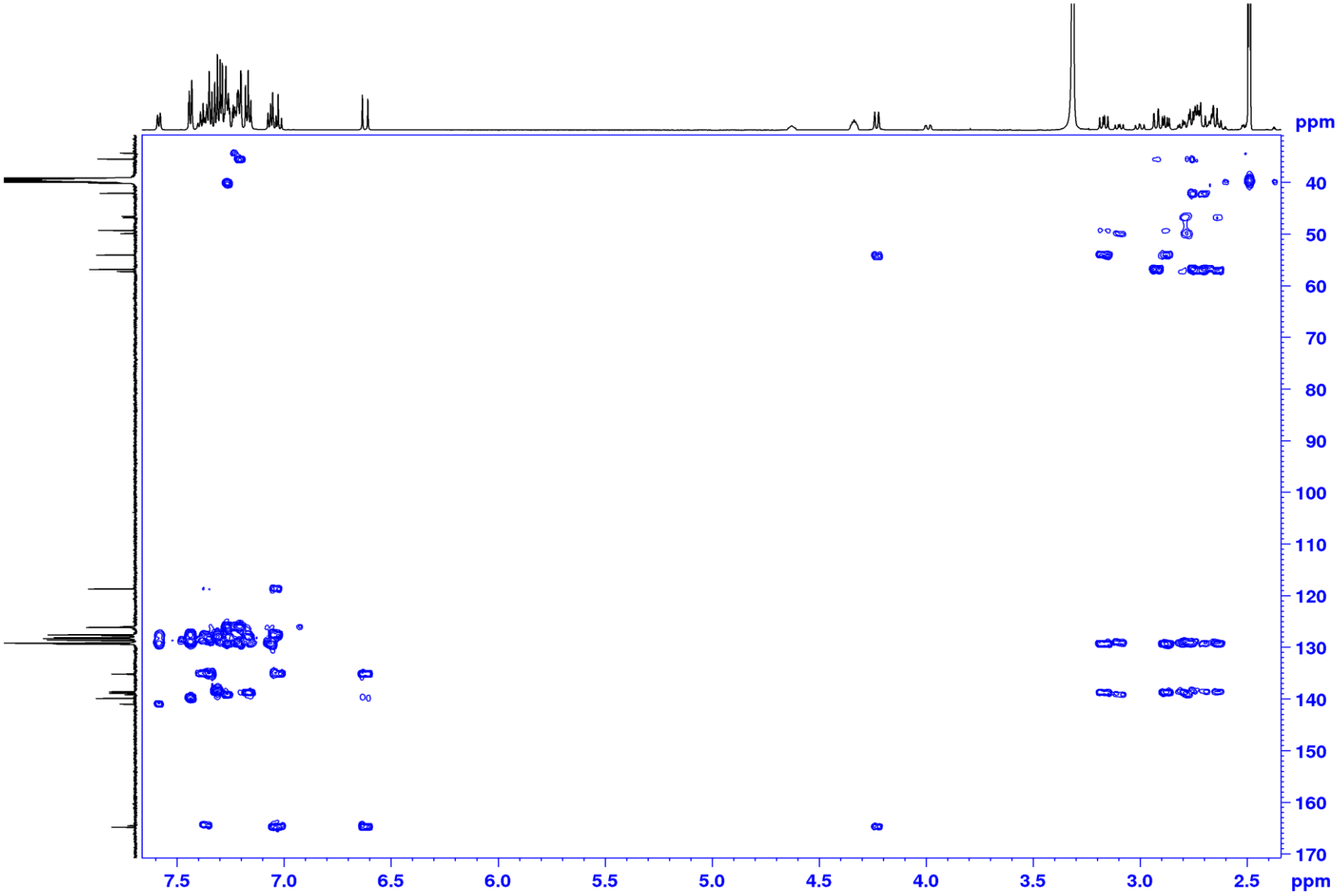

Figure S87. ^{1}H-^{13}C HMBC spectrum (600 MHz, DMSO-d_6) of xenocockiamide B (**11**)

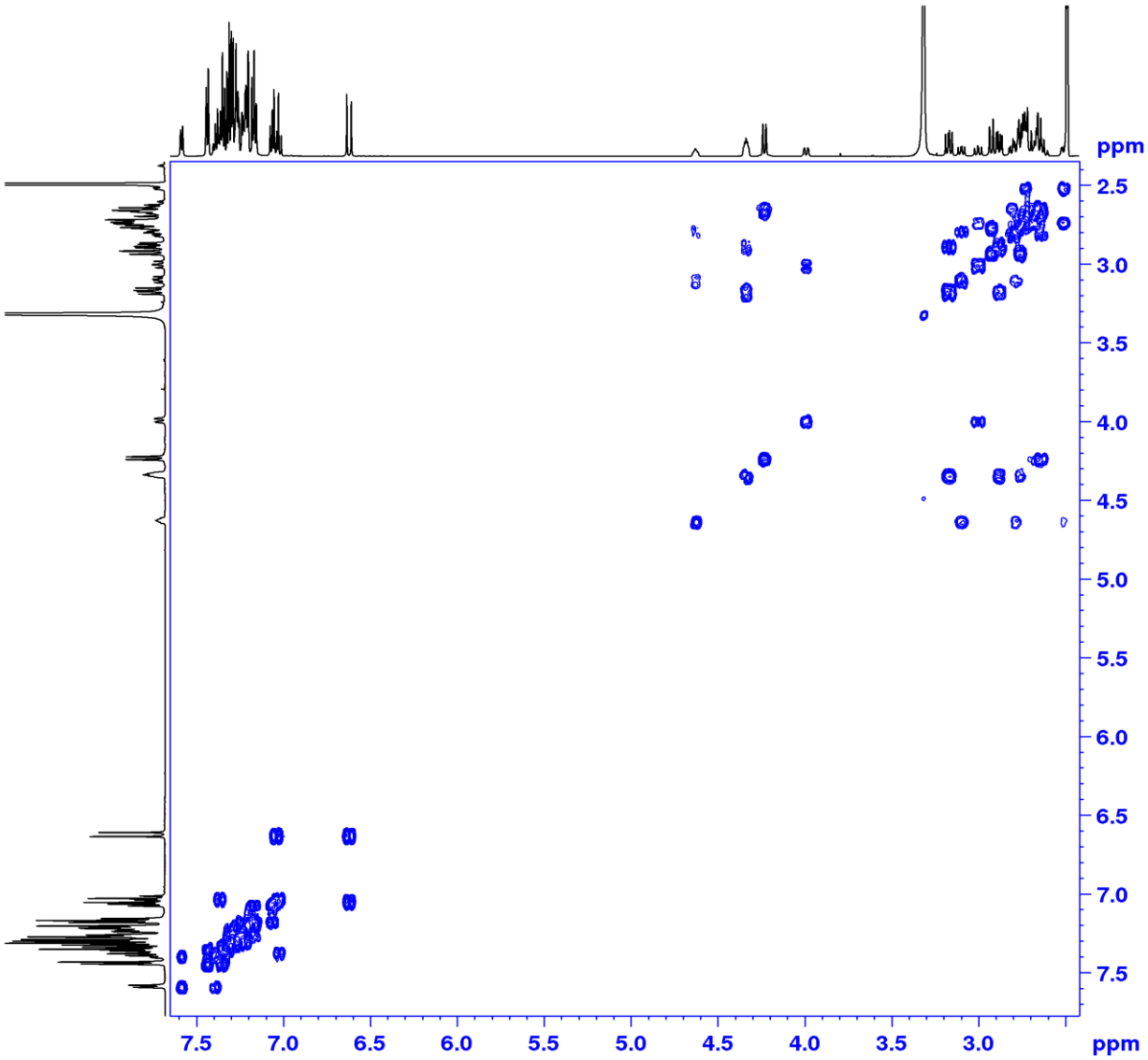

Figure S88. COSY spectrum (600 MHz, DMSO-d_6) of xenocockiamide B (**11**)

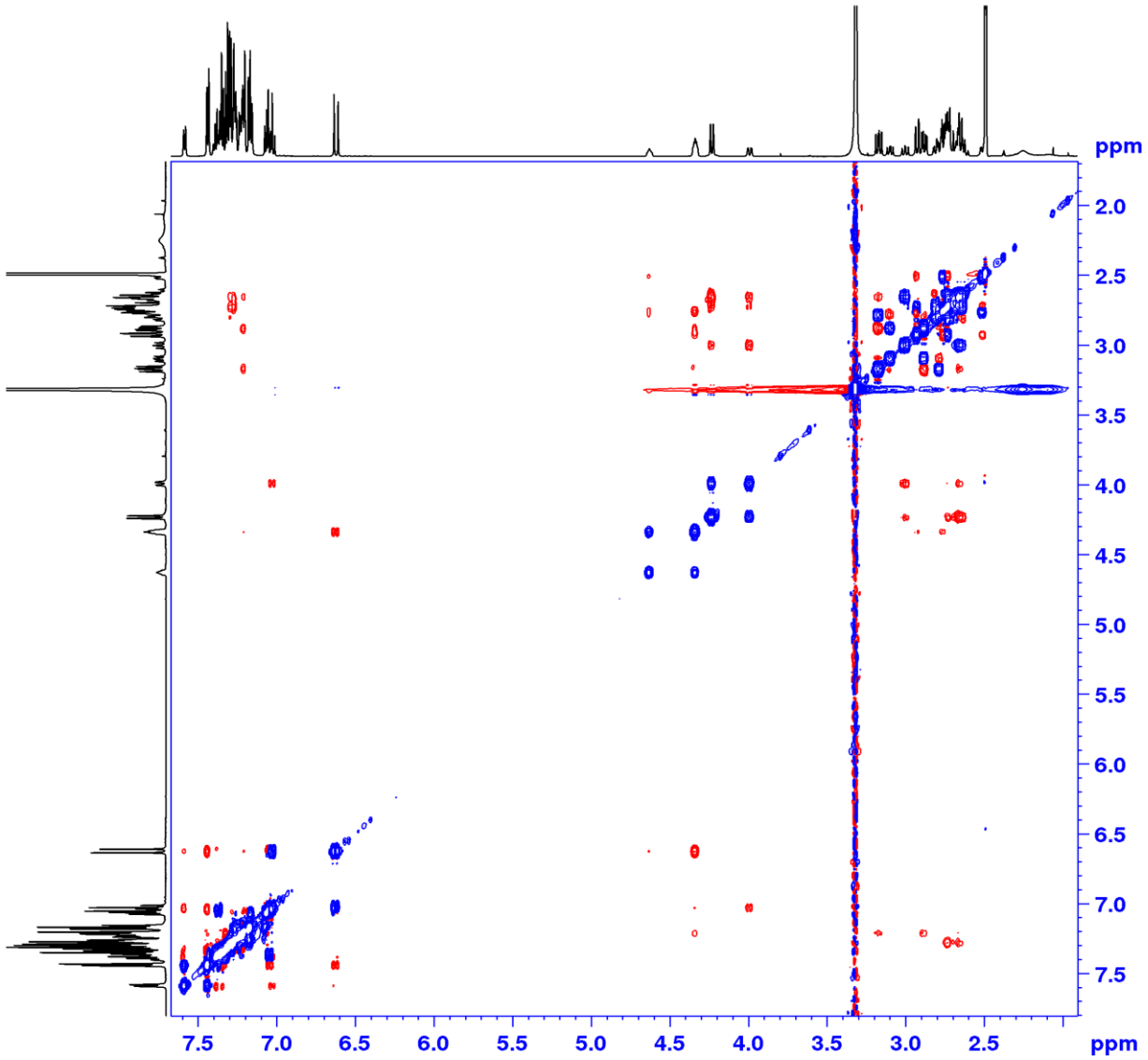

Figure S89. ROESY spectrum (600 MHz, DMSO-d_6) of xenocockiamide B (**11**)

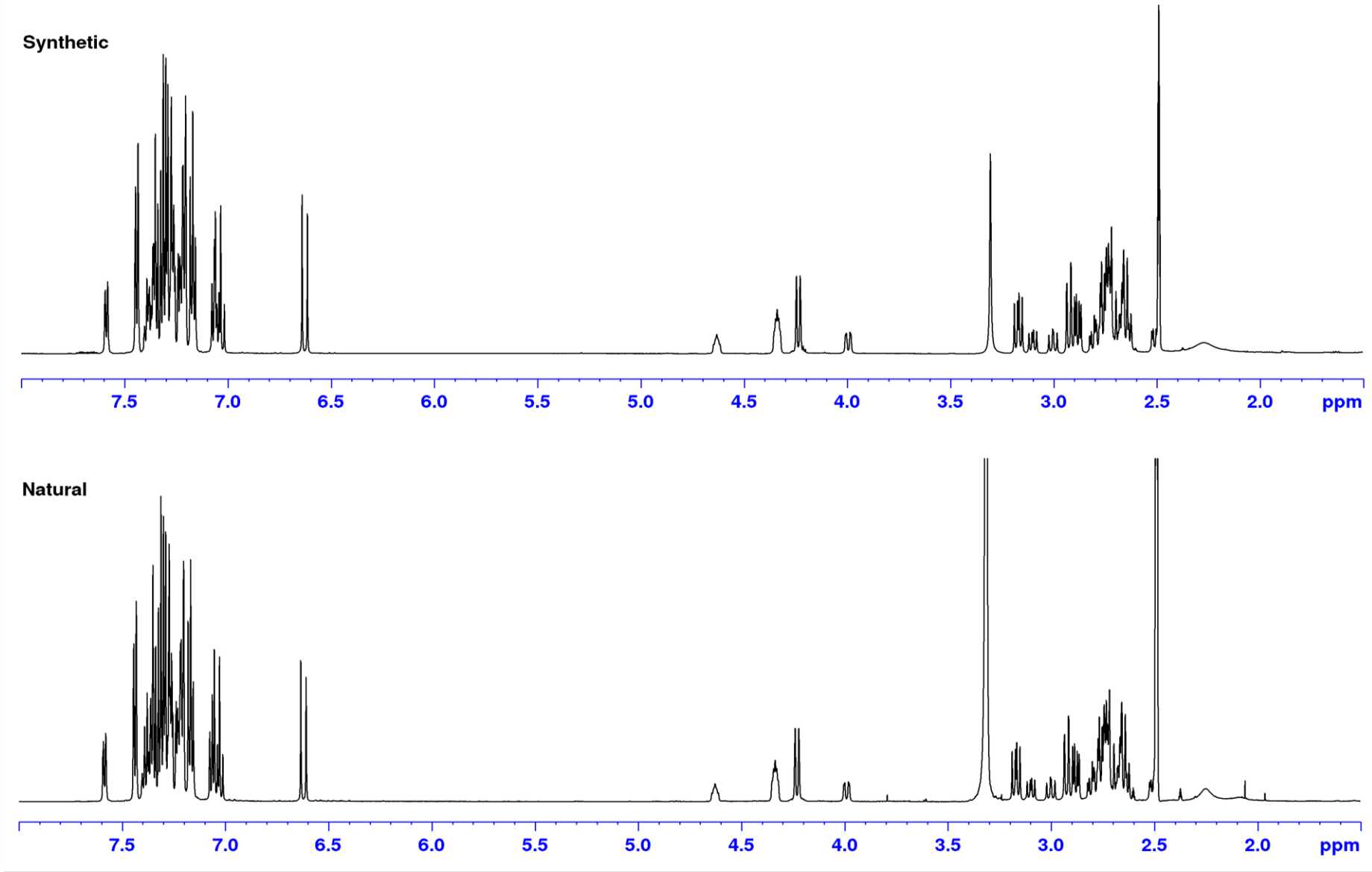

Figure S90. Comparison of ^{1}H NMR spectra (600 MHz, DMSO-d_6) of natural and synthetic xenocockiamide B (**11**)

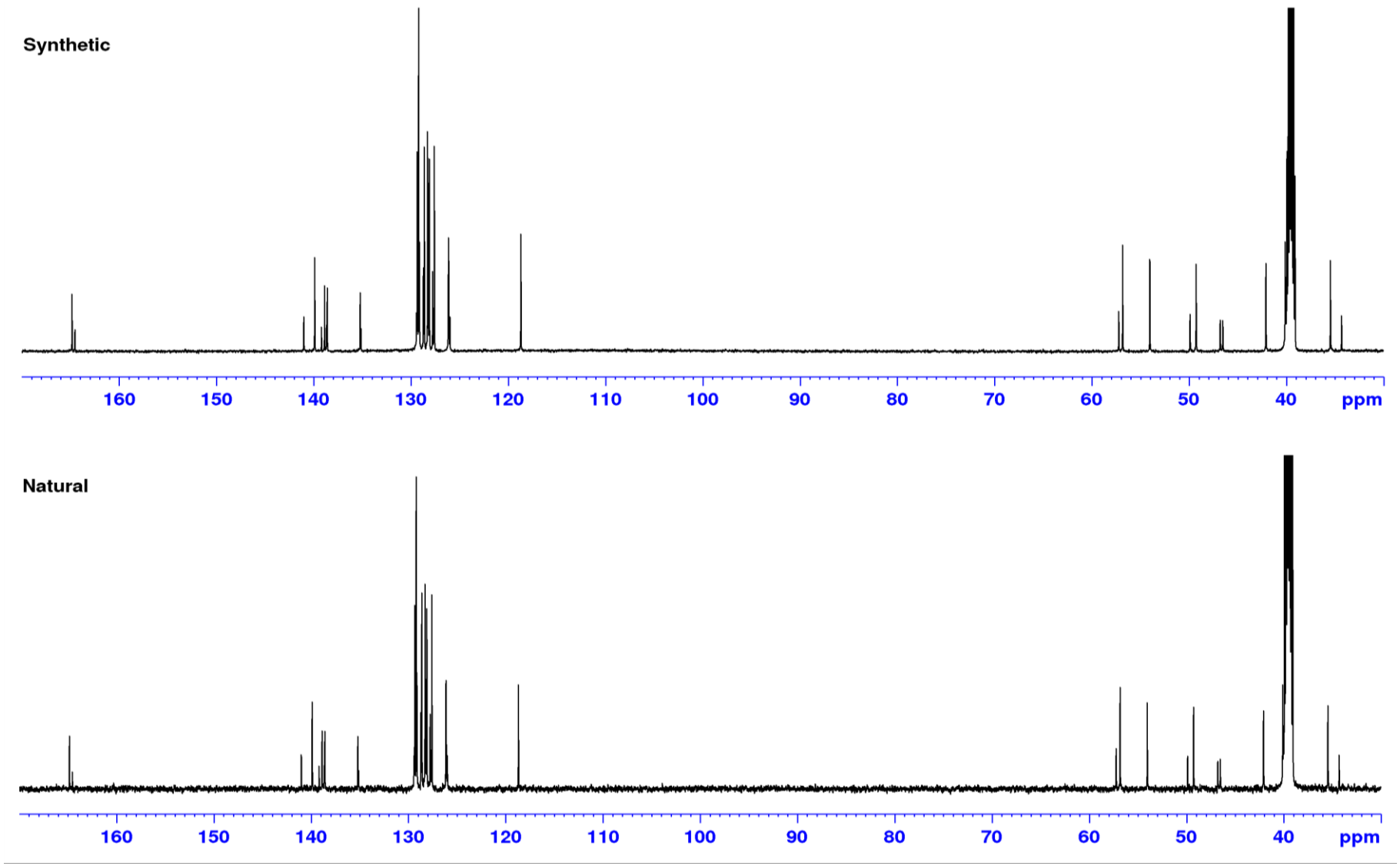

Figure S91. Comparison of ^{13}C NMR spectra (150 MHz, DMSO-d_6) of natural and synthetic xenocockiamide B (**11**)

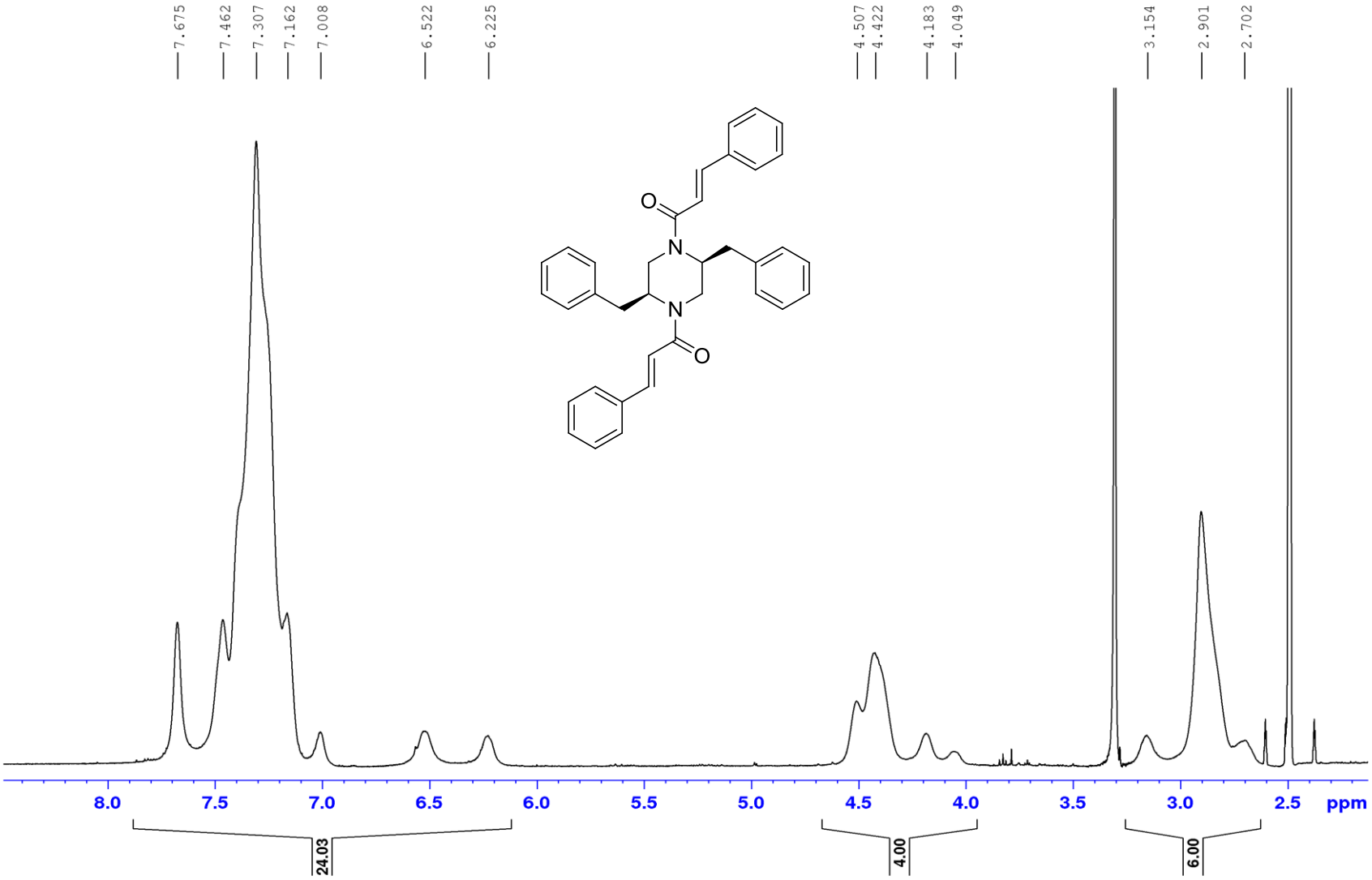

Figure S92. ^{1}H NMR spectrum (600 MHz, DMSO-d_6) of xenocockiamide C (**12**)

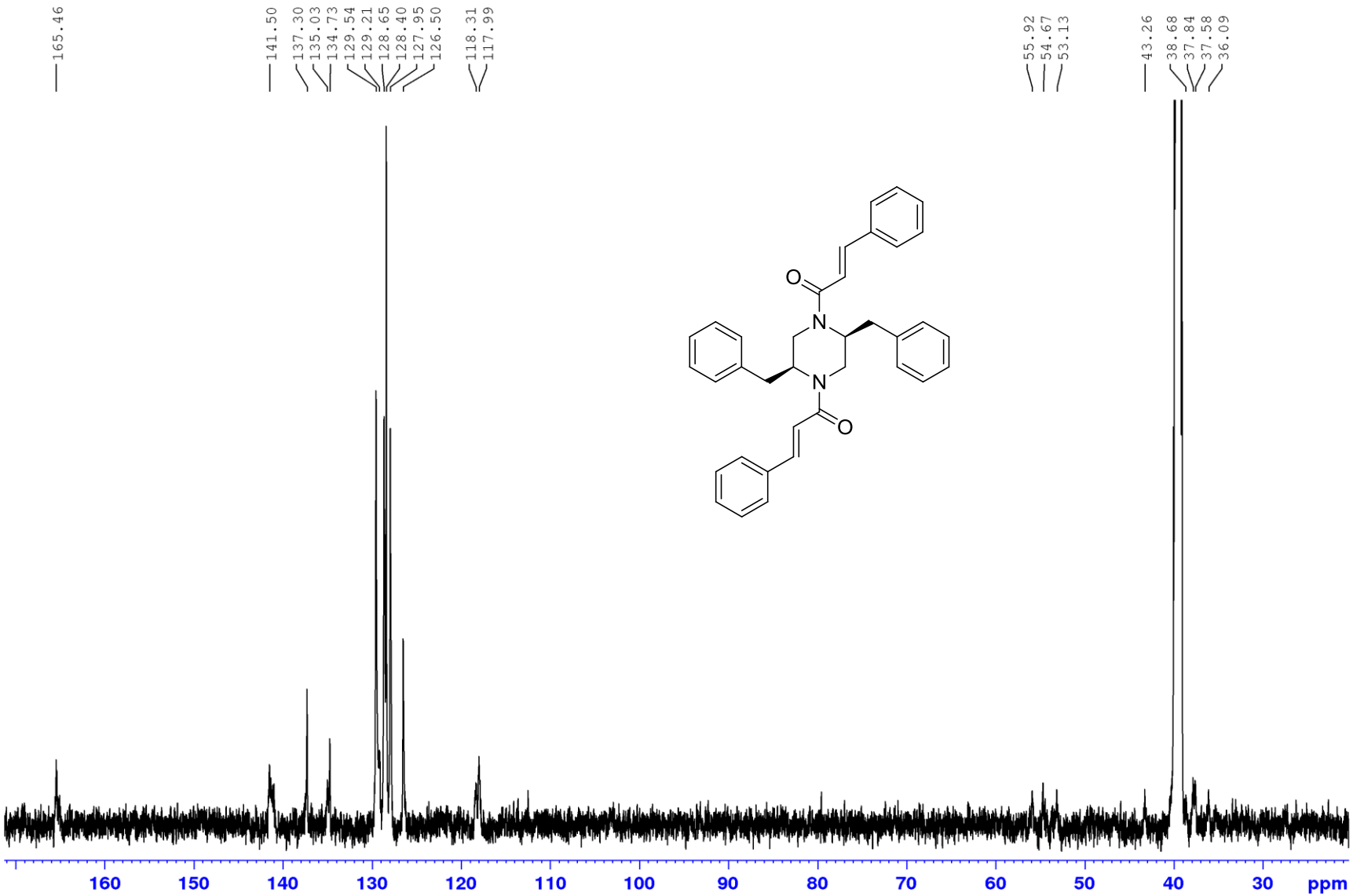

Figure S93. ^{13}C NMR spectrum (150 MHz, DMSO-d_6) of xenocockiamide C (**12**)

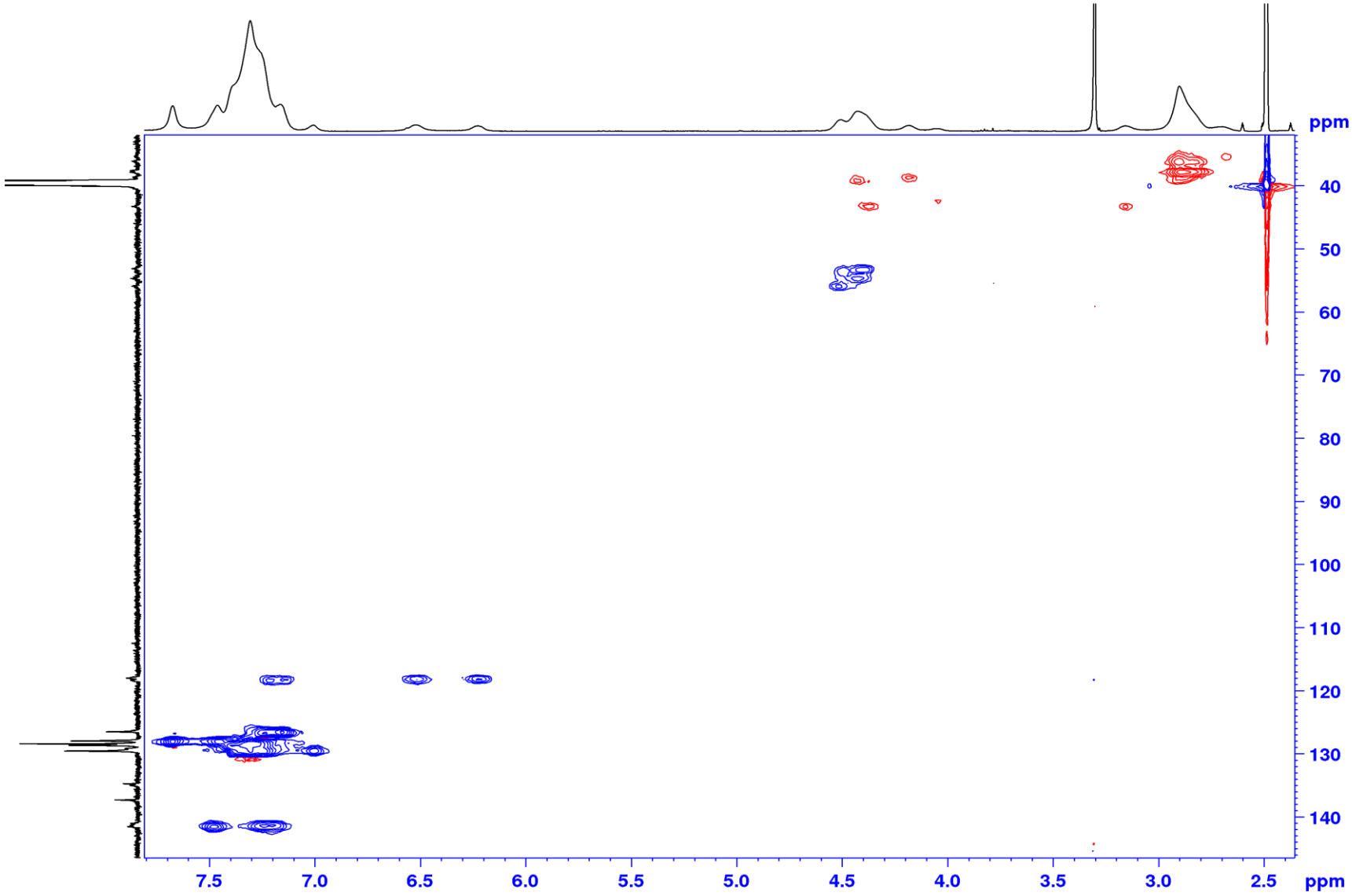

Figure S94. ^{1}H-^{13}C HSQC spectrum (600 MHz, DMSO-d_6) of xenocockiamide C (**12**)

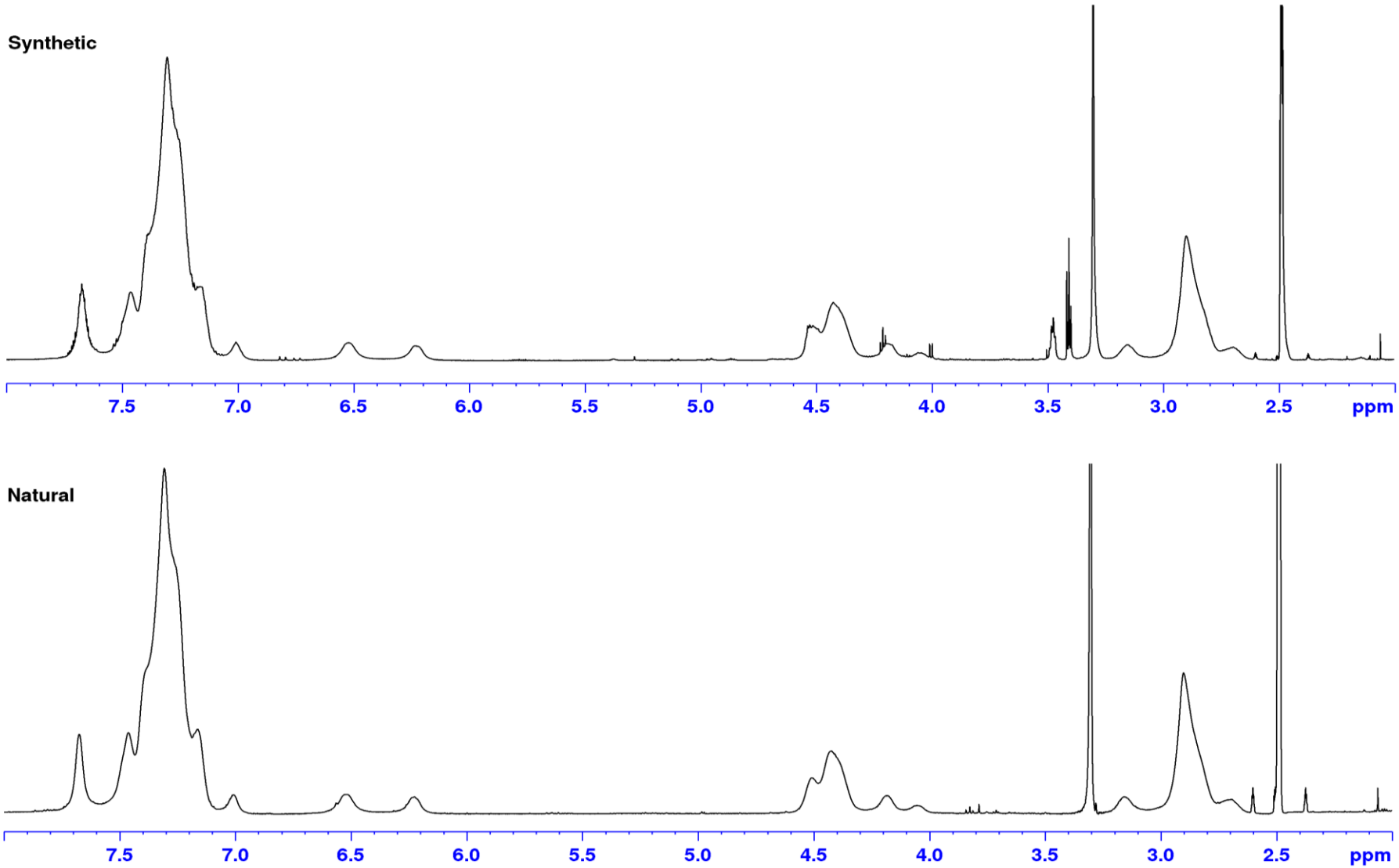

Figure S95. Comparison of ^{1}H NMR spectra (600 MHz, DMSO-d_6) of natural and synthetic xenocockiamide C (**12**)

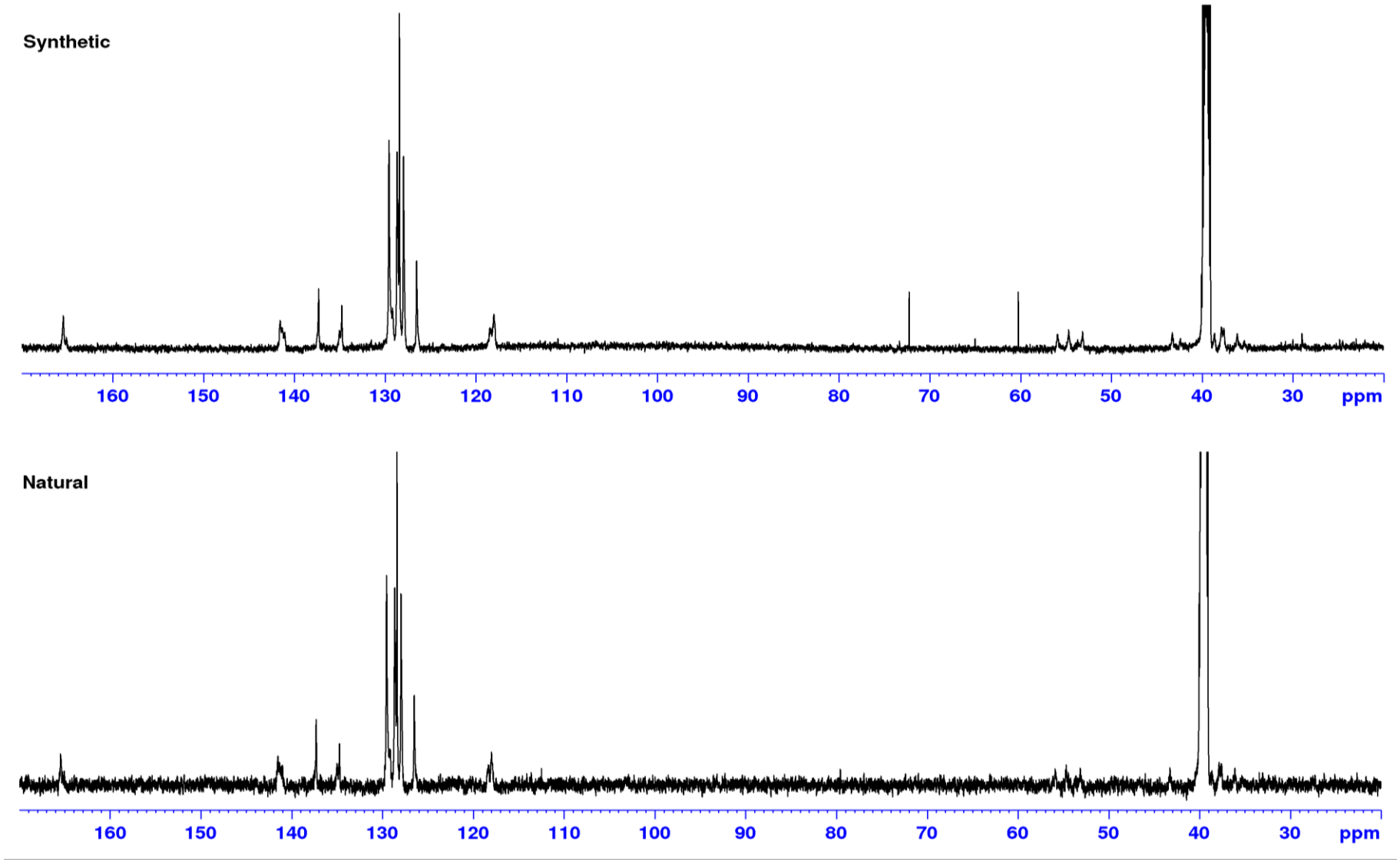

Figure S96. Comparison of ^{13}C NMR spectra (150 MHz, DMSO-d_6) of natural and synthetic xenocockiamide C (**12**)

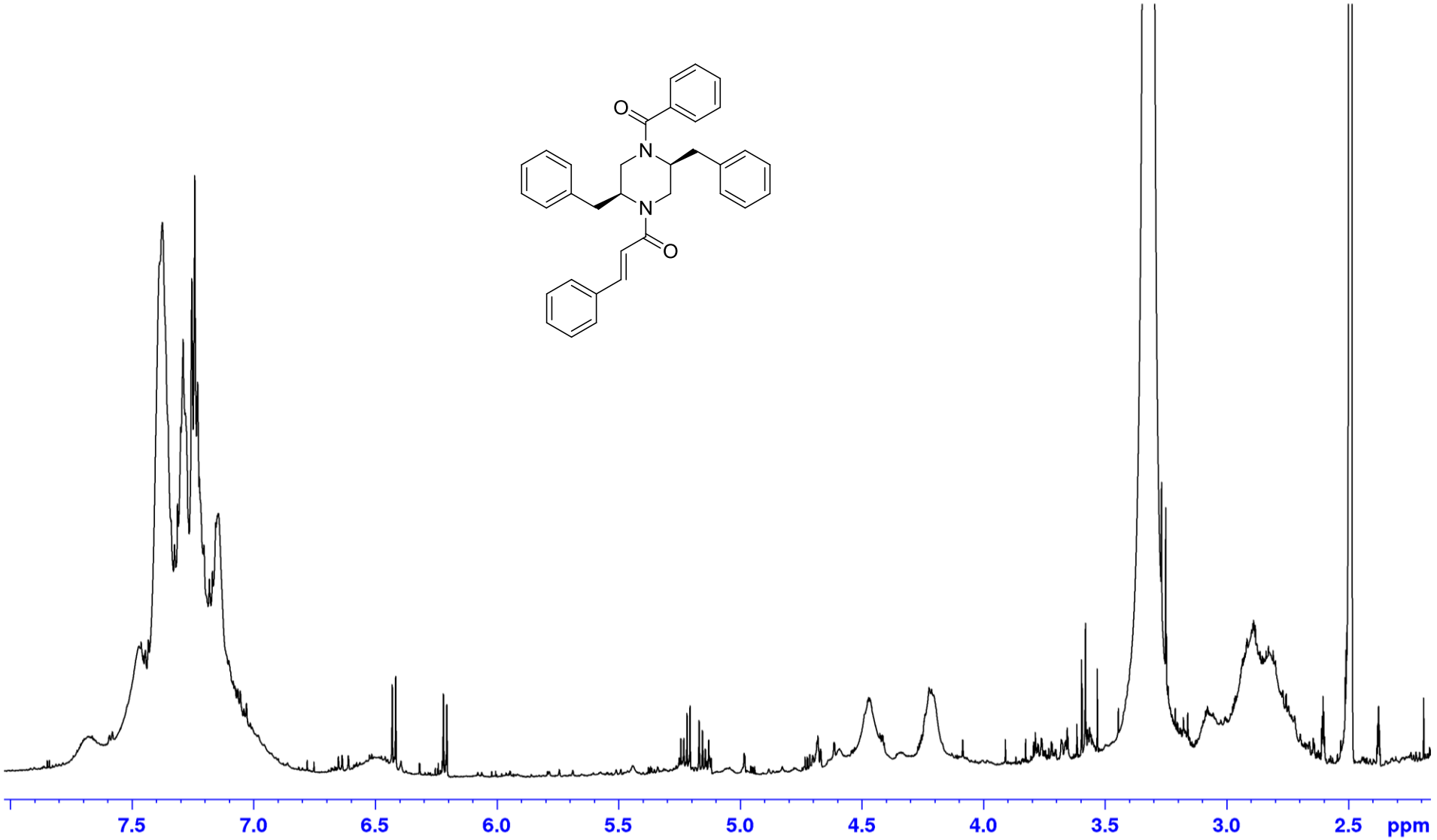

Figure S97. ^{1}H NMR spectrum (600 MHz, DMSO-d_6) of xenocockiamide D (**13**)

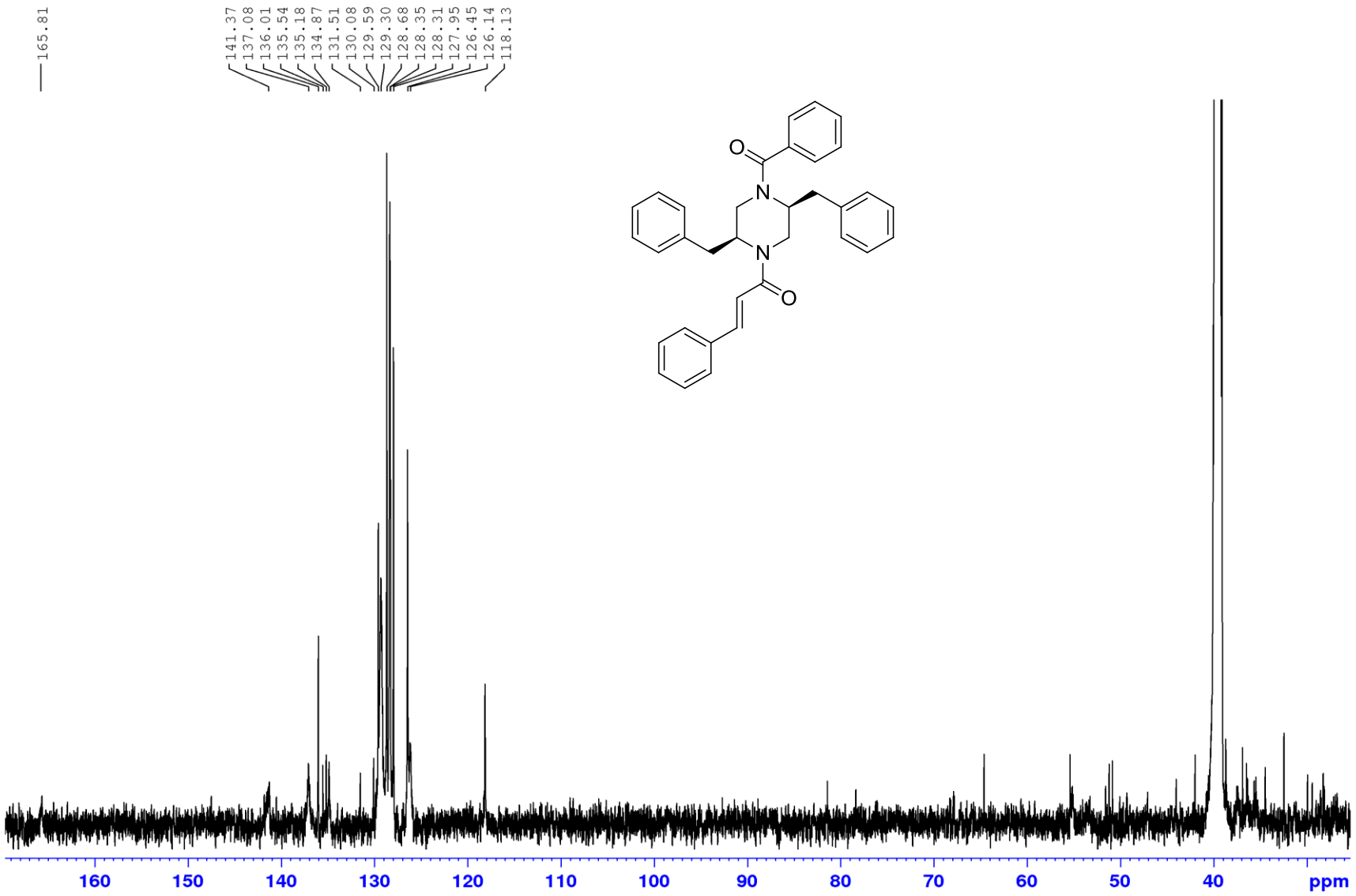

Figure S98. ^{13}C NMR spectrum (150 MHz, DMSO-d_6) of xenocockiamide D (**13**)

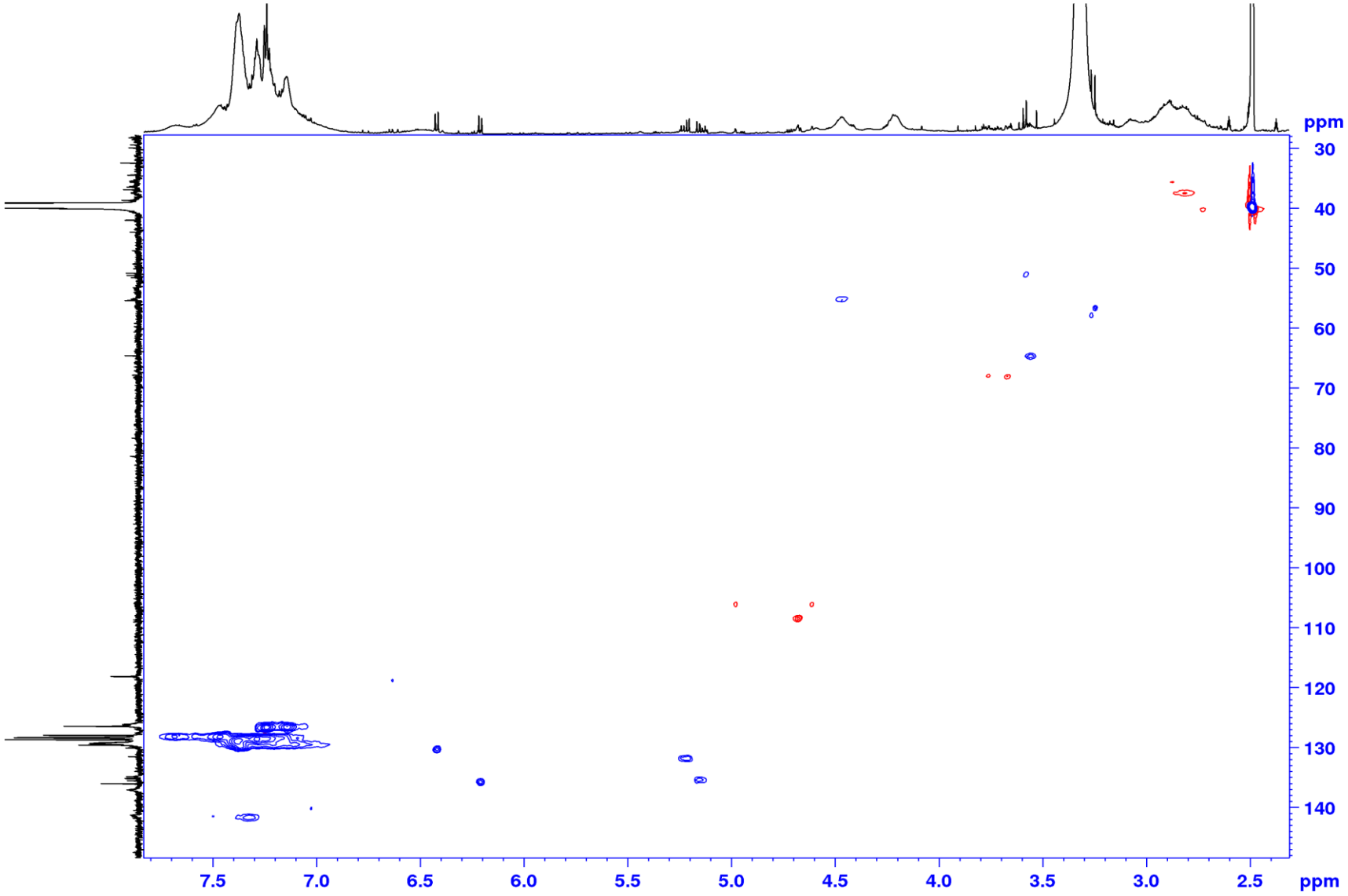

Figure S99. ^{1}H-^{13}C HSQC spectrum (600 MHz, DMSO-d_6) of xenocockiamide D (**13**)

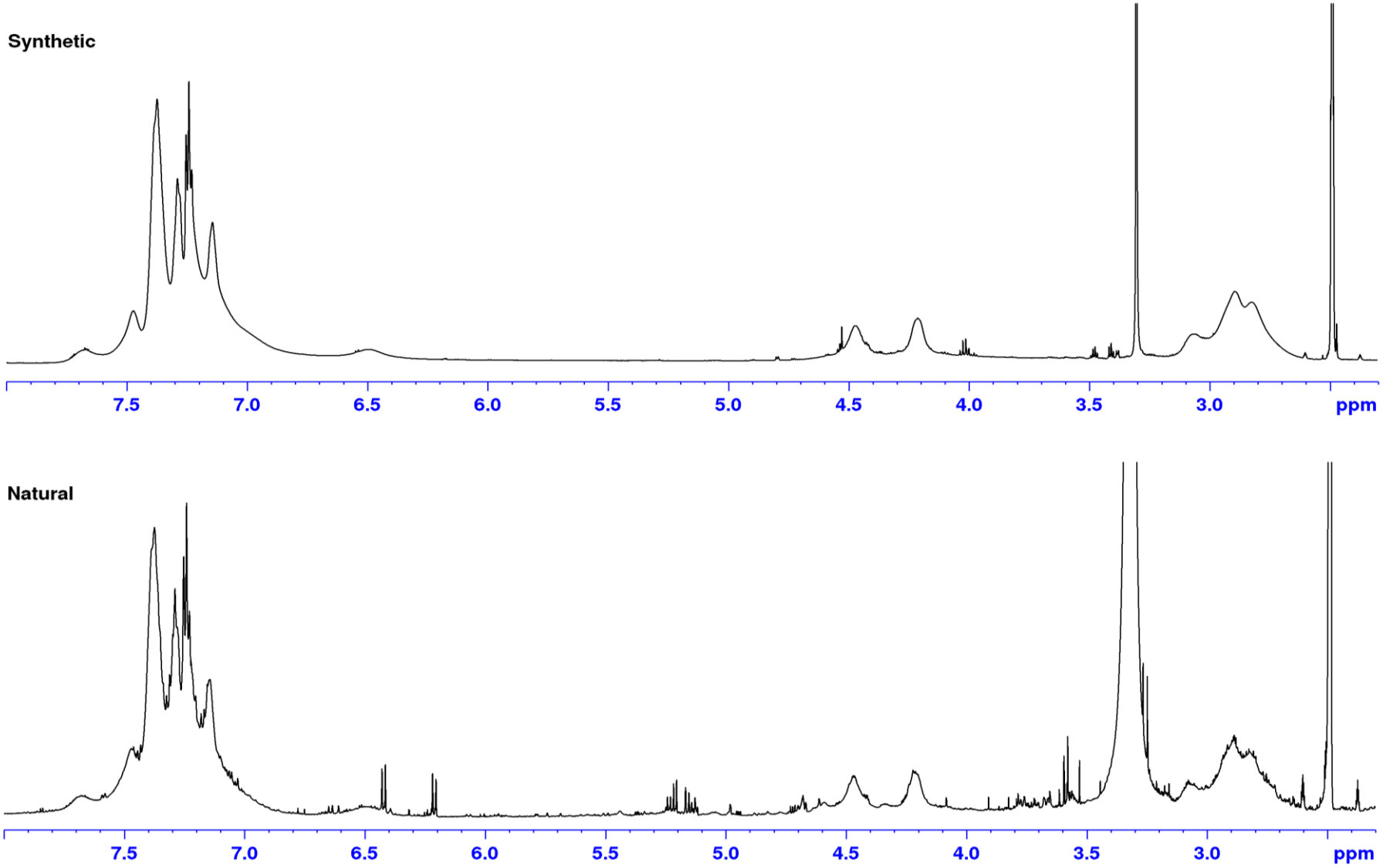

Figure S100. Comparison of ^{1}H NMR spectra (600 MHz, DMSO-d_6) of natural and synthetic xenocockiamide D (**13**)

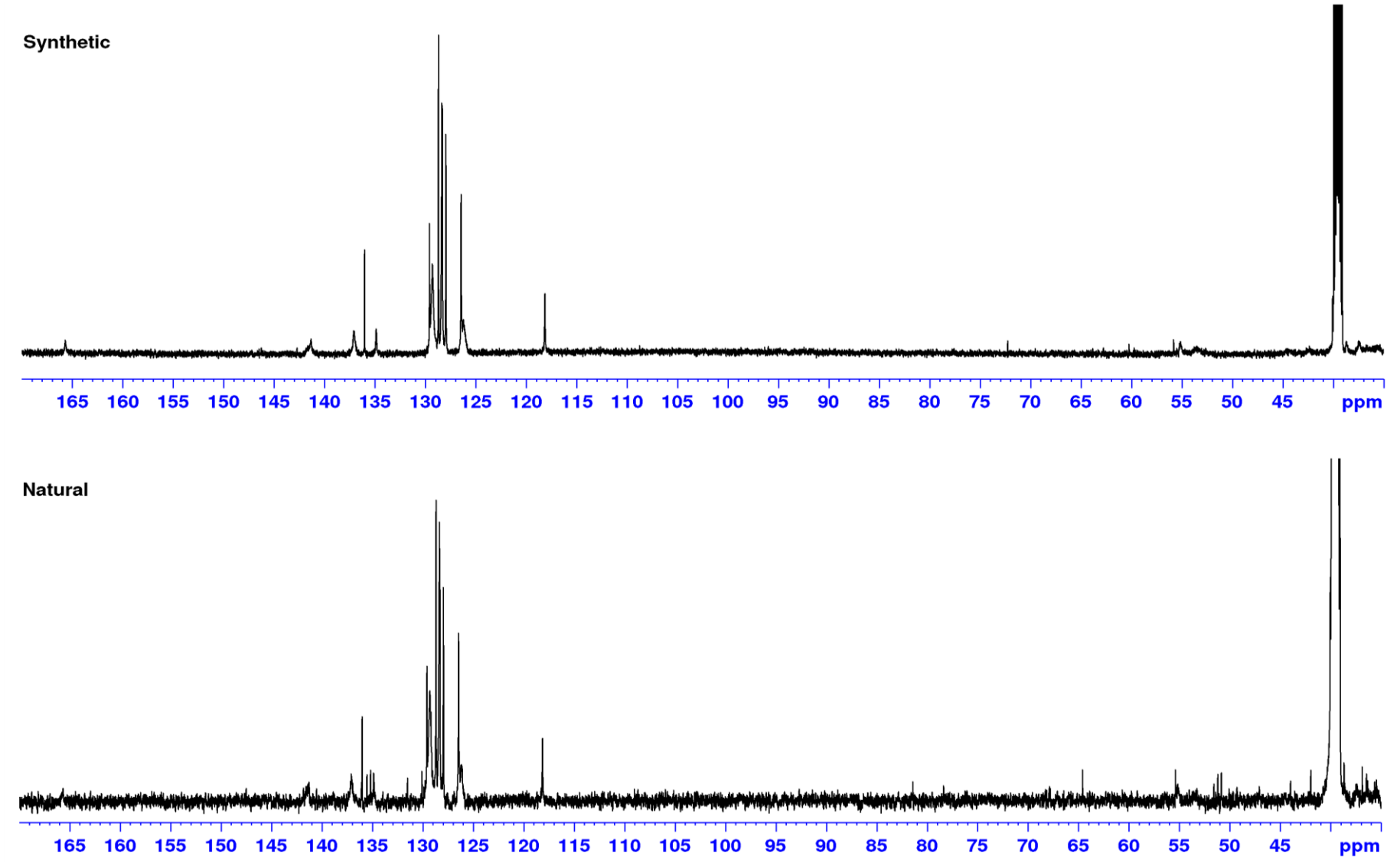

Figure S101. Comparison of ^{13}C NMR spectra (150 MHz, DMSO-d_6) of natural and synthetic xenocockiamide D (**13**)

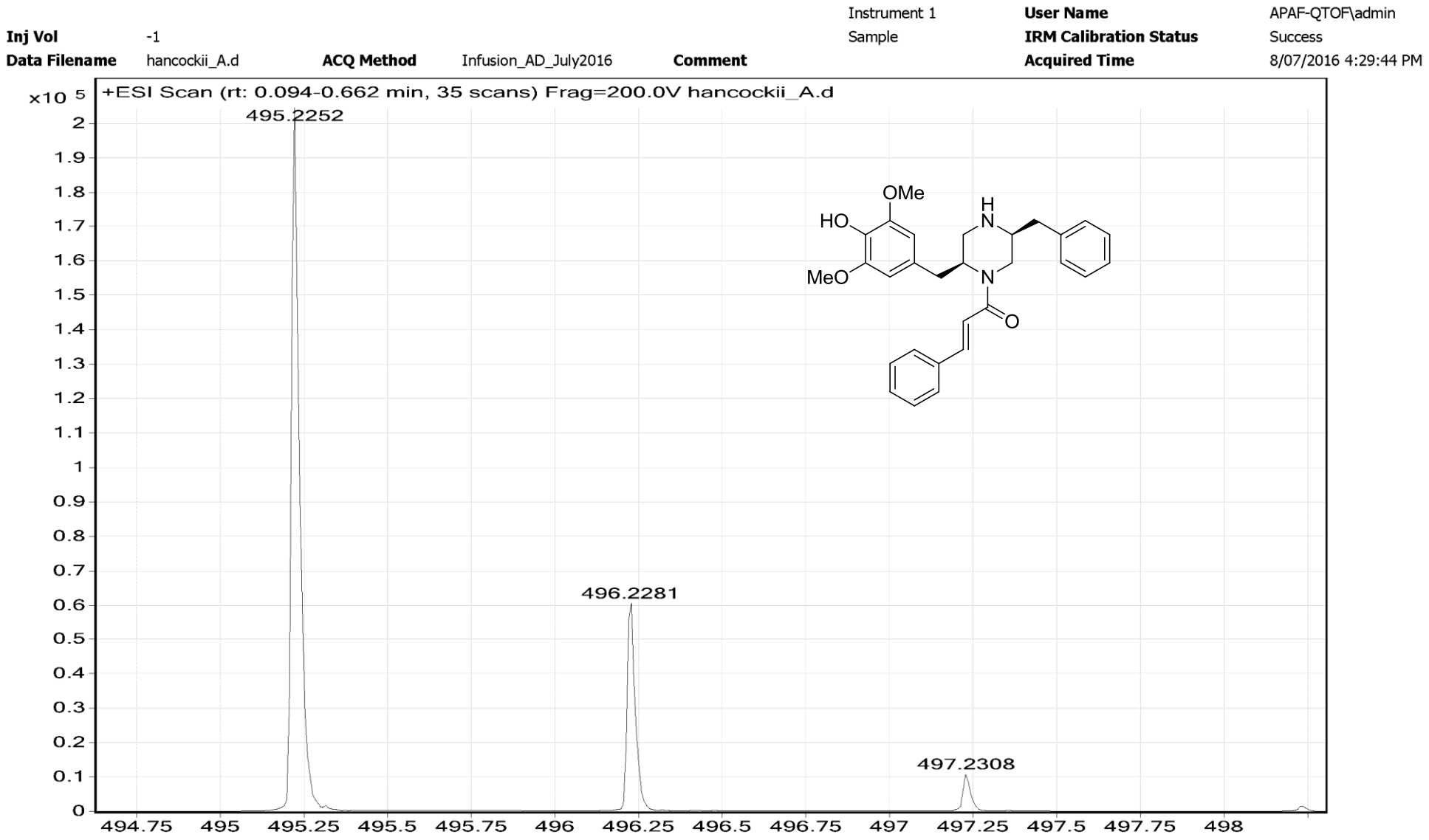

Figure S102. HRESI(+)MS spectrum of hancockiamide A (**1**)

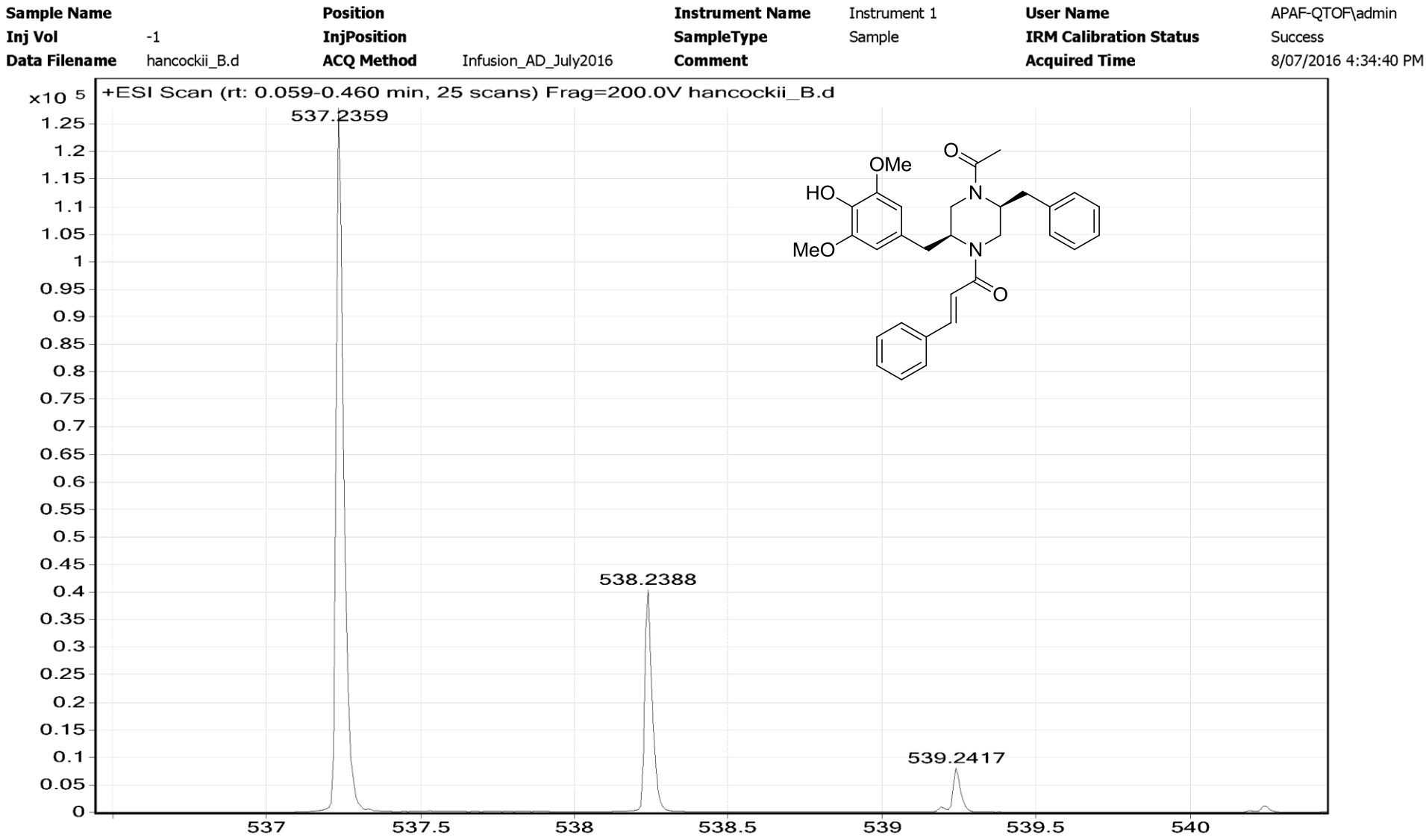

Figure S103. HRESI(+)MS spectrum of hancockiamide B (**2**)

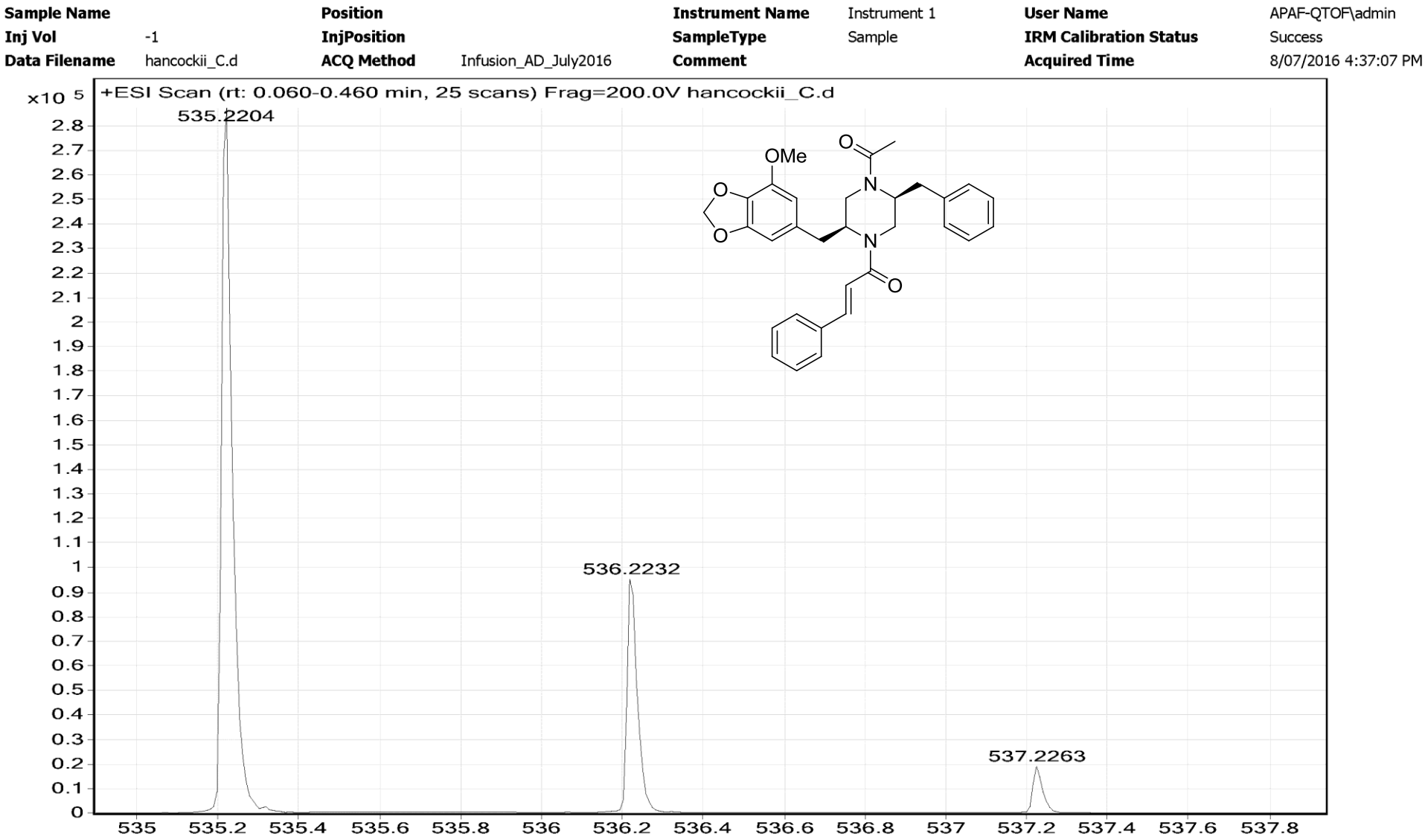

Figure S104. HRESI(+)MS spectrum of hancockiamide C (**3**)

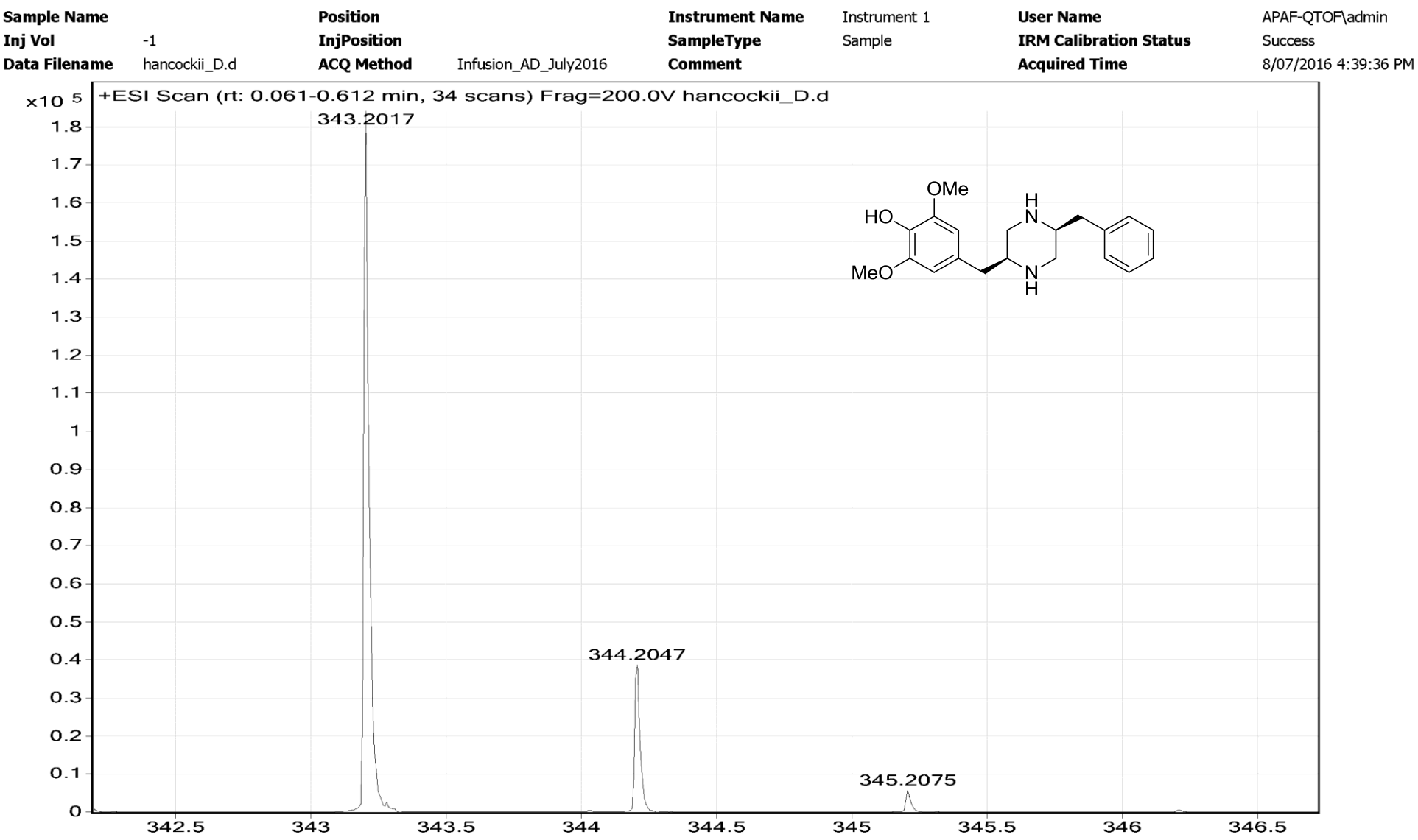

Figure S105. HRESI(+)MS spectrum of hancockiamide D (**4**)

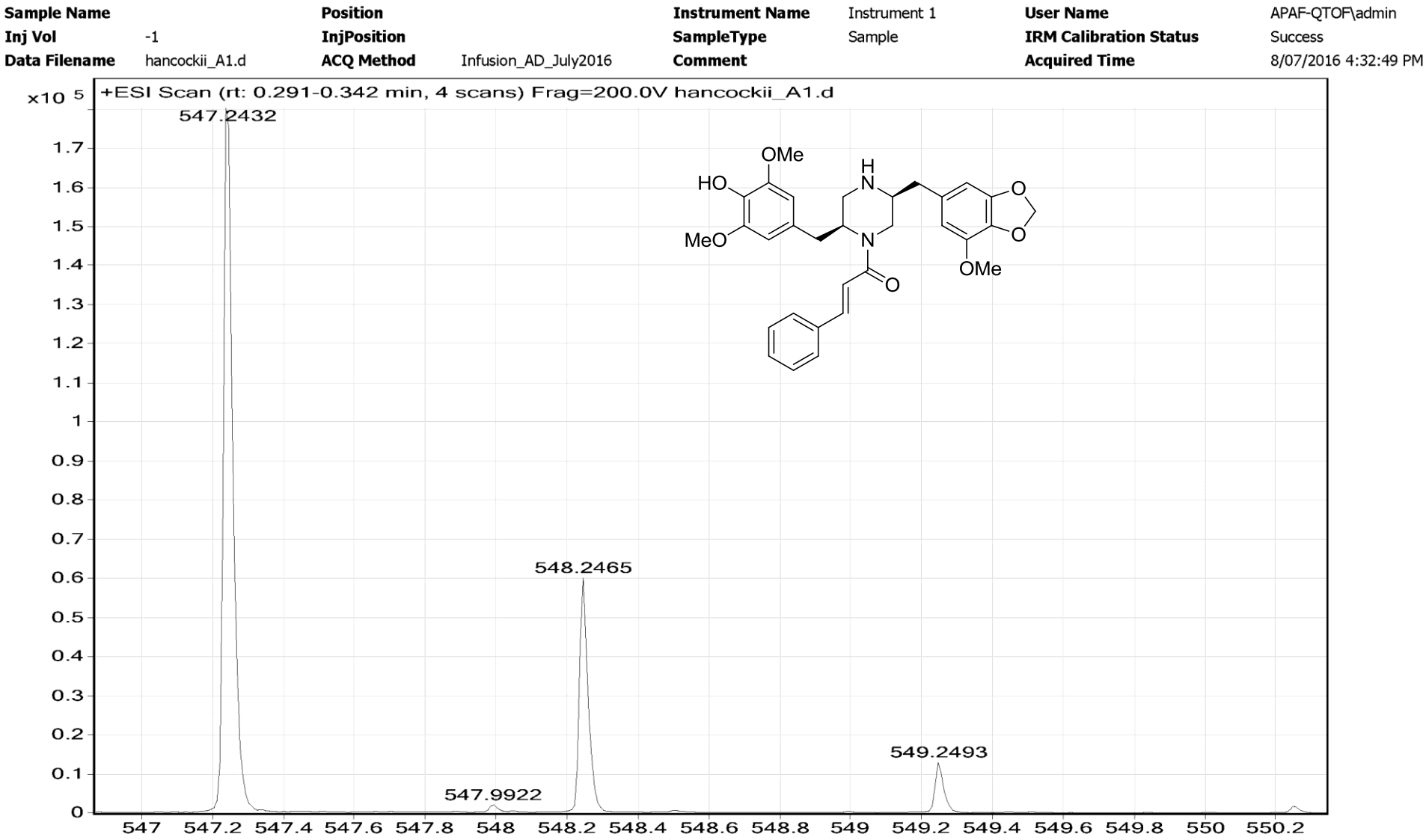

Figure S106. HRESI(+)MS spectrum of hancockiamide E (**5**)

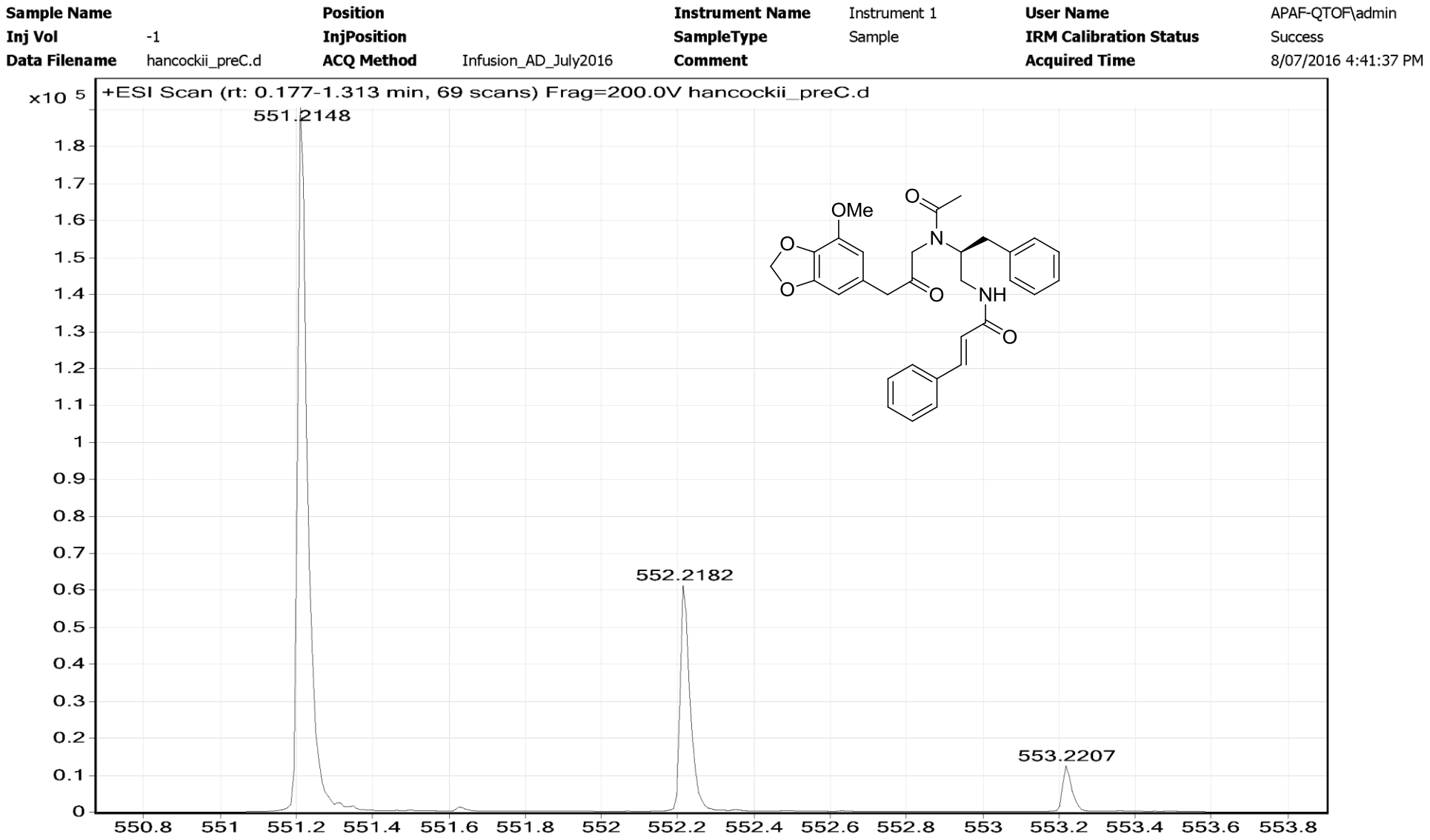

Figure S107. HRESI(+)MS spectrum of hancockiamide F (**6**)

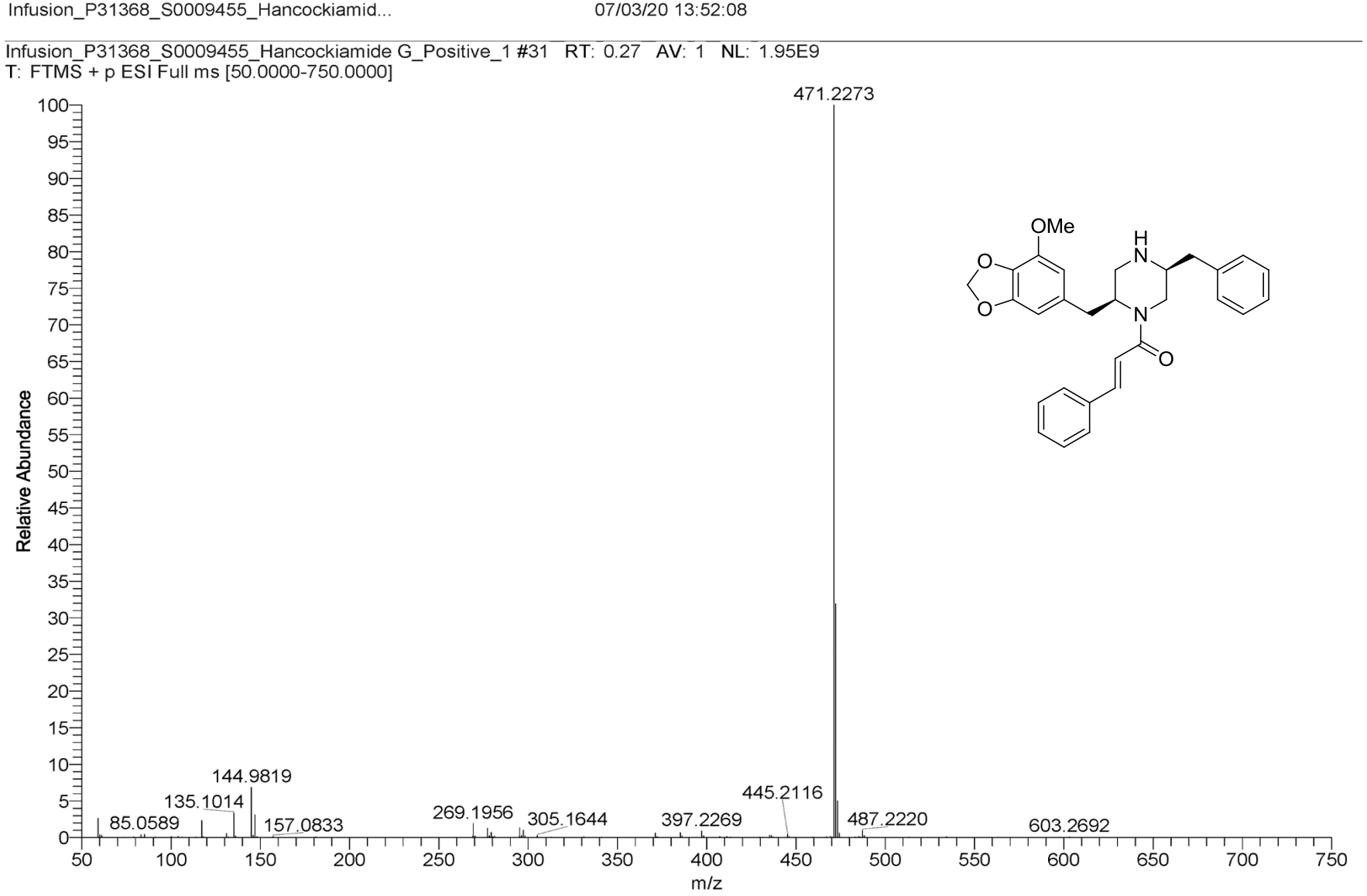

Figure S108. HRESI(+)MS spectrum of hancockiamide G (**7**)

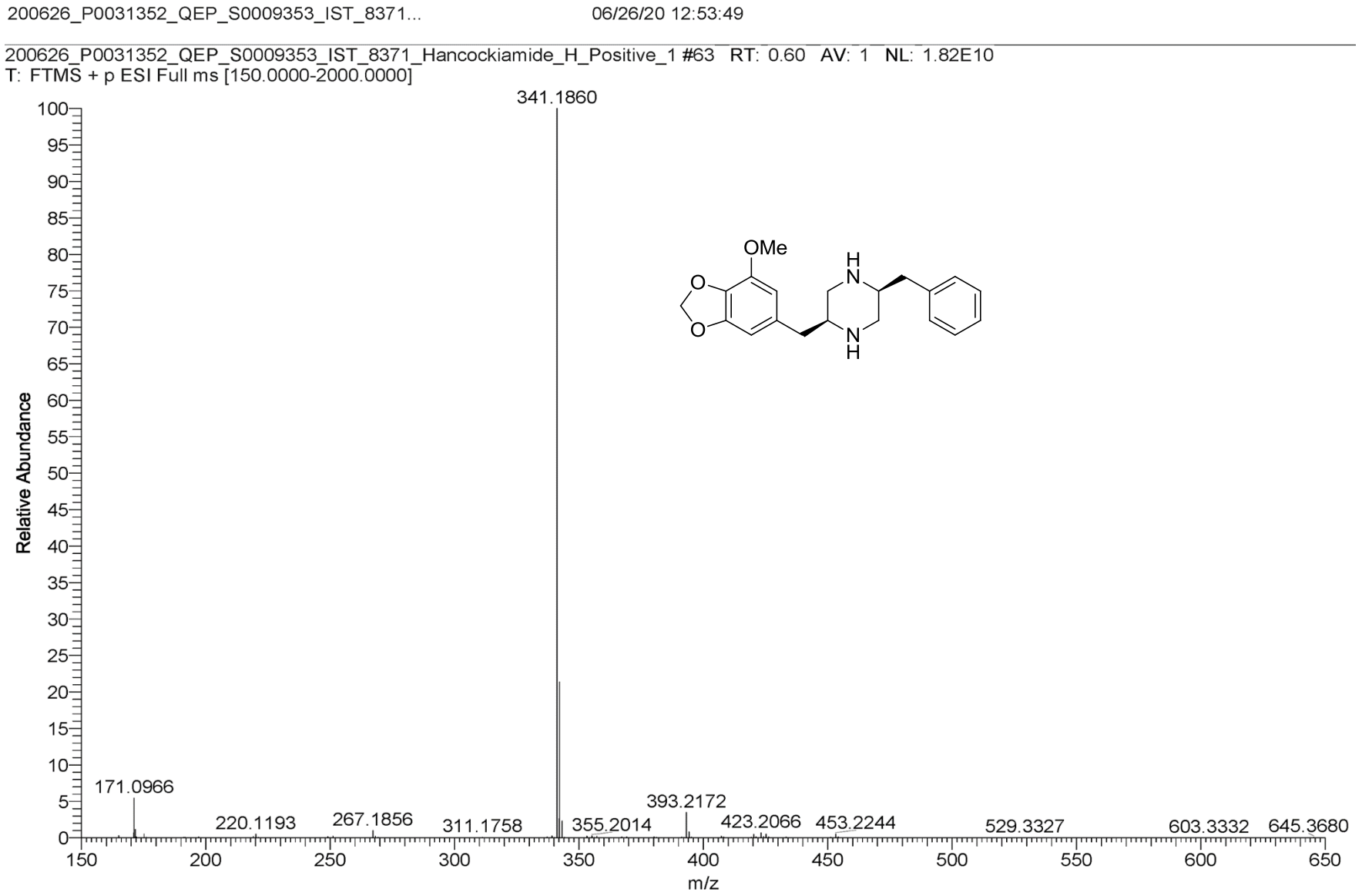

Figure S109. HRESI(+)MS spectrum of hancockiamide H (**8**)

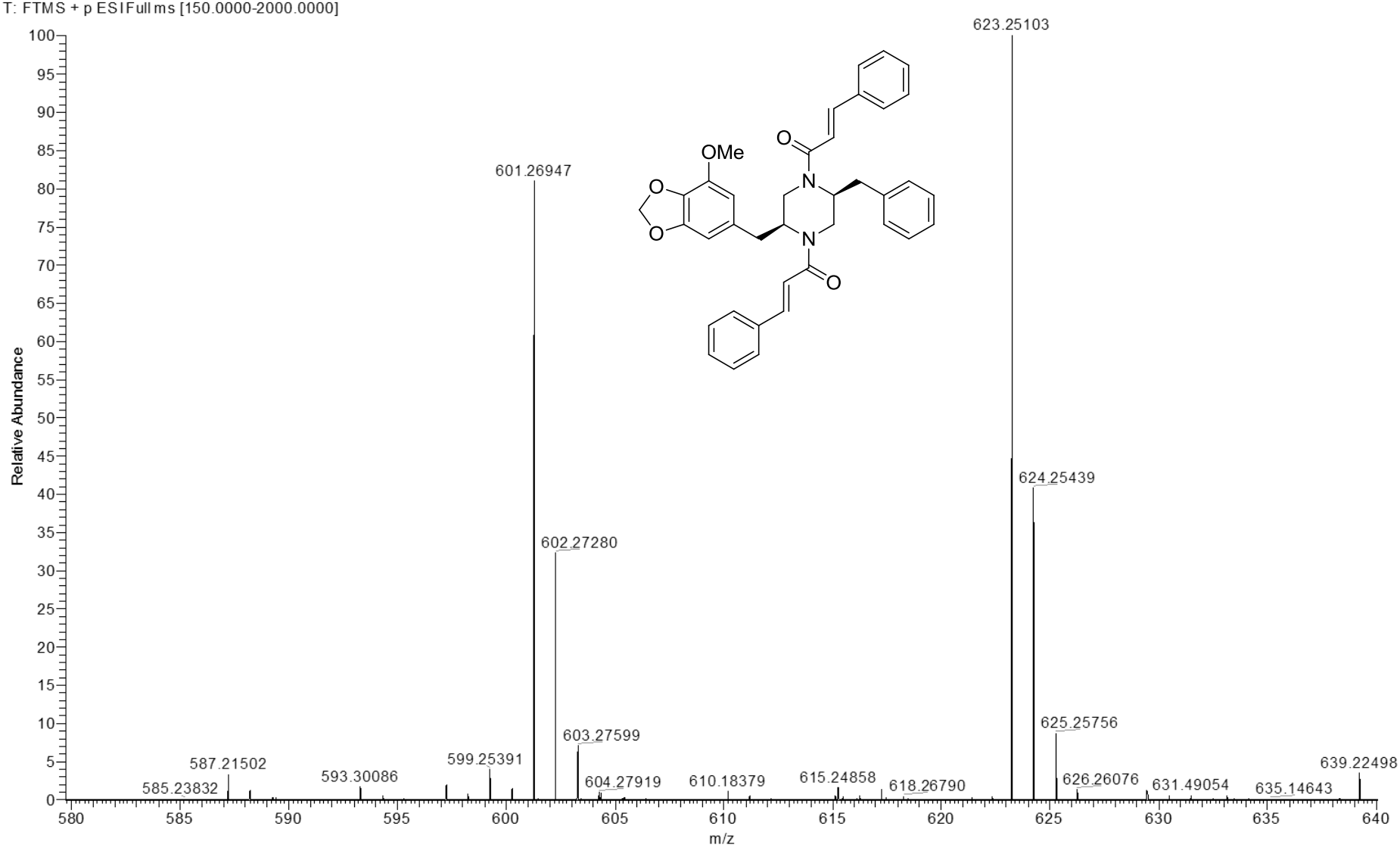

Figure S110. HRESI(+)MS spectrum of hancockiamide I (**9**)

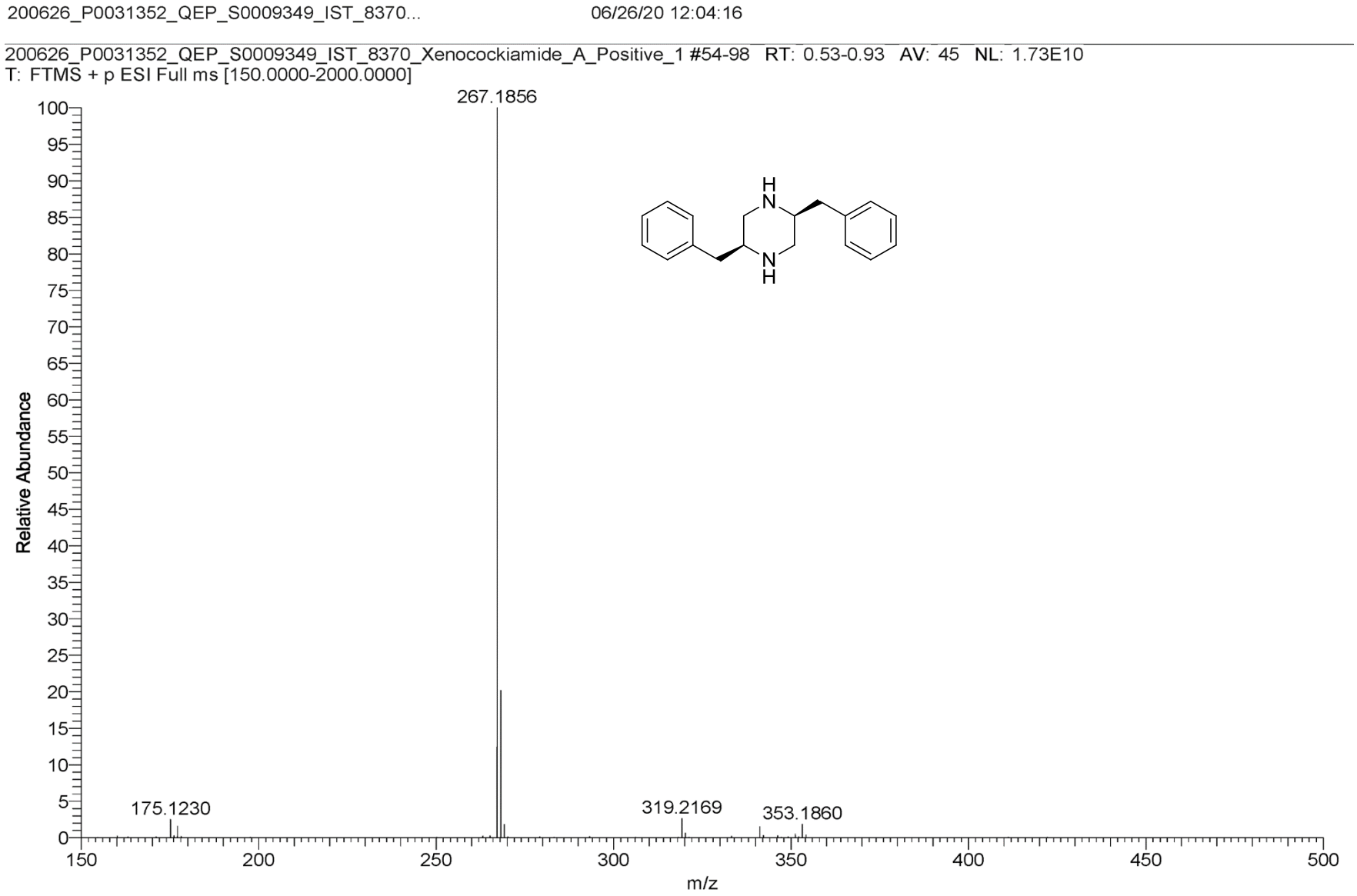

Figure S111. HRESI(+)MS spectrum of natural xenocockiamide A (**10**)

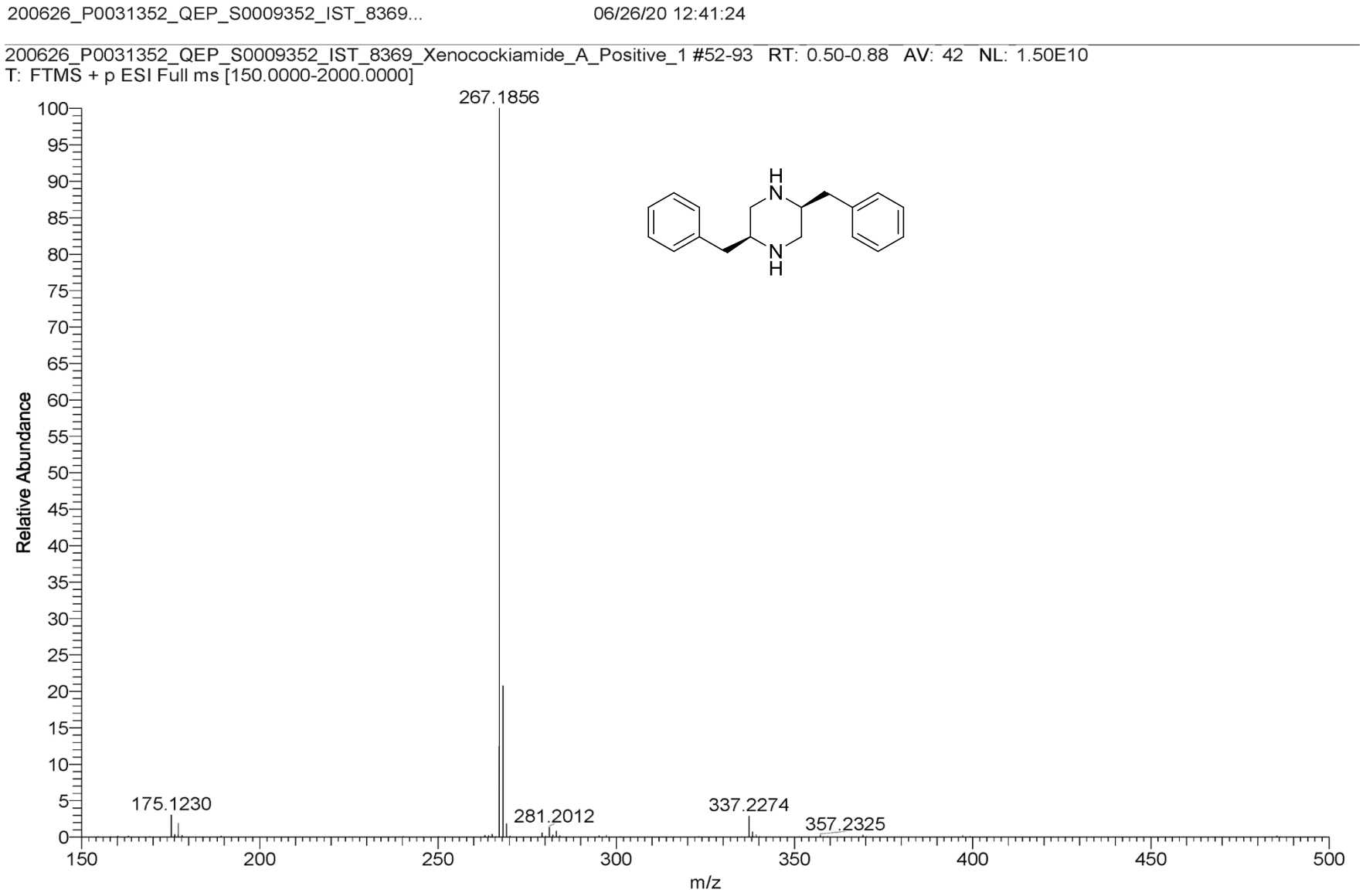

Figure S112. HRESI(+)MS spectrum of synthetic xenocockiamide A (**10**)

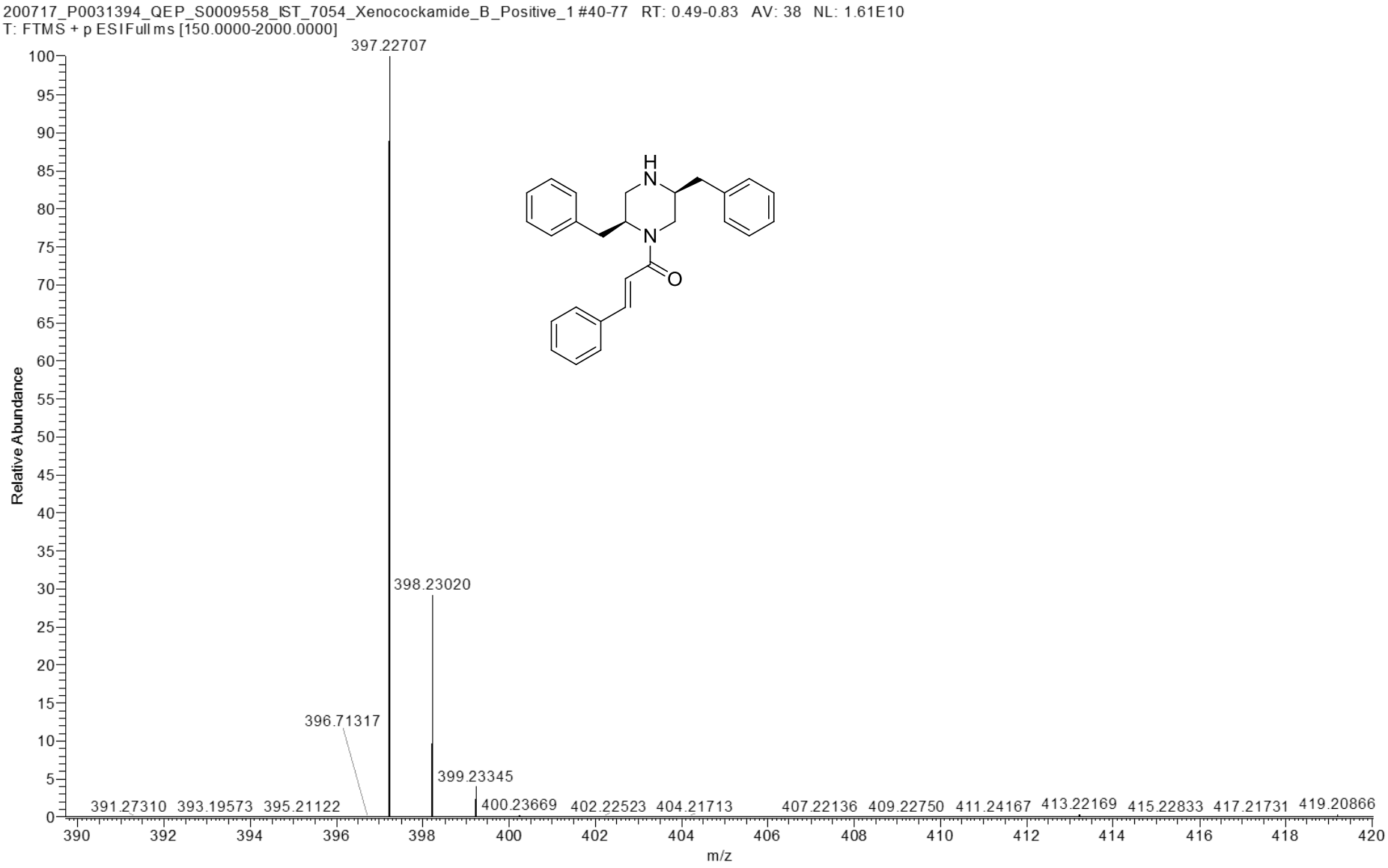

Figure S113. HRESI(+)MS spectrum of natural xenocockiamide B (**11**)

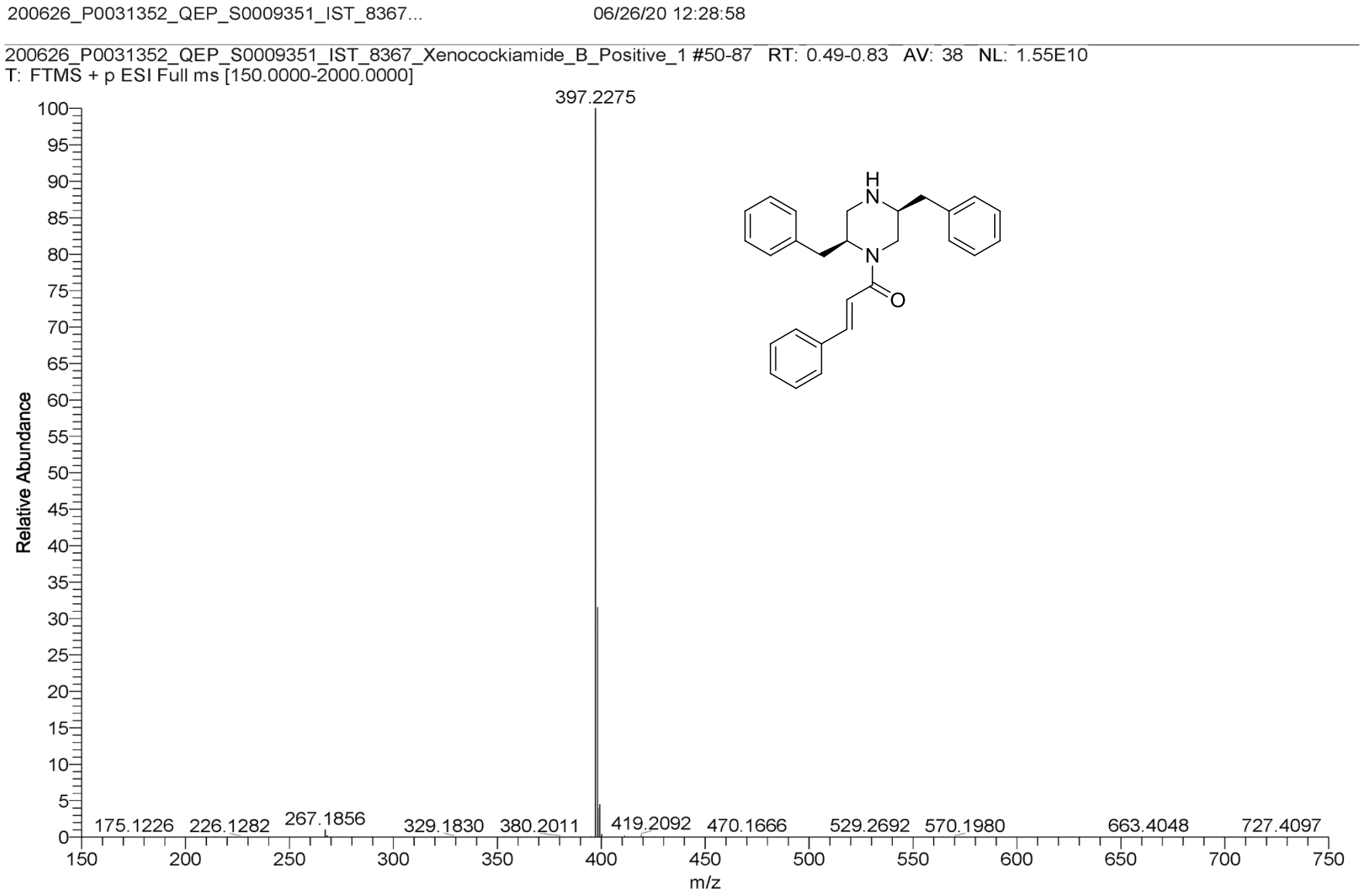

Figure S114. HRESI(+)MS spectrum of synthetic xenocockiamide B (**11**)

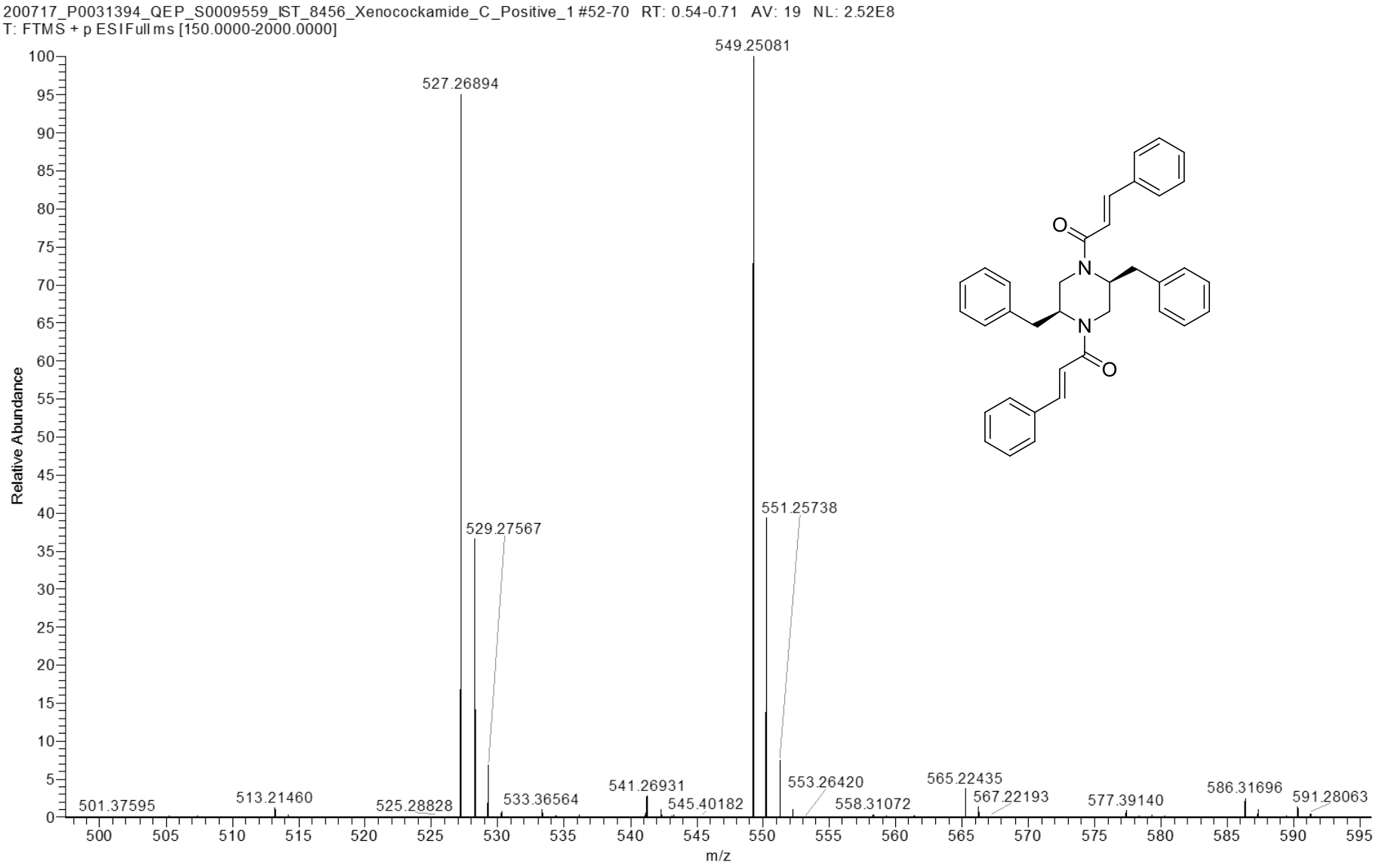

Figure S115. HRESI(+)MS spectrum of natural xenocockiamide C (**12**)

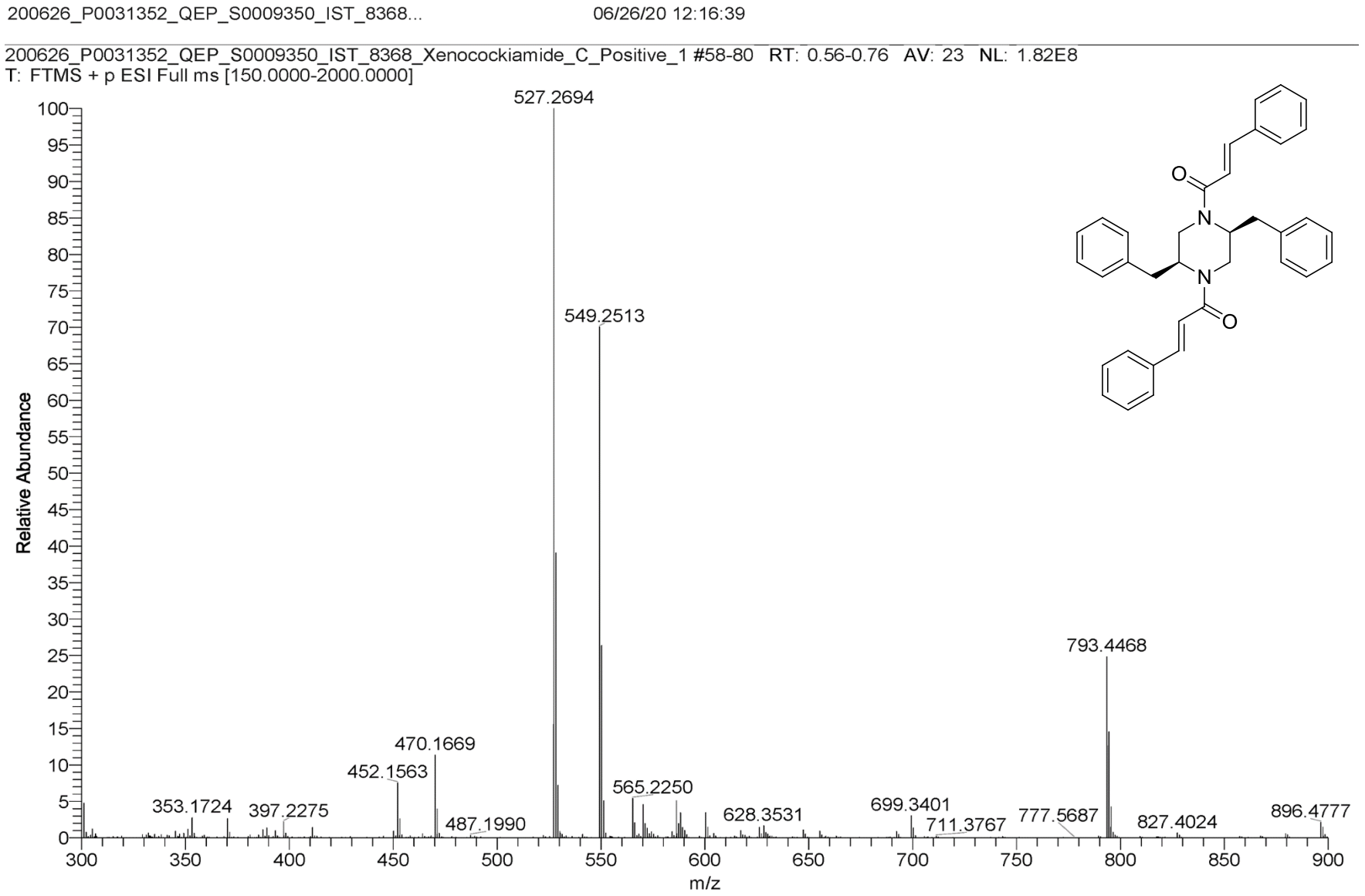

Figure S116. HRESI(+)MS spectrum of synthetic xenocockiamide C (**12**)

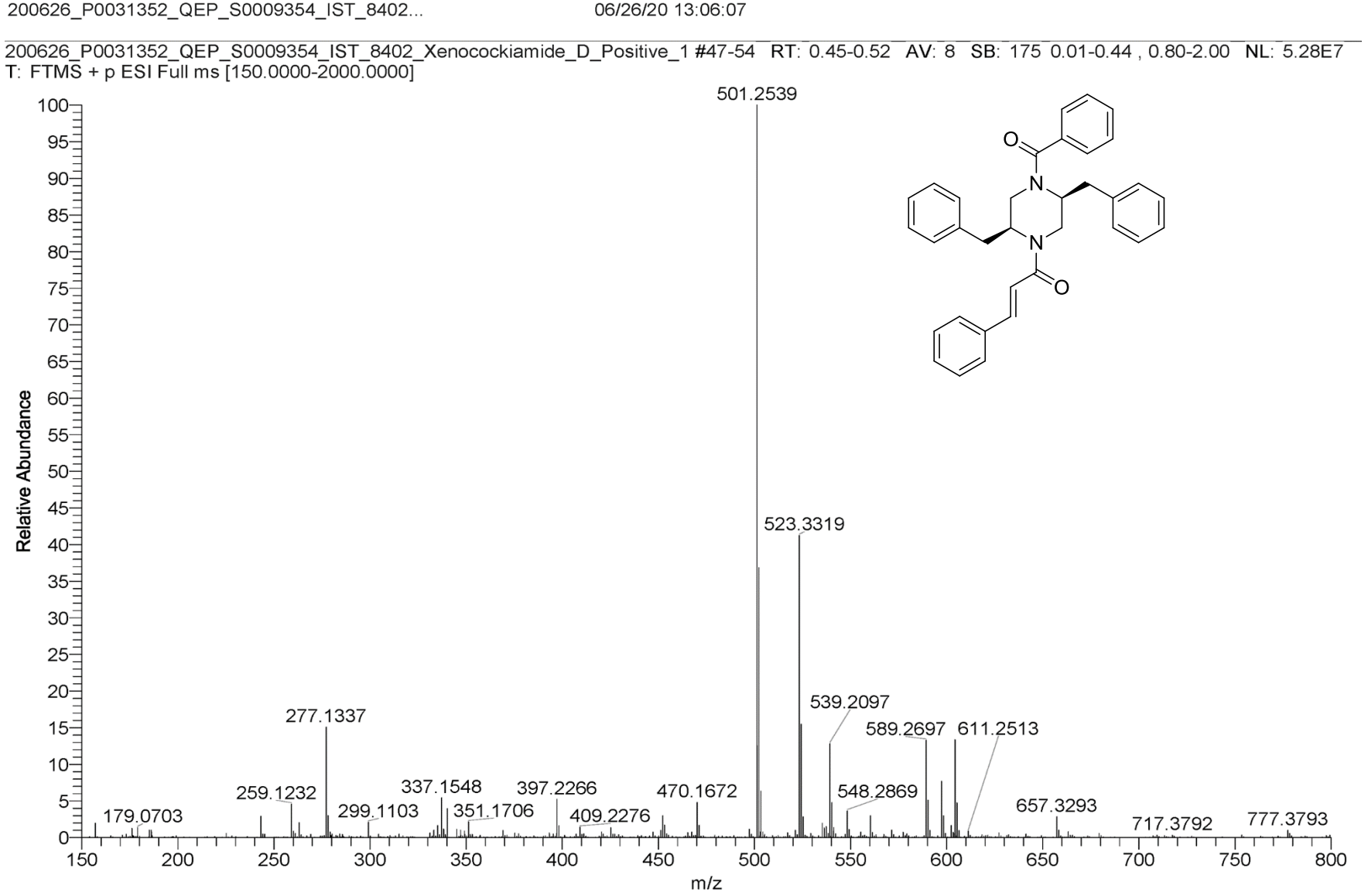

Figure S117. HRESI(+)MS spectrum of natural xenocockiamide D (**13**)

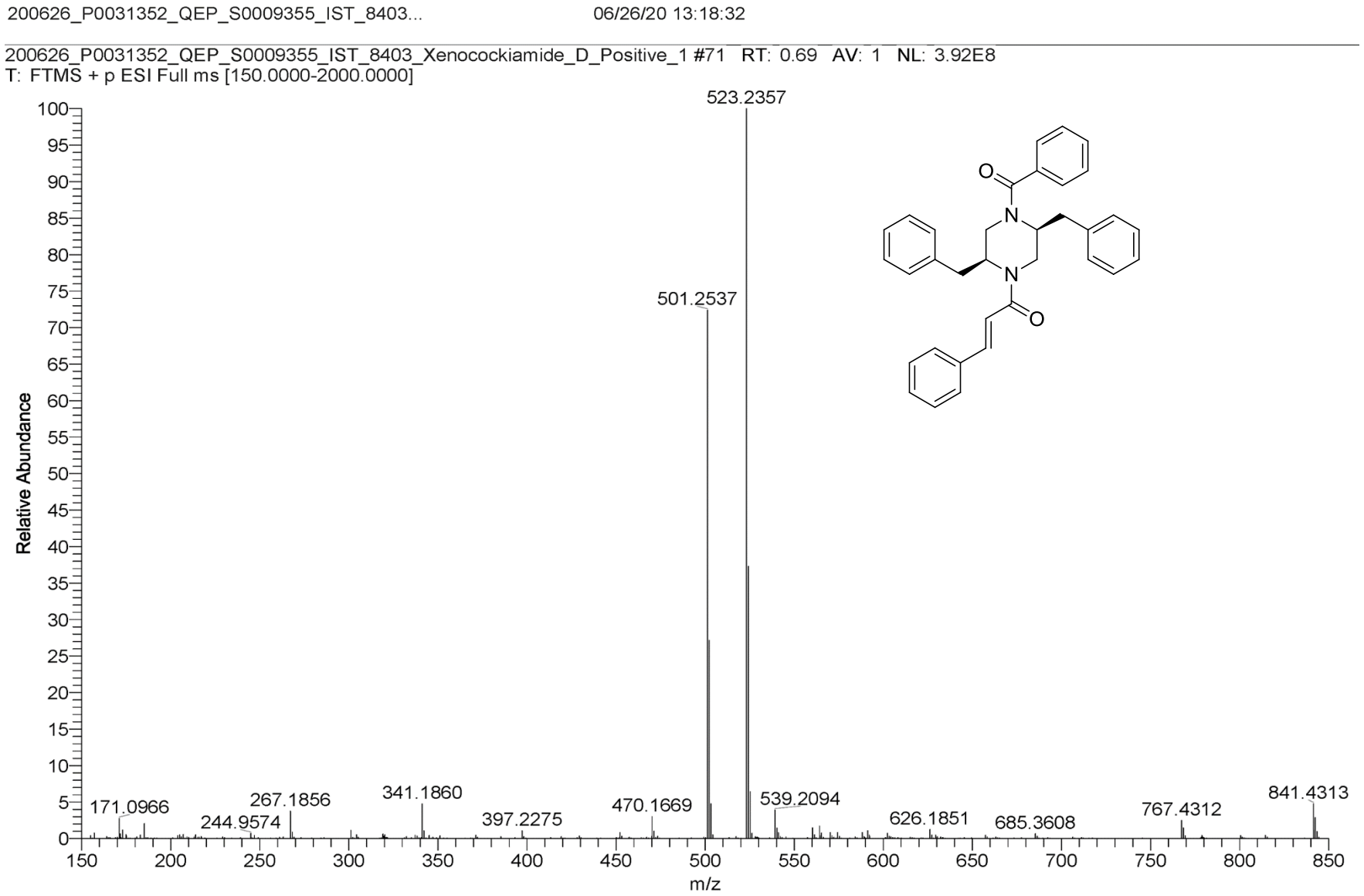

Figure S118. HRESI(+)MS spectrum of synthetic xenocockiamide D (**13**)

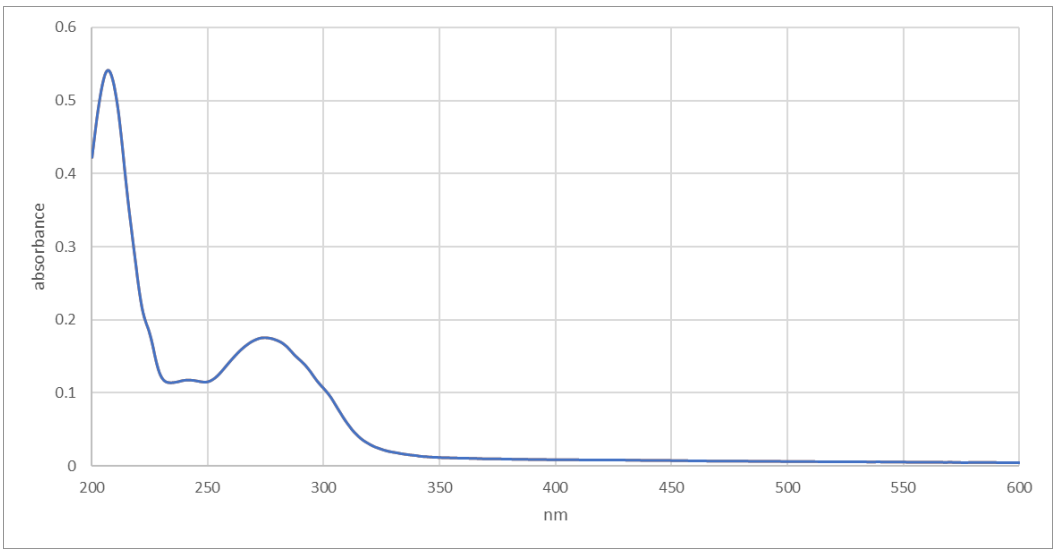

Figure S119. UV-vis spectrum of hancockiamide A (**1**)

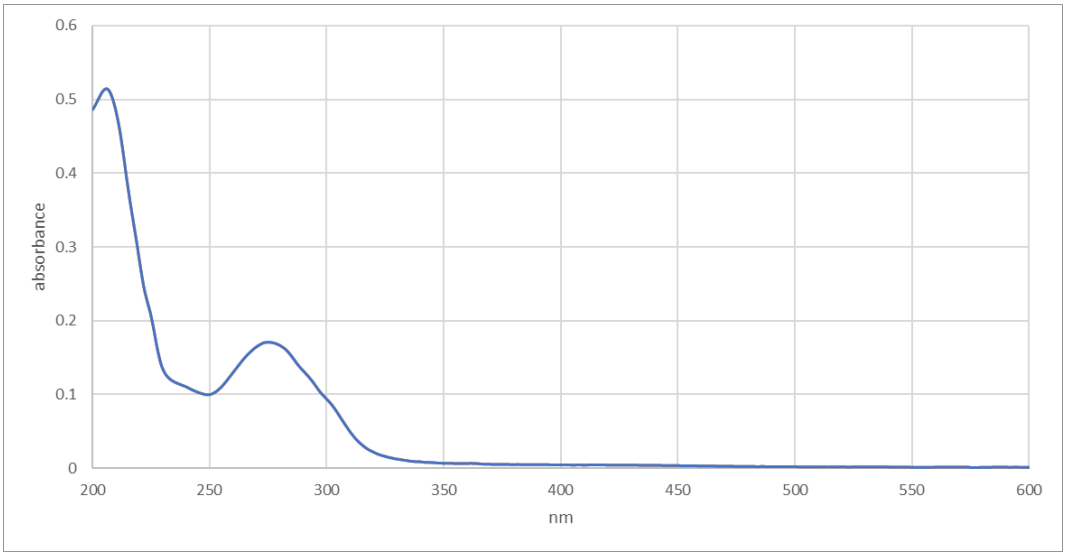

Figure S120. UV-vis spectrum of hancockiamide B (**2**)

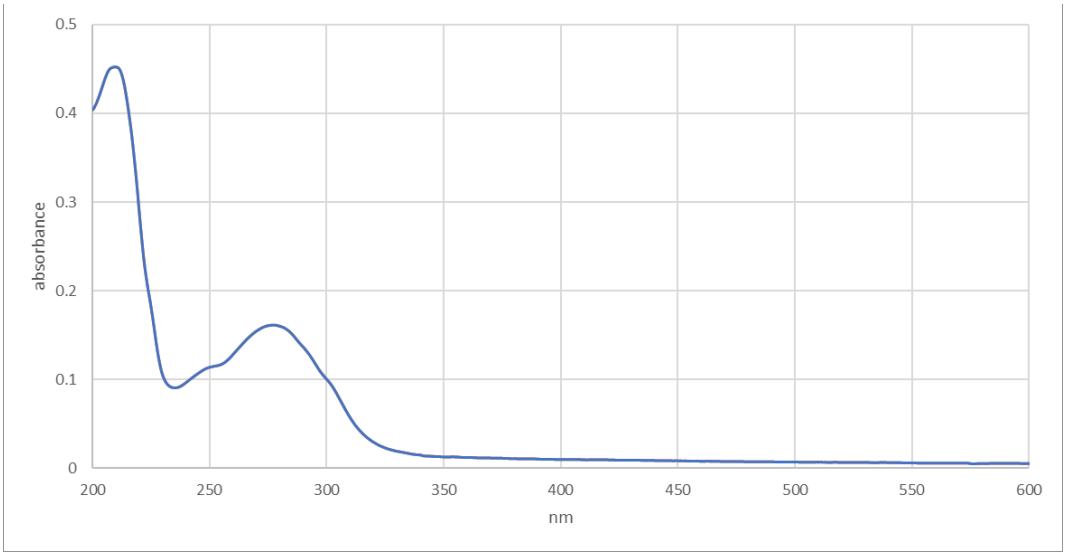

Figure S121. UV-vis spectrum of hancockiamide C (**3**)

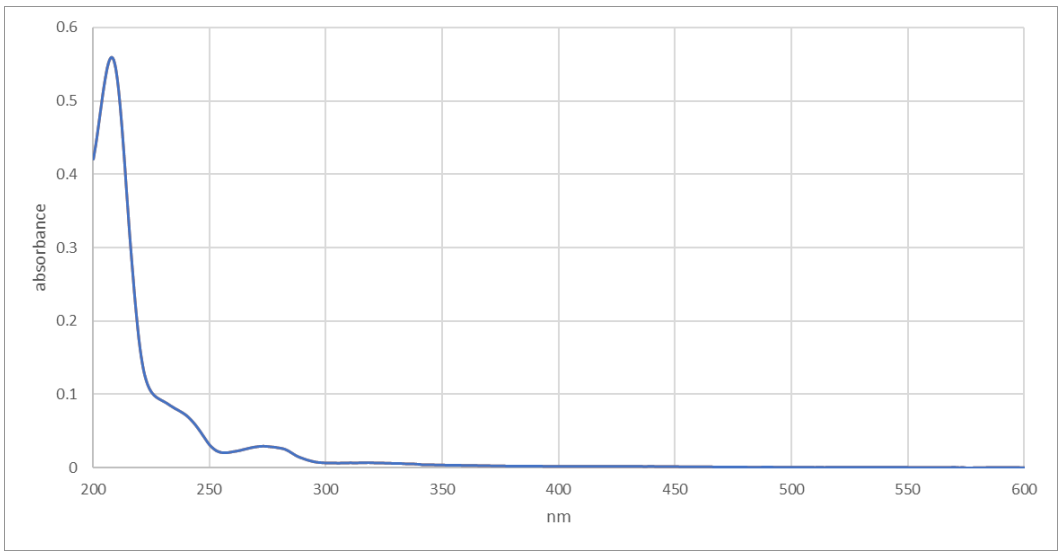

Figure S122. UV-vis spectrum of hancockiamide D (**4**)

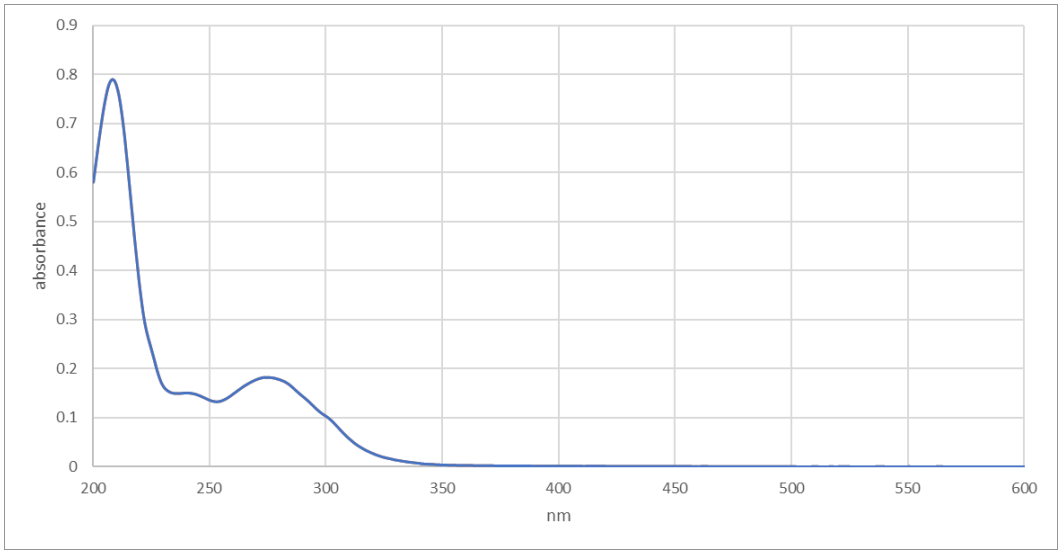

Figure S123. UV-vis spectrum of hancockiamide E (**5**)

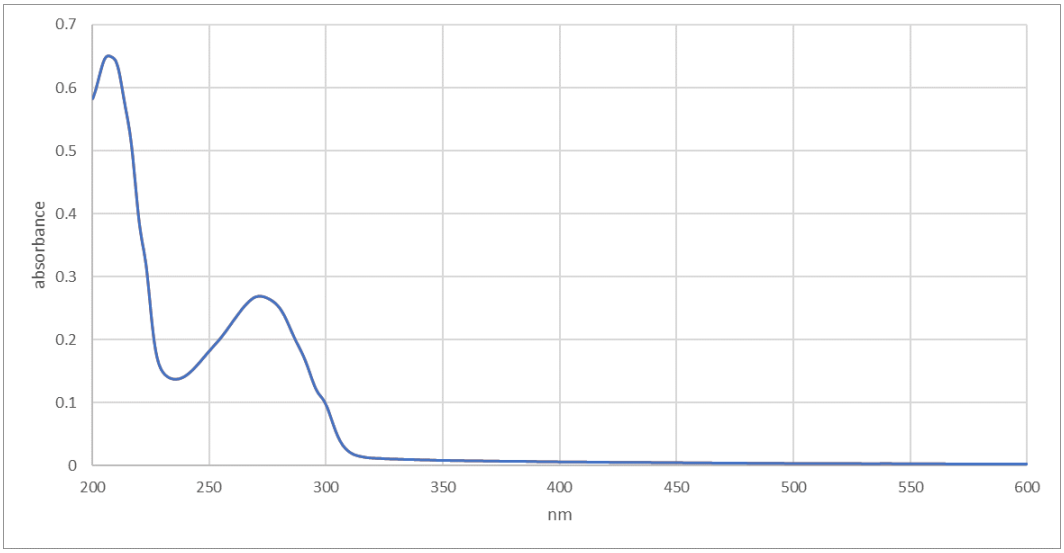

Figure S124. UV-vis spectrum of hancockiamide F (**6**)

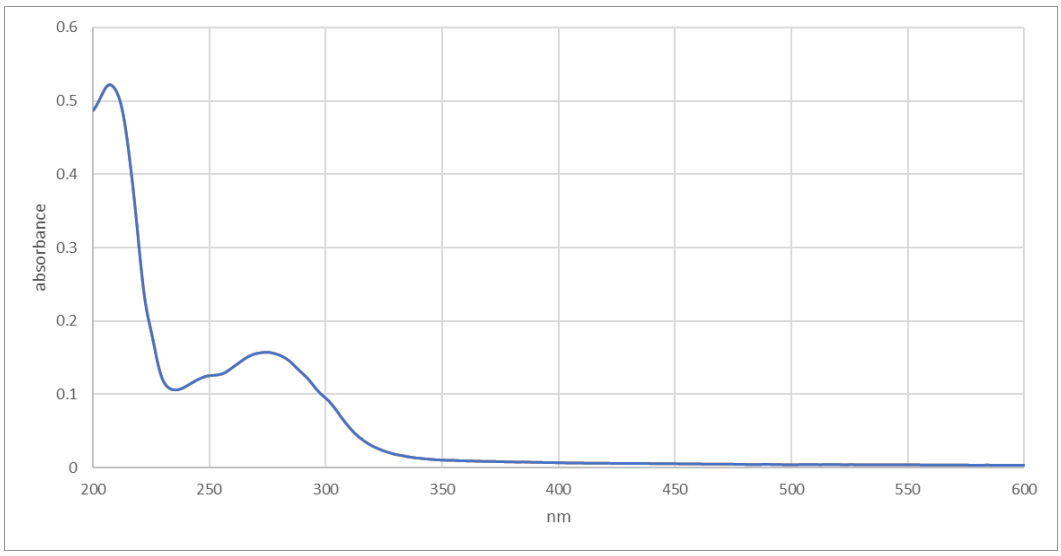

Figure S125. UV-vis spectrum of hancockiamide G (**7**)

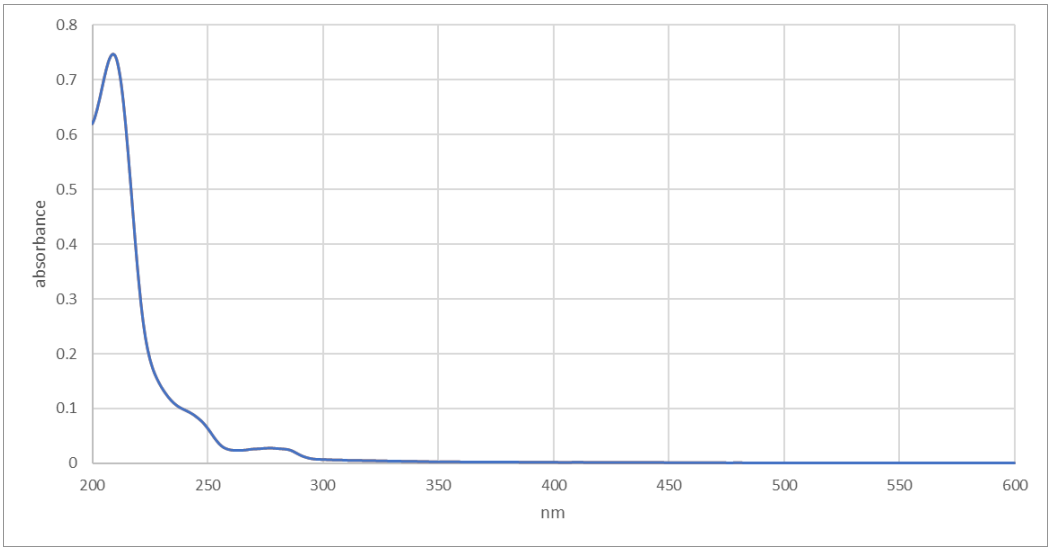

Figure S126. UV-vis spectrum of hancockiamide H (**8**)

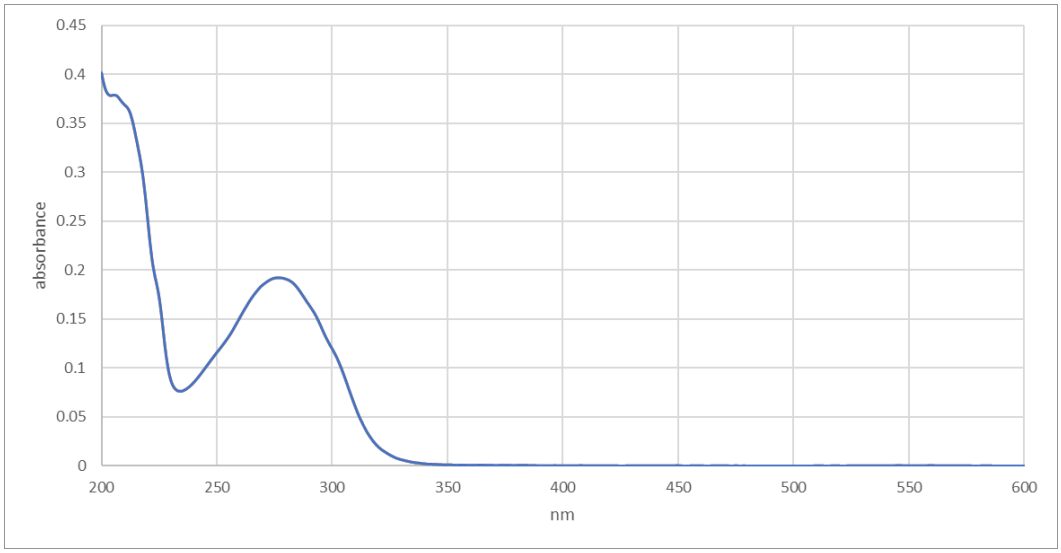

Figure S127. UV-vis spectrum of hancockiamide I (**9**)

(a) Natural

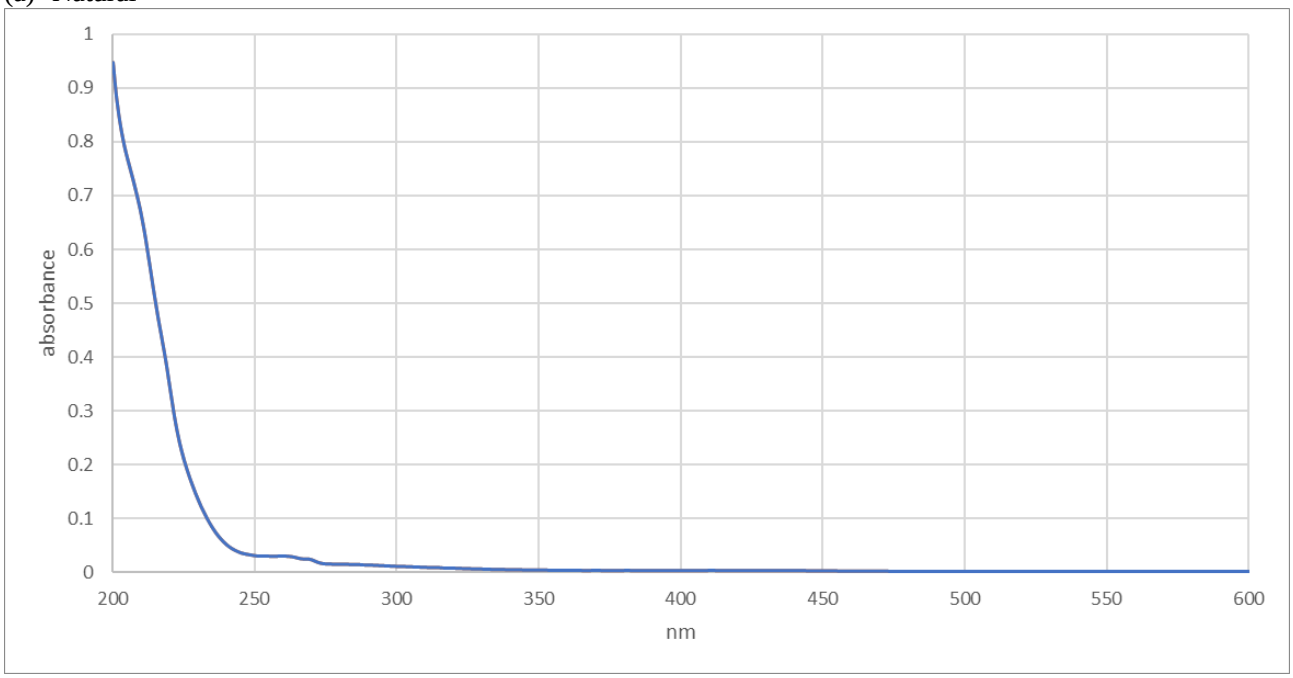

(b) Synthetic

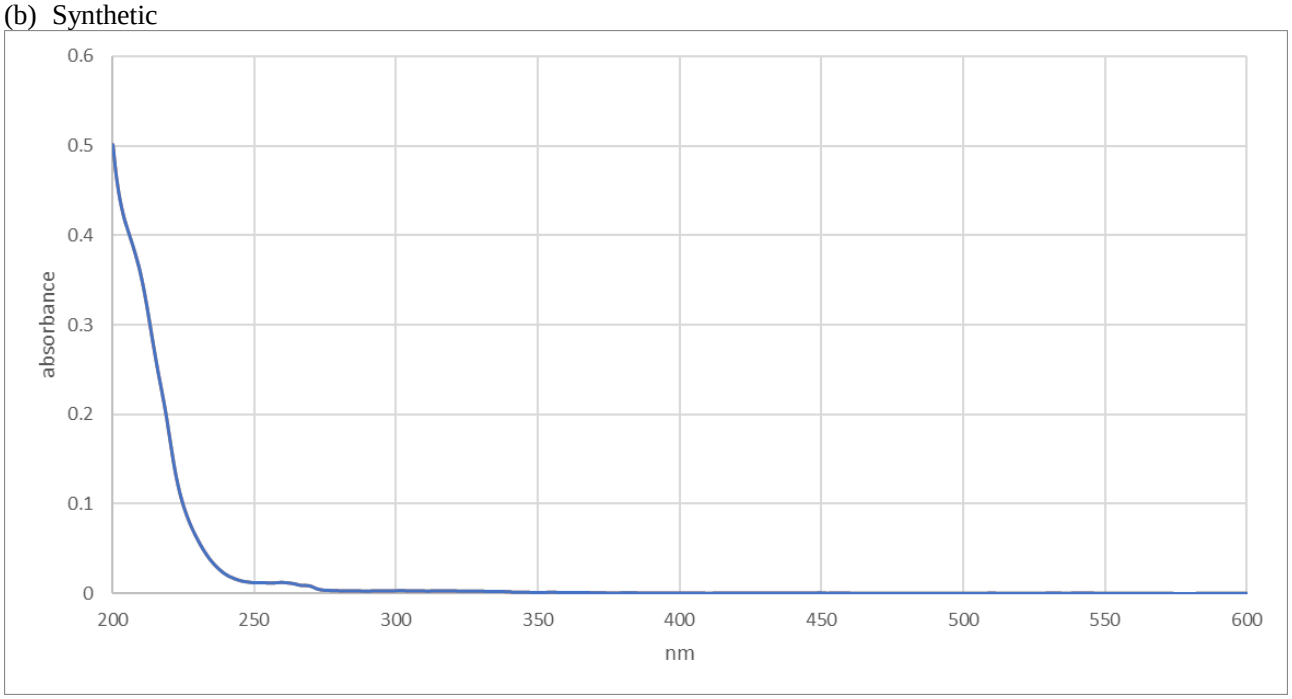

Figure S128. UV-vis spectrum of xenocockiamide A (**10**)

(a) Natural

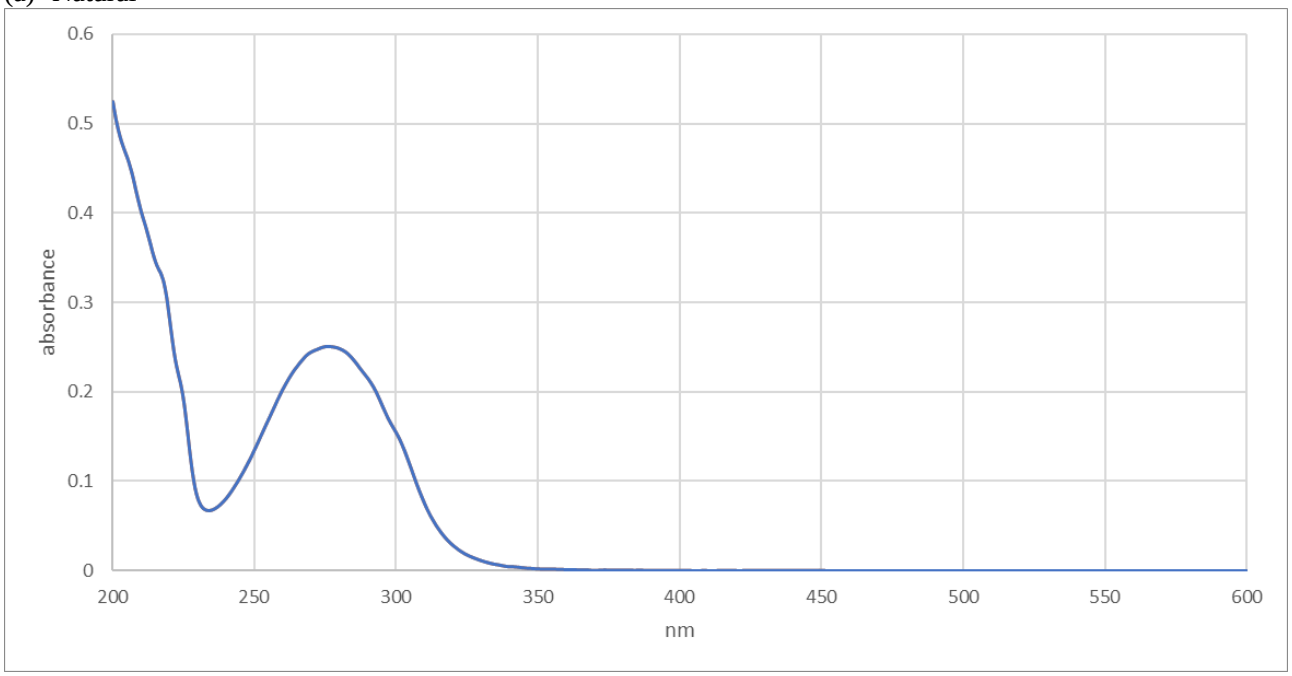

(b) Synthetic

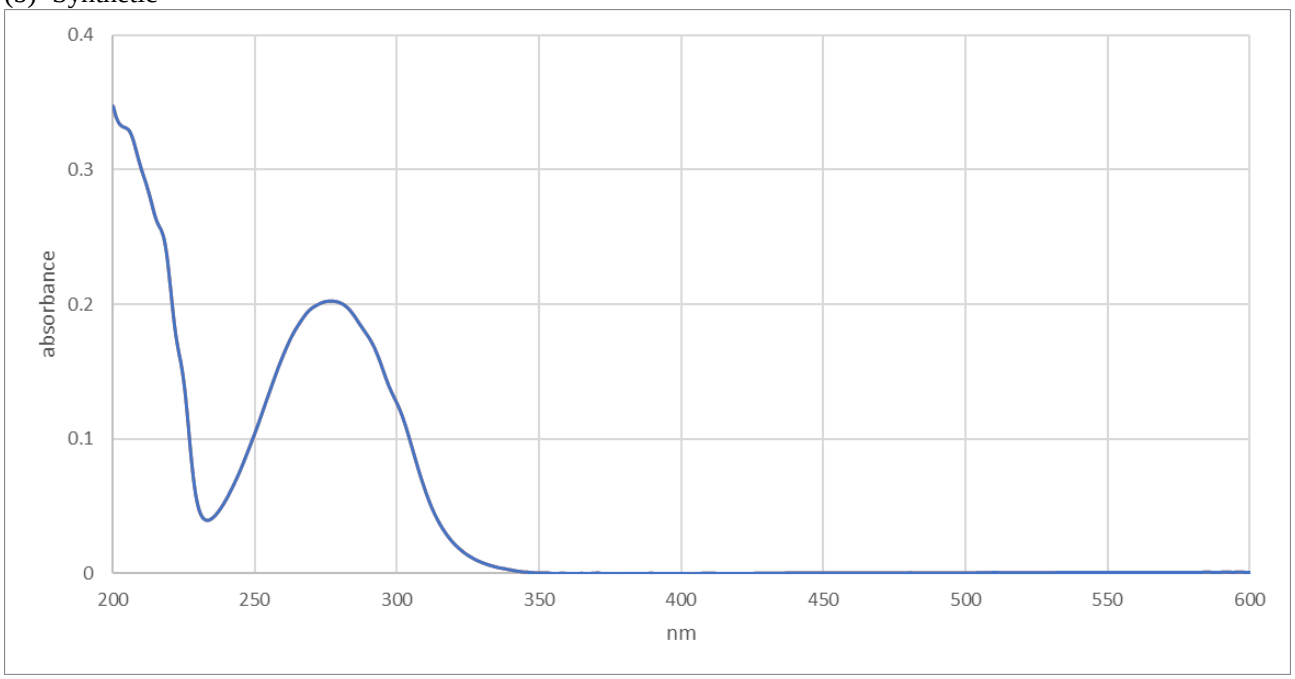

Figure S129. UV-vis spectrum of xenocockiamide B (**11**)

(a) Natural

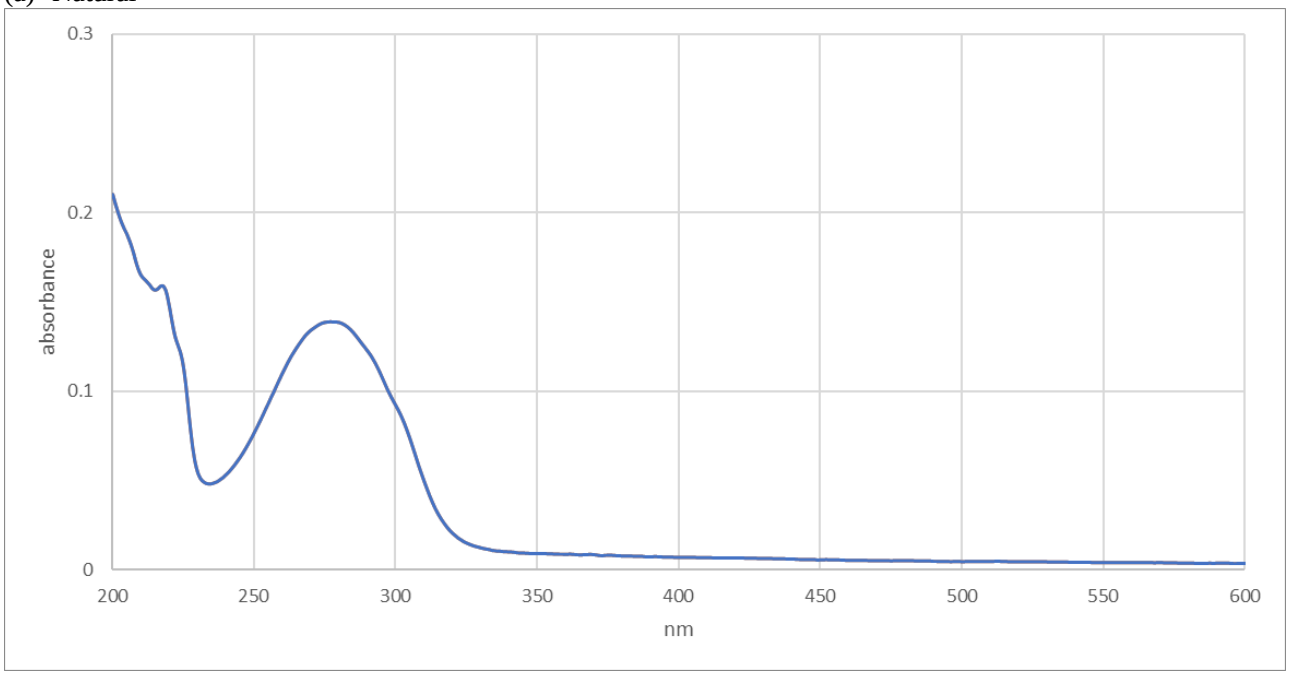

(b) Synthetic

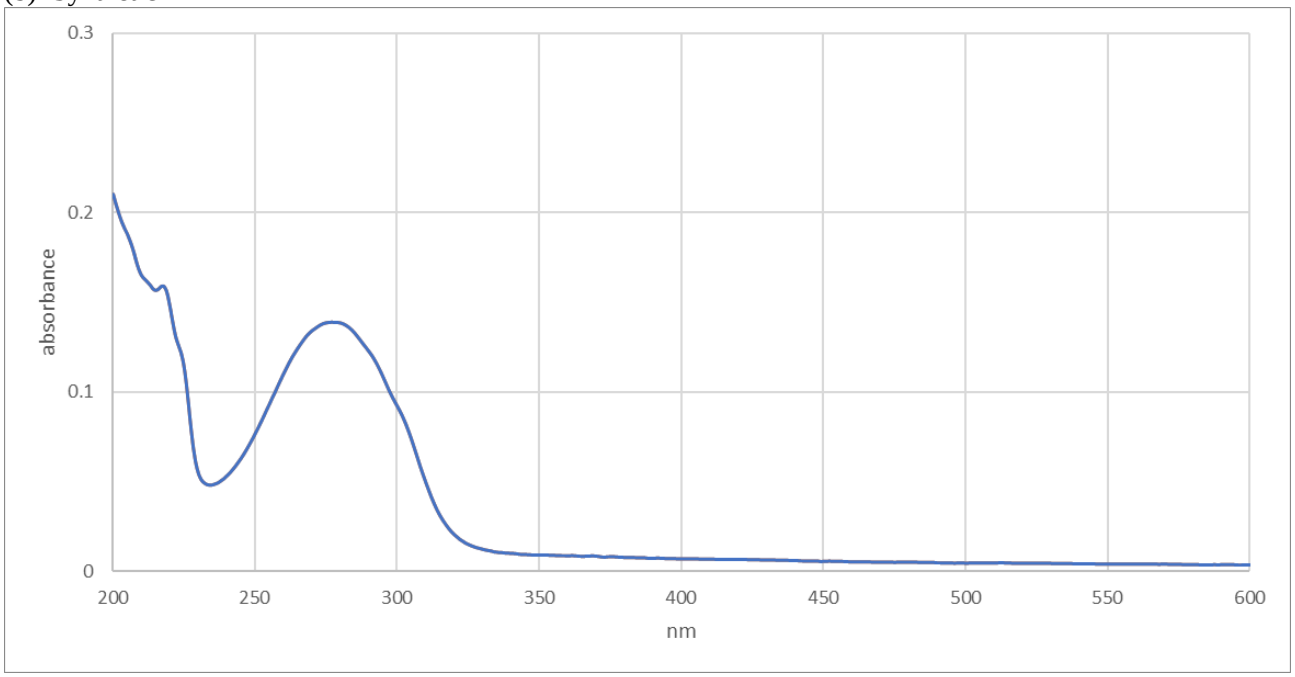

Figure S130. UV-vis spectrum of xenocockiamide C (**12**)

(a) Natural

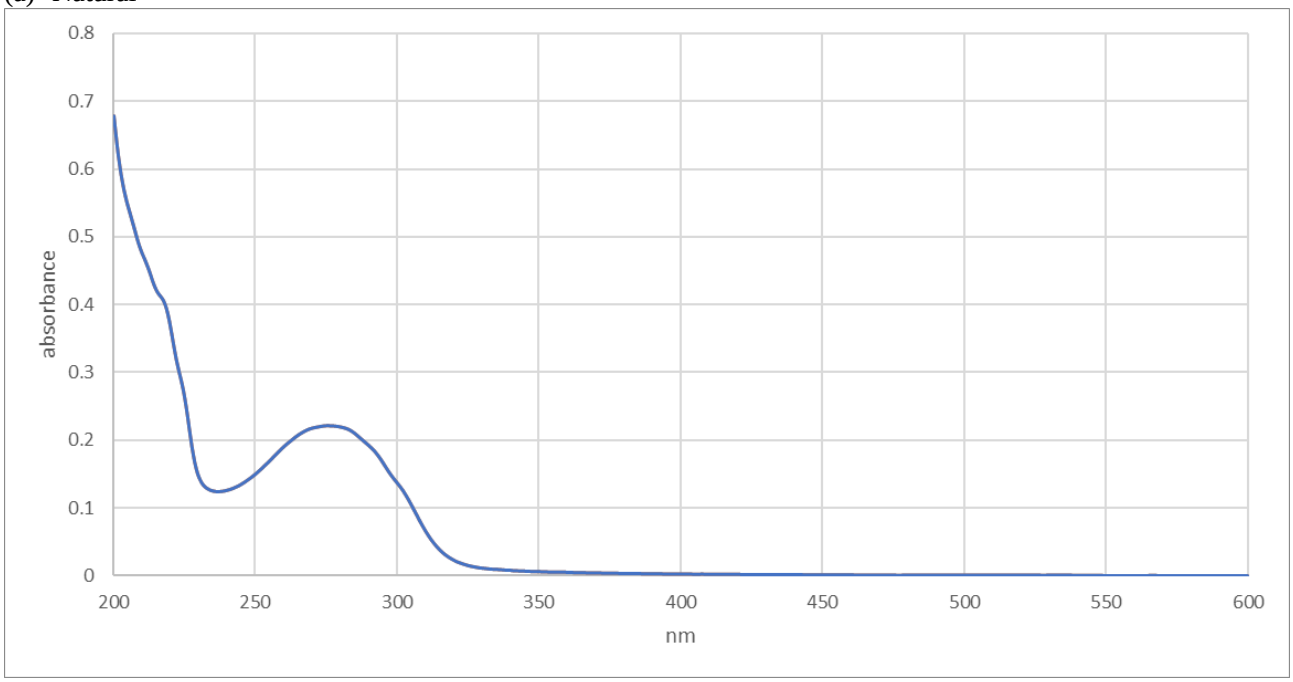

(b) Synthetic

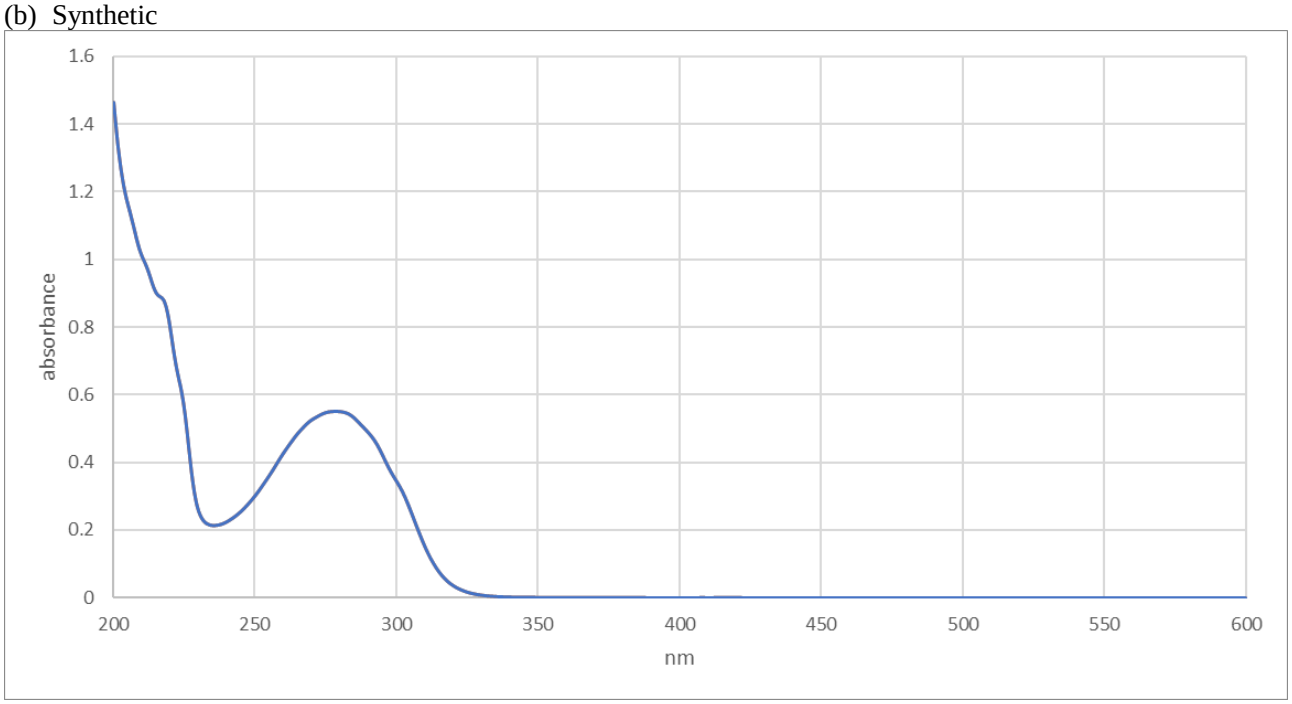

Figure S131. UV-vis spectrum of xenocockiamide D (**13**)

Supplementary references

1. Qiao, K.; Chooi, Y.-H.; Tang, Y., Identification and engineering of the cytochalasin gene cluster from Aspergillus clavatus NRRL 1. *Metab. Eng.* **2011,** *13*, 723−732.
2. Chiang, Y.-M.; Ahuja, M.; Oakley, C. E.; Entwistle, R.; Asokan, A.; Zutz, C.; Wang, C. C. C.; Oakley, B. R., Development of genetic dereplication strains in *Aspergillus nidulans* results in the discovery of aspercryptin. *Angew. Chem. Int. Ed.* **2016,** *55*, 1662−1665.
3. Yin, W.-B.; Chooi, Y. H.; Smith, A. R.; Cacho, R. A.; Hu, Y.; White, T. C.; Tang, Y., Discovery of cryptic polyketide metabolites from dermatophytes using heterologous expression in *Aspergillus nidulans*. *ACS Syn. Biol.* **2013,** *2*, 629−634.